

This year's cover celebrates the 100th anniversary of Einstein's General Theory of Relativity, depicting a conceptual gravitational well over the backdrop of a deep-sky image. The fabric of gravitational field-lines links images taken from our current Physics of the Cosmos (PCOS) Strategic Astrophysics Technology (SAT) projects, symbolizing that multiple technology developments are needed to enable future missions that will help expand our understanding of how the universe works.

Table of Contents

Executive Summary	4
1. Science Overview	7
2. Strategic Technology Development Process and Portfolio.	9
3. Technology Gaps	15
4. Technology Priorities and Recommendations.	41
5. Benefits and Successes Enabled by the PCOS SAT Program	44
6. Closing Remarks	48
References	49
Appendix A – Technology Development Quad Charts.	50
Appendix B – Technology Development Status	65
Appendix C – Training the Future Astrophysics Workforce	166
Appendix D – Acronyms	175

PCOS 2015 PATR

Executive Summary

What is NASA's Physics of the Cosmos (PCOS) Program?

From ancient times, humans have looked up at the night sky and wondered: Are we alone? How did the universe come to be? **How does the universe work?** PCOS focuses on that last question. Scientists investigating this broad theme use the universe itself as their lab. They investigate its fundamental laws and properties, testing Einstein's General Theory of Relativity to see if our current understanding of space-time is borne out by observations. They examine the behavior of the most extreme environments – supermassive black holes, active galactic nuclei, and others – and the farthest reaches of the universe, to expand our understanding. With instruments sensitive across the spectrum, from radio, through infrared (IR), visible light, ultraviolet (UV), to X rays and gamma rays, as well as gravitational waves, they peer across billions of light-years, observing echoes of events that occurred instants after the Big Bang.

One surprising recent discovery is that the universe is expanding at an ever-accelerating rate, the first hint of what we now call dark energy, estimated to account for 75% of mass-energy in the universe. Dark matter, so called because we can only observe its effects on regular matter, accounts for another 20%, leaving only 5% for regular matter and energy. Scientists now also search for special polarization in the cosmic microwave background to support the notion that in the split-second after the Big Bang, the universe inflated faster than the speed of light! Since this would have been an expansion of space itself, and not energy or matter moving faster than light, the Theory of Relativity would remain intact. The most exciting aspect of this grand enterprise today is that we can finally develop the tools needed for such discoveries.

Why is PCOS Technology Development Critical?

A 2008 Space Review paper noted that robust technology development and maturation is crucial to reducing flight project schedule and cost over-runs: “...in the mid-1980s, NASA's budget office found that during the first 30 years of the civil space program, no project enjoyed less than a 40% cost overrun unless it was preceded by an investment in studies and technology of at least 5 to 10% of the actual project budget that eventually occurred” [1]. Such a technology maturation program is most efficiently addressed through focused R&D projects, rather than in flight projects, where “marching armies” make the cost of delays unacceptably high. The 2010 Decadal Survey, [New Worlds, New Horizons in Astronomy and Astrophysics](#) (NWNH) stressed that “*Technology development is the engine powering advances in astronomy and astrophysics... Failure to develop adequately mature technology prior to a program start also leads to cost and schedule overruns*” [2].

NASA requires flight projects to demonstrate technology readiness level (TRL) 6* by Preliminary Design Review (PDR) for all technologies they need. However, this can only succeed with a process in place to correctly identify and adequately fund development of relevant “blue sky” technologies to TRL 3†, and then mature them to TRL 5‡ or 6, across the so-called “mid-TRL gap.” This enables robust mission concepts, letting the community focus its strategic planning on proposed missions’ scientific relevance.

What's in this Report? What's New?

This fifth Program Annual Technology Report (PATR) summarizes the Program's technology development activities for fiscal year (FY) 2015. It lists technology gaps identified by the astrophysics community

* TRL 6: “System/sub-system model or prototype demonstration in a relevant environment.” NPR 7123.1B, Appendix E.

† TRL 3: “Analytical and experimental critical function and/or characteristic proof-of-concept.” NPR 7123.1B, Appendix E.

‡ TRL 5: “Component and/or breadboard validation in relevant environment.” NPR 7123.1B, Appendix E.

(p. 17), with their priority ranking assigned by the PCOS Technology Management Board (TMB) (p. 43). Following this year's prioritization, the Program Office recommends NASA HQ first solicit and fund the following technologies:

- High-power, narrow-line-width laser sources;
- Highly stable, low-stray-light telescope;
- Large-format, high-spectral-resolution, small-pixel X-ray focal-plane arrays;
- Affordable, lightweight, high-resolution X-ray optics;
- Advanced millimeter-wave focal plane arrays for Cosmic Microwave Background (CMB) polarimetry; and
- High-efficiency cooling systems covering the range 20K to under 1K.

These recommendations take into account ongoing discussions between NASA and the European Space Agency (ESA) about potential US contributions to the Advanced Telescope for High ENergy Astrophysics (ATHENA), recently selected for ESA's L2 slot, and a yet-to-be-selected gravitational-wave mission for ESA's L3, planned to launch in the mid-2030s. In addition, the TMB considered a set of large mission concepts identified by the Astrophysics Division Director as candidates to be studied to inform the 2020 Decadal Survey. These studies include three of five "Surveyor" concepts described in the Astrophysics Roadmap, "[Enduring Quests, Daring Visions](#)," released in December 2013, as well as the Habitable Exoplanet Imaging Mission recommended by the NWNH. The PCOS Program Analysis Group (PhysPAG) along with the Program Analysis Groups (PAGs) for the Cosmic Origins (COR) program, COPAG, and Exoplanet Exploration Program (ExEP), ExoPAG, later concurred with this list. The PCOS Program Office and TMB are ready to respond to technology gaps identified by the studies as well as by US participants in ATHENA and the eventual L3 mission.

Meanwhile, the Program is pleased to announce three newly awarded PCOS Strategic Astrophysics Technology (SAT) projects for FY 2016 start (alphabetically, by Principal Investigator, PI):

- "Superconducting Antenna-Coupled Detectors and Readouts for Space-Borne CMB Polarimetry," James Bock, JPL;
- "Telescope Dimensional Stability Study for a Space-Based Gravitational-Wave Mission," Jeffrey Livas, Goddard Space Flight Center (GSFC); and
- "High-Efficiency Feedhorn-Coupled TES-based Detectors for CMB Polarization Measurements," Edward Wollack, GSFC.

Including these, the Astrophysics Division has awarded 22 PCOS SAT projects to date, funded by PCOS Supporting Research and Technology (SR&T), and intended to develop telescopes, optics, detectors, electronics, micro-thruster subsystems, and laser subsystems, applicable to future strategic PCOS missions. Nine of the 22 projects continue from previous years, each reporting significant progress, with several prepared for TRL advancement review. With one of the nine now complete and six new projects begun in FY 2015, this PATR reports on the progress, current status, and activities planned for the coming year for 14 projects funded in FY 2015. We thank the PIs of our ongoing projects for their informative progress reports (Appendix A – quad charts, p. 50; Appendix B – development status, p. 65), and welcome our new awardees, two of whom are returning PIs (abstracts at the end of Appendix B).

The following are some examples where Program-funded technologies were infused, or are planned to be infused, into projects and missions:

- Advancements made to X-ray mirror and detector/readout technologies is allowing meaningful NASA contribution to [ATHENA](#) (2028 launch);

- REgolith X-ray Imaging Spectrometer ([REXIS](#)), an MIT student instrument on the Origins-Spectral Interpretation-Resource Identification-Security-Regolith Explorer ([OSIRIS-REx](#)), is incorporating Program-funded directly deposited X-ray blocking filter technology on its engineering and flight CCDs (2016 launch); and
- Antenna-coupled transition-edge superconducting (TES) bolometer technology was deployed in the ground-based Background Imaging of Cosmic Extragalactic Polarization 2 ([BICEP2](#)) experiment to measure B-mode polarization, and performance-tested in a realistic environment on [Spider's](#) 2014/15 Antarctic season long-duration balloon flight.

Finally, this PATR introduces a new feature titled “Developing the Future Astrophysics Workforce,” (Appendix C, p. 166) This feature introduces the students and post-doctoral fellows who have worked on and contributed to our SAT projects, gaining the knowledge and experience that will enable them to push the field of astrophysics forward in the coming decades.

1. Science Overview

PCOS lies at the intersection of physics and astronomy. It uses the universe – the cosmic scale, the diversity of conditions, and the extreme objects and environments – as a laboratory to study the basic properties of nature. PCOS science addresses the fundamental physical laws and properties of the universe. The science objectives of the PCOS Program are to probe Einstein’s General Theory of Relativity and the nature of space-time, better understand the behavior of matter and energy in the most extreme environments, expand our knowledge of dark energy and the accelerating universe, precisely measure the cosmological parameters governing the evolution of the universe, test the inflation hypothesis of the Big Bang, and uncover the connection between galaxies and supermassive black holes.

The Program encompasses multiple scientific missions aimed at meeting Program objectives, each with unique scientific capabilities and goals. The Program was established to integrate those missions into a cohesive effort that enables each project to build on the technological and scientific legacy of its contemporaries and predecessors. Each project operates independently to achieve its unique set of mission objectives, which contribute to the overall Program objectives. The current operating PCOS missions are:

- Chandra X-ray Observatory;
- X-ray Multi-Mirror Mission (XMM–Newton); and
- Fermi Gamma-ray Space Telescope.

Two missions are in development in the PCOS portfolio, both led by ESA:

- Space Technology 7 (ST7)/Laser Interferometer Space Antenna (LISA) Pathfinder (LPF); and
- Euclid, a dark energy survey mission.

LPF, scheduled for launch in late 2015, is a technology demonstration mission. This mission is intended to validate a number of key technologies for gravitational-wave detectors, including inertial reference sensors, ultra-low-noise drag-free flight, and micro-Newton thrusters, retiring technical risks for a LISA-like mission. LPF contains two payloads, the European LISA Technology Package (LTP) and NASA’s ST7 experiment.

The NASA portion of Euclid is a PCOS project managed by JPL. Euclid, scheduled for a 2020 launch, will perform a six-year photometric and spectroscopic survey of about a third of the sky. Euclid’s scientific objectives, to improve our understanding of dark energy, gravity, and dark matter, are aligned with PCOS objectives. NASA will provide detectors and associated cryogenic electronics for one of Euclid’s two instruments, the Near Infrared Spectrometer and Photometer (NISP).

The PCOS portfolio currently focuses on technology studies in support of the priorities of the Astrophysics Division as outlined in the [Astrophysics Implementation Plan](#) (AIP), [updated in December 2014](#). The highly ranked NWNH priorities in the PCOS portfolio are:

- LISA – large mission category;
- International X-ray Observatory (IXO) – large mission category; and
- Inflation Probe – medium-size mission category.

The decadal committee ranked as the highest-priority large space mission the Wide-Field Infrared Survey Telescope (WFIRST). WFIRST, managed by the ExEP Program Office at JPL, is envisioned and designed to settle fundamental questions about the nature of dark energy, to perform studies of exoplanets, and to provide a highly capable near-IR observatory for large-field surveys. Following ESA’s announcement of themes for its large-class L2 and L3 launch opportunities, scheduled for 2028

and 2034 respectively, NASA is pursuing partnerships on the X-ray mission ATHENA for L2 and a future space-based gravitational-wave observatory for L3 (details below). Since the AIP prioritized the Inflation Probe lowest among the three, PCOS will not perform an Inflation Probe mission study before the completion of the mid-decadal review in 2016. However, the PCOS Program and the Astrophysics Division continue to support related technologies through SAT and Astrophysics Research and Analysis (APRA) funding.

ESA's L2 theme is "The Hot and Energetic Universe." In July 2014, ESA formally announced its selection of the [ATHENA X-ray mission concept](#) for L2. In accordance with the AIP, NASA has been actively pursuing a role in ATHENA, and has had a representative to the ATHENA Science Study Team (SST) since last year. Since the 2014 PATR, NASA solicited membership in the ATHENA SST Science Working Groups and selected 23 members of the US community for travel funding to participate in science workshops in support of ATHENA. NASA also issued a Request for Information (RFI) entitled "*Possible US Contributions to ESA's ATHENA Mission Focal Plane Instruments*." From this RFI it was determined there is one team in the US interested in participating in each of the two instruments (the X-ray Integral Field Unit, X-IFU; and the Wide Field Imager, WFI). Members of the US community have now joined the X-IFU consortium in Europe in preparation for the instrument Announcement of Opportunity (AO), anticipated for early 2016. Discussions are still under way for possible US roles in the WFI but, as of this writing, no formal role has been negotiated. The X-ray optics will be provided by ESA, rather than the ATHENA consortium (which is funded by the ESA member states), and any US role in the ATHENA optics is yet to be negotiated.

The L3 theme is the "The Gravitational Universe." While discussions have begun regarding possible NASA collaborations, these are at an earlier phase. NASA has selected four representatives to ESA's Gravitational Observatory Advisory Team (GOAT). The purpose of GOAT is to evaluate and recommend possible scientific and technical approaches for a gravitational-wave observatory envisaged for a planned launch date in 2034. [An intermediate report](#) was released in June 2015 with a number of preliminary findings, including that the LISA-type laser interferometer mission appeared to be the preferred mission architecture. ESA plans to release some technology funding to support L3 technologies within the next calendar year.

Meanwhile, NASA, through PCOS, continues to support the LPF mission. At the time of this writing, the LPF launch is anticipated for December 3, 2015. LPF will operate at the Earth-Sun L1 Lagrange point and is expected to commence its main operations in early 2016.

Moving forward, the Astrophysics Division plans to study several mission concepts that would explore the nature of the universe from its earliest moments, in its most extreme conditions, and at the largest scales. The candidate mission concepts identified by a December 2014 white paper written by the director of the Astrophysics Division are:

- Far-IR Surveyor;
- Habitable-Exoplanet Imaging Mission;
- UV/Optical/IR Surveyor; and
- X-Ray Surveyor.

The PhysPAG, COPAG, and ExoPAG have discussed these and other possible concepts, and in preliminary findings concurred that this list identifies the optimal set of large mission concepts to study, make science cases, assess cost and technology needs, and formulate design reference missions to be considered and prioritized by the upcoming 2020 Decadal Survey. The PAGs will submit a joint report to the Astrophysics Subcommittee on October 8, recommending which mission concept studies should be initiated. Note that all three PAGs have indicated they assume an L3 gravitational-universe mission study will occur concurrently with these flagship mission studies. The Program's technology development efforts will be guided by the outcome of these studies.

2. Strategic Technology Development Process and Portfolio

NASA HQ Science Mission Directorate (SMD) Astrophysics Division set up three program offices to manage all aspects of the three focused astrophysics programs: PCOS, COR, and ExEP. The Program Offices shepherd critical technologies toward the goal of implementation into program-relevant flight projects. These offices follow Astrophysics Division guidance, and base their recommendations on science community input, ensuring the most relevant technologies are solicited and developed. The PCOS Program Office, located at NASA GSFC, serves as HQ's implementation arm on PCOS Program-related matters. The Astrophysics Division achieves efficiency by having the same staff and physical facilities serve both PCOS and COR Program Offices. The Astrophysics Division funds technology development at all TRLs. Early-stage development ($TRL \leq 3$) and technologies related to non-strategic missions are typically funded by APRA. Final maturation ($TRL \geq 6$) is mission-specific and thus handled by flight missions. The SAT program, launched in 2009, funds maturation of technologies across the mid-TRL gap ($3 \leq TRL < 6$).

The PCOS Technology Development Process

The PCOS Program Office is charged to develop and administer a technology development and maturation program, moving innovative technologies across the mid-TRL gap to enable strategic PCOS missions. The Program Office facilitates, manages, and implements the technology policies of the Program. Our goal is to facilitate technology infusion into PCOS missions, including the crucial phase of transitioning nascent technologies into targeted projects' technology programs during mission formulation. PCOS SAT projects are funded by the PCOS SR&T budget. The process for achieving our goal is detailed in the PCOS technology management plan. Our work is guided by the priorities set forth in the AIP, the Astrophysics Roadmap, and any other current strategic guidance. The AIP describes the Astrophysics Division's planned implementation of space-based prioritized missions and activities identified in NWNH, and considering recent budgetary developments. The Roadmap strives to inspire and challenge the community to pursue the missions and technologies needed over the next three decades to address NWNH-identified science goals.

The process (Fig. 2-1), unchanged from prior years, places at the center of our efforts the science community's inputs through the Decadal Survey process and ongoing identification of technology gaps. The community is encouraged to submit gaps at any time via the PhysPAG or directly through the PCOS Program website. PhysPAG, through its science interest groups (SIGs) and science analysis groups (SAGs), reviews gaps submitted before the annual cutoff date, June 1 this year, consolidating, enhancing, and adding to them as needed to create a complete and compelling set of gaps for TMB evaluation. The Program Office charges its TMB annually to evaluate and determine which of the submitted technology developments would meet Program objectives, and prioritize them for further development consideration. The TMB ranks gaps based on Program objectives, strategic ranking of relevant science/missions, benefits and impacts, and urgency. The TMB, a Program-level functional group, thus provides a formal mechanism for input to, and review of, PCOS technology development activities.

TMB priority recommendations inform Astrophysics Division decisions on which technologies to solicit in the upcoming annual SAT call for proposals, and guide proposal selections. HQ's investment considerations are made within a broader context, and other programmatic factors apparent at the time of selection may affect funding decisions. HQ evaluates resulting technology development proposals, considering overall scientific and technical merit, programmatic relevance, and cost reasonableness given the scope of work. Awardees work to mature their technologies from their initial TRL, normally 3 or 4[§], through TRL 5. PIs report progress and plans to the Program Office periodically, and submit their technologies to TRL advancement review as appropriate. Progress in these projects allows infusion of newly mature technologies into NASA missions and studies, enabling and enhancing their capabilities with acceptable programmatic costs and risks.

[§] TRL 4: "Component and/or breadboard validation in laboratory environment." NPR 7123.1B, Appendix E.

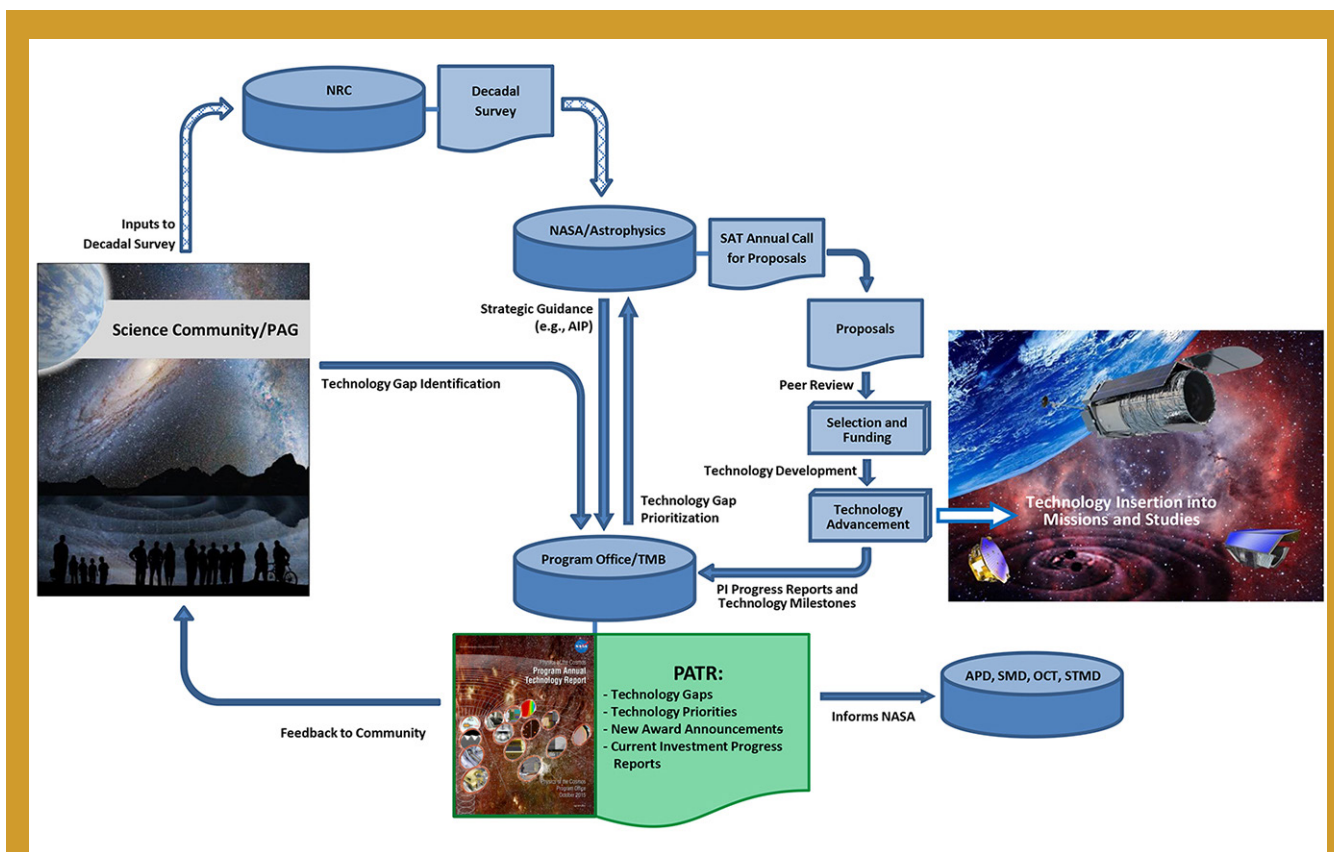


Fig. 2-1. The PCOS technology development process receives community input on technology gaps, recommends priorities, manages SAT-funded activities, and informs NASA and the science community about progress.

As seen in the process graphic, the PATR plays an important role in our technology development process. Through PI reports and quad charts, it describes the status of all strategic PCOS technologies. It captures technology gaps articulated by the scientific community, and recommends a prioritized list of technologies for future solicitation and funding. The PATR is an open source for the public, academia, industry, and the government to learn about the status of enabling technologies required to fulfill PCOS science objectives. The report informs NASA organizations, including but not limited to the Astrophysics Division, and updates the community regarding technology development progress, as input for future technology gap submissions. Technological progress and programmatic decisions change the landscape of requirements for PCOS needs; therefore, the process is repeated annually to ensure continued relevance of priority ranking. Indeed, in any given year, new SAT award decisions are informed by PATRs published over the prior two years, a new SAT solicitation is informed by the prior-year PATR and the current year's TMB report, and the current PATR provides recommendations for next year's SAT.

This technology development and maturation process identifies existing and emerging needs, improves the relevance of PCOS technology investments, provides the community a voice in the process, and promotes targeted external technology investments by defining needs and identifying NASA as a potential customer for innovative technologies. It also identifies providers of technologies and expertise, the Program PIs, to potential customers and collaborators within and beyond NASA. This encourages industry and other players to invest in enabling technologies for future missions, and promotes formation of productive collaborations. Beyond involvement in the Decadal Survey process and technology gap submission, the science community is a key stakeholder in Program technology development activities.

The community provides feedback and inputs to the technology development process; and participates in PhysPAG and other committees and workshops, ad-hoc studies, and in technology development by responding to SAT solicitations.

TRL Vetting

As mentioned above, the PCOS Program Office manages the Program's strategic technology development process. In prior PATRs, we described the overall technology development management effort. With several SAT projects reporting TRL progress, we now expand on our TRL vetting process.

SAT funding helps mature technologies expected to enable and/or significantly enhance future strategic astrophysics missions. These technologies typically enter the SAT program at TRLs 3 or 4, and are intended to progress toward higher TRLs. TRL assertions above a technology's approved entry level are not official until a TRL-vetting TMB concurs with the development team's assessment. When PIs believe their team has demonstrated the required progress, they may request a review to present their case for TRL update. The Program Office then convenes a TMB consisting of Program Office and HQ senior staff and subject matter experts to assess the request and, when warranted, approve the new TRL. The typical forum for such a request is during the PI's end-of-year presentation to the Program Office, but it can be made at any time. Several PIs with projects in the PCOS portfolio are considering undergoing TRL vetting this coming year.

Why review TRLs?

TRLs are used throughout the agency to help assess the maturity of technologies. The Program Office's charge includes a requirement that it monitor the progress of the Astrophysics Division's investments in technology maturation through SAT projects, relative to the TRL plan and milestones submitted by the PI in the SAT proposal. A key indicator of such progress is TRL advancement as vetted by the Program Office, providing a consistent method of assessing progress across our full portfolio of projects.

What does our vetting mean?

When the Program's TMB approves or vets a new, higher TRL asserted by the PI, it provides an independent assessment and verification that the project has achieved that TRL. The TMB consists of scientists, technologists and systems engineers from the Program, and subject matter experts from the community and Aerospace Corporation, who provide an objective and informed assessment. The primary purpose for issuing this assessment is to inform the Program Office of significant progress in preparing the technology for possible inclusion in strategic missions. It also informs the PI and the science community of the improved state of readiness.

What is expected?

The TRL vetting process is initiated when a PI notifies the Program Office that the milestones necessary for TRL advancement have been met. The PI then presents the progress to a TMB convened by the Program Office, which considers the TRL assertion, guided by TRL definitions in [NASA Systems Engineering Processes and Requirements](#), also known as NASA Procedural Requirements (NPR) 7123.1B. Recognizing that PI teams are busy and must concentrate their efforts on the work of maturing their technology, the Program Office is satisfied to rely on a cogent exposition of the same reports, graphs, and test results the team captures for its own records.

The PI team should prepare a brief but compelling presentation, making the case for the higher TRL. The Program Office has tools to help PIs assess their progress and is available to provide information on the TRL process. Finally, if the project is still ongoing, we recommend the PI present a plan for further TRL advances, if any, allowing the TMB to offer feedback and make recommendations.

What are the benefits for the PI and the Program?

The Program Office's TRL vetting process serves as an opportunity to collect and capture the needed documentary evidence and present it to a group of experts. This can strengthen a potential future TRL case presentation, whether in person or in writing, to flight projects, proposal teams considering adding the technology to their mission, and/or proposal reviewers. Another leveraging opportunity might be in collaboration opportunities. As alluded to above, the TMB can help the PI team fine-tune their plan for future work to achieve the claimed TRL if the current claim was not vetted, or for the next TRL if it was.

Finally, TRLs are NASA's technology development assessment language, and TRL advancement is one of the key success criteria for SAT projects. Our TRL vetting is an objective process, rendering an independent verification of achievement, increasing the credibility of the technology's maturity and its potential for continued funding or infusion into a flight mission.

The PCOS Technology Development Portfolio as of 2015

For FY 2015, the driving objective is to maintain progress in key enabling technologies for possible contributions to ESA L-class missions, such as ATHENA and an L3 gravitational-wave mission, a future US-led X-ray Surveyor, and a CMB polarimetry mission.

There have been 22 PCOS SAT projects awarded to date. Table 2-1 provides top-level information on the 14 projects that received funding in FY 2015, including where Appendices A and B describes each more fully. Appendix A provides one-page "quad chart" project summaries. Appendix B provides PI reports detailing development status, progress over the past year, and planned near-term development activities. Abstracts for the three recently awarded projects, slated to begin in FY 2016, are included at the end of Appendix B. The appendices provide technology overviews and status, not flight implementation details. For additional information, please contact the PCOS Program Office or the PIs directly. Contact information for each PI appears at the end of his or her report in Appendix B. The PCOS Program Office manages one SAT project co-funded with the Game-Changing Development Program of NASA's Space Technology Mission Directorate (STMD). When possible, the Programs leverage their limited funding to advance technologies that meet the goals of both. The laser-frequency stabilization investigation which appears in Table 2-1 fits that requirement, simultaneously ranking highly among all proposals submitted to both programs. Such collaborative investments are "win-win-win" opportunities for the Astrophysics Division, STMD, and the PI. The PCOS Program looks forward to continued relationship with STMD, creating more such opportunities in the future.

Similarly, one of the above SAT projects, developing 0.5-arcsec adjustable X-ray optics, follows up on a related project led by the same PI and co-funded by the APRA program and STMD. Indeed, since the two are so closely related, the PI summary in Appendix A and report in Appendix B describe progress in both.

Strategic Astrophysics Technology Selection for FY 2016 Start

The PCOS Program funds SAT projects to advance the maturation of key technologies to make feasible their implementation in future space-flight missions. The Program focuses on advancing those technologies most critical for substantive near-term progress on strategic priorities. Three technology areas were called out in the 2014 PCOS SAT solicitation as being of particular interest for the Program: X-ray astrophysics, gravitational-wave astrophysics, and CMB polarization.

Technology Development Title	PI	Institution	Start Year & Duration	Current TRL	Quad Chart & PI Report Locations
Demonstration of a TRL-5 Laser System for eLISA	J. Camp	GSFC	FY 14; 2 yrs	3	51, 66
Gravitational-Wave Phasemeter Technology Development	W. Klipstein	JPL	FY 14; 3 yrs	4	52, 72
Laser Frequency Stabilization (co-funded with STMD)	J. Lipa	Stanford U.	FY13; 3 yrs	3	53, 76
Telescope for Space-Based Gravitational-Wave Observatories	J. Livas	GSFC	FY13; 3 yrs	3	54, 85
Colloid Microthruster Propellant Feed System	J. Ziemer	JPL	FY13; 2 yrs	5	55, 93
Directly Deposited Blocking Filters for Imaging X-ray Detectors	M. Bautz	MIT	FY12; 4 yrs	5	56, 105
Fast Event Recognition for the ATHENA Wide-Field Imager	D. Burrows	PSU	FY15; 2 yrs	3	57, 115
Demonstrating Enabling Technologies for Hi-Res Imaging Spectrometer of Next NASA X-ray Astronomy Mission	C. Kilbourne	GSFC	FY13; 3 yrs	4	58, 121
Reflection Grating Modules: Alignment and Testing	R. McEntaffer	U. of Iowa	FY15; 2 yrs	4	59, 128
Development of 0.5 Arcsecond Adjustable Grazing-Incidence X-ray Mirrors for the SMART-X Mission Concept	P. Reid	SAO	FY15; 3 yrs	3	60, 135
Advanced Packaging for Critical-Angle X-ray Transmission Gratings	M. Schattenburg	MIT	FY15; 2 yrs	3	61, 140
Technology Development for an AC-Multiplexed Calorimeter for ATHENA	J. Ullom	NIST	FY15; 2 yrs	3	62, 145
Next-Generation X-ray Optics: High Angular Resolution, High Throughput, and Low Cost	W. Zhang	GSFC	FY15; 2 yrs	5	63, 150
Planar Antenna-Coupled Superconducting Detectors for Cosmic Microwave Background Polarimetry	J. Bock	Caltech/JPL	FY14; 2 yrs	3	64, 155

Table 2-1. PCOS Technology Development Portfolio as of FY 2015 (organized by science topic and PI name).

The PCOS SAT proposals selected for FY 2016 start, announced in August 2015, advance three technologies in two of these areas (Table 2-2). Two efforts advance CMB polarization measurement capabilities (superconducting antenna-coupled detectors and readouts, and feedhorn-coupled TES-based detectors), and one deals with a key technology required for a gravitational-wave mission (telescope dimensional stability). These are identified by the NWNH as key areas for technology maturation toward implementation of an Inflation Probe and a gravitational-wave observatory. Another SAT proposal received a highly favorable review, but the requested funding was greater than could be accommodated within Technology Development for PCOS (TPCOS). Since the proposed TES X-ray detector work is directly related to a technology that is a possible contribution to the ESA-led ATHENA mission planned to launch in 2028, it was funded independently of the SAT program, along with other ATHENA-related efforts.

Technology Development Title	PI	Institution	Duration	Initial TRL	Abstract Location
Superconducting Antenna-Coupled Detectors and Readouts for Space-Borne CMB Polarimetry	James Bock	JPL	2 years	3	163
Telescope Dimensional Stability Study for a Space-Based Gravitational-Wave Mission	Jeff Livas	GSFC	2 years	3	164
High-Efficiency Feedhorn-Coupled TES-based Detectors for CMB Polarization Measurements	Edward Wollack	GSFC	2 years	3	165

Table 2-2. PCOS SAT Development Starts in FY 2016 (alphabetically by PI).

These new SAT selections were based on the following factors:

- Overall scientific and technical merit;
- Programmatic relevance of the proposed work; and
- Cost reasonableness of the proposed work.

Since these projects have only recently been selected for funding, their status is not presented yet. First-year progress for each will appear in the 2016 PCOS PATR.

Studies Planned for 2016 – 2019 in Preparation for 2020 Decadal Survey

As mentioned in Section 1, the Astrophysics Division plans to study several mission concepts. These studies will guide efforts to mature technology components, architectures, and make the science cases to be considered and prioritized by the upcoming 2020 Decadal Survey. The candidate mission concepts are as follows (in alphabetical order):

- Far-IR Surveyor;
- Habitable-Exoplanet Imaging Mission;
- UV/Optical/IR Surveyor; and
- X-Ray Surveyor.

Each of these ambitious mission concepts promises breakthrough science results, but implementing them will require us to overcome daunting technology development challenges. The SAT program is certain to play a major role in funding these technology development efforts. We encourage all members of the community to support our efforts to identify the highest priority technology gaps we need to close to make these missions feasible, and continue to submit proposals in response to SAT solicitations. As of this writing, notices of intent to submit for the next SAT round are due January 22, 2016, with proposals due March 18, 2016.

Historic Record of TPCOS Proposals and Awards

The TPCOS section of the SAT program (Table 2-3) received 21 proposals in response to the 2010 solicitation, its first year; 26 for 2011; 10 for 2012; eight for 2013; and six for 2014. The 2013 solicitation was restricted to X-ray astrophysics-related technologies, partially explaining the smaller number of proposals. Of the first set, five proposals were selected, with five more the following year, three in the third year, six in year four, and as reported here, three selected in the latest round. This makes the historical selection rate for PCOS SAT proposals 31%, with the two latest round hitting 75% and 50%, respectively, very high for technology development solicitations.

Solicitation Year	TPCOS Proposals		Proposal Success Ratio
	Submitted	Selected	
2010	21	5	24%
2011	26	5	19%
2012	10	3	30%
2013	8	6	75%
2014	6	3	50%
Total to Date	71	22	31%

Table 2-3. Number of TPCOS SAT Proposals and Awards.

3. Technology Gaps

Anyone may identify a PCOS-related technology gap and submit it to the Program Office directly through the PCOS website, or via the PhysPAG. Technology gaps may be submitted throughout the year. However, to allow timely consideration by its TMB, the Program Office sets a deadline for inclusion in the current year's ranking. In 2015, the deadline was set for June 1, allowing the PhysPAG to review the list for completeness, merge overlapping gaps, and complete and improve entries where the submission did not adequately address the requested information. The final list provided by the PhysPAG was later assessed and prioritized by the PCOS TMB.

To maximize the likelihood of high priority ranking, the Program Office encourages submitters to include as much of the information requested as possible. More importantly, the Program Office asks submitters to describe a technology capability gap, not a specific implementation process or methodology. The technology's goals and objectives should be clear and quantified. Additionally, a complete description of the needed capability with specific performance goals based on mission needs is very valuable. Such information serves several important purposes:

1. The TMB is best able to understand and thus correctly assess the identified technology gap.
2. NASA HQ is best able to develop precise technology development proposal calls.
3. The community is clearly informed and best able to match candidate technologies to mission needs.

Aside from submitter information, the technology gap form requests the following information:

- **Technology gap name:** Identifies the gap, and optimally the type of mission filling it would enable.
- **Brief description:** Summarizes the technology gap and associated key performance criteria. In general, well-defined technology gaps receive higher priority than vague ones.
- **Assessment of current state of the art:** Describes the state of the art, allowing the TMB to appreciate the gap between what's available and what's needed.
- **TRL:** Specifies the current TRL(s) of the technology per NPR 7123.1B Appendix E with clear justification. The SAT program funds projects to advance technologies from TRL 3 up through TRL 5, so those already at TRL 6 will likely rank lower unless the existing technology is significantly deficient relative to the needs (see next point).
- **Target goals and objectives:** Details the goals and/or objectives for a candidate technology to fill the described gap. For example, "*The goal is to produce a detector with a sensitivity of X over a wavelength of Y to Z nm.*" Technology gaps with clearly quantified objectives may receive higher priority than those without quantified objectives.
- **Scientific, engineering, and/or programmatic benefits:** Describes the benefits of filling the technology gap. If the need is enabling, this should describe how and why. If the need is enhancing, it should describe, and if possible quantify, the impact. Benefits could be better science, lower resource requirements (e.g., mass, power, etc.), and/or programmatic (e.g., reduced risk, cost, or schedule). For example, "*Material X is 50% stronger than the current state of the art and will enable the optical subsystem for a 2-m telescope to be Y kg lighter.*" Technology gaps with greater potential mission benefits receive higher scores.
- **Application and potential relevant missions:** Technologies enabling or enhancing missions ranked highly by the AIP and/or the Astrophysics Roadmap, or at least by NWNH, will be scored higher. Technologies applicable to a wide range of PCOS missions, as well as COR and/or ExEP missions will rank better.

- **Urgency:** Specifies when the strategic mission enabled or enhanced by the technology is planned to launch. In certain cases where there is a more immediate driving need (*e.g.*, ESA requirements for achieving TRL 5 or 6 by a certain date to be considered for inclusion in a mission considered strategic by NASA Astrophysics Division), this driving requirement will also be considered. Technology gaps with shorter time windows relative to required development times receive higher priority.

Technology Gaps Submitted to the 2015 TMB

The technology gaps list for 2015 included 14 gaps from the 2014 TMB list, including three proposed revisions to those, plus 23 new entries submitted by the community, for a total of 37 gaps. To improve the comprehensiveness and quality of the list of gaps prioritized by the TMB, the PhysPAG Executive Committee (EC) agreed to review the list after the Program Office compiled it. The EC considered the full set of entries, consolidated those with significant overlap, improved the wording on some entries to make them more compelling to the TMB, added entries where appropriate, and recommended removing entries where those were too incomplete or too far outside the charge of the SAT program. At the conclusion of their effort, the EC sent back to the Program Office a list of 23 entries. Almost all technologies developed to close these gaps would enable and/or enhance high-priority strategic missions per the AIP, the Astrophysics Roadmap, and/or NWNH. We deeply appreciate the EC's efforts and look forward to continued collaboration in the future. Having the EC review gap entries prior to TMB prioritization serves several important purposes:

- It allows experts in relevant fields to clarify submissions and combine related and overlapping gaps, such that the resulting entries are more compelling and potentially merit higher priority ranking;
- It ensures the final list accurately reflects the community-assessed gaps; and
- It makes the process of generating unique technology gaps more transparent to the community.

The PCOS TMB reviewed the 23 gaps in the PhysPAG's list. In one case, the TMB combined two entries into a single gap. Then, the TMB scored and ranked the 22 unique technology gaps (Table 3-1), covering a broad range of PCOS science, including X-ray astronomy, gravitational waves, and the inflation epoch:

- Improvements in X-ray detection and optics (8 gaps);
- Millimeter-wave optics, detection, and polarization sensing (2 gaps);
- Highly stable telescopes, optical benches, and lasers (3 gaps);
- Phase measurement subsystems and gravitational reference sensors (2 gaps);
- Gamma-ray telescopes (1 gap);
- Ultra-high-energy cosmic-ray detectors, optics, and electronics (4 gaps);
- Lattice optical clock (1 gap); and
- Sub-Kelvin cooling (1 gap).

The Program Office continues to solicit and compile technology gap submissions from the community, and as was done this year, will collaborate with the PhysPAG EC to ensure the gaps ranked by the TMB are unique and compelling.

Table 3-1. Technology Gaps Evaluated by TMB in 2015

Table 3-1. Technology Gaps Evaluated by TMB in 2015	
Name of Technology	Fast, low-noise, megapixel X-ray imaging arrays with moderate spectral resolution
Description	<p>Strategic X-ray missions such as X-ray Surveyor require X-ray imaging arrays covering wide fields of view with excellent spatial resolution, i.e., megapixel or higher, and moderate spectral resolution.</p> <p>Fast readout time is needed to minimize event pileup and dead time, and radiation hardness must be sufficient to survive likely mission duration and environment.</p> <p>Finally, such detectors' power per pixel must be low enough to fit likely mission power budgets.</p> <p>Detector arrays meeting these requirements would also enable Explorer, and CubeSat missions with low power budgets, in potentially harsh orbital environments.</p>
Current State of the Art	Silicon active pixel sensors (APS) currently satisfy some of the requirements, but further work is needed to meet all requirements simultaneously. APS with 36 μm pixels are at TRL 6, but noise levels are still too high, and sensitivity to soft X rays needs to improve. Sparsified readout, limited to pixels with signals, allows fast frame rates and is at TRL 3.
Current TRL	3
Performance Goals and Objectives	<ul style="list-style-type: none"> • Pixel count > 1M/chip; • Multi-chip abutability; • Pixel size 16 μm or smaller; • Noise < 4e-; • Frame rates >100 frames/s; • Radiation tolerance > 10 krad(Si); > 10¹⁰ p cm⁻² 10 MeV proton equivalent non-ionizing dose; and • Power/sensor as low as 0.1 W.
Scientific, Engineering, and/or Programmatic Benefits	Enables X-ray imaging of wide fields with high spatial resolution and sufficient spectral resolution to meet science goals of strategic X-ray missions.
PCOS Applications and Potential Relevant Missions	Examples: X-ray Surveyor, ATHENA-WFI, JANUS/XTiDE-like, or any other focused X-ray optics, or coded-aperture wide-field X-ray monitoring, or X-ray grating mission.
Time to Anticipated Need	<p>Named missions: ATHENA (2020s)</p> <p>Development needed for 2020 Decadal</p> <p>Other drivers: General applicability to focused X-ray optics including the X-Ray Surveyor and Explorer opportunities.</p>

Table 3-1. Technology Gaps Evaluated by TMB in 2015 (continued)

Name of Technology	Large-format, high-spectral-resolution, small-pixel X-ray focal plane arrays
Description	<p>Covering a wide field (>5 arcmin) and spatial resolution matching future X-ray optics (< 1 arcsec) with X-ray focal-plane arrays providing excellent spectral resolution (< 4 eV FWHM in the 0.1 – 10 keV band) is needed to allow study of such questions as how and why matter assembles into galactic clusters, how black holes grow, and how they influence their surroundings.</p> <p>This would be done through observation of X-ray emission from the neighborhood of black holes, emitted by hot matter about to be swallowed.</p> <p>Current X-ray focal-plane arrays have insufficient pixel counts, and achieving large enough pixel counts makes energy resolution challenging.</p>
Current State of the Art	<p>Arrays of 32 pixels, with no multiplexing, are currently feasible (TRL 6).</p> <p>Transition-edge sensor (TES) microcalorimeters or magnetically coupled microcalorimeters (MCC) allow multiplexing which is necessary to achieve the required pixel counts.</p> <p>9:1 absorber:sensor multiplexing has been demonstrated at TRL 3-4.</p> <p>2:1 multiplexing with SQUIDs coupling GHz-frequency resonators has been demonstrated (TRL 2-3) and offers promise of 50:1 multiplexing.</p>
Current TRL	2-4
Performance Goals and Objectives	<ul style="list-style-type: none"> • Absorber (<i>i.e.</i> pixel): Sensor multiplexing of 20:1 with energy resolution < 4 eV and pixel pitch < 50 μm; • Sensor: readout channel multiplexing of > 400:1; and • Large-format arrays with pixel count > 100k and spectral resolution < 4eV FWHM, 0.2 – 10 keV.
Scientific, Engineering, and/or Programmatic Benefits	<p>Science benefits identified for IXO in NWNH and for X-ray Surveyor in 2014 Astrophysics Roadmap.</p> <p>Engineering benefits are simpler focal planes; less-demanding cryogenic requirements; and lower mass, power, and cost.</p>
PCOS Applications and Potential Relevant Missions	<p>Enabling technology for US contribution to ATHENA.</p> <p>Critical instrument for X-ray Surveyor.</p> <p>Studied as sole instrument for a stand-alone probe by Community Science Team.</p>
Time to Anticipated Need	<p>Named missions: ATHENA (2020s)</p> <p>Development needed for 2020 Decadal</p> <p>Other drivers: General applicability to X-ray spectroscopy including the X-Ray Surveyor and Explorer opportunities.</p>

Table 3-1. Technology Gaps Evaluated by TMB in 2015 (continued)

Name of Technology	Advancement of X-ray polarimeter sensitivity with the use of negative ion gas
Description	<p>Standard photoelectric X-ray polarimeter designs are both quantum-efficiency-limited and challenging to calibrate due to diffusion of electron signal as it drifts through the gas.</p> <p>Drifting negative ions decreases diffusion to the thermal limit, thereby decoupling sensitivity from drift distance and enabling larger detector areas that can be at the focus of larger-diameter mirrors and single-reflection concentrator.</p> <p>Negative-Ion Time Projection Chamber (NITPC) polarimeters also allow the selection of constituent gases and pressures to be based on the optimization of modulation and QE rather than diffusion properties. This versatility enables a large improvement in sensitivity without driving cost and with only moderate increase to mass and power of the detector and/or instrument. Furthermore, the energy band will be tunable to maximize science return.</p>
Current State of the Art	<p>Several photoelectric polarimeter concepts <i>e.g.</i>, Polarimeter for Relativistic Astrophysical X-ray Sources (PRAXyS previously GEMS), Imaging X-ray Polarimeter Explorer (IXPE), Polarimetry of Energetic Transients (POET) <i>etc.</i> were proposed in 2014 to provide the next substantial step exploiting X-ray polarization to answer key scientific questions for some of the brightest sources in the sky.</p> <p>However, proposed measurements remain photon-limited and the need for higher sensitivity polarimeters for both faint persistent sources such as AGN and bright transient sources such as SGRs by way of Explorer missions and probe-class missions in the next decade remains critical.</p> <p>The goal of this development is to make practical the technology that will provide an order-of-magnitude improvement in polarization sensitivity over current-generation instruments</p>
Current TRL	4
Performance Goals and Objectives	<p>Development of gas electron multipliers optimized for negative ion gas.</p> <p>Development of finer-pitch strip readouts to improve sensitivity at lower energies and higher pressures.</p> <p>Optimization of gas mixtures to maximize sensitivity (QE vs. track length).</p> <p>Demonstrate lifetime of the gas and detector materials is commensurate with mission requirements.</p>
Scientific, Engineering, and/or Programmatic Benefits	<p>These developments will allow a factor of 10 improvement in sensitivity without decreasing the sensitivity per unit mass and without increasing the relative cost of an instrument.</p>
PCOS Applications and Potential Relevant Missions	<p>Flagship and probe-class X-ray missions.</p> <p>Explorer-class X-ray missions.</p> <p>Sounding rocket experiments.</p>
Time to Anticipated Need	<p>Named missions:</p> <p>Development needed for 2020 Decadal: No</p> <p>Other drivers: Explorer, Probe, and MO opportunities.</p>

Table 3-1. Technology Gaps Evaluated by TMB in 2015 (continued)

Name of Technology	High-efficiency X-ray grating arrays for high-resolution spectroscopy
Description	<p>Light-weight, high-efficiency (> 40-50%), large-format X-ray grating arrays enable spectral resolving power $R > 3000$ in the soft X-ray band (~ 0.2 - 2 keV) for absorption- and emission-line spectroscopy using large X-ray telescopes.</p> <p>These would provide the resolving power needed to address key science goals in the soft X-ray band, such as finding the remaining ~50% of baryonic matter in the universe, detailing matter and energy feedback from supermassive black holes, and characterizing stellar lifecycles from birth to death.</p>
Current State of the Art	<p>Proven technologies (grating spectrometers on Chandra and XMM-Newton) fall short in efficiency, collecting area, and resolving power, by factors of 5-10. High-efficiency and high-spectral-resolving-power gratings have been demonstrated that place > 40% of the incident light into the diffracted orders while also achieving spectral resolving powers > 2000 in the soft X-ray band. These demonstrations place new gratings technologies at TRL 3 - 4.</p>
Current TRL	3 – 4
Performance Goals and Objectives	<p>Large-format grating arrays that place > 25% of incident (0.2 - 2 keV) X-rays in the diffraction spectrum (<i>i.e.</i>, excluding 0th order), taking all losses into account.</p> <p>Dispersion must be large enough to allow $R > 3000$.</p> <p>Grating mounting materials and grating-array assembly and alignment schemes must be developed.</p>
Scientific, Engineering, and/or Programmatic Benefits	<p>Spectrometers achieving $R > 3000$ throughout the soft X-ray band are mission-enabling, as micro-calorimeters cannot achieve that. Priority science goals for soft X-ray spectroscopy are listed in the NWNH report.</p>
PCOS Applications and Potential Relevant Missions	<p>A spectrometer using gratings with this performance is envisioned for X-ray Surveyor, has been studied by NASA as a probe, has been proposed for an Explorer, and will be flown on the Off-plane Grating Rocket Experiment.</p>
Time to Anticipated Need	<p>Named missions: ATHENA</p> <p>Development needed for 2020 Decadal: Yes, ATHENA, XRS</p> <p>Other drivers: Applicability to X-Ray Surveyor and Explorer opportunities.</p>

Table 3-1. Technology Gaps Evaluated by TMB in 2015 (continued)

Name of Technology	Affordable, lightweight, high-resolution X-ray optics
Description	<p>Future X-ray observatories need X-ray mirrors qualitatively and quantitatively better than any currently in operation. Improvements are needed in one or more of the following:</p> <ol style="list-style-type: none"> 1. Angular resolution. 2. Photon collecting area per unit mass. 3. Cost per unit photon-collecting area. <p>Proposed technology improvement methods may include: piezo, magnetic smart material (MSM) shaping with magnetic field; ion implantation, zero-stress Si, over-coating, coating the substrate back with a localized and controlled “stressy” material.</p>
Current State of the Art	<p>State-of-the-art lightweight X-ray optics is represented by GSFC-developed slumped glass optics, currently at TRL 5 for 10-arcsec mirror assemblies.</p> <p>Chandra optics:</p> <ul style="list-style-type: none"> • Angular resolution < 0.5 arcsec; • Effective area 400 cm² at 5 keV; and • Mirror mass 951 kg.
Current TRL	<p>3 to 5 depending on resolution</p>
Performance Goals and Objectives	<ul style="list-style-type: none"> • Effective area: up to 3 m² for X-ray Surveyor; up to 0.5 m² for several Explorers; • Angular resolution 0.5 arcsec for X-ray Surveyor; 5-10 arcsec for Explorers; • Photon-collecting area per unit mass up to two orders of magnitude greater than that of Chandra; and • Cost per photon-collecting area 50 times lower than Chandra.
Scientific, Engineering, and/or Programmatic Benefits	<p>This type of X-ray optics will enable study of the early universe to complement JWST, maintain US leadership in lightweight X-ray optics for space, and facilitate future missions and minimize their schedule and costs.</p>
PCOS Applications and Potential Relevant Missions	<p>Enabling technology for X-ray Surveyor. Possible US contribution to ESA’s ATHENA mission. Also enabling for several Explorer missions.</p>
Time to Anticipated Need	<p>Named missions: ATHENA (2020s)</p> <p>Development needed for 2020 Decadal: Yes, ATHENA, XRS</p> <p>Other drivers: Applicability to the X-Ray Surveyor and Explorer opportunities.</p>

Table 3-1. Technology Gaps Evaluated by TMB in 2015 (continued)

Name of Technology	Low-stress or stress-free coating for X-ray optics
Description	All X-ray optics need reflecting-surface coating with a heavy metal, such as iridium, platinum, or gold. Such a coating layer usually has strong residual stress from the deposition process. This residual stress will deform a mirror substrate, particularly a segmented thin substrate, and degrade its angular resolution dramatically. This is an especially serious issue for multilayer coatings required for hard X-ray ($E > 10$ keV) applications, as they can be very thick and their stress can be extremely high.
Current State of the Art	For soft-X-ray mirror coating, the residual stress can be minimized by thinning the surface coating, but it could slightly lower X-ray reflectivity. However, there is no real solution to this issue at this point for multilayer coating. The (multilayer) NuSTAR mirror suffers from stress and ends up with a 58 arcsec resolution, while the substrate was about 20 arcsec. Stress-free coating is crucial for future high resolution soft/hard-X-ray mirrors.
Current TRL	
Performance Goals and Objectives	To be able to coat a thick enough layer or a multilayer on a segmented thin mirror substrate, with substrate thickness of 0.2-0.4 mm, minimal distortion.
Scientific, Engineering, and/or Programmatic Benefits	Would enable some implementations of lightweight, high-resolution, affordable X-ray optics; and dramatically improve the angular resolution of large-area, hard X-ray optics.
PCOS Applications and Potential Relevant Missions	All future X-ray missions utilizing segmented thin X-ray optics, especially in the hard X-ray band, including Explorers, Probes, and missions of opportunity.
Time to Anticipated Need	Named missions: Development needed for 2020 Decadal: No Other drivers: Explorer, Probe, and MO opportunities.

Table 3-1. Technology Gaps Evaluated by TMB in 2015 (continued)

Name of Technology	Ultra-high-resolution focusing X-ray observatory telescope
Description	<p>Very high angular resolution in the X-ray band is needed to study the structure surrounding and jets emanating from SMBHs at the cores of galaxies. However, the Chandra X-ray observatory's 0.5-arcsec resolution is already near the best that can be expected from grazing-incidence reflection.</p> <p>Simulations suggest that above 4 keV, a transmitting diffractive-refractive pair in direct contact in which the focal length of the refractive component is minus twice that of the diffractive element can achieve milliarcsec resolution by nullifying chromatic aberration over a 15% bandwidth. However, a 1-m-diameter system would have a focal length of the order of 1000 km. Optics and detector would be aboard separate spacecraft that engage in "formation flying." Only one spacecraft can be in a true orbit; the other has to be powered by an engine to overcome the gravity gradient to maintain alignment and to reposition one spacecraft for target changes. The center of the detector spacecraft has to be < 10 cm from the optical axis or a designated position in a raster scan. The position of the optical axis has to be known to < 5 mm for milliarcsec resolution. Pointing direction of the optics and the distance between the two spacecraft are not critical.</p>
Current State of the Art	<p>This system requires new technology in two areas, X-ray optics and mission operations. Construction of the optics is not expected to be difficult, in fact, it should be much less demanding and much lower mass than a grazing-incidence optic. However, the very long focal length precludes laboratory tests of large-diameter optics. The principle but not the level of performance can be verified by testing miniature components at synchrotron radiation facilities with a very long vacuum pipe to accommodate the large distance between the optics and detector. Mission operations have to be studied analytically. No other high-energy mission or mission concept that this author knows of has had operational requirements comparable in difficulty to this, but there is no apparent reason why they cannot be satisfied.</p>
Current TRL	1
Performance Goals and Objectives	<p>The mission should be considered only after the development of a successor to Chandra ("X-ray Surveyor") has begun. It would begin with a study of formation flying of two spacecraft separated by 1000 km to determine the feasibility and costs of maintaining the position of the detector within 10 cm of the optical axis, or a designated point on the focal surface of a raster scan, with a positional uncertainty < 5 mm for a period of several years, during which time there will be target changes. Propulsion, most likely by ion engines, is needed for both maintaining pointing and changing targets. The quantity of propellant that can be accommodated determines the lifetime of the mission. The presence of either two optics or detector spacecraft will result in more efficient utilization of propellant. One spacecraft navigates to the next target position while the other is observing.</p>
Scientific, Engineering, and/or Programmatic Benefits	<p>This X-ray telescope system offers in theory three orders of magnitude higher angular resolution than any current or future grazing-incidence X-ray telescope and any single lens-telescope in any wavelength band. The formation-flying capability that would be developed for this mission is applicable to an even more ambitious project, X-ray interferometry with multiple lenses. Development of formation-flying capability between two or more spacecraft should be useful in other space projects.</p>
PCOS Applications and Potential Relevant Missions	<p>A very-high-angular resolution X-ray telescope would be enabled by the development of technology for long distance formation flying between two spacecraft with 5 cm pointing accuracy of the detector with respect to the optical axis or another direction of a raster scan, and changing targets. The principal objectives are observing the structure of the environment surrounding super massive black holes and the small clumps of material in their jets. The same would apply to the nebula surrounding neutron stars and the jets emanating from them.</p>
Time to Anticipated Need	<p>Named missions:</p> <p>Development needed for 2020 Decadal: No</p> <p>Other drivers: Applicability would be a decade after the next high angular resolution telescope, <i>i.e.</i> the "X-ray Surveyor" has operated for several years and has revealed specific targets that require higher-angular-resolution observations to probe more deeply.</p>

Table 3-1. Technology Gaps Evaluated by TMB in 2015 (continued)

Name of Technology	Very-wide-field focusing instrument for time-domain X-ray astronomy
Description	<p>The instrument is a soft-X-ray (0.5 to 15 keV) counterpart of Swift's hard X-ray (15-150 keV) BAT. It will operate in a much richer band of time-domain X-ray astronomy and detect a larger number of, and more distant, GRBs as well as have continuous coverage over several ster of diverse time-variable X-ray phenomena on all time scales $>10^{-3}$ sec. It will be orders of magnitude more sensitive than RXTE ASM and MAXI, neither, of which had continuous coverage of any region. The instrument would resolve and image all sources within its large field of view by focusing with ~ 100 cm² of effective area. The technology needed is a large-area lobster-eye focusing telescope, either a hybrid consisting of a 1-D focusing lobster-eye telescope integrated with a coded mask or a 2-D lobster-eye telescope. Neither of the two has been constructed on a sufficiently large scale. A Swift BAT-like 2-D coded mask would be much less effective in the 0.5 to 15 keV band. In addition to developing the very-wide-field focusing-optics technology, there is a corresponding need to develop an efficiently packed large-area cylindrical or spherical array of CCDs each with a 300-micron depletion depth. The total physical area of the CCD array is of the order of a square meter.</p>
Current State of the Art	<p>Small (~ 10 cm) 1-D and 2-D focusing lobster-eye telescopes made of an array of double-sided, metal-coated flat-glass reflectors have been constructed and tested. Also, small 2-D lobster-eye telescopes have been made from slumped-channel-plate glass. The problem of arraying telescope modules to form a very-large-area, large-field-of-view, mechanically and thermally rugged array has not been addressed. It seems straightforward, but mating a focusing 1-D lobster-eye telescope with a cylindrical coded mask has not been tested in the laboratory. Small 2-D slumped channel plate lobster-eye telescopes have been aboard the Mercury orbiter. We believe that the hybrid, which has larger effective area and bandwidth, will ultimately prove to be more effective as a telescope for time-domain X-ray astronomy. MIDEX-size versions of both types of telescope require a large array of CCD detectors that are efficiently packed. While a large-area array of optical CCDs has been developed for Kepler and PAN-STARRS, the few-ster field of view of these X-ray telescopes requires a much larger number of CCDs that are arrayed efficiently and have much larger depletion depth than the Chandra and XMM-Newton devices.</p>
Current TRL	2?
Performance Goals and Objectives	<p>The goal is to construct and X-ray-test a modular hybrid (or 2-D telescope) with a ~ 75 cm focal length. The hybrid (which this author believes will prove ultimately to be superior) consists of focusing double-sided 240-micron-thick flat-glass reflectors coated with 300 Å Pt plus a 100 Å C overcoat.</p> <p>The test-article telescope should have a field of view of at least 15 degrees (20 cm) along the azimuth and 70 degrees (1 m) in the polar direction. A cylindrical 2-D coded mask will be constructed and placed over the entrance aperture. The advocates of the slumped-channel-plate 2-D telescope would have a parallel development program.</p> <p>Either system will be tested in a quasi-parallel X-ray beam at MSFC or GSFC to measure its efficiency and ability to determine the 2-D direction of the beam with respect to various orientations of the telescope. We would also design a 1-cm or 2-cm CCD chip that can be produced in quantity and abutted as closely as possible on three sides. However, the X-ray telescope tests could be performed with only a few existing CCD chips. The test articles would be subjected to mechanical and thermal stress tests to verify their stability.</p>
Scientific, Engineering, and/or Programmatic Benefits	<p>The scientific benefit is a comprehensive study of time-domain X-ray astronomy over a large range of time scales. Only the shortest time scales, which require a very-large-area, narrow-field-of-view detector, are inaccessible.</p> <p>The high sensitivity for detecting gamma-ray bursts (the burst and X-ray afterglow phases blend seamlessly) should lead to the detection of the most distant galaxies in the universe.</p> <p>The instrument would be compatible with a Probe-class mission of size and cost similar to that of a MIDEX mission.</p>

PCOS Applications and Potential Relevant Missions	<p>This instrument is compatible with a dedicated Probe-class mission, similar in cost and complexity to Swift and possibly like Swift containing secondary instruments.</p> <p>Time-domain astronomy is much richer in the 0.5-to-15 keV band than it is in Swift's 15-to-150 keV band. More transients, bursts, and changes in state will be detected in the lower energy band. With larger gamma-ray burst sensitivity, their host galaxies will be found at greater distance, including perhaps the youngest galaxies in the universe.</p> <p>Focusing with either type of lobster-eye optics will resolve essentially all sources. Changes in intensity will be detected in multiple sources and their positions reported more rapidly to observers in other wavelength bands.</p> <p>Because several ster of sky are always in the field of view with activity in multiple sources, data would be open to all observers.</p>
Time to Anticipated Need	<p>Named missions:</p> <p>Development needed for 2020 Decadal</p> <p>Other drivers: Because there are no apparent unsolvable problems, a soft-X-ray time-domain astronomy mission could occur in this decade.</p>

Table 3-1. Technology Gaps Evaluated by TMB in 2015 (continued)

Name of Technology	Advanced millimeter-wave focal plane arrays for CMB polarimetry
<p>Description</p>	<p>The Inflation Probe requires arrays of detectors with background-limited sensitivity, dual-polarization detection capability, and control of systematic errors at multiple frequencies between ~30 and ~300 GHz for foreground removal.</p> <p>Architectures must be scalable to large arrays for the requisite sensitivity. Simultaneous multiband operation and high multiplexing factors may represent desirable design qualities. Detector systems must be compatible with the space environment. This includes low dielectric exposure to low-energy electrons and robust performance in the presence of cosmic rays</p> <p>Continued deployment in ground-based and balloon-borne platforms will benefit development efforts.</p>
<p>Current State of the Art</p>	<p>A great deal of progress has been made with a variety of approaches, including antenna-coupling into transmission-line micro-machined structures, waveguide probes, and absorber-coupled filled arrays.</p> <p>Transition-edge sensors are currently the leading candidate technology for the detecting element in these integrated sensors. Arrays of several thousand detectors are operating in ground-based CMB polarization experiments. Balloon experiments will operate detectors in the environment closest to space.</p>
<p>Current TRL</p>	<p>4</p>
<p>Performance Goals and Objectives</p>	<p>The detectors must demonstrate high efficiency over a wide spectral range (~30 to 300 GHz), scale to a focal plane architecture appropriate for space, and provide appropriate magnetic shielding, cosmic-ray immunity, and excellent noise stability. Process uniformity and high detector efficiency and yield are also important.</p>
<p>Scientific, Engineering, and/or Programmatic Benefits</p>	<p>Measurement of CMB polarization to search for evidence of, and characterize, inflation is a top NASA priority.</p> <p>Such detectors are a key enabling technology. A space-borne measurement can probe for a polarization pattern imprinted by a background of gravitational waves generated at the time of inflation in the early universe.</p> <p>Polarization measurements on finer angular scales probe large-scale structure sensitive to neutrino mass and dark energy.</p>
<p>PCOS Applications and Potential Relevant Missions</p>	<p>These are needed for measuring CMB polarization to search for and characterize the faint, polarized signature of inflation.</p> <p>The targeted mission is Inflation Probe as recommended in the NWNH report. Other possibilities include Explorer and international CMB polarization and absolute spectrum experiments.</p> <p>Development also has technological overlaps with superconducting far-IR and X-ray detectors.</p>
<p>Time to Anticipated Need</p>	<p>Named missions: Inflation Probe (2020s)</p> <p>Development needed for 2020 Decadal: Yes, IP</p> <p>Other drivers: Inflation Probe technology development is a NWNH priority that will be revisited by the mid-decadal review. International and Explorer implementations of the Inflation Probe will be proposed in the 2015-17 timeframe.</p>

Table 3-1. Technology Gaps Evaluated by TMB in 2015 (continued)

Name of Technology	Millimeter-wave optical elements
Description	<p>High-throughput telescope and optical elements with controlled polarization properties are required for the Inflation Probe. These require development of mm-wave filters and coatings.</p> <p>Measurement of CMB polarization on large scales may require rapid polarization modulation to separate sky-signal polarized intensity from instrumental effects. Employing modulators large enough to span the telescope primary aperture is an advantage in that sky polarization can be modulated before the signal is contaminated by the instrument.</p>
Current State of the Art	<p>Single-layer anti-reflection coatings in widespread use in various dielectrics.</p> <p>Several experiments in the field are currently using rapidly spinning half-wave plates as the primary means of modulating the signal and separating it from longer time variations.</p> <p>More experiments are coming online using both half-wave plates and variable-delay polarization modulators that endeavor to measure larger areas of the sky.</p>
Current TRL	2 – 5
Performance Goals and Objectives	<p>Develop robust multi-layer coatings for broadband applications. Develop thermal filtering technologies suitable for large focal plane arrays operating at sub-Kelvin temperatures.</p> <p>Develop space-compatible modulators, including work on frequency-selective surfaces and mechanisms compatible with the space radiation environment. Minimizing dielectric cross-section to low-energy electrons is a priority.</p> <p>Develop and compare strategies for instrument architectures with and without rapid modulators.</p>
Scientific, Engineering, and/or Programmatic Benefits	<p>Broadband optics can reduce the necessary focal-plane mass and volume for CMB polarization measurements. This may open options for compact optical systems appropriate for lower-cost Explorer opportunities; an international mission concept using broadband refracting optics is in the planning stages. Modulators are potentially a key enabling technology.</p>
PCOS Applications and Potential Relevant Missions	<p>Inflation Probe, Explorer, and international experiments to study CMB polarization and absolute spectrum.</p>
Time to Anticipated Need	<p>Named missions: Inflation Probe (2020s)</p> <p>Development needed for 2020 Decadal: Yes, IP</p> <p>Other drivers: Inflation Probe technology development is a NWNH priority that will be revisited by the mid-decadal review. International and Explorer implementations of the Inflation Probe will be proposed in the 2015 – 17 timeframe.</p>

Table 3-1. Technology Gaps Evaluated by TMB in 2015 (continued)

Name of Technology	High-power, narrow-line-width laser sources
Description	Gravitational-wave missions need lasers that are either intrinsically stable or can be stabilized using external signals. The laser fields also have to be modulated with different signals to exchange clock-noise information, ranging tones, and potentially data.
Current State of the Art	<p>The laser system is usually envisioned as a master laser power amplifier system although commercial (not space-qualified) single-stage laser systems with 2W output power exist that can be controlled to meet power and frequency noise requirements but lack capability to sufficiently modulate the laser field. The master laser could be the European LISA pathfinder laser (TRL 6) with an additional amplifier stage. The European TESAT company is expected to reach TRL 5 in 2015 for the entire laser system.</p> <p>US: A 2W laser amplifier was constructed by LGS, tested at GSFC, and is at TRL 4. The US version of the master laser is an ECL, prototyped at TRL 3. The full laser system in the US is at TRL 3.</p>
Current TRL	3
Performance Goals and Objectives	<p>The goal is to assemble and test a full space-qualified laser system meeting all requirements listed below. This includes laser power, frequency noise, intensity noise, and a possibility to modulate the laser with GHz sidebands, PRN codes, and maintain phase fidelity throughout the laser system.</p> <p>The key performance parameters are:</p> <ul style="list-style-type: none"> • Laser power > 1W; • Frequency noise: $\sim 100\text{Hz}/\sqrt{\text{Hz}}$; • Relative intensity noise: <ul style="list-style-type: none"> - $10^{-4}/\sqrt{\text{Hz}}$ in LISA band, - $10^{-8}/\sqrt{\text{Hz}}$ above ~ 2 MHz; • Phase fidelity of GHz phase modulation $< 6 \times 10^{-4}/\sqrt{\text{Hz}}$ in LISA band; and • Lifetime: > 3 years hot; 5 years with 3 yrs in cold redundancy. <p>All parameters measured at output of single-mode polarization-maintaining fiber.</p>
Scientific, Engineering, and/or Programmatic Benefits	<p>The laser is a potential US contribution to an ESA-led L3 mission addressing the “Gravitational Universe” science theme. It is also required for a potential future US-led laser-interferometric gravitational-wave mission. Laser technology is in general a critical technology for a vast range of future applications.</p> <p>All formation-flying plans in the 30-year Astrophysics Roadmap require laser systems that meet at least some of these requirements. Having a space-qualified commercial-off-the-shelf (COTS) laser system meeting the GW mission requirements should be a general goal of NASA.</p>
PCOS Applications and Potential Relevant Missions	<p>Space-based laser interferometric gravitational-wave detectors such as LISA or SGO-Mid or the European eLISA concept.</p> <p>Space-based geodesy missions, such as GRACE II, require low-power versions of these types of lasers.</p> <p>Future missions: Interferometry was named as one of the crosscutting, game-changing technologies in the Astrophysics Roadmap, and ultra-stable lasers are essential for this.</p>
Time to Anticipated Need	<p>Named missions: L3 (2030s)</p> <p>Development needed for 2020 Decadal: Yes, L3</p> <p>Other drivers: ESA schedule sets TRL 5 at 2020. The laser is a likely candidate for a NASA contribution to L3.</p>

Table 3-1. Technology Gaps Evaluated by TMB in 2015 (continued)

Name of Technology	Highly stable low-stray-light telescope
Description	<p>LISA-like missions need optical telescopes to expand and compress laser beams. The key performance parameters are: pm/√Hz stability at $f > 1 \text{ mHz} \sqrt{[1 + (3 \text{ mHz}/f)^4]}$; < 100 pW of stray light from the telescope back into the fundamental spatial mode on the optical bench (for up to 2 W input power); long-term imaging stability (set-and-forget focus adjustment or passive absolute stability) to generate 5-mm collimated beam on optical bench; aperture stop for transmitted beam. Phase-front quality: $\lambda/30$. Field of view (FOV): $\pm 200 \text{ mrad}$, diameter: 20-40 cm.</p> <p>The need for in-field guiding will depend on the orbits and progress in other areas, such as designs that allow correlating the two local lasers at the pm/√Hz level (back-link fiber or free-space link).</p>
Current State of the Art	<p>The most unusual performance parameters are the pm/√Hz stability and the stray-light requirements. Telescopes that meet the phase-front quality, FOV, and diameter requirements are fairly standard.</p> <p>The long-term imaging requirement with a set-and-forget focus adjustment is probably also standard. However, this adjustment mechanism might introduce unacceptable dimensional noise beyond the pm/√Hz level and some realizations have shown increased scattered-light levels. Relying on the passive absolute stability of the secondary/primary distance ($\sim \mu\text{m}$) would eliminate the need for a focus adjustment.</p> <p>The pm/√Hz stability has been tested for several spacer materials but never for a realistic telescope. The backscatter has been studied in small tabletop experiments for the secondary mirror for on-axis telescopes but not for a full telescope. On- and off-axis telescopes have been studied with ray-tracing programs, which are not ideal for laser interferometric applications. In-field guiding has not been integrated into any telescope test, and would require development of a mechanism.</p> <p>These tests and simulations put the telescope at TRL 4 without in-field guiding and below TRL 4 with it.</p>
Current TRL	4
Performance Goals and Objectives	<p>The goal is to build a prototype telescope (ideally two: one on-axis, one off-axis) and test for pm/√Hz stability and minimal backscatter while also evaluating the received and transmitted laser fields.</p> <p>Tests with a full telescope would increase this to TRL 5 and allow a decision between a simple on-axis design and a more complex off-axis design.</p> <p>In-field guiding should be studied through design and simulation first, and the need should be evaluated against progress in other areas including mission design (orbits, lifetime). In-field guiding would require development of a mechanism that could change the direction of propagation of a beam without inducing any change in the optical path length.</p>
Scientific, Engineering, and/or Programmatic Benefits	<p>The telescope is one of the potential US contributions to an ESA-led L3 mission that addresses the “Gravitational Universe” science theme. It is also required for a potential future US-led laser-interferometric gravitational-wave mission.</p>
PCOS Applications and Potential Relevant Missions	<p>Space-based laser-interferometric gravitational-wave detectors such as LISA, SGO-Mid, or the European eLISA concept.</p> <p>Potentially other precision interferometric measurement applications.</p>
Time to Anticipated Need	<p>Named missions: L3 (2030s)</p> <p>Development needed for 2020 Decadal: Yes, L3</p> <p>Other drivers: ESA schedule sets TRL 5 at 2020. The telescope is a likely candidate for a NASA contribution to L3.</p>

Table 3-1. Technology Gaps Evaluated by TMB in 2015 (continued)

Name of Technology	Low-mass, long-term-stability optical bench
Description	<p>Space-based laser-interferometric gravitational-wave missions need optical benches to prepare, split, direct, and combine the different laser fields to form all required beat signals.</p> <p>Key performance parameters are: $\sqrt{[1 + (1\text{mHz/f})^4]}$ pm/$\sqrt{\text{Hz}}$; long-term alignment stability; low mass; simple assembly procedures (a LISA-like mission requires six flight units).</p>
Current State of the Art	<p>Europe developed the optical bench for LISA Pathfinder using an all Zerodur, hydroxide bonded bench (TRL 6 now). It meets the stability requirement. However, the assembly of the bench took already very long and was always on or near the critical path. This technology does not scale well for the 4x larger LISA bench, which also carries 4x more components, and LISA requires six flight units instead of one.</p> <p>A different manufacturing technology, based on more classical mechanical mounts, has to be developed and tested to reduce this major programmatic risk. This different technology is probably at TRL 2 in the US.</p>
Current TRL	2
Performance Goals and Objectives	<p>An optical bench with classical mechanical mirror mounts and metal benches saves mass and time compared to an all-Zerodur hydroxide-bonded bench. However, it still has to be shown that such a bench can meet the pm/$\sqrt{\text{Hz}}$ requirement with components that can stay aligned during launch, or be realigned after it.</p>
Scientific, Engineering, and/or Programmatic Benefits	<p>A lighter and easier-to-assemble optical bench would significantly reduce cost and programmatic risks, which are associated with any complex assembly process.</p> <p>In addition, the bench could be a deliverable for NASA, should the US join the ESA-led mission which addresses the Gravitational Universe science theme (L3).</p>
PCOS Applications and Potential Relevant Missions	<p>ESA's L3 mission which asks for a NASA contribution.</p>
Time to Anticipated Need	<p>Named missions: L3 (2030s)</p> <p>Development needed for 2020 Decadal: Yes, L3</p> <p>Other drivers: ESA schedule calls for Phase A work starting 2017, an EM that will start 2019-2020. Therefore, TRL 4 by 2018.</p> <p>This work addresses the design and manufacturability of the optical bench, but the optical bench itself is not likely a NASA contribution to L3.</p>

Table 3-1. Technology Gaps Evaluated by TMB in 2015 (continued)

Name of Technology	Phase measurement subsystem (PMS)
<p>Description</p>	<p>Space-based laser-interferometric gravitational-wave missions measure the phase evolution of laser beat signals to monitor the minute length changes caused by gravitational waves (~pm/√Hz level), extract the phase of the clock noise tones (~0.1 millicycle/√Hz), measure absolute spacecraft distances at the sub-meter level, and provide signals for phase-locking and arm-locking the lasers and for aligning the constellation.</p> <p>This PMS includes the analog front end, quadrant photo-receivers, anti-aliasing filters, and ADCs. An ultra-stable oscillator (USO) and a frequency distribution system that includes frequency multipliers are also considered part of the PMS.</p>
<p>Current State of the Art</p>	<p>The system consists of many subcomponents which are at different TRLs. The most critical parts are the analog front end of the measurement system, which is at TRL 4.</p> <p>Quadrant photo-receivers based on COTS detectors have been developed at ANU, and a custom-designed detector with much lower capacitance (and therefore lower noise) has been developed through the SBIR program. Both alternatives need further development or at least flight qualification.</p> <p>The frequency multipliers in the frequency distribution system are at TRL 5. The phasemeter core is at TRL 6, although general advances in digital signal processing should be used to simplify and advance the capabilities of the PMS over time.</p>
<p>Current TRL</p>	<p>4</p>
<p>Performance Goals and Objectives</p>	<p>Quadrant photo-receivers and ADCs should be developed to meet the original LISA requirements (which serve as benchmarks for all currently discussed mission designs) and reach TRL 5. These analog parts present the largest remaining risks for the PMS. Further development of the frequency multipliers requires a final mission design that includes a frequency distribution plan.</p>
<p>Scientific, Engineering, and/or Programmatic Benefits</p>	<p>The PMS, in the form discussed here, meeting the requirements presented here, is critical for all LISA-like missions. A working PMS with an adequate analog front end is also important for many tests for other subsystems in LISA-like missions such as the optical bench or the telescope.</p> <p>The PMS is a strategic technology with multiple uses in many areas; the initial phasemeter evolved out of the Blackjack receivers used in GPS. The analog front end would allow application to optical signals, which vastly improves the sensitivity compared to GPS.</p>
<p>PCOS Applications and Potential Relevant Missions</p>	<p>Space-based laser-interferometric gravitational-wave detectors such as LISA, SGO-Mid, or the European eLISA concept.</p> <p>GRACE follow-on missions.</p> <p>Other future interferometric missions; interferometry has been named as one of the crosscutting, game-changing technologies in the Astrophysics Roadmap.</p>
<p>Time to Anticipated Need</p>	<p>Named missions: L3 (2030s)</p> <p>Development needed for 2020 Decadal: Yes, L3</p> <p>Other drivers: ESA schedule sets TRL 5 at 2020.</p> <p>The photo-receivers and ADCs are a likely NASA contribution to L3.</p>

Table 3-1. Technology Gaps Evaluated by TMB in 2015 (continued)

Name of Technology	Gravitational Reference Sensor (GRS) technologies
<p>Description</p>	<p>Space-based gravitational-wave observatories like LISA use free-floating test masses protected from all disturbing forces so they travel in near-perfect geodesics only subject to the tidal forces caused by gravitational waves.</p> <p>Laser interferometry is used to measure the variations in light travel time between test masses, caused by gravitational waves. A single test mass, together with its protective housing and associated components, including the electrode housing, caging mechanisms, vacuum systems, and front-end electronics, is referred to as a GRS.</p> <p>The GRS envisioned for LISA-like missions is a 2 kg gold/platinum cube, surrounded by electrodes used to sense the position of the test mass with respect to the spacecraft, and apply forces to the test mass in all non-sensitive directions. The free-floating test mass can become electrically charged due to cosmic-ray impacts and during release from the test-mass caging system. A charge management system is needed to discharge the test mass with respect to its housing.</p>
<p>Current State of the Art</p>	<p>ESA will test a GRS and disturbance reduction system in the LISA Pathfinder mission.</p> <p>ESA's Hg-lamp based charge management system is high TRL, and will be demonstrated in space in the LISA Pathfinder in 2015-16.</p> <p>As NASA has nothing comparable, it is difficult to assign a reasonable TRL to US technology readiness.</p>
<p>Current TRL</p>	<p>6 (< 3 in US)</p>
<p>Performance Goals and Objectives</p>	<p>The long-term target is to develop competency in the US in GRS technology.</p> <p>The immediate goals are to:</p> <ul style="list-style-type: none"> • Design and fabricate a TRL-3 electrode housing; • Develop capacitive readout and electrostatic actuation electronics, as well as an interferometric readout for calibration and high resolution measurements; • Develop a 240-255 nm UV LED-based charge management system that can be seamlessly integrated into the LISA Pathfinder GRS; with order-of-magnitude lower volume, mass, and power; and • Construct a torsion pendulum test facility to evaluate the performance of the GRS housing.
<p>Scientific, Engineering, and/or Programmatic Benefits</p>	<p>GRS technology is absolutely critical for any gravitational-wave detector mission.</p> <p>Having near-zero competency in the US puts NASA in an impossible position for a NASA-led mission to address one of the leading science goals of the last two Decadal Surveys</p> <p>A UV LED or comparable charge control system would allow the GRS to be smaller, lower-mass, and lower-power, while improving performance.</p>
<p>PCOS Applications and Potential Relevant Missions</p>	<p>LISA-like space-based gravitational-wave missions and, with relaxed requirements, geodesy missions.</p>
<p>Time to Anticipated Need</p>	<p>Named missions: L3 (2030s)</p> <p>Development needed for 2020 Decadal: Yes, L3</p> <p>Other drivers: ESA schedule sets TRL 5 at 2020.</p> <p>An entire GRS is not a likely NASA contribution to L3, but NASA achieving TRL 3 by 2018 mitigates risk in case the single vendor in Italy is not able to deliver.</p> <p>UV LED-based charge control is a possible candidate for a NASA contribution to L3. Note, that ESA doesn't plan to start development of any GRS-related technology (like charge management) until after the conclusion of the LISA Pathfinder mission in mid-2016.</p>

Table 3-1. Technology Gaps Evaluated by TMB in 2015 (continued)

Name of Technology	High-performance gamma-ray telescope
Description	<p>Two technologies are needed to enable gaseous detectors, <i>e.g.</i>, Time Projection Chambers (TPC), with large volumes, 10s to 100s of m³, to be inflated on orbit:</p> <ol style="list-style-type: none"> 1. The inflatable pressure shell must contain the detector gas at pressures up to ~3 Atm, be capable of self-sealing against micro-meteors, and have a surface density of < 1 g/cm². The TPC field-shaping electrodes are mounted on the inner surface of the inflatable shell and deploy as the shell inflates to positions accurate to ~1 mm. 2. The TPC readout structure at the bottom of the TPC must unfold within the gas volume, be rigid, and have position accuracy of ~1 mm.
Current State of the Art	<p>Thin Red Line Aerospace developed and supplied 20 full-fidelity inflatable pressure shells of up to 320 m³ volume for Bigelow Aerospace inflatable habitat Genesis spacecraft flight hardware.</p> <p>Thin Red Line designed, engineered, and manufactured the pressure-restraining hulls of Genesis 1 and 2 (launched 7/2006 and 6/2007, respectively), the first spacecraft on orbit successfully incorporating large-volume, high-stress inflatable architecture. See http://www.thin-red-line.com/projects.html for other projects.</p> <p>Large deployable mirrors have been developed for JWST. This technology could be adapted for the deployable TPC readout.</p>
Current TRL	6
Performance Goals and Objectives	<p>The goal is to enable construction of a ~100 m³ gamma-ray pair telescope with arc-minute angular resolution and continuum sensitivity of better than 5×10^{-7} between ~100 MeV and ~10 GeV.</p> <p>The objectives can be met by demonstrating an inflatable TPC gas shell with volume ~10 m³ at ~1 Atm and deployable readout electrodes with area of ~2 m².</p>
Scientific, Engineering, and/or Programmatic Benefits	<p>Inflatable gaseous detectors would enable gamma-ray telescopes to achieve arcmin angular resolution. Deployable 2-D readout structures within a large gas volume would increase telescope sensitivity.</p>
PCOS Applications and Potential Relevant Missions	<p>Arcmin gamma-ray telescope.</p>
Time to Anticipated Need	<p>Named missions:</p> <p>Development needed for 2020 Decadal: No</p> <p>Other drivers: Applicability to Explorer opportunities.</p>

Table 3-1. Technology Gaps Evaluated by TMB in 2015 (continued)

Name of Technology	Fast, few-photon UV detectors
Description	Near-UV (300-400 nm), single-photon detectors for measurements from space of atmospheric fluorescence light produced by particle cascades induced by ultra-high-energy cosmic rays (UHECR).
Current State of the Art	<p>Current SOTA are multi-anode vacuum photomultipliers. These are high TRL (quoted TRL applies only to these devices) and high performance, but are relatively costly per channel, heavy, sensitive to over-exposure, and delicate.</p> <p>Silicon photomultipliers (SiPM, also called multi-pixel photon counters or MPPC), based on arrays of avalanche-diode micro-pixels operating in quenched Geiger mode, are promising but the current SOTA SiPM have unacceptable noise without cooling to < 20°C. In the large imaging arrays needed with $2 \times 10^5 - 1 \times 10^6$ pixels, uncooled noise produces high false detection rate and cooling consumes unacceptable power. Also, most SiPM are not optimized for near-UV detection (although thinned, back-side-illuminated SiPM are possible).</p>
Current TRL	8
Performance Goals and Objectives	<ul style="list-style-type: none"> • Active area 8 mm² to 300 mm²; • Active-area fraction > 85%; • Read out at > 10 MHz; • Suitable for use in ≥ 4 m² arrays with $\geq 2 \times 10^5$ detectors (pixels); • QE at 330 nm $\geq 30\%$ (goal 60%); • Gain $\geq 10^4$ to allow few-photon (single-photoelectron) detection; • Noise < 10⁶ counts/(mm² sec) at half of single-photoelectron signal; • Signal duration < 10 ns; • Recovery time from single-photoelectron pulse to 99.9% resolution of 10³ photon pulse < 10 ns; • Inactive area < 20% when in array (< 5% goal), and scalable detector (pixel) dimensions to match the imaging optics; • Minimum mass (goal < 2 g/cm²); • Individual pixel readout is required; and • Active lifetime ≥ 5 years (goal 10 years) with integrated background exposure $\geq 3 \times 10^{14}$ photons/mm².
Scientific, Engineering, and/or Programmatic Benefits	This technology would enable focal planes for UHECR (see below) instruments to be built at a small fraction of the cost, mass, and power that would be required for the current SOTA. In turn, this would vastly increase the probability that a useful space-based UHECR instrument could be built. Coupled with light-weight, low-cost optics, this could enable a pathfinder instrument to be built as a MIDEX (possibly as a class-D SMEX, although this is ambitious).
PCOS Applications and Potential Relevant Missions	<p>Focal planes for missions to measure UHECR by imaging, from low-Earth orbit, the giant particle showers caused by UHECR ($E \geq 10^{18}$ eV) interacting in the Earth's atmosphere. This requires determining the time and spatial development of the UV light emitted by air fluorescence after excitation of atmospheric constituents, primarily N₂, by the particle cascade.</p> <p>A possible pathfinder mission, JEM-EUSO (JEM Extreme Universe Space Observatory), is in the Astrophysics Roadmap but development would also be applicable to the more advanced OWL (Orbiting Wide-angle Light Collectors) mission or other formulations. Detectors would also be important for ground Cherenkov arrays such as CTA and would have a variety of other astrophysics, accelerator, and medical imaging applications.</p>
Time to Anticipated Need	<p>Named missions:</p> <p>Development needed for 2020 Decadal: No</p> <p>Other drivers: Flight mission estimated no earlier than 2022 for JEM-EUSO or an OWL Pathfinder. Full balloon flight prototype 2019.</p>

Table 3-1. Technology Gaps Evaluated by TMB in 2015 (continued)

Name of Technology	Lightweight, large-area reflective optics
Description	Lightweight, easily deployable mirror as the primary of a Schmidt telescope (or similar) for measurements from space of atmospheric fluorescence light in the near UV (~330 - 390 nm) produced by particle cascades induced by UHECRs.
Current State of the Art	<p>SOTA is the optical system developed in NASA studies for the Orbiting Wide-angle Light Collectors (OWL) mission concept, based on smaller mirrors that have flown. This was an f/1 Schmidt with 45° full FOV. The deployable primary mirror diameter was 7.1 m (Schmidt corrector diameter was 3.0 m, and focal plane was 2.3 m). This had 8 petals and launched with the petals folded upward with four inner and four outer petals interleaved. After deployment, the outer ring of four petals unfolded and the inner ring unfolded and moved outward to form a uniform surface. The mass of the mirror and mechanisms was 581 kg.</p> <p>Publically accessible SOTA in inflatable mirror technology is a 7-m diameter microwave antenna in a convex-convex configuration with the reflective material on the inner surface of one of the sides. This requires highly UV-transparent material for the entrance surface.</p>
Current TRL	5
Performance Goals and Objectives	<p>Spherical or piecewise-spherical surface when deployed with $\geq 50\%$ (goal $\geq 90\%$) reflective area when compared to a complete spherical segment with the same solid angle.</p> <p>Reflector area $\geq 38 \text{ m}^2$ and full FOV $\geq 45^\circ$. Needed resolution is ~ 1 milliradian, $\geq 10^4$ larger than the diffraction limit, so inflatable optics are one possible solution.</p> <p>Goal is for a ~ 7-m diameter reflector to be compact enough when stowed for launch and light enough to facilitate a mission on a standard MIDEX-class launch vehicle or a vehicle similar to the SpaceX Falcon 9 using a ≤ 4.6-m-diameter fairing.</p> <p>Goal for mass of solid 7-m mirror and mechanism (if any) is < 300 kg. Goal for mass of inflatable 7-m mirror is ≤ 5 kg. Long-term goal is $1,400 \text{ m}^2$ reflector area with mass ≤ 100 kg.</p>
Scientific, Engineering, and/or Programmatic Benefits	<p>This technology would enable reflective optics for a UHECR (see below) mission to be built at a small fraction of the cost and mass of the OWL optics that represent the current SOTA. In turn, this would vastly increase the probability that a useful space-based UHECR instrument could be built.</p> <p>Coupled with a light-weight, low-cost, high-performance focal plane and electronics, this could enable a pathfinder instrument to be built as a MIDEX (possibly as a class-D SMEX, although this is ambitious).</p>
PCOS Applications and Potential Relevant Missions	<p>Optics for missions to measure UHECR by imaging, from low-Earth orbit, the giant particle showers caused by UHECR ($E > 10^{18}$ eV) interacting in the Earth's atmosphere. This requires determining the time and spatial development of the UV light emitted by air fluorescence after excitation of atmospheric constituents, primarily N_2, by the particle cascade. A possible pathfinder mission, JEM-EUSO, using refractive (Fresnel) optics is in the Astrophysics Roadmap. However, this has not been selected for flight by any space agency.</p> <p>It is generally agreed that a full UHECR mission would use reflective optics similar to the Schmidt telescope designed for the NASA OWL mission. It is possible that an OWL-like pathfinder could fly in the same timeframe as JEM-EUSO.</p> <p>To extend the full measurement aperture down to 10^{18} eV to enable measurements of neutrinos from UHECR interactions with the CMB would require a 42-m-diameter reflector. This could only be achieved using a very light mirror such as an inflatable. If the lightweight technology could be applied to mirrors with better resolution, then a wide variety of missions would be enabled.</p>
Time to Anticipated Need	<p>Named missions:</p> <p>Development needed for 2020 Decadal: No</p> <p>Other drivers: Flight mission estimated no earlier than 2022 for JEM-EUSO or an OWL Pathfinder. Full balloon flight prototype 2019.</p>

Table 3-1. Technology Gaps Evaluated by TMB in 2015 (continued)

Name of Technology	Low-power time-sampling readout
Description	Time-sampling low-power readout electronics to measure pulse amplitude and photon-arrival time for detection from space of atmospheric fluorescence light in the near UV (~330 - 390 nm) produced by particle cascades induced by UHECRs using fast photodetectors (<i>e.g.</i> , multi-anode vacuum photomultiplier or silicon photomultiplier).
Current State of the Art	<p>SOTA are switched capacitor arrays with ~1024 sampling cells per channel and switching using a “domino” strobe that causes the input to be sampled continuously until stopped by an external signal. Some devices include onboard digitizer and others clock out charge to an external digitizer. Channels can be cascaded to increase depth.</p> <p>Effective resolution 9 to 11.5 bits. Reported power consumption at 200 MS/s (mega-samples per second) sampling (10× faster than needed) ~4 mW/channel.</p> <p>Development push is toward faster sampling rather than lower power consumption. Sample-to-sample timing is not constant, but can be calibrated.</p> <p>Most implementations require an external amplifier. A competing technology uses a series of delay lines acting as a circular analog memory. Sampling depth depends on the total delay that can be achieved. Depth of 1024 samples has been reported at 500 MS/s but same delay would have a depth of only 40 samples at 20 MS/s.</p>
Current TRL	6
Performance Goals and Objectives	<ul style="list-style-type: none"> • Sampling rate ≥ 20 MS/s for ~100 ns photon-arrival-time resolution (allowing photodetector pulse to overlap two samples); • Full time sampled 3×10^{-4} s so depth 6000 samples at 20 MS/s; • Usable dynamic range ≥ 11 bits per sample; • Charge resolution ~0.25 pC; • Readout clock speed ~10 MHz – 33MHz; • Operating power at 20 MS/s ≤ 0.5 mW/channel (goal 0.25 mW/channel) including any required amplification; • Area required including ancillary components ≤ 8 mm²/channel; and • Channels/ASIC ≥ 9.
Scientific, Engineering, and/or Programmatic Benefits	<p>This technology would enable readout electronics for UHECR (see below) instrument focal planes to be built with a small fraction of the cost and power that would be required for the current SOTA. In turn, this would vastly increase the probability that a useful space-based UHECR instrument could be built.</p> <p>Coupled with light-weight, low-cost optics and high-performance photodetectors, this could enable a pathfinder instrument to be built as a MDEX (possibly as a class-D SMEX, although this is ambitious).</p>
PCOS Applications and Potential Relevant Missions	<p>Readout electronics for the focal planes of missions to measure UHECR by imaging, from low Earth orbit, the giant particle showers caused by UHECR ($E \geq 10^{18}$ eV) interacting in the Earth’s atmosphere. This requires determining the time and spatial development of the UV light emitted by air fluorescence after excitation of atmospheric constituents, primarily N₂, by the particle cascade.</p> <p>A possible pathfinder mission, JEM-EUSO, is in the Astrophysics Roadmap but development would also be applicable to the more advanced OWL mission or other formulations.</p>
Time to Anticipated Need	<p>Named missions:</p> <p>Development needed for 2020 Decadal: No</p> <p>Other drivers: Flight mission estimated no earlier than 2022 for JEM-EUSO or an OWL Pathfinder. Full balloon flight prototype 2019.</p>

Table 3-1. Technology Gaps Evaluated by TMB in 2015 (continued)

Name of Technology	Low-power comparators and logic arrays
Description	Low-power space-qualified pulse comparators and logic arrays to implement the event trigger logic for detection from space of atmospheric fluorescence light in the near UV (~330 - 390 nm) produced by particle cascades induced by UHECRs using fast photodetectors (<i>e.g.</i> , multi-anode vacuum photomultiplier or silicon photomultiplier).
Current State of the Art	<p>Comparators: SOTA for low-power space-qualified comparators are CMOS devices with 1.2 V output voltage. There are many devices available, but lowest power consumption is ~10 mW/channel. No development of low-voltage output (0.5 V) comparators for mobile devices seems to be underway.</p> <p>Logic: General SOTA for low-power, space-qualified logic implementations are flash-based FPGAs using 1.2 V logic. It is difficult to define a specific SOTA because of the wide variation in numbers of logic cells and I/O lines. However, devices with 6×10^5 logic cells suitable for UHECR applications, and ≥ 100 MHz maximum clock speed (2.5\times faster than needed), are available with power consumptions ≤ 100 mW. There is tremendous effort toward low-voltage (0.5 V) logic for mobile device applications, but to date this has not been fully realized in space-qualified versions.</p>
Current TRL	9
Performance Goals and Objectives	<p>Comparator:</p> <ul style="list-style-type: none"> • Voltage threshold range 2 mV to 0.5 V; • Nominal input voltage to 1 V, but overdrive tolerant to 5 V; • Response time ≤ 50 ns; • Output pulse 0.5 V; • Drive capability ≤ 600 Ohms; • Supply voltage $\leq \pm 5V$; and • Quiescent power consumption ≤ 0.7 mW/channel (goal 0.2 mW/channel). <p>Logic:</p> <ul style="list-style-type: none"> • FPGA or similar programmable logic with $\geq 6 \times 10^5$ cells per device; • Clock speed 40 MHz; • I/O lines ≥ 210; • Internal logic and I/O logic 0.5 V; and • Power consumption ≤ 25 mW per unit at 40 MHz (goal 10 mW per unit).
Scientific, Engineering, and/or Programmatic Benefits	<p>This technology would enable trigger electronics for UHECR (see below) instrument focal planes to be built with a small fraction of the power that would be required for the current SOTA. In turn, this would vastly increase the probability that a useful space-based UHECR instrument could be built.</p> <p>Coupled with light-weight, low-cost optics and high-performance photodetectors and readout electronics, this could enable a pathfinder instrument to be built as a MIDEX (possibly as a class-D SMEX, although this is ambitious).</p>
PCOS Applications and Potential Relevant Missions	<p>Event trigger components for missions to measure UHECR by imaging, from low-Earth orbit, the giant particle showers caused by UHECR ($E \geq 10^{18}$ eV) interacting in the Earth's atmosphere. This requires determining the time and spatial development of the UV light emitted by air fluorescence after excitation of atmospheric constituents, primarily N_2, by the particle cascade.</p> <p>A possible pathfinder mission, JEM-EUSO, is in the Astrophysics Roadmap but development would also be applicable to the more advanced OWL mission or other formulations. The proposed technology developments would enable a wide variety of other missions from flagships down to the nano-sat class.</p>
Time to Anticipated Need	<p>Named missions:</p> <p>Development needed for 2020 Decadal: No</p> <p>Other drivers: Flight mission estimated no earlier than 2022 for JEM-EUSO or an OWL Pathfinder. Ground tests (in conjunction with Telescope Array) or limited balloon flight tests ~2017. Full balloon flight prototype 2019.</p>

Table 3-1. Technology Gaps Evaluated by TMB in 2015 (continued)

Name of Technology	Lattice optical clock for Solar Time Delay mission and other applications
<p>Description</p>	<p>There are a number of probable applications of optical clocks in future PCOS missions. However, one particularly attractive one is looking for a suspected breakdown in General Relativity [see <i>e.g.</i>: T. Damour and G. Esposito-Farese, Phys. Rev. D 53, 5541-5578 (1996)].</p> <p>Probably the most promising place to look for such a breakdown is in the possible small deviation of the space-curvature parameter γ from unity suggested by string theory or theories with additional dimensions.</p> <p>The present accuracy for γ as determined by Doppler measurements of the solar time delay during the Cassini mission is 2.3×10^{-5}. A new determination with 3×10^{-8} or better accuracy could be made with a high-performance optical clock on a spacecraft near the L-1 point of the Earth-Sun system.</p>
<p>Current State of the Art</p>	<p>Both Sr-87 and Yb-131 optical clocks have reached accuracies in the laboratory of better than 5×10^{-18} over periods of 10^4 s. This is better than precision of $1 \times 10^{-14}/(\sqrt{\text{Hz}})$ down to 1×10^{-6} Hz needed for a high-accuracy Solar Time Delay mission, but has not yet been demonstrated at frequencies below 1×10^{-4} Hz.</p> <p>Also, the PTB in Germany and the INFN in Italy have jointly developed a transportable Sr-88 optical clock with a short term noise level of 4×10^{-15} at 1 second that is nearly ready for field use.</p> <p>Other groups in Europe are investigating other types of transportable optical clocks. Some of the components for cold-atom systems are being tested at a drop tower in Bremen, Germany, for future use in space.</p>
<p>Current TRL</p>	
<p>Performance Goals and Objectives</p>	<p>A proposed Solar Time Delay mission was described by N. Ashby, P.L. Bender, J.L. Hall, <i>et al.</i> in "Measurement of gravitational time delay using drag-free spacecraft and an optical clock" [Relativity in Fundamental Astronomy, Proc. IAU Symp. No. 261, 2009, P.K. Seidelman, S. Klioner, and M. Soffel, Eds., Int. Astron. Union].</p> <p>Optical time delay measurements would be made from a drag-free spacecraft near the L-1 point to a small transponder satellite during a period of about 20 days when the optical path between the satellites passed by the Sun. The transponder satellite would be in a 2-year period orbit with an eccentricity of 0.37. The clock performance required is a precision of $1 \times 10^{-14}/(\sqrt{\text{Hz}})$ down to 1×10^{-6} Hz and an accuracy of 1×10^{-17}.</p> <p>Other versions of Solar Time Delay missions are expected to be proposed in response to future PCOS requests for proposals.</p>
<p>Scientific, Engineering, and/or Programmatic Benefits</p>	<p>The primary scientific benefit of a Solar Time Delay mission would be a very strong test of General Relativity. Looking for a small offset of 1×10^{-7} or less in the parameter γ from solar time delay measurements is fairly widely believed to be the best candidate for detecting an effect on GR of the merger of quantum physics with General Relativity.</p> <p>Optical clocks are also expected to have high value in connection with spacecraft communications and navigation applications, and are listed under TA 5.4.1.3 in the May 2015 Draft NASA Technology Roadmaps. A Technology Candidate Snapshot for Cold Atom Lattice Optical Clocks is listed on page TA5-94. However, in view of the scientific benefits of a future PCOS Solar Time Delay Mission, technology development of optical clocks to the necessary TRL should be listed under TA 8.1 also.</p>

PCOS Applications and Potential Relevant Missions	<p>Before the proposed Solar Time Delay mission can be fully evaluated, a demonstration of the necessary optical clock performance on the International Space Station (ISS) may be needed. This will require vibration isolation and some additional precautions because of the on-board noise level. In view of the problem of frequency comparison between the ISS and ground, two clocks on the ISS operating under somewhat different conditions will need to be compared.</p> <p>This demonstration will facilitate applications to other NASA missions, as well as to the expected future PCOS Solar Time Delay mission. The operation on the ISS of the PHARAO clock based on cooled Cs atoms with an accuracy of about $1e-16$ and of a mercury trapped-ion clock will help provide experience on the requirements for optical clock operation.</p>
Time to Anticipated Need	<p>Named missions:</p> <p>Development needed for 2020 Decadal: No</p> <p>Other drivers: Discovery opportunities would benefit from TRL 6 by 2019.</p>

Table 3-1. Technology Gaps Evaluated by TMB in 2015 (continued)

Name of Technology	High-efficiency cooling systems for temperatures covering the range 20K to below 1K
Description	Stable and continuous cooling systems with high thermal-lift capacity and efficiency are needed for the Inflation Probe and planned X-ray and Far-IR missions. The demonstrated open-cycle dilution refrigerator on Planck does not scale to higher power loading. Approaches based on adiabatic demagnetization refrigeration (ADR), ³ He sorption cooling, or closed-cycle dilution offer avenues to provide improved performance.
Current State of the Art	The Planck satellite demonstrated continuous cooling to 20 K and 4 K for four years, and continuous cooling to 0.1 K for 2.5 years.
Current TRL	6
Performance Goals and Objectives	Continuous and stable cooling to 100 mK without cryogenes. The cooling power must be increased beyond that provided by the Planck system for large focal planes, and the implementation simplified for lower-cost mission opportunities.
Scientific, Engineering, and/or Programmatic Benefits	Enables next-generation measurements of CMB polarization. Eliminates cryogenes which limit mission life. Simplified approach lowers cost.
PCOS Applications and Potential Relevant Missions	Inflation Probe, Explorer, and international CMB polarization and absolute spectrum experiments; X-ray applications with cryogenic detectors; and Far-IR instrumentation.
Time to Anticipated Need	Named missions: Inflation Probe (2020s) Development needed for 2020 Decadal: Yes, IP Other drivers: Inflation Probe technology development is a NWNH priority that will be revisited by the mid-decadal review. International and Explorer implementations of the Inflation Probe will be proposed in the 2015-17 timeframe.

4. Technology Priorities and Recommendations

Background

As part of its annual technology prioritization process, the Program Office convened a TMB to prioritize the technology gaps submitted. The TMB followed an agreed-upon set of evaluation criteria, resulting in the priorities shown below. TMB membership included senior staff from NASA HQ Astrophysics Division, the Program Office, STMD, and the Aerospace Corporation. For 2015, the TMB used a prioritization approach similar to that used in prior years, with a streamlined set of four criteria. These included strategic alignment, benefits and impacts, scope of applicability, and urgency.

- **Strategic alignment:** How well does the technology align with PCOS science and/or programmatic priorities of the AIP or current programmatic assessment (*e.g.*, the Astrophysics Roadmap)?
- **Benefits and impacts:** How much impact does the technology have on applicable missions? To what degree does it enable and/or enhance achievable science objectives, reduce cost, and/or reduce mission risks?
- **Scope of applicability:** How crosscutting is the technology? How many Astrophysics programs and/or mission concepts would it benefit?
- **Urgency:** When are the enabled/enhanced missions' launches anticipated and/or by when do other schedule drivers require progress?

The TMB assigned weighting factors, reflecting the relative importance placed on each criterion. Each technology gap received a score of 0 to 4 for each criterion. The scores were multiplied by their respective weights, and the products were summed. Some technologies could be scored based on several missions or mission classes. In such cases, the TMB scored each scenario independently, assigning the highest overall score (*e.g.*, a gap might receive an overall score of 91 for a highly aligned mission, but only 75 for a less-aligned class of missions, in which case it would be assigned the higher score). Table 4-1 details the criteria descriptions, weighting factors, and TMB scoring guidelines.

This process provides a rigorous, transparent ranking of technology gaps based on the Program's goals, community scientific rankings of relevant missions, Astrophysics Division priorities as outlined in the AIP and Roadmap, and the external programmatic environment. Since the SAT program is intended to promote development and maturation of technologies relevant to missions and concepts identified as strategic, the strategic alignment criterion is driven by the AIP, which is in turn based on NWNH. The AIP details highly ranked science missions and technology development, which for PCOS include dark energy, gravitational waves, X-ray astronomy, and cosmic inflation; and prioritizes those based on current budget realities. This year, the TMB also considered the five potential "Surveyor" missions envisioned by the Astrophysics Roadmap, as well as the Habitable Exoplanet Imaging Mission recommended by the NWNH, several of which will be studied as concept missions in preparation for the 2020 Decadal Survey.

Criterion	Weight	Max Score	Max Weighted Score	General Description/ Question	4	3	2	1	0
Strategic Alignment	10	4	40	How well does the technology align with PCOS programmatic priorities of the AIP or current programmatic assessment (e.g., Astrophysics Roadmap)?	Applicable PCOS mission concept receives highest AIP consideration	Applicable PCOS mission concept receives medium AIP consideration, or is envisioned as a "Surveyor" in the Roadmap	Applicable PCOS mission concept receives low AIP consideration	Applicable PCOS mission concept not considered in the AIP but was positively addressed in NWNH	Not considered by the AIP, Roadmap, or NWNH for PCOS
Benefits and Impacts	8	4	32	How much impact does the technology have on applicable mission(s)? To what degree does the technology enable and/or enhance achievable science objectives, reduce cost, and/or reduce mission risks?	Critical and key enabling technology; required to meet mission concept objectives; without this technology, applicable missions would not launch	Highly desirable; not mission-critical, but provides major benefits in enhanced science capability, reduced critical resources need, and/or reduced mission risks; without it, missions may launch, but science or implementation would be compromised	Desirable; not required for mission success, but offers significant science or implementation benefits; if technology is available, would almost certainly be implemented in missions	Minor science impact or implementation improvements; if technology is available would be considered for implementation in missions	No science impact or implementation improvement; even if available, technology would not be implemented in missions
Scope of Applicability	3	4	12	How cross-cutting is the technology? How many Astrophysics programs and/or mission concepts could it benefit?	Applies widely to PCOS mission concepts and both COR and ExEP mission concepts	Applies widely to PCOS mission concepts and either COR or ExEP mission concepts	Applies widely to PCOS mission concepts	Applies to a single PCOS mission concept	No known applicable PCOS mission concept
Urgency	4	4	16	When are launches and/or other schedule drivers of missions enhanced or enabled by this technology anticipated?	Launch anticipated in next 5-9 years (2020-2024) or other schedule driver requires progress in 3-4 years (2018-2019)	Launch anticipated in next 10-14 years (2025-2029) or other schedule driver requires progress in 5-9 years (2020-2024)	Launch anticipated in next 15-19 years (2030-2034)	Launch anticipated in next 20-24 years (2035-2039)	Launch anticipated in 25 or more years (2040 or later)

Table 4-1. Clear, strategic criteria provide a rigorous, transparent process for prioritizing technology gaps.

Prioritization Results

As mentioned above, in 2015, the PCOS TMB received 23 technology gap entries. After combining two of these, the TMB scored a final set of 22 gaps. Reviewing the scores, the TMB binned the technology gaps into three groups based on a number of factors, including primarily a natural grouping of overall scores. These groups were as follows (entries within a group are numbered for convenience, but are ranked equally):

Priority 1: Technologies the TMB determined to be of the highest interest to the PCOS Program. Filling these gaps would provide key enabling technologies for the highest-priority strategic PCOS missions including potential US contribution to ESA's ATHENA X-ray mission, gravitational-wave missions such as participation in ESA's L3 mission, and a potential Inflation Probe mission. The TMB recommends SAT calls and award decisions address these technology gaps first.

1. High-power, narrow-line-width laser sources.
2. Highly stable, low-stray-light telescope.
3. Large-format, high-spectral-resolution, small-pixel X-ray focal-plane arrays.
4. Affordable, lightweight, high-resolution X-ray optics.
5. Advanced millimeter-wave focal plane arrays for CMB polarimetry.
6. High-efficiency cooling systems covering the range 20K to under 1K.

Priority 2: Technologies the TMB believes would be critical, highly desirable, or desirable for a variety of strategic missions. The TMB recommends that sufficient funding be available, SAT calls and award decisions address closing these technology gaps as well.

1. Phase-measurement subsystem (PMS).
2. Millimeter-wave optical elements.
3. Low-stress or stress-free coating for X-ray optical elements.
4. Low-mass, long-term stability optical bench.
5. Fast, low-noise megapixel X-ray imaging array with moderate spectral resolution.
6. High-efficiency X-ray gratings for high-resolution spectroscopy.
7. Gravitational reference sensor (GRS).

Priority 3: Technologies the TMB deemed supportive of PCOS objectives, but scoring lower than Priority 1 and 2 technology gaps.

1. Very-wide-field focusing instrument for time-domain X-ray astronomy.
2. Ultra-high-resolution focusing X-ray observatory telescope.
3. Advancement of X-ray polarimeter sensitivity with the use of negative-ion gas.
4. Fast, few-photon UV detectors.
5. Lightweight large-area reflective optics.
6. Low-power time-sampling readout.
7. Low-power comparators and logic arrays.
8. Lattice optical clock for Solar Time Delay mission and other applications.
9. High-performance gamma-ray telescope.

From 2011 through 2015, nearly all gaps achieving Priority 1 maintained that rank or changed by one level due to minor shifts in how priority scores break up naturally into groups. Also, funded projects have addressed high-priority gaps, mostly Priority 1, and occasionally Priority 2. For example, five of six of the 2015 Priority 1 gaps have already been addressed by SAT projects, as have two of the seven Priority 2 gaps. Over the years, certain high-urgency Priority 1 gaps were funded directly rather than by SAT grants.

5. Benefits and Successes Enabled by the PCOS SAT Program

The main benefit of the SAT program is in maturing technologies across the mid-TRL gap, so they can be infused into strategic PCOS missions and/or enable international collaboration on projects relevant to Program goals. Where appropriate, newly matured technologies are also likely to be implemented in ground-based and suborbital experiments, as well as Explorers and Probe-class missions. These may well extend beyond the PCOS Program, to COR, ExEP, and even outside the Astrophysics Division.

For example, several SAT projects have advanced X-ray optics, detector, and readout technologies, providing a range of possible options or meaningful US contributions to ATHENA. As a result, the TES calorimeter array approach developed by one of the PCOS SAT projects has been provisionally selected for ATHENA's X-IFU X-ray spectrometer. Additionally, X-IFU endorsed the continued development of time-division Superconducting QUantum Interference Device (SQUID) multiplexing supported by SAT funding as backup to their baseline readout, which is currently at a lower TRL. In the gravitational-wave arena, phasemeter technology funded by PCOS SAT program, including phase locking and laser stabilization, was infused into the Laser Ranging Interferometer (LRI) on the Gravity Recovery and Climate Experiment (GRACE) Follow-On mission. Advances accomplished as a result of this LRI work are now being leveraged by the PI back into his SAT project.

Perez *et al.* [3] reported that PCOS-funded projects have provided significant positive outcomes. One example is the SAT-supported development of an antenna-coupled TES bolometer. This technology was deployed in the BICEP2 experiment in Antarctica, helping search for B-mode polarization in the CMB signal. The technology provided an order-of-magnitude increase in measurement speed compared to the BICEP1 experiment. Detector-array technology from this SAT project was then incorporated into the BICEP3 and Keck Array ground-based experiments, and flown on the Spider long-duration balloon mission during the 2014/15 Antarctic season, measuring CMB polarization at 90 and 150 GHz with excellent low-frequency stability and low cosmic-ray event rates.

Another success story is the incorporation of directly deposited optical blocking filters developed by another SAT project onto flight CCDs of REXIS, an MIT student instrument on the OSIRIS-REx mission (2016 planned launch). This filter technology meets the stringent performance requirements without straining the experiment's technical budgets. The experiment went through its pre-environmental review in the summer of 2015. As a bonus, this provides the SAT project a nearly free opportunity to space-qualify its development.

Beyond supporting technology maturation, selection for SAT funding offers additional benefits to PIs, research groups, institutions, and the community. During the preparation of this PATR, the Program Office surveyed current PIs about additional benefits resulting from their SAT funding.

Eleven of 14 PIs reported they were able to leverage SAT funding to generate matching internal research and development funding; fellowships (*e.g.*, Smithsonian Astrophysical Observatory, SAO, internal funding including the Leon Van Speybroeck Fellowship in X-ray Optics; GSFC Internal Research and Development, IRAD; Nancy Grace Roman Technology Fellowship, RTF; and Presidential Early Career Award for Scientists and Engineers, PECASE); contributed labor, parts, and/or infrastructure funding; industry contracts; Small Business Innovation Research (SBIR) grants; and/or funded parallel efforts on related projects. Nine of the 14 PIs hired students and/or post-doctoral fellows to assist their technology development work (on average, three or four per project), helping train the next generation of researchers and technologists needed to support future missions. At least two of those students converted to full-time employment status within their respective organization, and one launched a small business, proving that the Program is helping train and shape the future astrophysics work force. Many

Involving Students and Postdocs in SAT Projects

The PCOS SAT projects have involved dozens of students and postdocs, helping train the future astrophysics workforce (see Appendix C for details). As can be seen in the following quotes, the Program is making a deep impact on these future technologists, and through them promotes astrophysics missions over many decades to come.

"I feel well-prepared to lead efforts in optical design, modeling and simulation, and experiment design and implementation."

"Immersed in an environment of frequent discussion, compelling ideas, and passionate problem-solving, I had the opportunity to constantly inquire and learn."

"By graduation, I will be prepared to serve as a PI for future missions and a contributor to the fields of space technology and astrophysics."

"The SAT project enabled me to gain understanding of the systems-level engineering challenges further up the optical path."

"I've gained valuable microfabrication knowledge and skills that I know will serve me well in future efforts to ready new technology for broader use."

The Broad Impacts of the SAT Program

Figure 5-2 depicts the geographic breadth of SAT program (both PCOS and COR) impacts, showing the locations of our PI institutions, their collaborators and partners, and the universities and colleges where the students and post-doctoral fellows involved in SAT projects attend school and work.

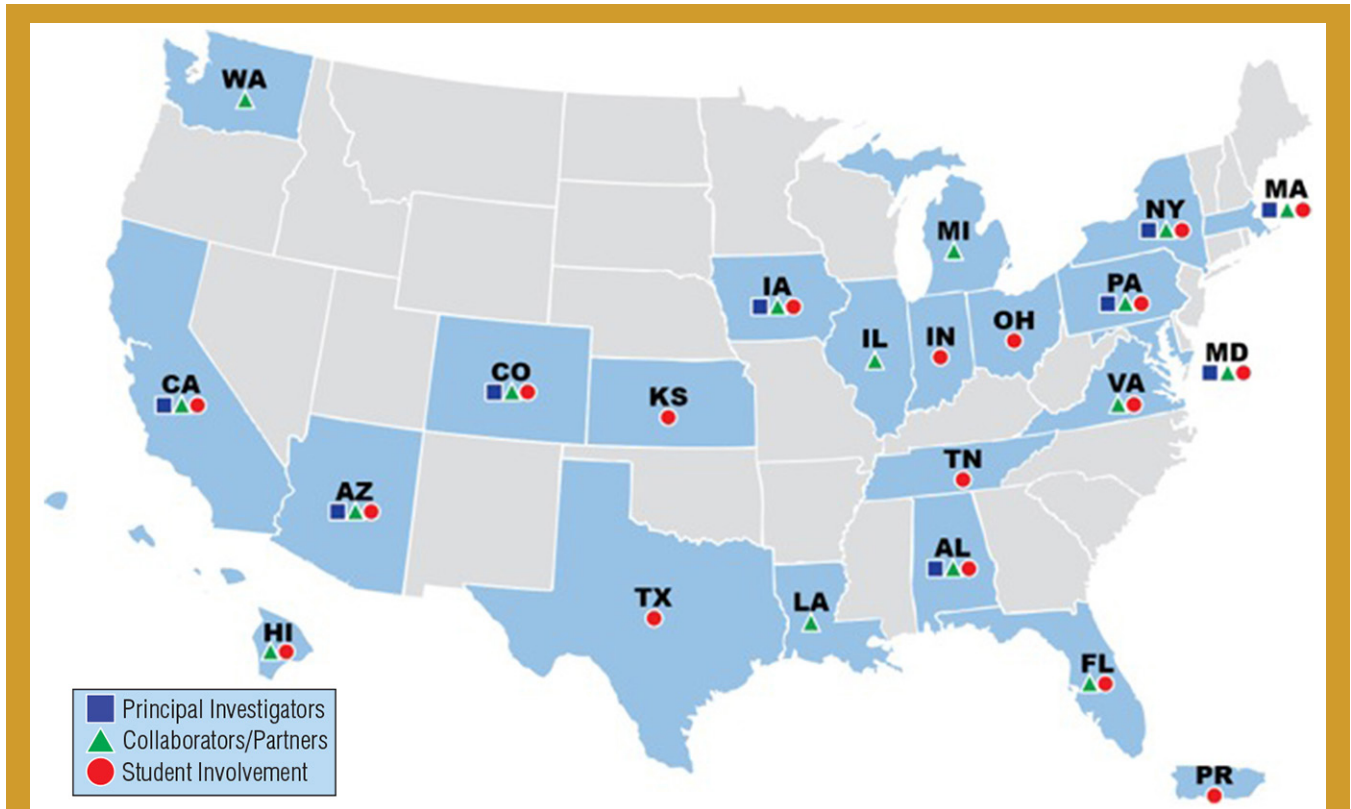


Fig. 5-2. SAT Program Impacts Map. The Program supports research efforts of PIs and collaborators/partners, and develops our future astrophysics workforce through student involvement (locations shown for both COR and PCOS Programs).

6. Closing Remarks

This 2015 PCOS PATR serves as a snapshot of the dynamic state of technology development managed by the Program Office and provides future directions for technology planning and maturation. As we complete another year of PCOS technology development activities, we see many positive developments.

Our technology development portfolio is growing, and continues to deliver significant advancements. All funded technologies are maturing toward higher TRLs, with several providing direct benefit to ground-based experiments and flight missions. New SAT awards slated to start in FY 2016 will fund additional CMB and gravitational-wave technology work, while new X-ray technology work is being funded directly. PCOS SAT investments are also generating benefits beyond direct advancement of strategic technologies. This includes leveraging internal and external (including non-NASA) funding; contributed materials, parts, and facility/equipment usage; hiring students and post-docs, thereby training our future astrophysics workforce; and generating research collaborations and industry partnerships, in support of PCOS science goals.

Our established and streamlined technology gap prioritization process continues to adhere to strategic guidance based on the AIP, NWNH, and now the Astrophysics Roadmap “Surveyor” concepts, with the TMB assigning the most significant weight in technology gap prioritization to strategic alignment. As a result, the Astrophysics Division continues to fund projects addressing technology gaps identified by the TMB as having the highest priority. The latest set of highest-priority TMB recommendations submitted to the Astrophysics Division include technology developments related to gravitational-wave missions, X-ray focal plane arrays and optics, millimeter-wave focal planes for CMB polarimetry, and high-efficiency cooling systems reaching temperatures below 1K.

To continue and support the ever-evolving technology needs of the PCOS community, we continue to interact with the broad scientific community through the PhysPAG, through various workshops, via public outreach activities, and at public scientific conferences. These activities identify and incorporate the astrophysics community’s ideas about new science, current technology progress, and new needs for technology in an open and proven process. Each year, we incorporate new lessons learned and make appropriate improvements to our process.

We would like to thank the PCOS scientific community, the PIs and their teams, and the PhysPAG for their efforts and inputs that make this annual report current and meaningful. We welcome continued feedback and inputs from the community in developing next year’s PATR, which should be sent to [Thai Pham](#) at the Program Office. For more information about the Program and its activities, or to provide your feedback and inputs, please visit the [PCOS website](#).

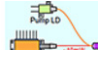




References

- [1] J. Mankins, “*The critical role of advanced technology investments in preventing spaceflight program cost overrun*”, The Space Review, December 1, 2008. Available at www.thespacereview.com/article/1262/1. Accessed May 2014.
- [2] National Research Council, “*New Worlds, New Horizons in Astronomy and Astrophysics*,” Washington, DC: The National Academies Press, 2010. Available at www.nap.edu/catalog.php?record_id=12951. Accessed May 2014.
- [3] M. Perez, B. Pham, and P. Lawson, “*Technology maturation process: The NASA strategic astrophysics technology (SAT) program*,” Proc. SPIE, Montreal, June 2014.


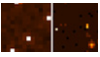

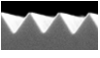
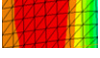



Appendix A

Technology Development Quad Charts

Gravitational Waves

	Jordan Camp – “Demonstration of a TRL-5 Laser System for eLISA”	51
	William Klipstein – “Gravitational-Wave-Mission Phasemeter Technology Development”	52
	John Lipa – “Laser Frequency Stabilization”	53
	Jeffrey Livas – “Telescopes for Space-Based Gravitational-Wave Observatories”	54
	John Ziemer – “Colloid Microthruster Propellant Feed System”	55

X Rays

	Mark Bautz – “Directly Deposited Optical Blocking Filters for Imaging X-ray Detectors”	56
	David Burrows – “Fast Event Recognition for the ATHENA Wide-Field Imager”	57
	Caroline Kilbourne – “Demonstrating Enabling Technologies for the High-Resolution Imaging Spectrometer of the Next NASA X-ray Astronomy Mission”	58
	Randall McEntaffer – “Reflection Grating Modules: Alignment and Testing”	59
	Paul Reid – “Development of 0.5-Arcsecond Adjustable Grazing-Incidence X-ray Mirrors for the SMART-X Mission Concept”	60
	Mark Schattenburg – “Advanced Packaging for Critical-Angle X-ray Transmission Gratings”	61
	Joel Ullom – “Technology Development for an AC-Multiplexed Calorimeter for ATHENA”	62
	William Zhang – “Next-Generation X-ray Optics: High Angular Resolution, High Throughput, and Low Cost”	63

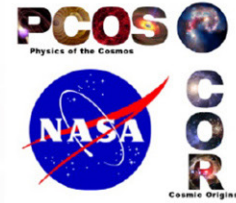
Cosmic Microwave Background

	James Bock – “Planar Antenna-Coupled Superconducting Detectors for CMB Polarimetry”	64
---	--	----

For more information, see full status reports starting on page 65

Demonstration of a TRL-5 Laser System for eLISA

PI: Jordan Camp / GSFC



Objectives and Key Challenges:

- Develop 1.5W light source for eLISA gravitational wave (GW) mission using a Master Oscillator Power Amplifier design with a novel diode laser oscillator (External Cavity Laser, ECL) followed by a 1.5W Yb fiber amplifier, providing a highly stable, compact, and reliable system
- Develop with industrial partner (Redfern Integrated Optics) space-qualified, ultra low-noise oscillator
- Test the laser system for reliability, and for amplitude and frequency stability, achieving the required noise performance
- Demonstrate low-noise power amplifier with servo controls
- Demonstrate system TRL 5 as well as noise performance and reliability of full laser system

Significance of Work:

- Required for eLISA or any similar gravitational wave mission

Approach:

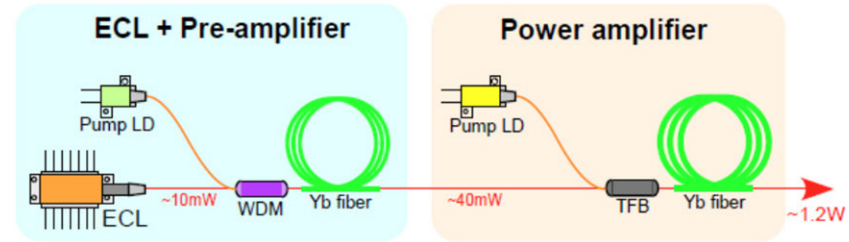
- Noise optimization of 1064 nm External Cavity Laser (RIO)
- Reliability study of External Cavity Laser
- Implementation of amplitude and frequency servo controls on full laser system, achieving $RIN=10^{-4}$ at 10^{-3} Hz, frequency noise = 300 Hz / $\text{Hz}^{1/2}$ at 10^{-2} Hz, and differential phase noise = 6×10^{-4} rad/ $\text{Hz}^{1/2}$ at 10^{-2} Hz

Key Collaborators:

- Kenji Numata, Mike Kraniak (NASA/GSFC)
- Lew Stolpner (Redfern Integrated Optics)

Development Period:

May 2014 – May 2016



Master Oscillator / Power Amplifier (MOPA) configuration of eLISA laser, including ECL, preamp, and diode-pumped Ytterbium (Yb) fiber amplifier

Recent Accomplishments:

- ✓ Developed and constructed 1.5W laser amplifier
- ✓ Fabricated world's first butterfly package layout 1064 nm ECL

Next Milestones:

- ECL optimization contract start (July 2015)
- Noise tests of optimized laser amplifier (Nov 2015)
- Preliminary laser system test with ECL (Jan 2016)
- ECL reliability tests (Feb 2016)
- Full laser system noise testing (Mar 2016)
- Full laser system reliability testing (May 2016)

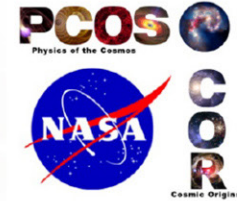
Applications:

- Laser source for eLISA GW mission
- Oscillator for ground-based GW LIGO project
- Oscillator for GRACE-II mission

TRL_{In} = 3 TRL_{Current} = 3 TRL_{Target} = 5

Gravitational-Wave-Mission Phasemeter Technology Development

PI: William Klipstein / JPL



Objectives and Key Challenges:

- Advance our phase-measurement system from TRL 4 to 5 through significant system-level hardware fidelity increase and greater fidelity of signal test environment by adding low light levels
- Mature the TRL of phase readout with high strain sensitivity through micro-cycle/ $\sqrt{\text{Hz}}$ precision on a 4-16 MHz beat-note in the presence of laser frequency noise and local clock noise, already demonstrated in a lab testbed

Significance of Work:

- High-performance phase readout is an enabling technology for multi-spacecraft laser-interferometer-based missions such as LISA-like gravitational-wave missions

Approach:

- Advance component technologies
 - Infuse compatible EM hardware from GRACE Follow-On Laser-Ranging Interferometer (LRI)
 - Demonstrate wavefront sensing with quadrant photoreceivers
- System-level testing
 - Modify interferometer testbed to include low-light signals
 - Replace COTS components in interferometer testbed with LRI EM hardware and demonstrate performance

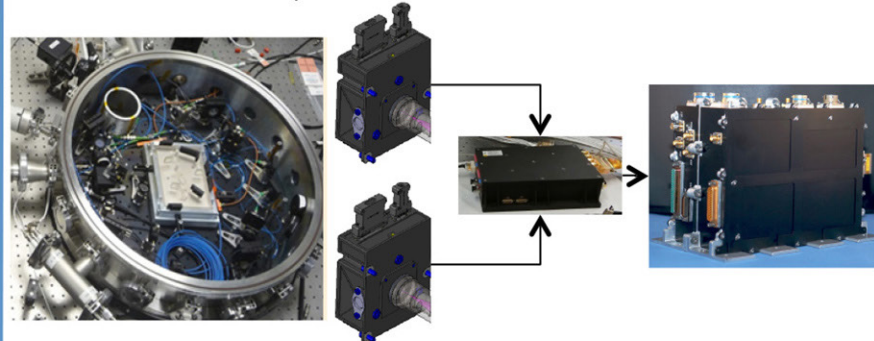
Key Collaborators:

- Jeff Dickson, Brent Ware, Bob Spero, Kirk McKenzie, Andrew Sutton, and Chris Woodruff (JPL)

Current Funded Period of Performance:

Apr 2014 – Sep 2016

EM Hardware (QPD Photoreceivers, Pre-Amp, and Phasemeter) infused into the LISA Testbed



Recent Accomplishment:

- ✓ Demonstrated phase readout with micro-cycle/ $\sqrt{\text{Hz}}$ precision in the presence of laser frequency noise and local clock noise in an interferometer testbed

Next Milestones:

- Incorporate Quadrant Photoreceivers into testbed
- Demonstrate wave-front sensing
- Migrate additional photoreceiver algorithms from LabView phasemeter to EM
- Demonstrate tracking of low visibility signals with EM Phasemeter
- Incorporate EM photoreceivers and signal chain
- Demonstrate testbed performance at TLR 5 or better

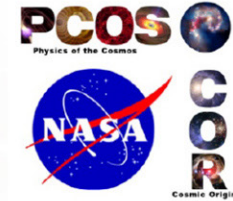
Applications:

- Inter-spacecraft laser interferometry and pm-precision interferometer readout electronics for future missions, *e.g.*, LISA
- Other interferometry concepts (*e.g.*, planet searches)

$TRL_{In} = 4$ $TRL_{Current} = 4$ $TRL_{Target} = 5$

Laser Frequency Stabilization

PI: John Lipa / Stanford University



Objectives and Key Challenges:

- Develop a laser operating near 1570 nm with improved noise performance and mid-term frequency stability for missions that could use a highly coherent light source near the telecom band
- Performance goals are to achieve substantially lower noise than iodine-stabilized lasers, the current gold standard for transportable systems; goal is an Allan deviation of $\sim 2 \times 10^{-15}$ in a one-second measurement time
- Noise performance and frequency stability of lasers on short and intermediate time scales requires dual locking scheme (see figure)

Significance of Work:

- A highly stable laser simultaneously locked to a cavity and a molecular transition at a telecom wavelength will enable a range of high-precision measurements including gravitational-wave observations

Approach:

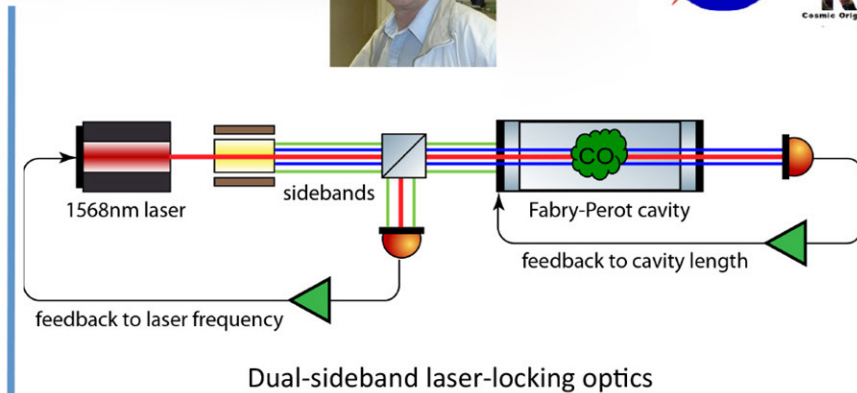
- Set up a bench-top model of laser system for CO based on existing system at JILA for C₂H₂ near 1064 nm
- Perform functional tests on system
- Set up a system to allow detailed noise performance measurements
- Upgrade optics and electronics to achieve noise performance goal

Key Collaborators:

- Jan Hall (JILA)
- Bob Byer and Sasha Buchman (Stanford University)
- Shailendhar Saraf (SN&N Electronics, CA)

Current Funded Period of Performance:

Jan 2013 – Jun 2015



Recent Accomplishments:

- ✓ First-ever CO-stabilized laser
- ✓ Initial noise measurement
- ✓ System noise in 10^{-13} range

Next Milestones:

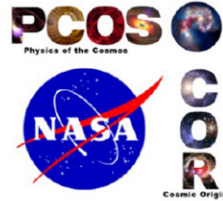
- Additional noise measurements with frequency comb (Jun 2015)
- Documentation of final TRL (Jul 2015)

Applications:

- Tests of fundamental physics, gravitational-wave observation, precision spectroscopy and Doppler, formation flying, trace gas detection

TRL_{In} = 3 TRL_{Current} = 3 TRL_{Target} = 4

Telescopes for Space-Based Gravitational-Wave Observatories



PI: Jeffrey Livas / GSFC



Objectives and Key Challenges:

- Establish a complete telescope design meeting optical, mechanical, thermal, and manufacturability requirements for the US contribution to the eLISA L3 mission
- Fabricate and test a prototype
- Validate stray-light model

Significance of Work:

- First demonstration of a validated scattered-light model; combined with previous demonstration of dimensional stability, provides a firm basis for realistic engineering-model design for a flight-qualifiable off-axis telescope.

Approach:

- Use SGO-Mid and the ESA eLISA concept as a reference
- Generate requirements per the ESA/SRE “Yellow Book”
- Use design study results (off-axis SiC recommended)
- Fabricate a prototype from the design
- Verify for compliance with specifications
- Concentrate on stray-light model validation

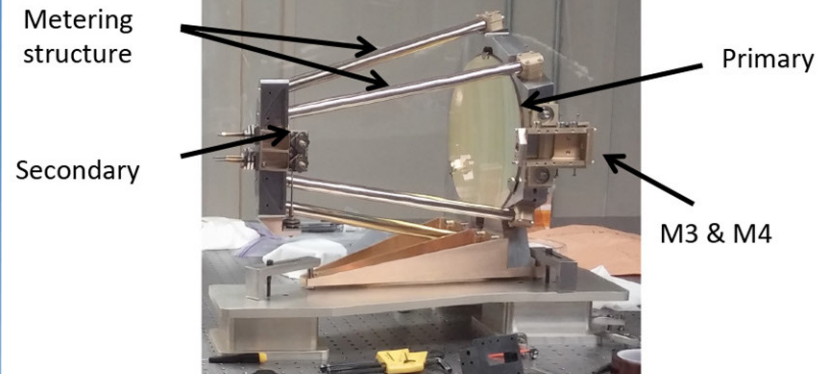
Key Collaborators:

- Joe Howard, Garrett West, Peter Blake, Len Seals, and Ron Shiri (GSFC Code 551)
- John Crow and Justin Ward (GSFC Code 543)

Current Funded Period of Performance:

Oct 2012 – Sep 2015

Off-axis Prototype Delivered



Recent Accomplishments:

- ✓ Signed prototype model contract
- ✓ Prototype CDR
- ✓ Prototype telescope delivered to GSFC
- ✓ Aligned prototype telescope at GSFC

Next Milestone:

- Validate system-level scattered-light model (Sep 2015)

Applications:

- Flagship gravitational-wave missions (eLISA)
- Laser ranging; precision metrology applications
- Laser communications

TRL_{In} = 3 TRL_{Current} = 3 TRL_{Target} = 3

Colloid Microthruster Propellant Feed System

PI: John Ziemer / JPL



Objectives and Key Challenges:

- Replace the heavy (up to 15 kg) spring-loaded bellows design from ST7 with a light-weight pressurized diaphragm tank (≤ 1 kg)
 - O1: Design tank and feed system with full redundancy
 - O2: Design, fabricate, and test stainless steel diaphragm tank
- Use new Busek Microvalve (Phase II SBIR and Phase IIe) to reduce complexity while providing redundancy
 - O3: Design, fabricate, and test new Busek Microvalves
 - O4: Integrate and test feed system components to TRL 5

Significance of the Work:

- A new, flight-like, fully redundant, higher-capacity colloid thruster feed system at TRL 5 can support any gravitational-wave observatory concept
- A clear path to TRL 6 once the mission and system are defined

Approach:

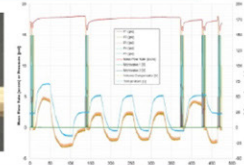
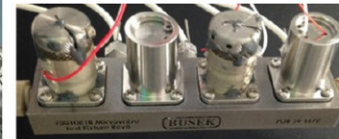
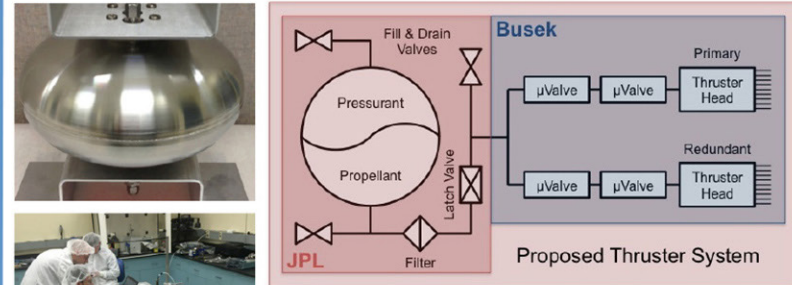
- Teaming arrangement between flight tank vendor Keystone, microvalve vendor Busek, and JPL to manage, perform I&T
- Use standard liquid-fed propulsion flight design guidelines and practices – the new technology is in the assembled pieces working together, not the propulsion engineering approach
- Four tasks related to each objective, plus a management task, each with a JPL expert lead
- Hold peer reviews at each meaningful milestone: requirements definition, design, and test

Key Collaborators:

- Busek Co., Inc. on microvalve and systems engineering
- Keystone Engineering on flight-like tank manufacture and test
- JPL electric / chemical propulsion and flight propulsion groups

Development Period:

Jan 2013 – Jan 2015



Accomplishments:

- ✓ Tank fabrication and TRL 5 tests are complete
- ✓ Microvalve fabrication and environmental tests are complete
- ✓ Redundant Microvalve subassembly, including accumulator and volume compensator, has been fabricated and tested for TRL 5
- ✓ Complete feed system has been integrated and tested in a relevant, laboratory environment to reach TRL 5
- ✓ Integrated tests spanned expected beginning-to-end-of-life operating conditions, including testing redundant configuration

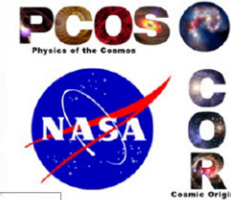
Applications:

- Drag-free gravitational-wave observatories
- Removing reaction wheels allows precision pointing of exoplanet observatory and next generation space telescopes
- Small spacecraft main propulsion

$TRL_{In} = 3$ $TRL_{PI-Asserted} = 5$ $TRL_{Target} = 5$

Directly Deposited Optical Blocking Filters for Imaging X-ray Detectors

PI: Mark Bautz / MIT MKI



Objectives and Key Challenges:

- Silicon Imaging X-ray detectors require thin filters (<300 nm) to block noise/background from UV and optical light
- State-of-the-art, free-standing filters use fragile, thin substrates
- Objective: deposit blocking filter directly on CCD X-ray detector, eliminating substrate
- Challenges:
 - Deposit filter directly without compromising CCD performance
 - Deposit sufficiently thin, uniform filters

Significance of Work:

- Filter deposited on detector requires no fragile substrate
- Allows cheaper, more robust sensors (with no vacuum housing)
- Improves QE and makes larger focal planes practical

Approach:

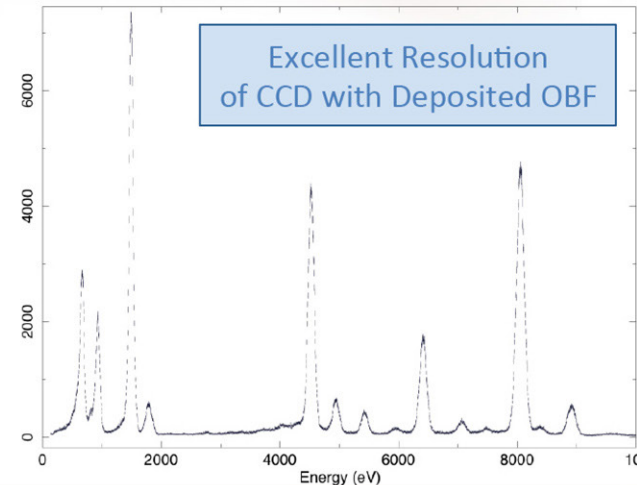
- Exploit existing stocks of (engineering grade/flight spare) X-ray CCD detectors at MIT Lincoln Laboratory
- Screen, thin, passivate, package, and apply filters to detectors
- Filter is Al with AlO₂ cap
- Start thick (220 nm Al) and get progressively thinner
- Use existing MIT facilities for X-ray characterization
- Use existing and upgraded facilities for optical characterization

Key Collaborators:

- Bautz, Kissel *et al.* (MIT Kavli Institute)
- Suntharalingam, Ryu, Burke, O'Brien (MIT Lincoln Laboratory)

Current Funded Period of Performance:

Jul 2012 – Jun 2016



Recent Accomplishments:

- ✓ Reduced pinhole fraction to < 1% (OD<7) for 220 nm OBF
- ✓ Tested 70 nm & 100 nm thick Al OBF; optical blocking as expected
- ✓ Identified leakage paths through CCD edges, support wafer, and epoxy bond line; significant for REXIS (large visible-light flux)
- ✓ With REXIS, developed and qualified underside coating as effective countermeasure against leakage
- ✓ Began long-term stability test; no degradation evident in 8 months

Next Milestone:

- Support environmental tests of REXIS flight CCDs/OBFs, achieve TRL 6, surpassing project goals

Applications:

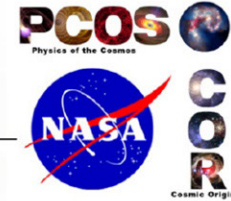
Every X-ray imaging or grating spectroscopy mission, including:

- Explorers (Lobster, Arcus, *etc.*)
- Probes (AEGIS, N_XGS, AXSIO, WFXT, *etc.*)
- Flagship (ATHENA, X-ray Surveyor)

TRL_{In} = 5 TRL_{Current} = 5 TRL_{Target} = 6

Fast Event Recognition for the ATHENA Wide-Field Imager

PI: David Burrows / PSU

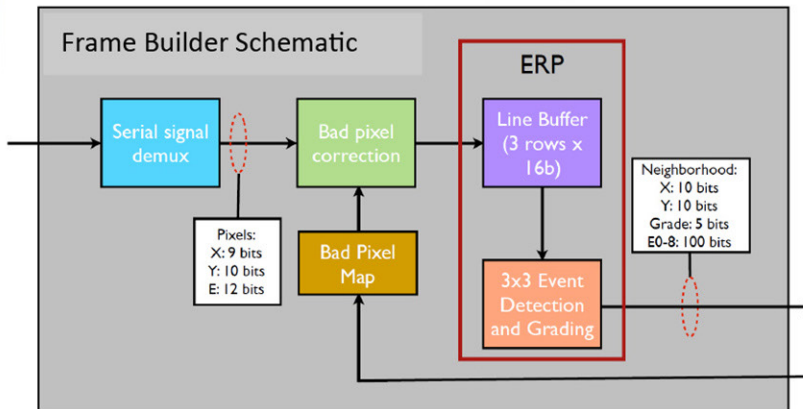


Objective and Key Challenges:

- High-speed event recognition and data compression

Significance of Work:

- Required for future proposed X-ray imagers, including ATHENA WFI (ESA L2), JANUS XCAT (EX), XTIDE XCAT (SMEX), Arcus (ISS), and X-ray Surveyor (Astrophysics Roadmap)



Approach:

- FPGA coding/simulation/testing
- Testing with fixed patterns up to 1GB/s
- Testing with real X-ray data up to 1GB/s

Key Collaborators:

- Dr. Karl Reichard and Eli Hughes (PSU/ARL)
- Dr. Zach Prieskorn and Dr. Tyler Anderson (PSU/ECOS)
- Dr. Mark Bautz (MIT)
- Dr. Steve Murray (SAO)

Development Period:

Jan 2015 – Dec 2016

Recent Accomplishment:

- ✓ Initiated internal funding codes, ordered development kit

Next Milestone:

- Design Review (July 2015)
- Test breadboard version (Aug 2015)
- Test Readiness Review (Oct 2015)

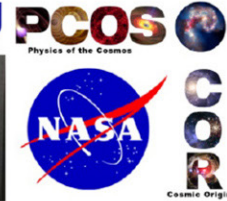
Applications:

- ATHENA WFI (ESA L2)
- JANUS XCAT (EX)
- XTIDE XCAT (SMEX)
- Arcus (ISS)
- X-ray Surveyor (Astrophysics Roadmap)

TRL_{In} = 3 TRL_{Current} = 3 TRL_{Target} = 4

Demonstrating Enabling Technologies for the High-Resolution Imaging Spectrometer of the Next NASA X-ray Astronomy Mission

PI: Caroline Kilbourne / GSFC Code 662



Objectives and Key Challenges:

- Develop large-format arrays of X-ray microcalorimeters and their readout that meet the challenging requirements of high-resolution X-ray imaging spectrometers for astrophysics
- Advance the key components of an X-ray microcalorimeter imaging spectrometer from TRL 4 to 5, and advance a number of important related technologies to at least TRL 4

Significance of Work:

- This solid demonstration of core technologies coupled with a demonstration of targeted enhancements will enable a number of mission concepts to be confidently considered
- This development has enabled NASA participation in ESA's ATHENA mission

Approach:

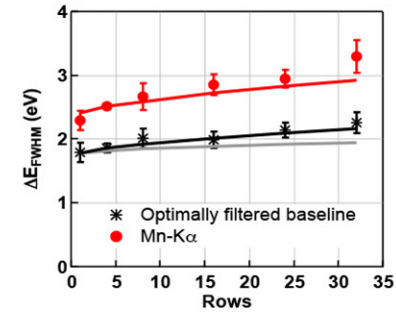
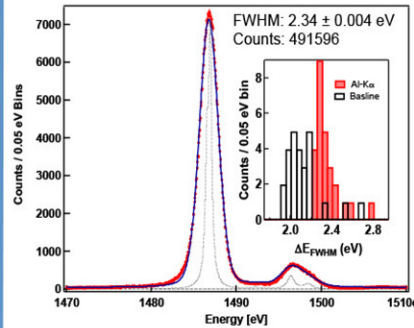
- Optimize SQUID time-division multiplexer (TDM) components and back-end electronics for low crosstalk, acceptable power dissipation, and bandwidth sufficient to allow frame times of <320 ns (goal of 160 ns)
- Integrate state-of-the-art 32 × 32 TES arrays (Mo/Au TES with Au/Bi absorbers) with optimized multiplexed readout
- Advance code-division multiplexer (CDM) readout
- Investigate component technologies for focal-plane assembly

Key Collaborators:

- J. Adams, S. Bandler, R. Kelley, F.S. Porter, S. Smith (GSFC 662)
- J. Chervenak (GSFC 553)
- J. Ullom, W.B. Doriese, C. Reintsema (NIST)
- K. Irwin (Stanford)

Current Funded Period of Performance:

Oct 2012 – Sep 2015



Left: Combined spectral results for Al-K α for 32-row TDM. The inset shows the resolution distributions. Right: Resolution vs. multiplex factor at 6 keV and the baseline (noise only).

Recent Accomplishments:

- ✓ Multiplexed 16 rows in a single column with an average resolution of 2.86 ± 0.17 eV at 6 keV and 2.34 ± 0.1 eV at 1.5 keV
- ✓ Many improvements in the design of TDM and CDM components

Next Milestone:

- Demonstrate multiplexed (3 columns × 16 rows) readout of 96 different flight-like pixels with 0.25 mm pitch in a 32 × 32 array with > 95% of pixels achieving better than 3 eV resolution at 6 keV

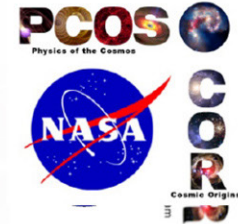
Applications:

- Potential contribution to the X-ray Integral Field Unit instrument on ESA's ATHENA mission.
- Other potential missions needing high-resolution imaging X-ray spectroscopy

TRL_{In} = 4 TRL_{Current} = 4 TRL_{Target} = 5

Reflection Grating Modules: Alignment and Testing

PI: Randall L. McEntaffer / University of Iowa



Objectives and Key Challenges:

- Implement an alignment methodology specific to off-plane reflection gratings
- Populate a module with aligned gratings capable of achieving spectral resolutions $> 3000 (\lambda/\delta\lambda)$ with high throughput over the 0.2 – 2.0 keV band
- Advance the OP-XGS technology to TRL 5

Significance of Work:

- Enables high throughput and high spectral resolving power below 2 keV where the majority of X-ray spectral features reside
- This will be the first time that multiple off-plane gratings have been aligned at this tolerance level with associated performance testing

Approach:

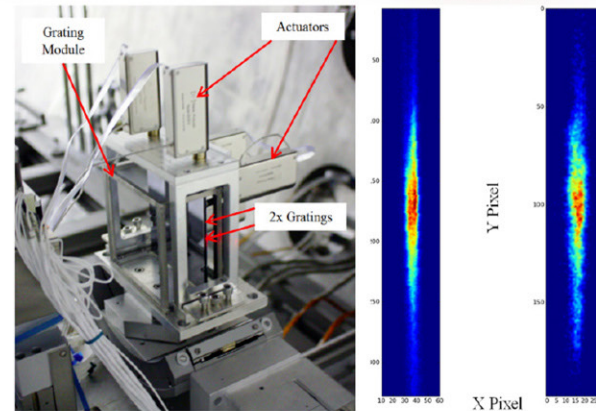
- Quantify alignment tolerances
- Formulate alignment methodology
- Implement alignment methodology
- Performance- and environmental-test an aligned module
- Evaluate process and repeat in Year 2

Key Collaborators:

- Will Zhang (NASA/GSFC)
- Jessica Gaskin (NASA/MSFC)

Current Funded Period of Performance:

Jan 2015 – Dec 2016



Left: Aligned gratings at PANTER
Right: SPO focus (left) vs. OP-XGS focus (right)

Recent Accomplishments:

- ✓ Quantified alignment tolerances for suborbital and Explorer spacecraft
- ✓ Completed design phase of alignment methodology and grating module; entering implementation
- ✓ Aligned and tested two gratings with SPO telescope at PANTER

Next Milestones:

- Implement new alignment methodology (3rd quarter 2015)
- Performance-test aligned gratings at MSFC (4th quarter 2015)

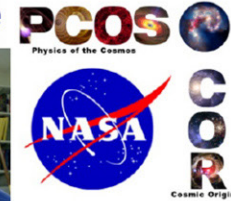
Applications:

- Large X-ray observatories
- Explorer class missions
- Suborbital rocket investigations

$TRL_{In} = 4$ $TRL_{Current} = 4$ $TRL_{Target} = 5$

Development of 0.5-Arcsecond Adjustable Grazing-Incidence X-ray Mirrors for the SMART-X Mission Concept

PI: Paul Reid / Smithsonian Astrophysical Observatory



Objectives and Key Challenges:

- Develop an alignment and mounting scheme consistent with a large-area ($> 2\text{m}^2$), high-resolution ($< 0.5''$) X-ray telescope that accommodates many (~ 100) close-packed mirror segments - align to $0.25''$ (= Chandra alignment) with mounting distortions $< 1\ \mu\text{m}$ P/V (correctable with adjusters)
- Approach must allow calibration of mirror surface figure as each segment is mounted so that figure can be corrected before aligning the next segment
- Incorporate developments in high-connection-density flexible cabling and row-column addressing to minimize and simplify electrical connections for mirror adjuster command and control

Significance of Work:

- Enables adjustable optics to correct mounting-induced distortion and on-orbit thermal changes with LCD-display electrical simplicity

Approach:

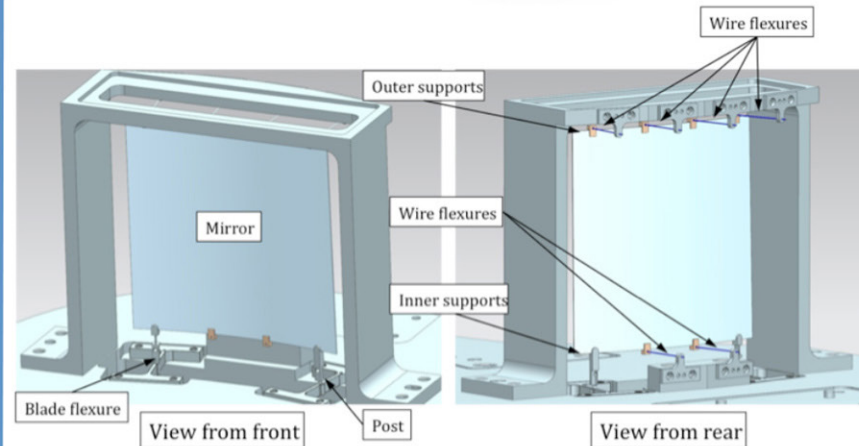
- Investigate anisotropic conductive films for high connection density (up to 100 contacts/mm)
- Develop ZnO thin-film transistor over-layer with insulating top layer for row-column addressing and ease of electrical contact routing
- Through structural and thermal analysis and design, incorporate and extend alignment and mounting approach being developed for APRA TRL-4 X-ray test.

Key Collaborators:

- Susan Troler-McKinstry and Margeaux Wallace (PSU)
- Brian Ramsey and Steve O'Dell (MSFC)

Current Funded Period of Performance:

Apr 2015 – Mar 2017



Single-shell mounting concept that will be modified for multiple shells

Recent Accomplishment:

- ✓ Completed initial thermal sensitivity analysis of thin piezoelectric film adjustable mirror in mounting concept

Next Milestones:

- Ray-tracing analysis of thermal modeling – 9/15
- Generation of thermal requirements for mirror ass'y – 10/15
- Structural Analysis and design for multi-shell ass'y – 2/16

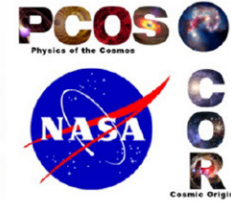
Application:

- X-ray Surveyor (formerly SMART-X) mission concept

$TRL_{In} = 3$ $TRL_{Current} = 3$ $TRL_{Target} = 4$

Advanced Packaging for Critical-Angle X-ray Transmission Gratings

PI: Mark Schattenburg / MIT MKI



Objectives and Key Challenges:

- Develop key technology to enable a Critical-Angle X-ray Transmission Grating Spectrometer (CATGS), advancing to TRL 6 in preparation for proposed mid- and large-size missions over the next two decades
- Develop improved grating fabrication processes
- Develop frame mounting, alignment, and assembly techniques for CAT grating arrays

Significance of Work:

- Improved diffraction efficiency and resolving power for CATGS
- Ability to manufacture large-area, light-weight grating arrays

Approach:

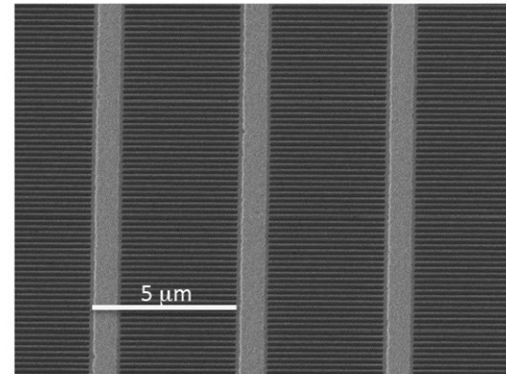
- Integrated wafer front/back-side fabrication process using silicon-on-insulator (SOI) wafers
- Wafer front side: CAT grating and Level 1 support structure
- Wafer back side: Level 2 support mesh structure
- CAT grating fabricated by deep reactive-ion etching (DRIE) followed by KOH polishing
- Bonded to expansion-matched metal support frame (Level 3)
- X-ray testing of prototypes at synchrotrons and MSFC facility

Key Collaborators:

- William Zhang (GSFC)
- Steve O'Dell (MSFC)

Current Funded Period of Performance:

FY 2015 – FY 2016



Scanning Electron Micrograph (SEM) of a free-standing CAT grating membrane after DRIE and KOH polish

Recent Accomplishments:

- ✓ Optimized combined dry- and wet-etch processes to obtain smooth grating bar sidewalls and narrow L1 supports and produced free-standing, large-area gratings with hierarchy of low-blockage supports
- ✓ Achieved record absolute X-ray diffraction efficiency (> 30%)

Next Milestones:

- Demonstrate CAT grating resolving power in an X-ray imaging system (Oct 2015)
- Develop integrated grating design with frame assembly (Oct 2016)

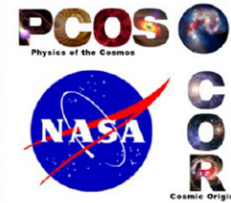
Applications:

- Flagship X-ray missions
- Explorer-type X-ray missions
- Laboratory X-ray analysis (materials science, energy research)

TRL_{In} = 3 TRL_{Current} = 3 TRL_{Target} = 6

Technology Development for an AC-Multiplexed Calorimeter for ATHENA

PI: Joel Ullom / NIST



Objectives and Key Challenges:

- Increase TRL of AC-biased Transition-Edge Sensor (TES) X-ray microcalorimeters from 3 to 4
- To achieve this, we seek to demonstrate that AC-biased TESs can meet the anticipated performance requirements of ESA's ATHENA mission, and in particular that AC-biased TESs can routinely achieve energy resolutions of 2.5 eV or better at 6 keV
- The key challenge is that, so far, TESs under AC-bias do not have as good energy resolution as under DC-bias

Significance of Work:

- AC-biased TESs and Frequency Division Multiplexing (FDM) are the baseline readout architecture for ATHENA; the performance of this approach strongly impacts mission design and success

Approach:

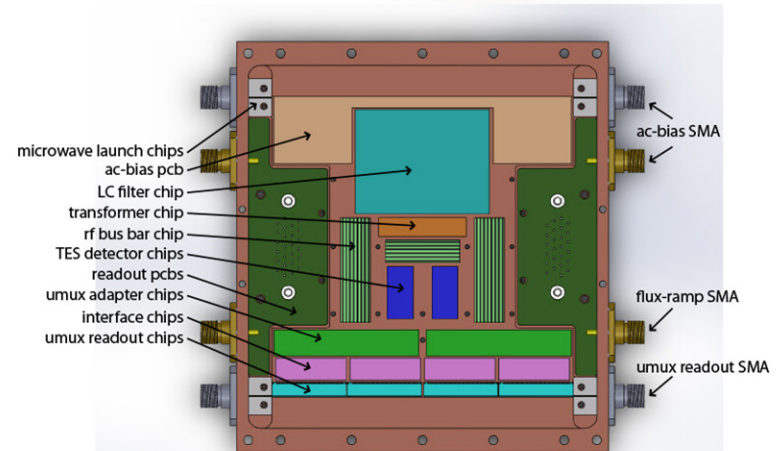
- Study the behavior of single GSFC TESs under AC-bias
- In one experiment, maximize the use of readout components from the European ATHENA team
- In a second experiment, separate the effects of the readout system from the TES by using a novel, open-loop readout architecture based on microwave SQUID amplifiers
- Study interactions among small numbers of AC-biased TES sensors

Key Collaborators:

- Caroline Kilbourne, Simon Bandler, and Richard Kelley (GSFC)
- Kent Irwin (Stanford University)

Current Funded Period of Performance:

FY 2015 – FY 2016



Sample box design for readout of AC-biased TESs using open-loop microwave SQUIDs

Recent Accomplishments:

- ✓ Designed sample box for microwave SQUID readout of AC-biased TESs
- ✓ Designed microwave SQUID amplifier with optimized input bandwidth
- ✓ Coordinated with European ATHENA team on joint experiments and exchange of sensor and readout components

Next Milestones:

- Fabricate microwave SQUID amplifier (end of 2015)
- First operation of AC-biased TES (end of 2015)

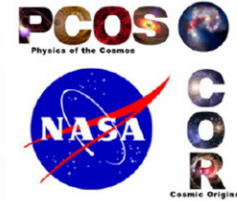
Applications:

- ATHENA and future X-ray missions based on TES microcalorimeters

$TRL_{In} = 3$ $TRL_{Current} = 3$ $TRL_{Target} = 4$

Next-Generation X-ray Optics: High Angular Resolution, High Throughput, and Low Cost

PI: William W. Zhang / GSFC



Objectives and Key Challenges:

- Develop lightweight X-ray mirror technology achieving better than 10-arcsec HPD angular resolution while minimizing cost and schedule; advance to TRL 5 to enable missions planned for 2010s and 2020s
- Prepare ways to achieve significantly better than 10-arcsec resolution while keeping the mass and cost at similar levels
- Fabrication and metrology of mirror segments
- Coating mirror segments with 20 nm of iridium w/o distortion
- Alignment and bonding of mirror segments

Significance of Work:

- Enables major X-ray observatories such as ESA's ATHENA and NASA's Astrophysics Roadmap's X-ray Surveyor

Approach:

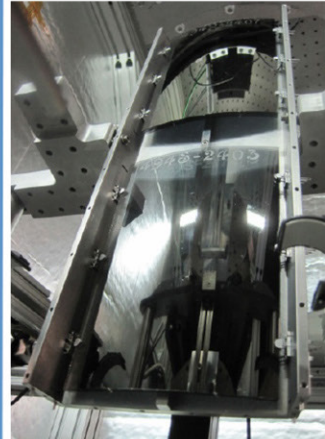
- Precision glass slumping to make mirror substrates
- Use magnetron sputter or atomic layer deposition to maximize X-ray reflectance
- Use interferometer, null lens, and interferometric microscope to conduct measurements
- Use Hartmann tests to align mirror segments
- Develop precision epoxy-bonding techniques

Key Collaborators:

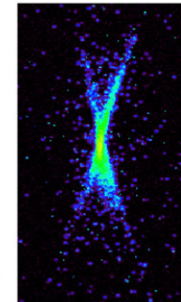
- Michael Biskach, Kai-Wing Chan, Ryan McClelland, and Timo Saha (GSFC)
- Stephen O'Dell (MSFC)

Current Funded Period of Performance:

Oct 2014 – Sep 2016



Technology Development Module (TDM) containing three pairs of parabolic-hyperbolic mirror segments



X-ray image with 8-arcsec HPD

Recent Accomplishments:

- ✓ Slumped mirror substrates achieving better than 10-arcsec HPD
- ✓ Coated mirror substrates with 15 nm of iridium without distortion
- ✓ Repeatedly co-aligned and bonded multiple mirror pairs, achieving 8-arcsec HPD X-ray images

Next Milestones:

- Refine mirror bonding process to fully realize mirror segment potential of 6.5-arcsec HPD
- Reduce gravity distortion by building a vertical X-ray beam to test mirror modules

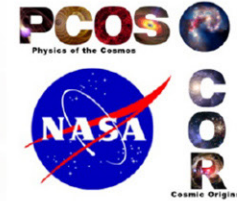
Applications:

- Flagship and probe class X-ray missions
- Explorer type X-ray missions
- Medical research and diagnosis

TRL_{In} = 3 TRL_{PI-Asserted} = 5 TRL_{Target} = 6

Planar Antenna-Coupled Superconducting Detectors for CMB Polarimetry

PI: James Bock / JPL



Objectives and Key Challenges:

Advance antenna-coupled superconducting detector technologies for space requirements:

- RF propagation properties
- Beam control and polarized matching
- Extended-frequency antennas
- Detectors stability and cosmic-ray response
- Readout-noise stability
- Modular focal-plane units

Significance of Work:

- Antenna designs for all bands required by the Inflation Probe
- Detector sensitivity, stability, and minimized particle susceptibility appropriate for space-borne observations

Approach:

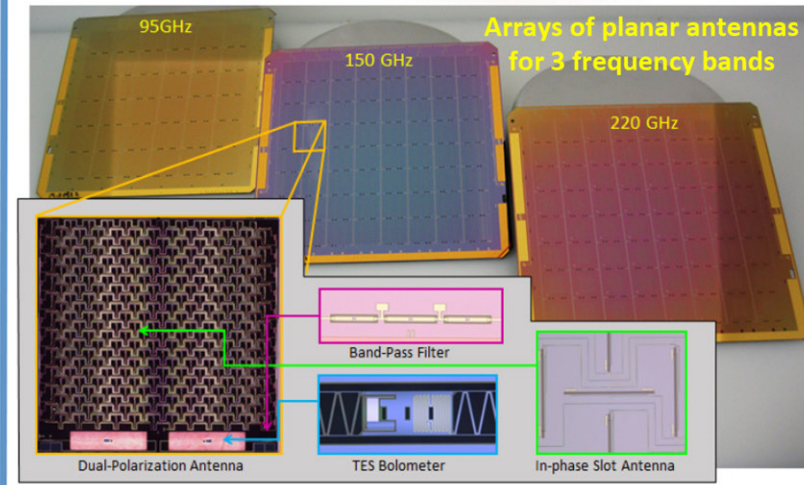
- Planar antennas provide entirely lithographed fabrication with no coupling optics
- Detectors provide photon-limited sensitivities in space
- Antennas provide excellent polarization and beam-matching properties
- Modular focal plane unit for large focal plane arrays

Key Collaborators:

- Koko Megerian, Hien Nguyen, Roger O'Brient, Anthony Turner, and Alexis Weber (JPL)
- Jon Hunacek, Howard Hui, and Sinan Kefeli (Caltech)
- Chao-Lin Kuo (Stanford)

Current Funded Period of Performance:

Jan 2014 – Dec 2015



Recent Accomplishments:

- ✓ 90- and 150-GHz focal planes flew on SPIDER balloon experiment
- ✓ Fabricated 40-GHz antennas; fielded 220-GHz arrays
- ✓ Tested first-generation dual-color antenna
- ✓ Tested tapered antennas with refracting optical system
- ✓ Measured white noise of uMUX SQUID readout

Next Milestones:

- Beam-line particle tests of frame events
- Develop second-generation dual-color antenna

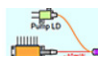




Applications:

- NASA Inflation Probe mission
- Explorer & international CMB missions
- Technology commonalities with Far-IR and X-Ray missions


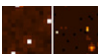





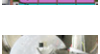
$TRL_{In} = 3$ $TRL_{Current} = 3$ $TRL_{Target} = 4$

Appendix B Technology Development Status

Gravitational Waves

	Jordan Camp – “Demonstration of a TRL-5 Laser System for eLISA”	66
	William Klipstein – “Gravitational-Wave-Mission Phasemeter Technology Development”	72
	John Lipa – “Laser Frequency Stabilization”.	76
	Jeffrey Livas – “Telescopes for Space-Based Gravitational-Wave Observatories”	85
	John Ziemer – “Colloid Microthruster Propellant Feed System”	93

X Rays

	Mark Bautz – “Directly Deposited Optical Blocking Filters for Imaging X-ray Detectors”	105
	David Burrows – “Fast Event Recognition for the ATHENA Wide-Field Imager”	115
	Caroline Kilbourne – “Demonstrating Enabling Technologies for the High-Resolution Imaging Spectrometer of the Next NASA X-ray Astronomy Mission”	121
	Randall McEntaffer – “Reflection Grating Modules: Alignment and Testing”.	128
	Paul Reid – “Development of 0.5-Arcsecond Adjustable Grazing-Incidence X-ray Mirrors for the SMART-X Mission Concept”	135
	Mark Schattenburg – “Advanced Packaging for Critical-Angle X-ray Transmission Gratings”	140
	Joel Ullom – “Technology Development for an AC-Multiplexed Calorimeter for ATHENA”.	145
	William Zhang – “Next-Generation X-ray Optics: High Angular Resolution, High Throughput, and Low Cost”.	150

Cosmic Microwave Background

	James Bock – “Planar Antenna-Coupled Superconducting Detectors for CMB Polarimetry”	155
---	--	-----

Abstracts of SAT Projects Starting in 2016

James Bock – “Superconducting Antenna-Coupled Detectors and Readouts for Space-Borne CMB Polarimetry”	163
Jeffrey Livas – “Telescope Dimensional Stability Study for a Space-Based Gravitational-Wave Mission”.	164
Edward Wollack – “High-Efficiency Feedhorn-Coupled TES-Based Detectors for CMB Polarization Measurements”.	165

Demonstration of a TRL-5 Laser System for eLISA

Prepared by: Jordan Camp (NASA/GSFC)

Summary

The gravitational-wave (GW) space mission Laser Interferometer Space Antenna (LISA) [1] is likely to be chosen for the European Space Agency (ESA) L3 GW astronomy opportunity, and NASA intends to contribute instruments to the mission. LISA's eventual flight will open a spectacular new window on the universe, using gravitational waves to reveal the physics and astronomy associated with the merger of massive black hole systems. The backbone of LISA is a highly stable laser of ~ 1.5 W power, which enables the picometer interferometry necessary to record the passage of a gravitational wave; such a laser is listed as a top priority of the Physics of the Cosmos (PCOS) Program Analysis Group (PhysPAG) technology roadmap. LISA is now under technology development in Europe, and the Europeans have expressed interest in the laser system as a possible contribution from the US. To enable this contribution, we will provide a Technology Readiness Level (TRL) 5 demonstration of the full LISA laser system by 2016, allowing maximum flexibility for mission implementation. The laser system includes a state-of-the-art master-oscillator power-amplifier approach. The oscillator is a compact, low-mass, low-noise, semiconductor External Cavity Laser (ECL) that is robust for operation in space. In addition, our custom-designed fiber amplifier will demonstrate the full range of LISA noise and power requirements.

The activity described here, funded through our Strategic Astrophysics Technology (SAT) grant, involves two steps. First, the understanding gained from our lab prototypes' noise and reliability testing will be incorporated into a rebuilt oscillator and amplifier. Second, with the oscillator and amplifier development complete, we will do a full-system test of the laser, using control systems to achieve the laser power, frequency, intensity, and differential phase noise. This will demonstrate a TRL-5 LISA laser system in 2016.

Background

LISA will use laser interferometry to observe the disturbance of freely floating test masses, caused by the passage of a GW. The detection of these GWs will allow LISA to observe the mergers of supermassive black holes, giving unprecedented views of tests of General Relativity at high precision, as well as the astrophysics of merging galaxies back to very high redshift. Because gravity is a very weak force, the GW test-mass disturbance is expected to be very small, of the order of 10^{-21} in strain, or 10^{-12} m displacement over a 10^9 m arm length, with a timescale of $\sim 10^3$ seconds. This displacement sensitivity and timescale flows through the LISA laser requirements [2], shown in Table 1.

Power (W)	λ (nm)	Intensity Noise ($1/\sqrt{\text{Hz}}$)	Frequency Noise ($\text{Hz}/\sqrt{\text{Hz}}$)	Differential Phase Noise ($\text{rad}/\sqrt{\text{Hz}}$)	Lifetime (Years)
1.5	1064	10^{-4} (at 10^{-3} Hz) 10^{-8} (at 10^7 Hz)	300 (at 10^{-2} Hz)	6×10^{-4} (at 10^{-2} Hz)	2.5

Table 1. Laser requirements for LISA

The design of the LISA laser system consists of a low-noise ECL oscillator and preamp, followed by a fiber power amplifier (Fig. 1).

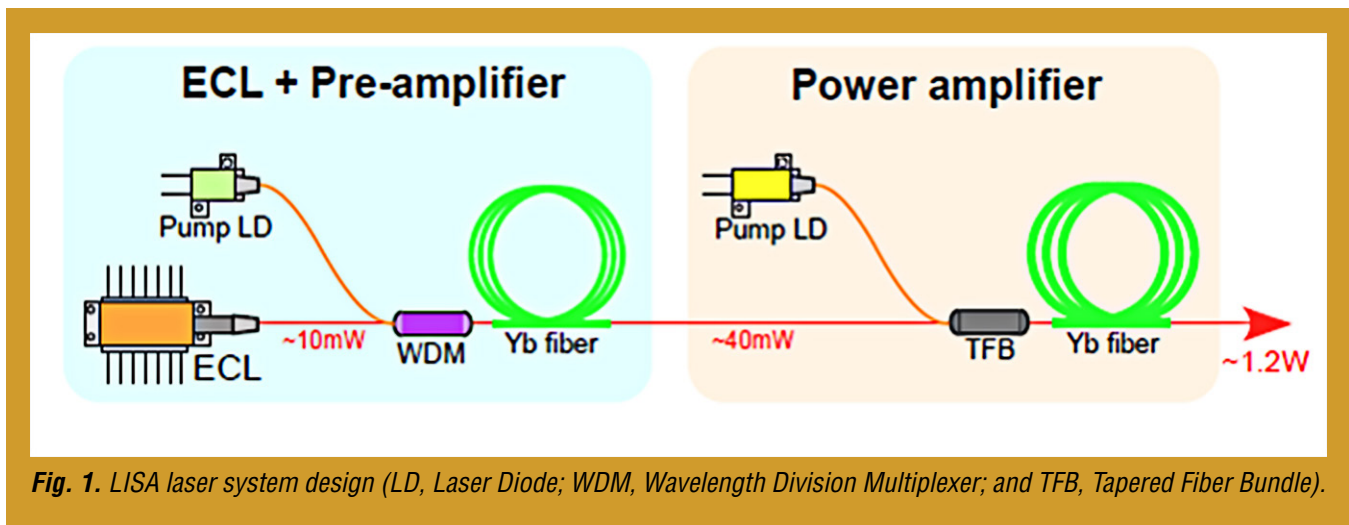


Fig. 1. LISA laser system design (LD, Laser Diode; WDM, Wavelength Division Multiplexer; and TFB, Tapered Fiber Bundle).

The ECL is a low-mass, low-cost, compact, simple, and highly reliable semiconductor laser, provided by a US vendor [3, 4]. These characteristics make it a compelling choice for the oscillator. The preamp is a simple and highly reliable subsystem that amplifies the ECL output by a factor of four.

For the amplifier, a laser design utilizing optical fibers presents many advantages over solid state bulk crystals, including:

- Insensitivity to contamination problems and ease of alignment, since the light is maintained within the fiber core and waveguide;
- Conveniently redundant design, since higher-risk components such as pump diodes are easily made redundant by splicing them into the gain fiber; and
- Ability to leverage the large resources of the telecommunications fiber industry.

The stringent noise requirements shown in Table 1 are achieved in the laser system design through the use of well-known amplitude- and frequency-stabilization techniques described below, with which our group has had extensive experience. The power and wavelength requirements are compatible with the overall oscillator and power amplifier configuration.

Objectives and Milestones

The objectives involve three main aspects:

- Optimization of the oscillator (ECL);
- Construction of a preamp and laser amplifier; and
- Systems testing of the full laser system (oscillator, preamp, and amplifier).

Optimization of the ECL will take place at the laser vendor (Redfern Integrated Optics, RIO). The first version of a 1064 nm wavelength ECL in the preferred Butterfly package was produced in 2014, and allowed us to incorporate this low-mass, compact oscillator [5] into our laser design. The next step in the ECL development will be the optimization of its design to provide lower phase noise and high reliability. This will be done by iterating the design of the planar Bragg grating which forms the reflector for the ECL optical cavity, and by performing accelerated aging tests on the laser-gain chip.

The laser amplifier will be constructed using a mechanically robust design to survive shake-testing and thermal cycling. It will also include temperature stabilization which is necessary to limit amplitude

noise. This construction involves use of a fiber splicer to combine fibers from the pump diode to the gain elements and a fiber coater to provide a coating layer with varying index of refraction to keep the light propagating through the fiber with low loss. The laser amplifier will be tested for required output power, frequency noise, differential phase noise, and amplitude noise. It will then be environmentally tested for mechanical and thermal robustness.

Finally, the full laser system (oscillator and amplifier) will be tested for noise and environmental robustness, as shown in Fig. 2. When TRL 5 is achieved individually for the oscillator and amplifier, we will demonstrate TRL 5 through a full-system-level test of the entire laser system, including power, frequency, intensity, and differential phase noise measurements. These studies will take place in the 2nd year of this SAT grant.

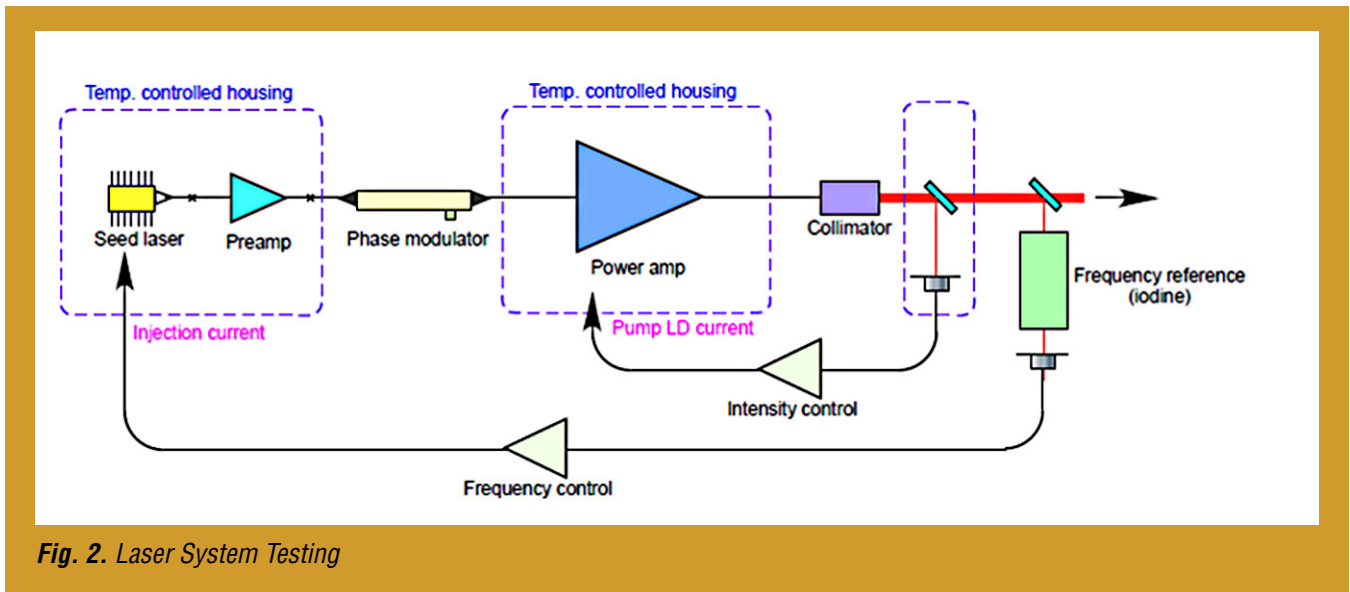


Fig. 2. Laser System Testing

The system test uses the fully fiber-coupled setup shown in Fig. 2 and incorporates the understanding gained in the measurements of the separate components. To simulate the stable space thermal environment, the oscillator and amplifier will be located in a temperature-controlled housing, stabilized to 0.1°C over a one-hour timescale. The experimental arrangement of Fig. 2 presents the amplifier, preamp, phase modulator, and amplifier as a single integrated system.

The milestones for these activities are:

- Procurement of long-lead items (completed) Mar 2015
- Preliminary 1.5 W laser amplifier (completed) Apr 2015
- Preliminary laser amp test with non-optimized ECL (completed) May 2015
- ECL optimization contract start. Jul 2015
- Optimized 1.5 W laser amplifier Sep 2015
- Noise tests of stabilized 1.5 W laser amplifier Nov 2015
- Noise optimization of ECL complete. Jan 2016
- Reliability testing of ECL complete Feb 2016
- Laser system test with optimized ECL. Feb 2016
- Full-laser-system noise testing Mar 2016
- Full-laser-system environmental testing Jun 2016

By June 2016 we will have characterized the full-laser-system noise and demonstrated compliance with environmental testing, establishing TRL 5 for this laser.

Progress and Accomplishments

We received notice of our SAT award in March 2014, and the funding arrived at GSFC in May 2014. Thus all progress should be measured against a start date of May 2014. We describe progress on the five major activities of procurements, ECL optimization, preamp build, laser amplifier build, and laser systems testing.

Procurement of Long-Lead Items: We have prepared a temperature-stabilized enclosure for the laser systems testing. We have also procured all long-lead instruments necessary for the systems testing, including a frequency reference cavity, a fiber fusion splicer, two fiber coaters, and a mechanical shaker.

ECL Optimization: This activity involves a redesign of the planar linear cavity that provides the optical feedback to control the lasing from the laser gain chip. It is funded through a procurement from this SAT, matched with funds from a Small Business Innovation Research (SBIR) Phase IIE award (RIO was funded in their ECL development through an SBIR Phase II grant). A difficulty in getting this work started was that RIO was acquired by a large company (QinetiQ) during the Phase IIE contract acquisition, requiring significant negotiation with NASA Shared Services Center (NSSC) lawyers and contract novation. As of June 2015, the contract preparation work is concluded and we expect RIO to be funded and start ECL optimization in July 2015.

Preamp Build and Test: A counter-pumped preamp with a gain of 5 was constructed, using a gain fiber of 1 m length. A clean output spectrum was observed, with low Amplitude-Stimulated Emission (ASE) floor, no output leakage, and an efficiency of ~20%. The preamp is shown in the left panel of Fig. 3, along with the ECL oscillator mounted with its low-noise current driver. The right panel of Fig. 3 shows the preamp output power plotted against its pump diode power. A preamp enclosure was designed and ordered. It will house two seed ECLs and two pump diodes for redundancy. Its fiber tray design was taken from the Lunar Atmosphere and Dust Environment Explorer (LADEE) flight mission.

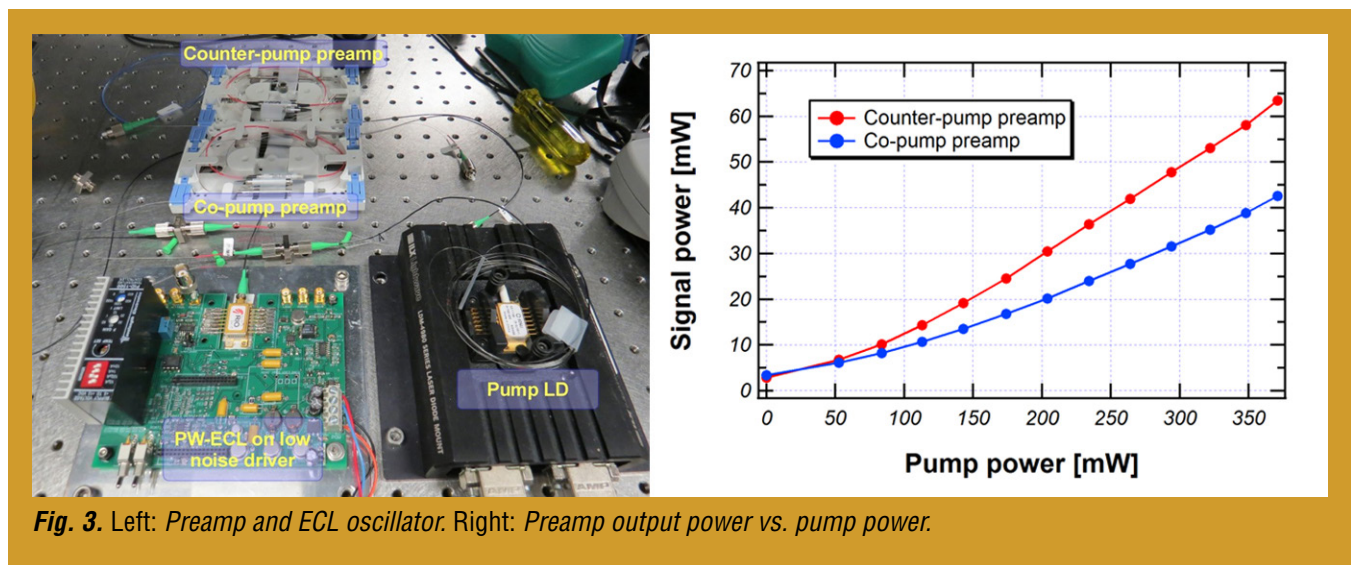
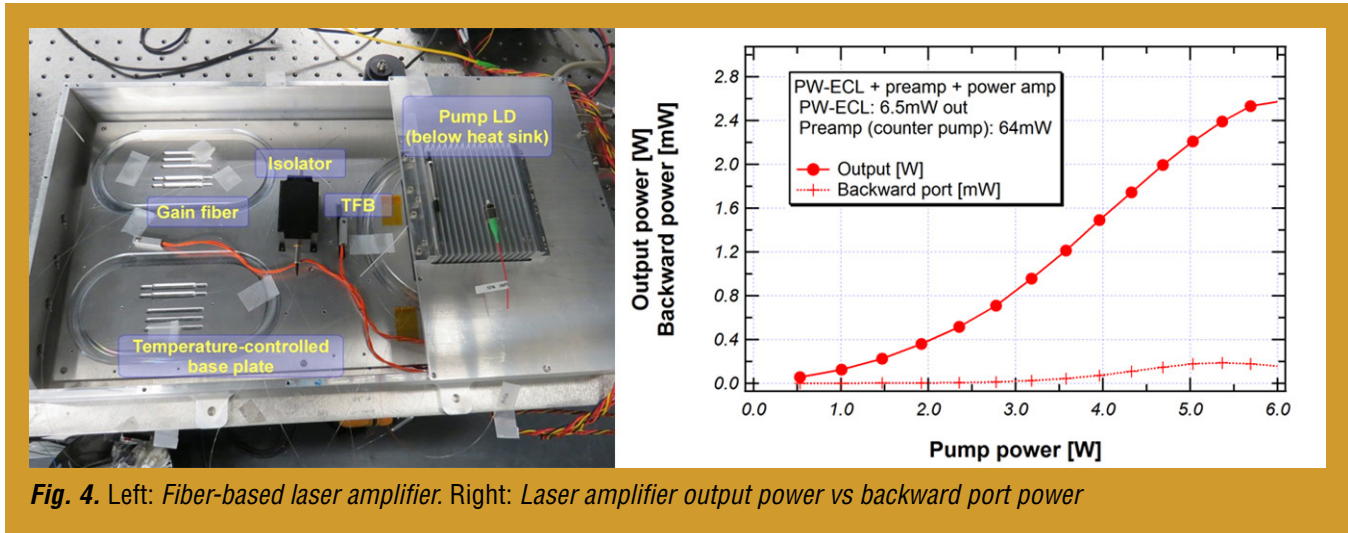


Fig. 3. Left: Preamp and ECL oscillator. Right: Preamp output power vs. pump power.

Amplifier Build and Test: the newly built 1.5 W fiber amplifier is shown in the left panel of Fig. 4. As shown schematically in Fig. 2, it includes a pump diode to provide power, a TFB to allow redundant power input, and a 2.3 m length, 10- μ m core, double-clad, large-mode-area gain fiber that converts the

pump power to amplification gain. The forward-pumped design and optical isolator minimize potential sources of feedback. The amplifier uses a robust mechanical design and temperature stabilization to suppress fiber-length variations.



Testing of the amplifier has shown an unstabilized amplitude variation of about 1% root mean square (rms), and an output power of 2.5 W, significantly above the 1.5 W requirement, as shown in the right panel of Fig. 4. The constant backward-port power as a function of output power indicates that Stimulated Brillouin Scattering (SBS) is likely not a noise concern. Approximately 20 dB polarization extinction ratio (PER) was achieved at the output. A 1064 nm ECL with 6 mW output, followed by a preamplifier of gain ~10, was used as input to the amplifier.

Laser System Testing: We have performed some preliminary laser systems tests by amplitude- and frequency-stabilizing the ECL and amplifier. By stabilizing the amplifier pump-diode current, an amplitude noise attenuation of ~5 was achieved at a frequency of 1 mHz (still a factor of ~10 from the LISA requirement). This noise will decrease significantly once temperature stabilization of the amplifier is applied. The laser system was also frequency-stabilized by locking a small fraction of the amplifier’s output to the frequency reference cavity, using either the laser current or an Acousto-Optical Modulator (AOM) as frequency actuator. A control bandwidth of ~10 kHz was achieved; future work will increase this to order 1 MHz by optimizing the AOM driver. Finally, the phase-meter necessary to measure LISA phase variations between the lasers on separate spacecraft has been implemented in our lab. It will be used to demonstrate phase locking of a free-running ECL oscillator to an ECL stabilized to the reference cavity.

Path Forward

The following activities will be undertaken in the second year of this SAT grant, starting in June 2015, and will be concluded by June 2016.

Completion of Amplifier Rebuild: The final, optimized, coated and spliced fibers and associated optical components will be installed in the amplifier chassis (Sep 2015).

Stabilized Laser System Test with Non-Optimized ECL: The amplifier will be fed with light from a (non-optimized) 1064 nm ECL seed laser. This will not be sufficient for the final noise tests, but will allow us to look at many aspects of the laser functionality, including power output, amplitude stability, and frequency stability (Nov 2015).

Design Optimization of ECL: This work will be done at RIO, and will involve modeling and analysis of the current-gain chip and Planar Linear Cavity (PLC) that comprise the ECL, and then modeling of the full oscillator. This will feed a redesign of the PLC. The next step will be the manufacturing and then integration of the new components, followed by characterization to verify the improved phase-noise performance, and then final reliability testing (accelerated aging) of the laser gain chip. The final oscillator will then be delivered to GSFC (Jan 2016).

Laser System Test with Optimized ECL: We will use the optimized ECL as the new seed laser for the amplifier. The seed laser will be frequency-stabilized using the optical reference cavity. Testing will include power, amplitude noise, and frequency noise (Feb 2016).

Full-Laser-System Noise Testing: The final, full-laser-system testing will proceed by enabling the temperature stabilization provided by the laser enclosure. The measurements will include power, amplitude stability, differential phase noise, and frequency stability; they will be shown to meet the requirements listed in Table 1. We will also carefully examine the incidence of SBS and ASE with an increase in laser power, to determine the maximum power at which the amplifier can operate. The noise testing will then be completed (Mar 2016).

Full-Laser-System Environmental Testing: Meeting the goal of demonstrating a TRL-5 laser system requires environmental testing, including vibration and thermal cycling. We will also monitor the laser output at high power and at elevated temperature (50°C) as part of accelerated aging measurements. Finally the oscillator, preamp, and amplifier components and gain fibers will be subjected to radiation exposure at the expected integrated LISA levels. TRL 5 will be demonstrated with the conclusion of all these tests (Jun 2016).

References

- [1] T. Prince *et al.*, “*LISA: Probing the Universe with Gravitational Waves*,” LISA-LIST-RP-436 Version 1.2 (2009)
- [2] O. Jennrich and G. Heinzel, “*Laser requirements for a gravitational wave mission*” (2013)
- [3] *Redfern Integrated Optics Products Page*
- [4] K. Numata *et al.*, “*Performance of planar-waveguide external cavity laser for precision measurements*,” *Optics Express* **18** 22781 (2010)
- [5] K. Numata *et al.*, “*Characteristics of the single-longitudinal mode planar-waveguide external cavity diode laser at 1064 nm*,” *Optics Letters* **39** No. 7, 2101 (2014)

For additional information, contact Jordan Camp: jordan.b.camp@nasa.gov



Gravitational-Wave-Mission Phasemeter Technology Development

Prepared by: William Klipstein (PI; JPL); Jeff Dickson, Kirk McKenzie, Robert Spero, Andrew Sutton, Brent Ware, and Chris Woodruff (JPL)

Summary

The proposed work in the framework of this Strategic Astrophysics Technology (SAT) project will advance the Technology Readiness Level (TRL) of our phase measurement electronics, and demonstrate their performance in an upgraded interferometer system-level test bed; the test bed will provide signals representative of gravitational-wave (GW) missions, such as the Laser Interferometer Space Antenna (LISA). Our technology-development effort starts with demonstrating the “photons-to-bits” phase measurement system (interferometer readout electronics) as a system to TRL 4 in an interferometer test bed providing signals representative of a LISA-like mission. Some components, most notably the digital phasemeter board, have been developed beyond TRL 4, as assessed by NASA’s Earth Science Program.

Background

LISA-like GW mission concepts rely on heterodyne laser interferometry to measure picometer-level fluctuations in the separation between three widely separated spacecraft. The transmit and receive beams from a spacecraft pair are mixed optically (interfered) on a beam combiner, resulting in a detected signal varying sinusoidally at the frequency difference between the local transmit laser and the laser received from the distant spacecraft. Picometer-level displacement sensitivity requires microcycle-level precision in measuring the phase difference compared to the micron-scale wavelength of the laser light.

Since 2005, we have been developing phase measurement systems to validate and support the photons-to-bits interferometer-signal readout based on the mission parameters described in the LISA Technology Development Plan. Future variants of GW missions all (except the less-mature atom interferometer concepts) involve laser interferometry between widely separated spacecraft. Thus, they will all rely on a LISA-like phasemeter and time-delay interferometry to mitigate the impact of laser frequency noise on mission performance.

Elements of our phase measurement system include quadrant photoreceivers, an analog signal chain, analog-to-digital converters, and digital signal processing for the phase measurement. In addition to measuring the phase (distance) change in the interferometer, the phasemeter also controls laser frequency and provides an optical communication link between spacecraft. We have recently used the phasemeter from the Gravity Recovery and Climate Experiment (GRACE) Follow-On to implement differential wavefront sensing using our LISA four-quadrant photoreceivers, and used that signal to maintain relative pointing of incoming and outgoing lasers by feeding back to a steering mirror in the transmitted light path.

Objectives and Milestones

The objective of this project is to advance our phase measurement system from TRL 4 to 5, through significant system-level hardware fidelity increase and greater fidelity of the signal-test environment by adding low light levels.

Key project milestones:

1. Incorporate quadrant photoreceivers into test bed.
2. Demonstrate wave-front sensing.
3. Migrate additional photoreceiver algorithms from LabView phasemeter to an Engineering Model (EM).
4. Demonstrate tracking of low-visibility signals with EM phasemeter.
5. Incorporate EM photoreceivers and signal chain.
6. Demonstrate test bed performance at TRL 5 or better.

Progress and Accomplishments

Work on this task was postponed in order to take advantage of synergistic developments on the Earth Science mission, GRACE Follow-On, which will carry a Laser Ranging Interferometer (LRI) based on technology development of the phasemeter for a GW mission. LRI will demonstrate inter-spacecraft interferometry with requirements quite similar to the former LISA mission by design. LRI is a partnership between the US and Germany, relying on partners from LISA formulation. The phasemeter team's share in LRI includes the phasemeter, laser, and laser stabilization cavity. LRI will fly LISA phasemeter algorithms implemented and advanced to flight maturity. The hardware complement is shown in Fig. 1. An EM of the quadrant photoreceivers and signal chain has been delivered to the US to support testing and will be made available to support this task as a complement to the US-developed photoreceivers. A comparison of LRI requirements to LISA requirements is shown in Table 1.

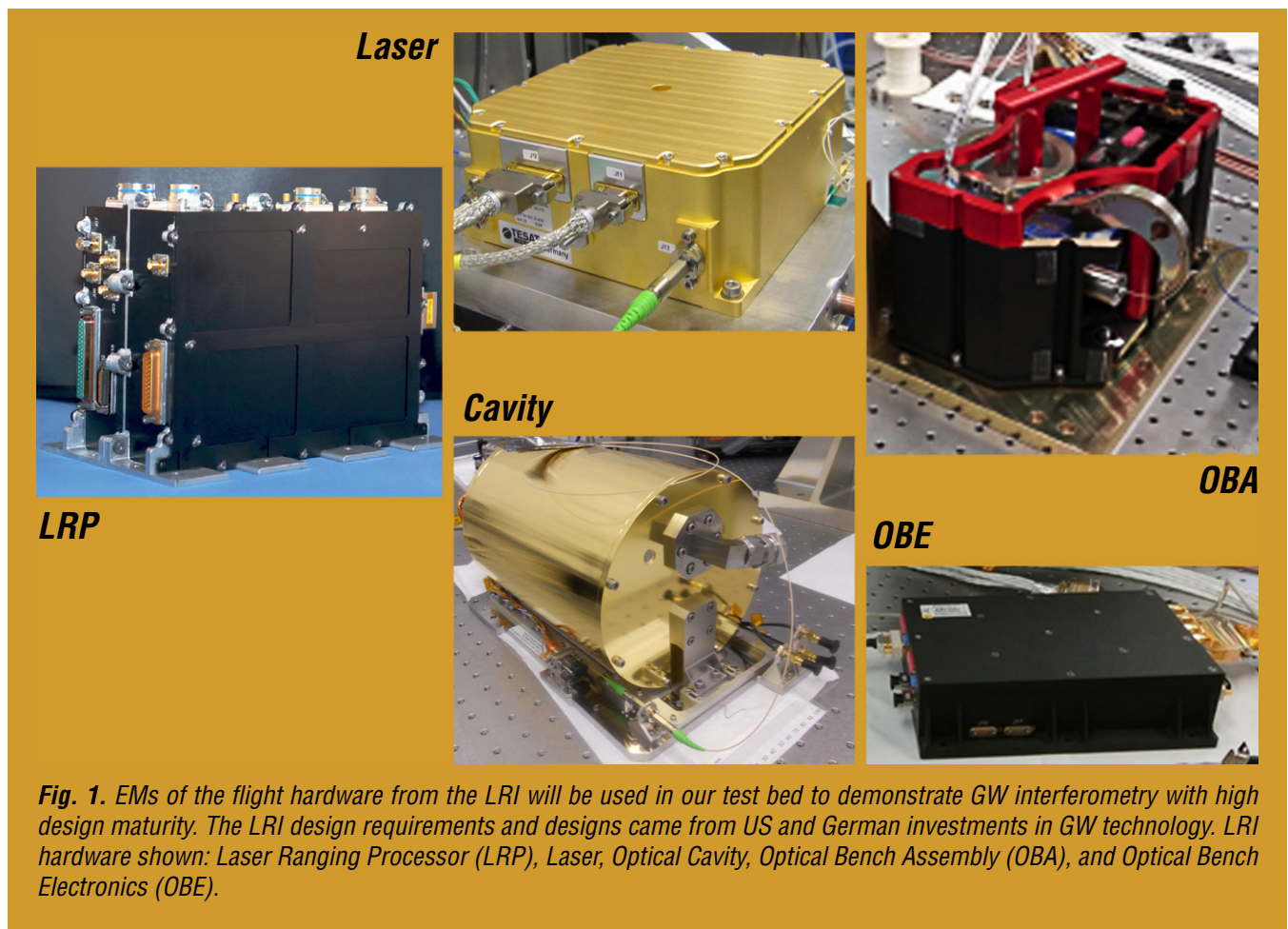


Fig. 1. EMs of the flight hardware from the LRI will be used in our test bed to demonstrate GW interferometry with high design maturity. The LRI design requirements and designs came from US and German investments in GW technology. LRI hardware shown: Laser Ranging Processor (LRP), Laser, Optical Cavity, Optical Bench Assembly (OBA), and Optical Bench Electronics (OBE).

Parameter	LRI	LISA
Measurement noise	0.08 micron/ $\sqrt{\text{Hz}}$	2×10^{-5} micron/ $\sqrt{\text{Hz}}$
Shot noise	10 pm/ $\sqrt{\text{Hz}}$	7 pm/ $\sqrt{\text{Hz}}$
Photoreceiver noise	1 nm/ $\sqrt{\text{Hz}}$	
Phasemeter noise	1 nm/ $\sqrt{\text{Hz}}$	
Optical path-length noise	30 nm/ $\sqrt{\text{Hz}}$	
Laser frequency noise	35 nm/ $\sqrt{\text{Hz}}$	
Ultra-Stable Oscillator noise	1 nm/ $\sqrt{\text{Hz}}$	
Satellite separation	170 – 270 km	5 million km
Satellite relative velocity	$< \pm 3$ m/s	$< \pm 15$ m/s
Wavelength	1064 nm	1064 nm
Phase precision	40 microcycle/ $\sqrt{\text{Hz}}$	1 microcycle/ $\sqrt{\text{Hz}}$
Nominal carrier-to-noise density ratio (CNR)	>75 dB-Hz (single phasemeter channel)	>75 dB-Hz (single phasemeter channel)
Intermediate Frequency (IF) Signal frequency	4-16 MHz	2-18 MHz
IF Signal dynamics (@1Hz)		
Before frequency stabilization	50 kHz/ $\sqrt{\text{Hz}}$	5 kHz/ $\sqrt{\text{Hz}}$
After frequency stabilization	30 Hz/ $\sqrt{\text{Hz}}$	300 Hz/ $\sqrt{\text{Hz}}$
Science bandwidth	2 mHz to 0.1 Hz	0.1 mHz to 1 Hz
Rx optical power	80 pW	80 pW
# of phasemeter channels	4	64
Analog-to-Digital Converter (ADC) clocking rate	38.656 MHz	50 MHz
Time coordination	GPS (laser ranging could be used)	Laser ranging code
Laser phase locking	Required	Required
Pointing information	Wavefront sensing	Wavefront sensing

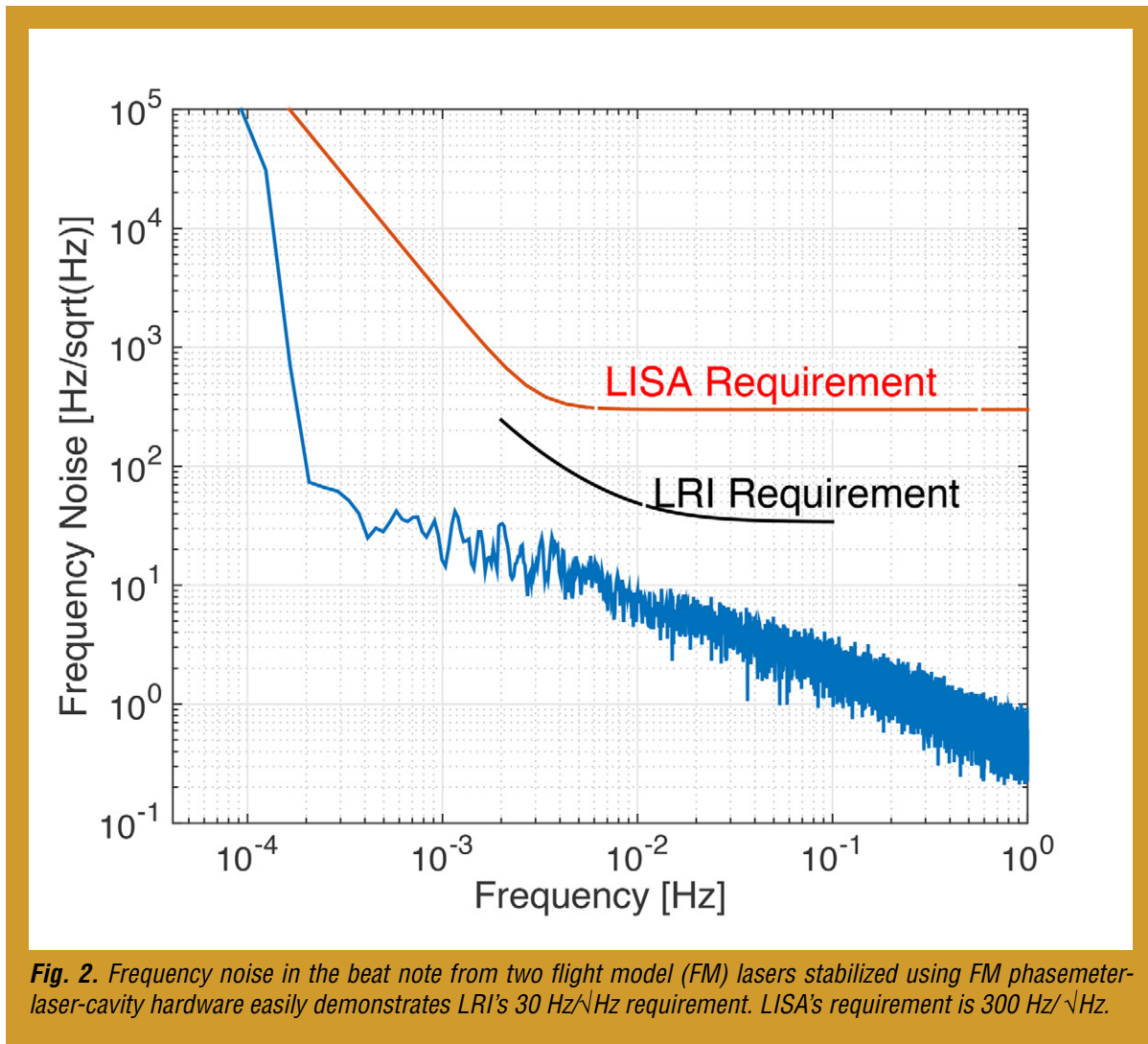
Table 1. LRI requirements are closely matched to LISA requirements. The primary differences are that LRI has tighter laser-frequency-noise requirements (demonstrated) and LISA requires more tracking channels, including multiple channels per signal stream. LRI will fly LISA phasemeter algorithms.

The LRI phasemeter has demonstrated the following LISA-relevant requirements:

- Microcycle phase measurement of heterodyne signals with CNR of 70 dB-Hz from 4-16 MHz from quadrant photoreceivers
- Differential wavefront sensing and steering mirror control
- Phase locking of a flight non-planar ring oscillator (NPRO) laser at 70 dB-Hz
- Laser stabilization of a flight NPRO laser to a flight cavity (data shown in Fig. 2)

The primary functions being added to the LRI phasemeter are the ability to track multiple tones, tracking of a clock-correction signal, and the time/range code used to align time from multiple data streams. These algorithms will be migrated using the same process that was used to migrate the LabView phasemeter algorithms for phase tracking, phase locking, and Pound-Drever-Hall laser-frequency stabilization.

Incorporating these EMs into our LISA phase-measurement test bed, modified to provide low-visibility signals, will advance the GW technology development, just as it was instrumental in seeding the application to Earth Science. GRACE Follow-On is scheduled to launch in August 2017.



Path Forward

Once our work is completed on LRI for the GRACE Follow-On mission, we plan to restart our efforts on this SAT project, building on our LRI work.

For additional information, contact William Klipstein: bill.klipstein@jpl.nasa.gov



William Klipstein

Laser Frequency Stabilization

Prepared by: John Lipa (Stanford University)

Summary

Missions such as the Laser Interferometer Space Antenna (LISA) and the Space-Time Asymmetry Research (STAR) mission [1, 2], require the ultimate in laser stability. Highly stable lasers are also important for a number of other astrophysical and fundamental physics missions that have been proposed, from the Gravity Recovery and Climate Experiment II (GRACE-II) to the Laser Astrometric Test of Relativity (LATOR) [3], and more recent alternatives to LISA.

When combined with a space-qualified optical frequency comb (currently under development at the Jet Propulsion Laboratory, JPL [4]), extremely high-sensitivity spectroscopy over the entire near-infrared band is possible. This allows easy detection of trace gases in acquired samples, such as within the International Space Station, from a cometary surface, or with a Mars rover, achieving sensitivities up to 100 times that of conventional techniques [5]. This technology could also contribute to crew safety via early fire detection on long duration missions, and improve exploration capability in distant environments. The capability would also be available for ground applications such as advanced atomic clocks, gravity gradiometers, and optical-frequency standards. Other longer-range uses include medical applications, such as detection of volatile organic compounds for cancer screening and forensics, and in trace atmospheric gas studies using Light Detection and Ranging (LIDAR) [6].

Our technical objective is to advance the development of a laser-stabilization scheme with very low noise into a compact, low-power unit that can be used in space for missions requiring extreme optical-frequency-stabilization performance. The device will operate at a wavelength near 1565 nm using low-pressure carbon monoxide (CO) gas as a molecular reference, with the possibility of later migrating to near 1064 nm. The core technology has been demonstrated in the laboratory over the past 15 years. The ultimate performance as a stabilization system using CO is based on calculation, and is expected to approach the performance of ultra-cold neutral-atom clocks requiring multiple lasers and an extensive amount of equipment. Our project objectives are:

1. Demonstrate the lowest short-term noise performance to date using a molecular gas transition as the reference medium.
2. Upgrade the device design from the optical bench level toward a brass-board level, focusing on compactness, power, and portability.

Our team consists of the principal investigator, John Lipa, and members of Stanford University's optics groups, with consulting from Prof. Jan Hall of the Joint Institute for Laboratory Astrophysics. Project start date was January 1, 2013, with a two-year period of performance. A six-month no-cost extension was obtained to allow additional measurements to be made.

The main accomplishments for the past year have been continued improvement of the entire laser-stabilization system's performance, making noise measurements with reference to an independent standard, and starting the move towards a brass-board configuration.

Background

This project supports the goals of the Astrophysics Division by raising the Technology Readiness Level (TRL) of hardware that will increase our knowledge of fundamental laws of nature through improved

laser-frequency stability in space missions. It directly supports the Strategic Astrophysics Technology (SAT) program “Physics of the Cosmos” (PCOS) theme. When applied in new space missions, the technology would have a direct impact on cosmology and astrophysics by improving our knowledge of the physics of the early universe. The primary NASA science question supported by this project is given in the 2010 Science Plan for the Science Mission Directorate (SMD): “*How do matter, energy, space, and time behave under the extraordinarily diverse conditions of the cosmos?*” This is derived from the goal: “*Discover how the universe works, explore how the universe began and developed...*” Our objective is to develop an extremely stable laser using advanced molecular-transition interrogation techniques. The instrument can support improved signal/noise in gravitational-wave detection; scientific measurements related to the isotropy of space and the variation of clock frequencies with gravitational potential; and frontiers of research in testing the limits of Einstein’s theories of space, time, and gravity.

The second baseline objective for Astrophysics in the NASA Science Plan for 2007-2016 is: “*Investigate the nature of space-time through tests of fundamental symmetries.*” Improved laser stability is an important aspect of technology development to support this objective. In the case of the search for Lorentz violations in the velocity of light due to boost, one needs to compare a cavity ‘clock’ with another reference such as a spectral line. This is the modern analog of the Kennedy-Thorndike experiment [7], one of the essential experimental foundations of special relativity. Atomic- or molecular-clock stability and noise performance are critical features of such an experiment. Hardware development for a space experiment of this type is proceeding at a low level as the STAR program, mentioned earlier.

Our project supports the National Research Council (NRC) 2010 Decadal Survey, New Worlds, New Horizons in Astronomy and Astrophysics (NWNH) via improved technology for gravitational-wave detection in space. LISA requirements appear to be satisfied with free-running YAG lasers [8] using a combination of time-delay interferometry [9] and arm-locking [10]. However, it should be remembered that 14 orders-of-magnitude noise reduction is needed for a free-running laser to make the measurements, a tall order for any electronic processing system. A prudent design would carry a very high margin of safety for dealing with real-world electronics issues on the LISA spacecraft. With the elimination of the American contribution to LISA and the search for cheaper alternatives by the science community and core teams established by the PCOS Program Office, it is clear that improved lasers would lessen the strain on some of the electronic systems contributing to the overall error budget. This would then allow a wider trade space to potentially reduce mission cost and architecture complexity, for example by using a shorter baseline than LISA, but with improved strain resolution.

Improved frequency stabilization using molecular gases allows lower-noise measurements or shorter measurement times for various physical phenomena. We project a theoretical improvement of up to a factor of 50 in noise reduction for measurement times of up to 10^4 sec using a CO molecular-referenced laser as opposed to an iodine-stabilized laser, the current state-of-the-art. An example of the current status of iodine-laser frequency control is given in Argence *et al.* [11]. The demonstrated noise performance of this iodine system ‘meets’ LISA specs but requires 14 orders-of-magnitude further noise reduction using interferometry and arm-locking techniques. Our approach tries to reduce the basic laser noise further, allowing some relaxation of signal processing requirements and broadening the trade space for the optics system. An essential feature of our approach is the use of cavity resonance techniques to enhance the signal from a low-pressure gas sample with a very narrow molecular-transition line-width. The top-level development plan is to develop the spectroscopy setup for the CO transition of interest at the laboratory instrument level, then transition to a design closer to flight prototype level, with which the desired performance can be demonstrated.

Objectives and Milestones

The overall aim of our work is to develop greatly improved laser-frequency stabilization using a molecular gas. The intent is to advance the state of the art from TRL 3 to 4+. The approach is to use a resonant optical cavity to amplify the optical field applied to a low-pressure gas contained in a specially designed cell, and create the conditions for very-high-resolution molecular spectroscopy. The spectroscopic signal is then used to lock the laser frequency to a quantum-mechanical transition in the molecule.

The work is loosely divided into four main phases. The first phase involved setting up a basic benchtop spectroscopy system operating with a CO gas cell. This part was completed on schedule. We also set up a medium-finesse Ultra-Low Expansion (ULE) cavity and thermal control system to act as a short-term optical reference system. This system has now been integrated into the main optics assembly and testing has commenced.

The second phase involved converting the instrument to the breadboard level. The optics system has been simplified and repackaged into a more-compact instrument using fiber-coupled components where possible. A significant step in this process involved placing the gas cell in a small vacuum chamber to provide easier pressure and thermal control of critical optical components. This setup was not intended to replicate the vacuum environment of space, but to eliminate conductive and convective heat transfer, reducing thermal drift and frequency fluctuations from air gaps in the optics that existed in earlier cell designs. It did not include the free-space components of the system because these are commercial parts, not designed for use in vacuum. Nevertheless, the vacuum operation gave some information related to space behavior. The more-extensive round of vacuum testing envisaged in our proposal was curtailed to allocate more resources for solving the cell and laser development difficulties encountered in the first year of the project.

The third phase involved operating the system extensively to demonstrate functionality and start performance testing. To demonstrate frequency-stability performance, we need a second independent unit to allow comparison measurements. Originally, we planned to construct a second set of optics and gas cell, and a duplicate set of electronics. Due to the difficulties encountered early in the program with laser stability and cell development, we opted instead to make use of a frequency-stabilized optical-comb system that became available in another part of the building. This comb was fortuitously set up to cover the wavelength of interest in our project: near 1565 nm. As a backup, a temperature-controlled high-finesse cavity was also set up for short-term noise measurements.

The final phase is ongoing and involves upgrading the system using the lessons learned to date, and implementing some critical electronics items at the board level to reduce noise and provide a path to flight-like designs. To minimize unnecessary development effort, board-level work has been restricted to functions not already demonstrated elsewhere at TRL 5 or above. Testing and upgrading has become a continuous process during this period. A major technology milestone in this phase will be performance demonstration at a fractional frequency stability f/f of 2×10^{-15} or better with 1 sec averaging. This is about seven times the estimated photon noise-limited performance with CO, and an order of magnitude better than iodine.

Key Milestones

Status

- | | |
|--|---------------------|
| 1. First turn-on of complete bench-top system | completed June 2013 |
| 2. First turn-on of optical cavity reference setup | completed Oct 2013 |
| 3. Bench-top system operational with CO. | completed Oct 2014 |
| 4. Completion of flight prototype gas cell | completed May 2014 |
| 5. Completion of breadboard instrument assembly. | completed Sep 2014 |
| 6. Start testing in vacuum environment | deleted |

7. Complete first round of vacuum testing deleted
8. Complete upgrade of bench-top system completed May 2015
9. Complete breadboard performance testing (in progress). July 2015

Progress and Accomplishments

During the past 12 months, we have succeeded in developing a laser-stabilization system based on a rotational-vibrational molecular transition in low-pressure CO gas. It is configured to act as a highly stable frequency standard. To our knowledge, this is the first time such a system has been set up. The only comparable system [12] used deuterated ethane gas, C₂HD. The use of CO is expected to lead to a higher-stability system and also allows the use of optical components readily available in the telecom optical waveband near 1550 nm. A block diagram showing the main components of the system is shown in Fig. 1.

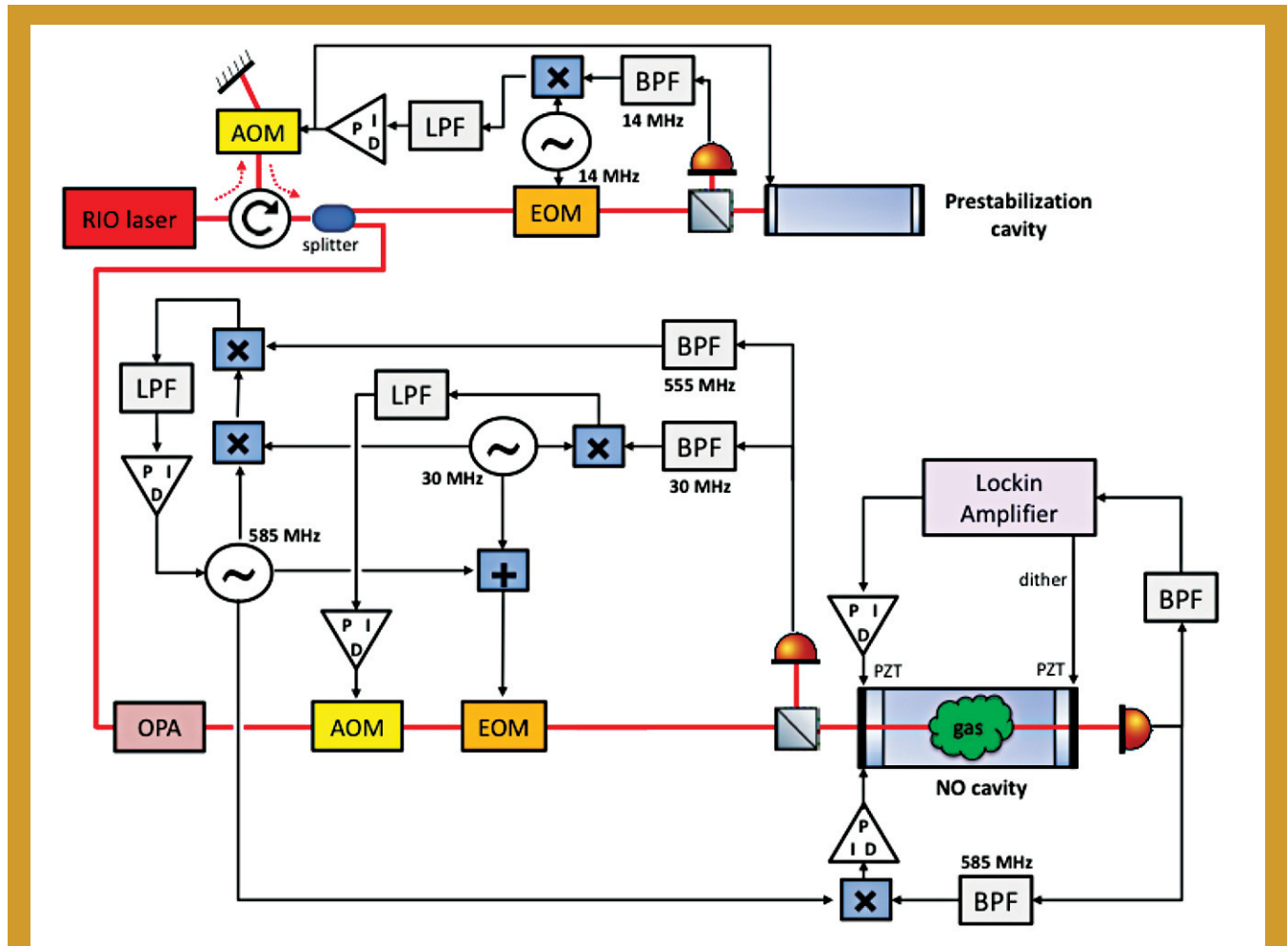


Fig. 1. Functional block diagram of laser control system showing main feedback loops (AOM, Acousto-Optic Modulator; BPF, Band-Pass Filter; EOM, Electro-Optic Modulator; LPF, Low-Pass Filter; NO, NICE-OHMS, Noise-Immune Cavity-Enhanced Optical Heterodyne Molecular Spectroscopy; OPA, Optical Power Amplifier; PID, Proportional Integral Differential controller; PZT, PieZo-electric Transducer; RIO, Redfern Integrated Optics; x, mixer; +, summing amplifier). Red lines are optical paths, black are electrical.

The laser (shown in red) is first pre-stabilized using an optical cavity-locking scheme that compensates for the frequency noise via an AOM. The servo loop has a high bandwidth and reduces the laser noise by more than an order of magnitude. A second, slow loop adjusts the resonant frequency of the cavity to track the average frequency of the laser light. This pre-stabilized light is then fed into the gas cavity via an optical power amplifier for further stabilization. In this second stage, the frequency of the light is locked to the resonant frequency of a very-high-finesse cavity using a second AOM. This cavity is filled with the low-pressure CO gas. Sidebands are added to the input light using an EOM at a frequency corresponding to the free-spectral range of the cavity, near 585 MHz. These sidebands pass through the cavity and are detected by a photo-detector in transmission. The interference between the sidebands and the carrier on the photo-detector generates a phase signal that encodes the difference between the carrier frequency and the resonant frequency of the gas molecular transition. This signal is then used to adjust the resonant frequency of the cavity to that of the transition using a piezo-electric transducer. Since the input light is locked to the cavity, it is then also locked to the gas transition. The cavity provides another function, greatly boosting the laser intensity where it interacts with the gas to narrow the transition linewidth to the so-called ‘sub-Doppler’ region. In this region, the photons preferentially interact with molecules traveling transverse to the beam, reducing thermal motion broadening. An additional optional stabilization loop using a lock-in amplifier is shown in the figure. This loop uses a low-frequency (~ 500 Hz) modulation or dither of the cavity length to allow second-harmonic detection of the phase signal from the gas. To study the noise on the stabilized light, we transmit a portion of it to another laboratory via a fiber-optic link where it can be compared with other frequency standards using an optical frequency comb.

As noted last year, significant problems were encountered with the development of the gas cell and with the laser. Overcoming these issues required a great deal of unplanned effort, and put us behind schedule. We now have a fully working system and are engaged in performance testing and iterative upgrades of the electronics. The successful laser configuration involved a planar external cavity laser with a Bragg grating from RIO, coupled with the pre-stabilization cavity we built, operating near 1565 nm. The successful gas cell was the third generation unit in which a high-finesse optical cavity was immersed in a small vacuum system that can be filled with low pressure gas. The internal construction of the device is shown in Fig. 2. The central tube in the figure is made from ULE glass to reduce the need for active

temperature control. There are piezo-electric transducers and low-loss mirrors on each end of the tube to form an optical resonator with a slightly adjustable length. With this design, the only optical losses are from the cavity mirror coatings and the gas itself. This allowed us to achieve optical saturation of the gas molecular transitions, needed for laser stabilization. This so-called sub-Doppler effect [5] produces a narrow line feature on top of the Doppler-broadened line as shown in Fig. 3. The trace shows the optical power transmitted through the cell as a function of its resonant frequency at a pressure of 10^{-2} Torr. The inner portion of the Doppler line is shown by the wide parabola. The sub-Doppler feature is the small peak near the minimum of the parabola. Its presence indicates all optics conditions for locking the laser to the gas spectral line are met.

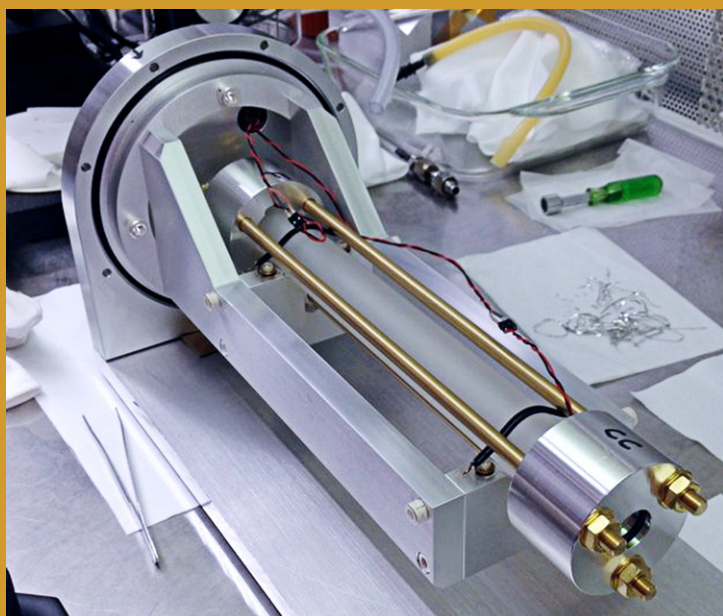
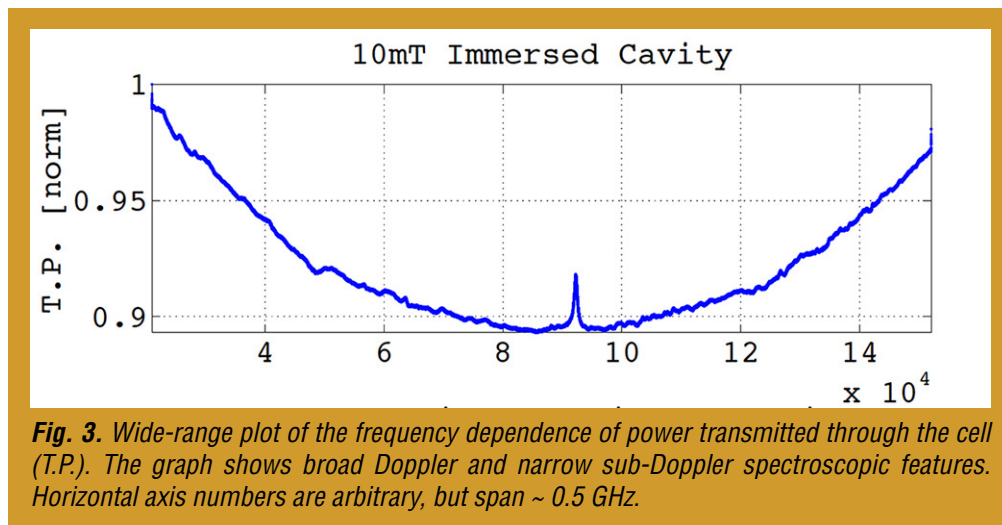
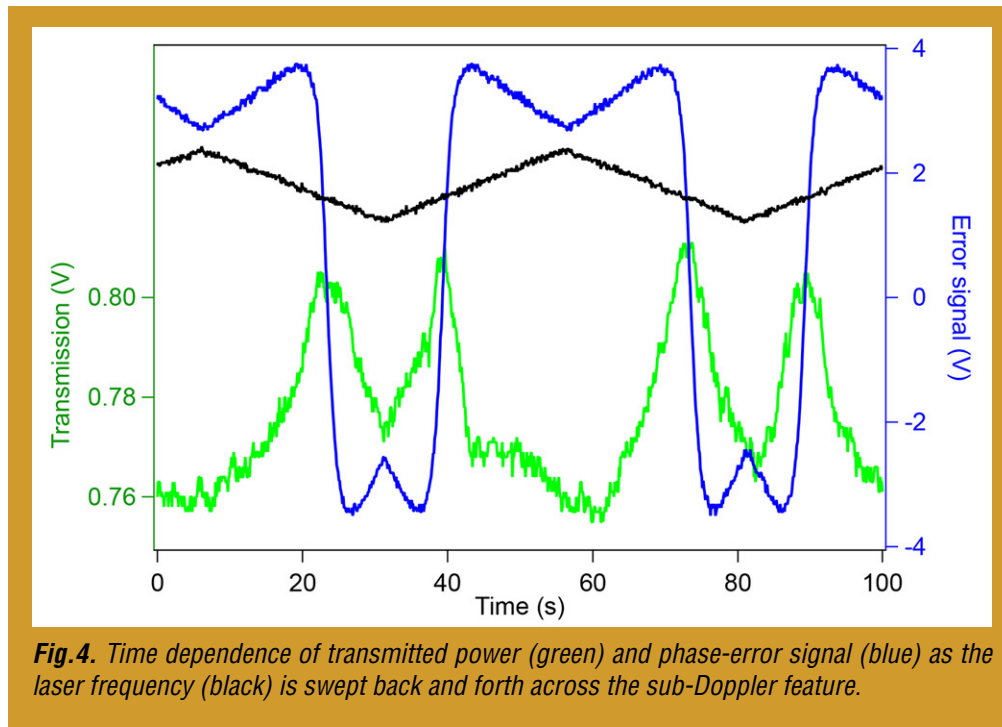


Fig. 2. Optical cavity installed in vacuum can.



The most important feature for locking the laser to the sub-Doppler feature is the variation of the optical phase of the demodulated transmission signal as the feature is crossed. The phase and transmitted intensity as a function of optical frequency are shown in Fig. 4.



The associated opto-electronics consists of multiple commercial optical components and detectors operating at a wavelength of 1565 nm, mounted on a highly stable optical table. Two views of the setup are shown in Fig. 5. In the section near the laser, the components are fiber-coupled, while near the optical cell they are free-space-coupled. Some free-space components are inevitable because of the need for precision control of the wavefront shape at the cell entrance mirror. However, most of the optics can be converted to fiber-coupled components, well-suited for brass-board demonstrations. Loops of excess fiber shown in the figure can easily be eliminated in a flight design.

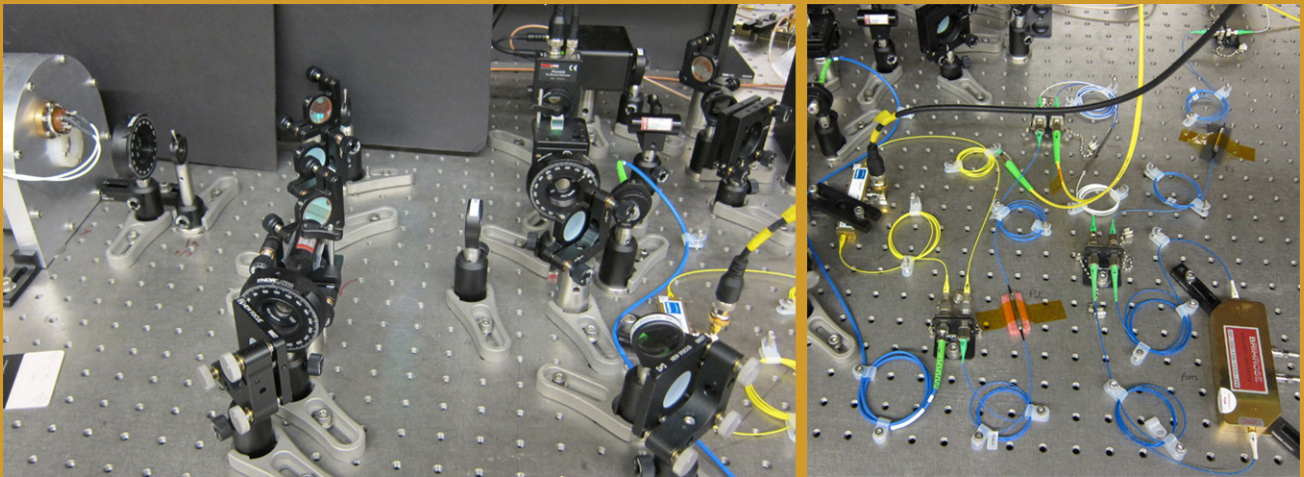


Fig. 5. System optics. Left: free-space optical components; right: fiber-coupled components.

Figure 6 shows the pre-stabilizer cavity system, a modified version of the reference cavity system described in our 2014 report. The main changes were adding a piezo transducer to the cavity in the vacuum system and fiber-coupling the light from the laser to the optics used to lock the cavity frequency to that of the laser. A new, higher-quality reference cavity has now been built and is under test.

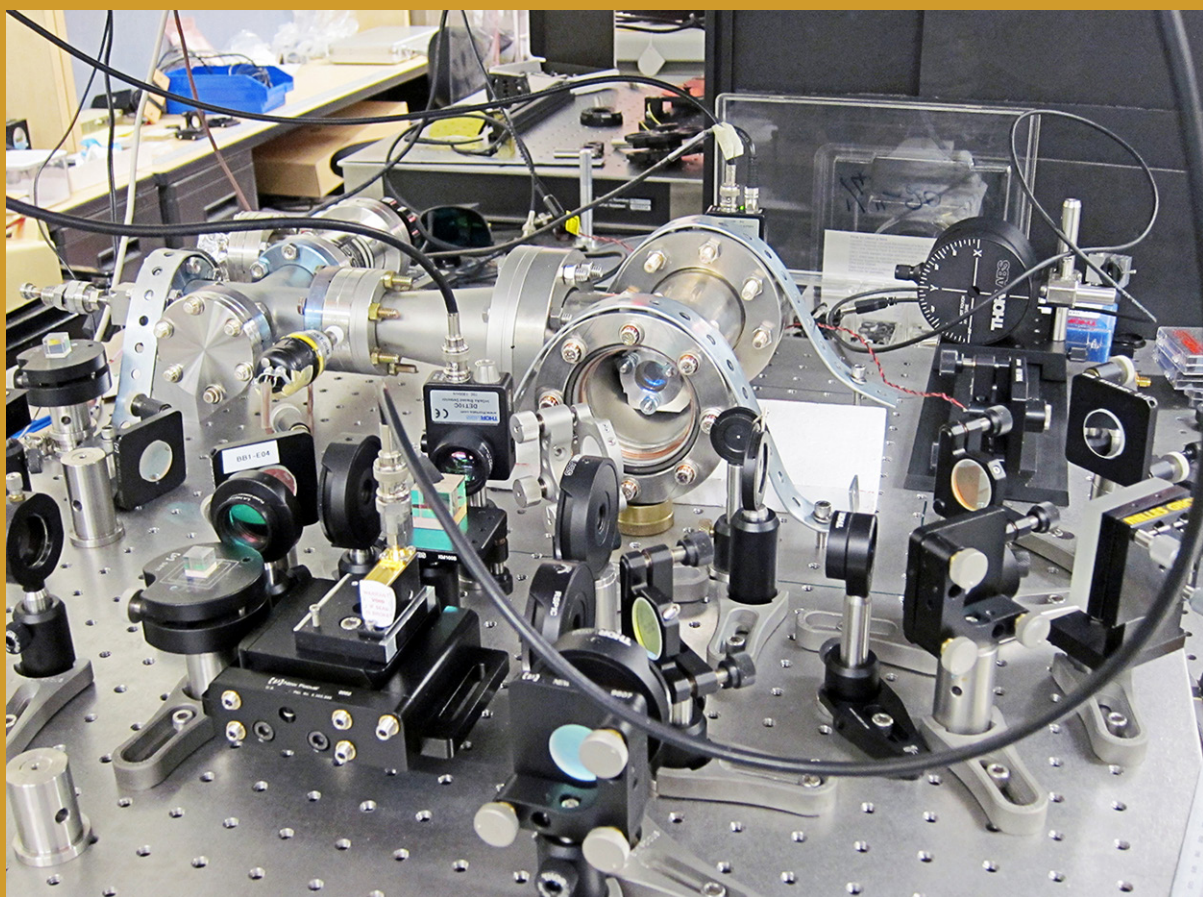


Fig. 6. Pre-stabilizer cavity optical system.

As mentioned above, system noise tests were conducted using an optical-frequency comb available in another laboratory. This setup can be stabilized using either Global Position System (GPS) timing signals or by reference to a highly stable optical resonator. Some Allan deviation results from this comparison are shown in Fig 7. The purple trace shows a measure of the comb stability when it is locked to GPS. The pale blue trace is the CO system relative to the comb. It is clear that over most of the band, stability is limited by the GPS. The green trace shows the CO system compared to the comb locked to the reference Fabry-Perot cavity (FPC), showing better stability than with GPS. We are currently working on additional noise reduction strategies including using a resonant photo-detector for the gas servo and a lock-in amplifier technique mentioned above. This method has recently produced the sub-Doppler signal shown in Fig. 8 that looks very promising. The next step will be to extract phase information from this signal.

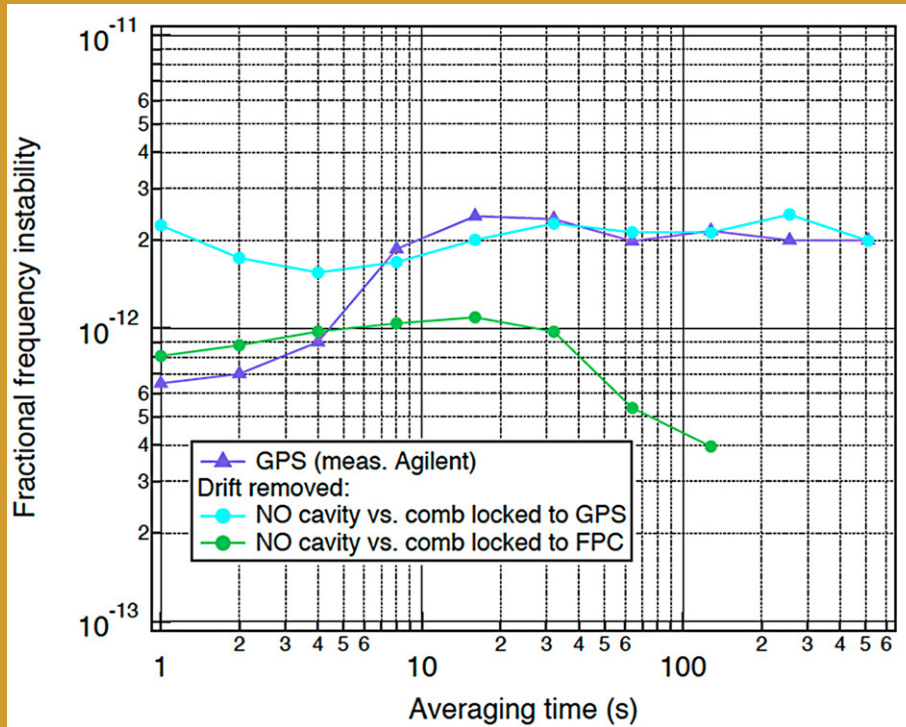


Fig. 7. Allan deviation results for gas stability. See text for explanation of curves.

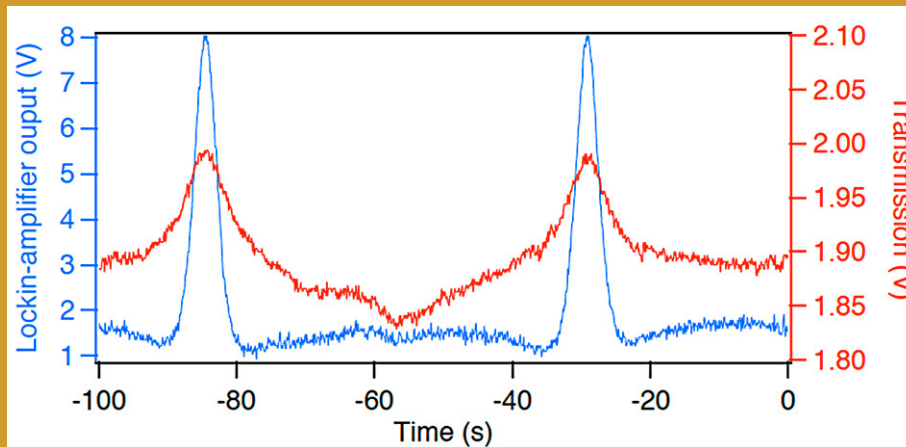


Fig. 8. Comparison of raw transmission sub-Doppler data (red) with that from the lock-in technique (blue).

Path Forward

We are rapidly approaching the end of the project and will be concentrating our efforts on noise reduction. The project will be continued for at least another year with separate funding.

References

- [1] C. Braxmaier *et al.*, “*The Space-Time Asymmetry Research (STAR) Program*,” Proc. 24th Eur. Freq. and Time Forum, EFTF 2010 (April 2010)
- [2] J. A. Lipa *et al.*, “*Prospects for an advanced Kennedy-Thorndike experiment in low Earth orbit*,” arXiv: 1203.3914 (2012)
- [3] S. G. Turyshev *et al.*, “*Space-based research in fundamental physics and quantum technologies*,” Proc. Quantum to Cosmos-II Mtg (Bremen, June 2007), to be published
- [4] N. Yu, JPL, private communication (Jan. 2012)
- [5] A. Foltynowicz *et al.*, “*Noise-immune cavity-enhanced optical heterodyne molecular spectroscopy: Current status and future potential*,” Appl. Phys. B **92**, 313 (2008)
- [6] P. Meras Jr. *et al.*, “*Laser frequency stabilization for coherent LIDAR applications using novel all-fiber gas reference cell fabrication technique*,” 24th International Laser Radar Conference (ILRC), Boulder, CO (2008)
- [7] R.J. Kennedy and E.M. Thorndike, “*Experimental Establishment of the Relativity of Time*,” Phys. Rev. **42**, 400 (1932)
- [8] “*LISA Mission Formulation: Requirement Breakdown*,” EADS Astrium Technical Note, LISA ASDTN-5001 (27 Nov. 2009)
- [9] M. Tinto, F.B. Estabrook, and J.W. Armstrong, “*Time-delay interferometry for LISA*,” Phys. Rev. D **65**, 082003 (2002)
- [10] K. McKenzie, R.E. Spero, and D.A. Shaddock, “*The performance of arm locking in LISA*,” arXiv:0908.0290v2 [gr-qc] (2009)
- [11] B. Argence *et al.*, “*Molecular laser stabilization at low frequencies for the LISA mission*,” Phys. Rev. D, 82002 (2010)
- [12] L-S. Ma *et al.*, “*Ultra-sensitive frequency-modulation spectroscopy enhanced by a high-finesse optical cavity*,” J. Opt. Soc. Am. B, **16**, 2255 (1999)

For additional information, contact John Lipa: jlipa@stanford.edu



John Lipa

Telescopes for Space-Based Gravitational-Wave Observatories

Prepared by: Jeffrey Livas (NASA/GSFC)

Summary

Telescope development for gravitational-wave detection began in Fiscal Year (FY) 2012 with a funding award from the Physics of the Cosmos (PCOS) Program, and is funded until FY 2014 with a two-year Strategic Astrophysics Technology (SAT) grant. A no-cost extension will enable work to continue through the end of FY 2015. A follow-on SAT grant has just been awarded to continue this work through FY 2017.

The goal is to develop a telescope suitable for precision metrology for a space-based gravitational-wave observatory [1-4], where the baseline application is to measure the separation of two spacecraft with a precision of 10^{-11} m/ $\sqrt{\text{Hz}}$ (10 pm/ $\sqrt{\text{Hz}}$) over several million kilometers. The telescope technology study effort will develop a set of suitable requirements for the gravitational-wave metrology application and investigate the two key design challenges with modeling, analysis, and experiments. We have adopted the evolved Laser Interferometer Space Antenna (eLISA) [3] as the reference mission.

The work is supported by a team of engineers from the NASA Goddard Space Flight Center (GSFC) Optics Branch; a mechanical engineer from the GSFC Mechanical Engineering Branch; and a postdoctoral fellow, Shannon Sankar, currently a CRESST/USRA (Center for Research and Exploration in Space Science & Technology/Universities Space Research Association) scientist (detailed listing in Table 1).

Name	Expertise
Jeff Livas	PI
Peter Blake	Mirror fabrication
Edward Bragg	Procurement/alignment
John Crow	Mechanical
Joseph Howard	Optical designer
Shannon Sankar	Stray light measurement
Lenward Seals	Stray light
Ron Shiri	Electro-magnetic (EM) modeling
Garrett West	Optical design

Table 1. The eLISA Prototype Telescope Team.

The most significant accomplishments from the past year are the construction of a scattered-light test-bed and the delivery of a prototype telescope that we plan to use to validate our scattered-light model. A summary of the telescope requirements, design, and results has been published previously [5].

Background

The telescope technology development targets the requirements for displacement measurement for space-based gravitational-wave detection. Gravitational waves are generated by any mass distribution with a time-changing quadrupole moment [6]. The simplest example is a pair of gravitationally bound masses orbiting around a common center of mass. The efficient generation of gravitational waves requires large compact objects moving at a large fraction of the speed of light. The canonical source is a pair of million-solar-mass black holes colliding. It is believed that black holes of this size are co-located at the centers of galaxies, and therefore this type of source represents collisions of pairs of galaxies, one of the ways large-scale structure is formed in the universe. The estimated event rate is between 10 and 100 mergers per year, *i.e.*, from once per month to twice per week.

LISA addresses a number of science goals [7-9] and was specifically endorsed by the 2010 Decadal Survey, “*New Worlds, New Horizons in Astronomy and Astrophysics*” (NWNH) as the third-priority large-scale space mission (NWNH, Table ES.5, p. 8.) for three specific reasons:

- Measurements of black-hole mass and spin will be important for understanding the significance of mergers in the building of galaxies;
- Detection of signals from stellar-mass compact stellar remnants as they orbit and fall into massive black holes would provide exquisitely precise tests of Einstein’s theory of gravity; and
- Potential for discovery of waves from unanticipated or exotic sources, such as backgrounds produced during the earliest moments of the universe or cusps associated with cosmic strings.

Examples of other expected science returns are the study of galactic populations of binary stars [10] and precision determination of cosmological distances in a manner independent from electromagnetic determinations [11].

The function of the telescope for the LISA baseline space-based gravitational-wave observatory mission is to function as a precision beam expander to deliver optical power efficiently from one spacecraft to another [12]. The telescope design for a space-based gravitational-wave mission is based on a near-diffraction-limited classical Cassegrain-style reflecting optical system. However, since the application is precision-displacement measurement rather than image formation, the normal requirements for high-quality image formation must be augmented by two challenges that require development:

1. The requirement for picometer-level optical-path-length dimensional stability through the telescope in the presence of both axial and transverse temperature gradients.
2. The requirement for low scattered-light levels. Scattered-light levels must be extremely low because the distance measurement uses interferometric techniques that are very sensitive to low light levels and because the telescope must simultaneously transmit a 1W beam and receive a 100 pW beam.

Typical imaging applications do not have these additional requirements.

The long-term goal of this telescope technology-development effort is to make a prototype telescope that meets the basic requirements for a space-based gravitational-wave observatory and bring it to Technology Readiness Level (TRL) 5 in time to be a serious candidate for a mission within the European Space Agency (ESA) L3 Cosmic Visions program. As of 2015, the best indication we have from ESA is for the technology to be ready by 2019 (see next section), which requires sustained development for the telescope. The immediate goal of the effort as currently funded should result in a prototype with TRL 3 that can be used to validate a model of the scattered-light performance of the complete telescope and relate it to the properties of the individual mirrors. Additional work, not currently funded, will be required to reach TRL 4 and then 5.

Objectives and Milestones

Overall Objectives in the Context of the International Community

Although the situation is both uncertain and fluid, Fig. 1 shows one possible timeline for development activities for an ESA-led mission up to the time of the next Decadal Survey. Activities in Europe (top section) and the US (center section with gray background) are shown separately. Shown is the launch and mission of the LISA Pathfinder technology demonstration mission, and development activities associated with ESA’s L2 Cosmic Visions program. Not shown are the activities associated with the L1 Cosmic Visions mission, Jupiter ICy moons Explorer (JUICE), scheduled for a 2022 launch. Also not shown are expected discoveries of gravitational waves by ground-based detectors (operations shown in bottom section), including the Laser Interferometer Gravitational-Wave Observatory (LIGO)/Virgo, and pulsar timing arrays such as the North American Nanohertz Observatory for Gravitational waves (NANOGrav). These anticipated discoveries may change the scientific landscape and context for a space-based mission.

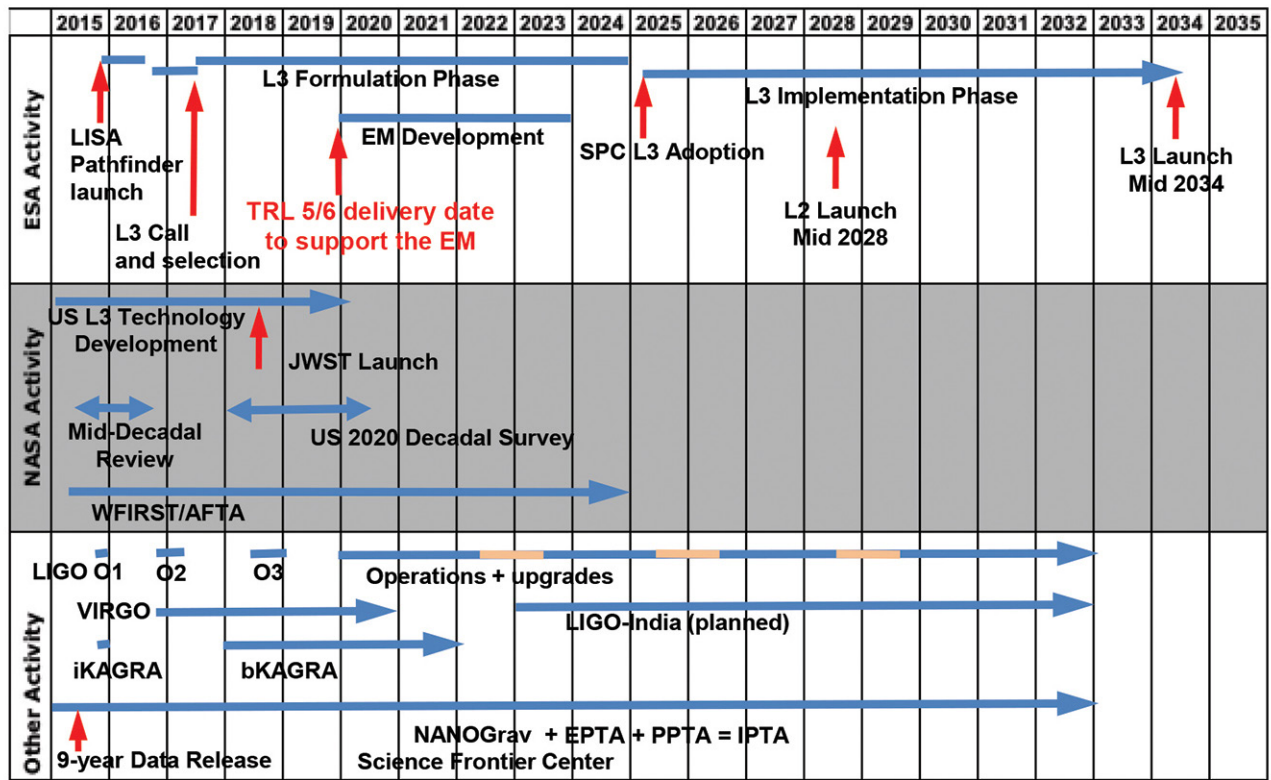


Fig. 1. A possible timeline for an ESA-led mission as part of the L3 Cosmic Visions Opportunity showing work in the US (middle section) and Europe (top section). Not shown are expected discoveries in the 2017-2018 timeframe by ground-based gravitational detectors (operations shown in bottom section), such as the LIGO/VIRGO network, KAmioka GRAvitational-wave telescope (KAGRA), and/or pulsar timing arrays (PTAs) such as the NANOGrav consortium.

The “Gravitational Universe” was selected as the science theme for ESA’s third large-class mission for the Cosmic Vision Program. With a nominal launch date in 2034, mission selection would nominally occur in 2022. However, ESA has established a special committee, the Gravitational Observatory Advisory Team (GOAT) [13] that is scheduled to provide a report to ESA in early 2016. ESA has also recently indicated that it has technology development funding available and may select a mission by the end of 2016, with an engineering model development program beginning in 2020. Therefore, technologies to be considered for the engineering model need to be at TRL 5-6 by 2019. We have adopted this timeline as a working schedule for now.

In this context, the objective of this work over the next few years is to advance the knowledge needed to build a telescope meeting the requirements so that the US can be a credible international partner for an ESA-led mission, as well as providing a compelling candidate for consideration in the next US Decadal Survey.

Objectives and Milestones Specific to Telescope Technology Development

The tasks and milestones specific to the work in progress are summarized in Fig. 2. The two milestones with notes in the blue framed box were key milestones in the original SAT proposal, and actual completion dates for some activities are also indicated at far right. Specific tasks that have been added include:

- Construction of an M3/M4 scattered-light test-bed;
- Procurement of the prototype telescope – contract kick-off June 19, 2014;
- Prototype telescope delivery – completed June 5, 2015 (originally March 28, 2015); and
- M3/M4 initial mirror delivery – completed September 25, 2014.

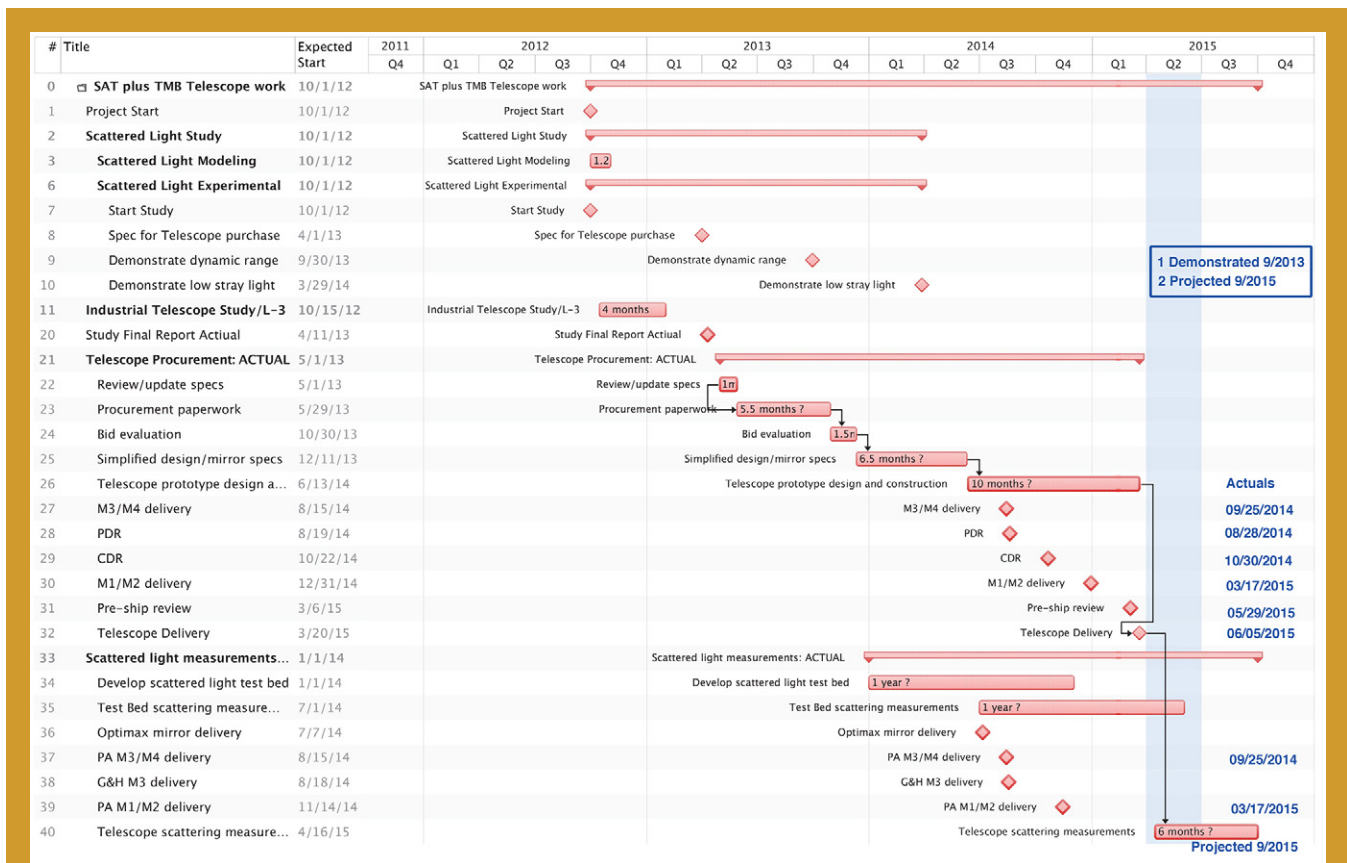


Fig. 2. Key project tasks and milestones. Two of the three original key milestones are framed in blue on the right-hand border of the schedule. The third is no longer planned due to cost constraints. Actual dates are listed at far right for some of the key sub-milestones. See Table 2 for the redefined milestones.

Overall, the work has been delayed by approximately one year, but with a no-cost extension, funding is sufficient to accomplish Key Milestone #2. Key Milestone #3, dimensional stability, has already been demonstrated on a telescope metering structure [14], but a full demonstration with a complete telescope including optics is outside the scope of the current project due to cost.

Progress and Accomplishments

Previous Accomplishments

The major accomplishment during 2012-2013 was to complete a study of the telescope design with an industrial contractor. The study included a complete thermal, optical, and a partial mechanical analysis of two implementations – an on-axis design and an off-axis design, and two material systems – carbon-fiber composite and silicon carbide. The study contractor was also required to develop plans for manufacturing and verification testing of these designs. The main results and recommendations are summarized below.

- An on-axis design does not meet the stray-light requirement, so use an off-axis design (on- vs. off-axis manufacturing complexity is similar);
- Use silicon carbide to avoid the unknown effects on dimensional stability from water absorption and subsequent out-gassing with composite materials; and
- The estimate for a ground prototype was a 16-month delivery with a cost of \$2.5M, including:
 - \$1.5M recurring engineering;
 - \$0.26M non-recurring engineering;
 - \$0.43M testing; and
 - \$0.22M focus mechanism.

Immediately after the study concluded on April 11, 2013, we initiated a request for quotes (RFQ) for building a prototype telescope based on the study results. The RFQ process ended October 24, 2013 with two bids. The lowest bid was approximately twice the available funding, and the proposal was not adequate technically. The other bid was about four times the available funding. At this point, we were forced to de-scope the work to extract the most value. We chose to concentrate on developing and validating a scattered-light model, rather than achieving a specific performance level for scattered light. This amounts to a redefinition of Key Milestone #2 (Table 2). In addition, we had to postpone testing the complete telescope for dimensional stability, since cost considerations forced us to choose materials for a room-temperature test-bed instead of the expected soak temperature of -70°C. We previously investigated silicon carbide for the metering structure and showed it can be stable enough. Given the cost limitations for this project, it seemed best to concentrate on developing experience with scattered light. We therefore fabricated the structure of the telescope out of conventional low coefficient-of-thermal-expansion (CTE) materials instead of the more expensive silicon carbide. A telescope meeting both the dimensional-stability and scattered-light requirements can be produced at a later time by combining the designs.

Year	Milestone	Date	Milestone Description	Redefinition	New Date
FY 2013	1	9/13	Stray light measurement capability	No redefinition – achieved. Demonstrated dynamic range of 10^{-10}	Achieved
FY 2014	2	3/14	Demonstration of scattered-light performance of $<10^{-10}$ of transmit power	Develop and validate a scattered-light model	9/15
FY 2014	3	9/14	Demonstration of optical-path-length stability	Not possible – materials and construction of a prototype that could be environmentally tested are too expensive	N/A

Table 2. Key milestones as redefined. No change from 2014.

We modified the telescope design from the one developed in the study, simplifying it while retaining its essential features. We then designed the mirrors for the simplified telescope design. We ordered a complete set of mirrors to build a prototype, as well as several sets of the two mirrors the model shows are the largest sources of scattered light, M3 and M4. The idea is to try different combinations of surface roughness and coatings to better understand how to achieve the scattered-light requirement and demonstrate we understand the physics.

Recent Accomplishments

We were able to find a vendor who agreed to build a complete prototype telescope to meet our requirements at room temperature, and held a kick-off meeting on June 19, 2014. We supplied a set of mirrors as Government Furnished Equipment (GFE). The critical design review (CDR) was held October 30, 2014, and the telescope was delivered to GSFC on June 5, 2015. Delivery was delayed by a 2-month delay in the primary and secondary mirrors from the mirror vendor, but the telescope integrator also experienced unanticipated problems with alignment. Ultimately, they were able to meet an important requirement, which is a wavefront error of $1/30^{\text{th}}$ of a wavelength through the telescope.

In parallel with the construction of a complete telescope, we designed a test-bed consisting of just M3 and M4, where we can test those two mirrors individually and as a subsystem. The test-bed is nearly aligned and almost ready to begin testing.

Figure 3 shows the telescope, a 4-mirror afocal design with a 200-mm-diameter primary, and a 5-mm collimated output beam. The left panel shows the path of the central ray through the telescope. The right panel shows a photo of the telescope as it was finally aligned in the vendor’s clean facility.

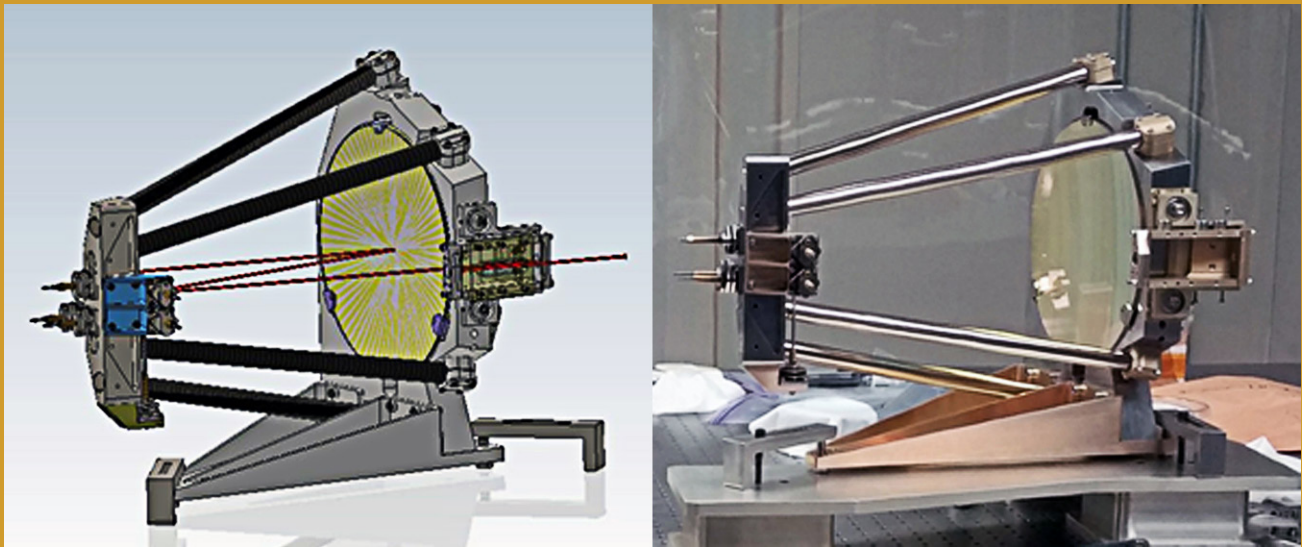


Fig. 3. *Prototype telescope. Left: drawing of the telescope with the central, or “gut” ray’s path through the telescope indicated by the solid brown line. The secondary is in the light blue mount to the left of the primary. Right: photo of the telescope as aligned in the vendor’s cleanroom.*

Both the telescope and the scattered-light test-bed are installed in the Laser Communication Relay Demonstration (LCRD) cleanroom, where we have arranged to share the space through the end of the calendar year. This arrangement allows us access to the clean room environment, which helps postpone the degradation we expect from particulate contamination. It also enables access to a key piece of test equipment (an interferometer). In return, LCRD has access to a key piece of our test equipment, a point-source microscope.

The immediate next step is to re-assemble and re-align the telescope. We expect alignment to take approximately three weeks, and then we will begin stray-light testing. The goal is to complete these measurements, and measurements with the scattered-light test-bed, by September 2015 (see Fig. 2). The desired result is a validation of the scattered-light model we have developed, not necessarily to achieve a specific level of performance. Understanding the model will allow us to better design a follow-on telescope to meet the required level of performance. In some cases this may result in a reduction in risk and cost as we understand which aspects of the design, particularly the mirror design, are essential and which are not.

Scattered-light suppression work was augmented with funding received by Ron Shiri through the GSFC Internal Research and Development (IRAD) program for development of partially transparent petaled masks. This funding enabled Ron to engage with the University of Delaware for fabrication of partially transparent masks.

Experimental efforts continue with Shannon Sankar making transmission measurements of the petaled masks designed by Ron. The goal is to understand the challenges and limitations of the different steps that must be followed to progress from a theoretical design to a working mask. A number of fabrication methods have been tested, and we are in the process of a quantitative comparison between theory and experiment for a circular mask for which we can calculate the expected response analytically. A publication is in preparation.

Successful implementation of these masks may allow us to adopt an on-axis telescope design, which may be less expensive to build and better suited to the application’s environmental requirements compared to an off-axis design.

Path Forward

The key milestones for the project are shown in Table 2 as originally proposed for the SAT grant. The first milestone is to demonstrate the ability to detect low levels of scattered light. This was successfully accomplished in the summer of 2013.

The second milestone is to demonstrate low-scattered-light performance with a prototype telescope. This milestone is still in progress. The telescope has just been delivered to GSFC at the beginning of June, almost three months later than the original date shown. The primary reason for this delay was late delivery of the primary and secondary mirrors. Now that the telescope is delivered, the immediate task is to realign it. The telescope was shipped disassembled to avoid damage to the mirrors during shipping. Alignment is in progress, and the new estimated completion date for scattered-light results remains September 2015.

As described in the previous section, we also intend to begin making measurements of scattered-light performance with a test-bed containing only M3 and M4, which we believe are the largest contributors to scattered light from the telescope. The test-bed has been assembled in the clean room, and needs only a final alignment with an interferometer before testing can begin. We expect the alignment to proceed in parallel to telescope alignment, since the same equipment is needed and we can practice on the test-bed before trying to align the complete telescope.

The third milestone is to demonstrate the optical-path-length stability requirement. This milestone is currently outside the capability of this development effort. It is not necessary to develop the path-length-stability measurement capability because the original plan was to take advantage of the capability already developed for measuring a silicon carbide spacer at the University of Florida [14-16]. In practice, some work will be required to adapt the existing setup to a real telescope with optics instead of just a metering structure, and to improve the temperature-measurement instrumentation, but the basic capability exists. A second iteration of the prototype telescope with more flight-like materials will be required to demonstrate dimensional stability. This second iteration is not currently funded, and would be undertaken ideally as follow-on work to the current grant. We submitted a grant application, “Telescope Dimensional Stability Study for a Space-based Gravitational-Wave Mission” for funding through the SAT program this year. We also contributed as a Co-PI toward a grant application with the title “Ultra-Stable Structures,” which is to investigate similar dimensional-stability requirements for large telescopes such as the Advanced Technology Large-Aperture Space Telescope (ATLAST) and a Large Ultra-Violet Optical Infra-red (LUVOIR) telescope.

An important extension of this work is to examine the possibility of including a small moving mirror as part of the design. This design extension is referred to as “in-field pointing,” which allows the telescope in principle to accommodate a large change ($\pm 1^\circ$) in the line-of-sight of the input beam without physically moving the telescope. The current baseline design has the telescope mounted as a complete assembly with the optical bench and the gravitational reference mass so that the entire assembly can be moved on a pivot. Preliminary work indicates that the basic design with a small steerable mirror may be optically possible, but that it may have implications on the scattered-light performance. This is a system-level aspect of the telescope design that no one else has investigated, and has the potential to be a show-stopper for this concept. We will evaluate the in-field pointing concept and its implications for scattered light to determine if it is feasible or not.

Acknowledgements

The author would like to thank P. Bender, G. Mueller, J. Sanjuan, A. Spector, R. Stebbins, and the members of the Gravitational-Wave Study Team for advice, support, and stimulating discussions.

References

- [1] P. Bender, K. Danzmann, and LISA Study Team, “*LISA for the Detection and Observation of Gravitational Waves*,” Max-Planck-Institut für Quantenoptik, Garching Technical Report No. MPQ233 (1998)
- [2] “*LISA Unveiling a Hidden Universe Assessment Study Report*” (Yellow Book), ESA/SRE (2011) 3
- [3] P. Amaro-Seoane *et al.*, “*The Gravitational Universe*,” eLISA L2 White Paper
- [4] “*Gravitational-Wave Mission Concept Study Final Report*,” (2012)
- [5] J. Livas, P. Arsenovic, J. Crow, P. Hill, J. Howard, L. Seals, and S. Shiri, “*Telescopes for Space-based Gravitational Wave Missions*,” *Opt. Eng.* **53** (9), 091811 (2013). doi: 10.1117/1.OE.52.9.091811
- [6] B.F. Schutz, “*Gravitational waves on the back of an envelope*,” *Am. J. Phys.* **52** 412 (1984)
- [7] P. Amaro-Seoane *et al.*, “*Low-frequency gravitational-wave science with eLISA/NGO*,” *Class. Quantum Grav.* **29** (12), 124016 (2012)
- [8] P. Amaro-Seoane *et al.*, “*Intermediate and extreme mass-ratio inspiral astrophysics, science applications, and detection using LISA*,” *Class. Quantum Grav.* **24** (17) (2007)
- [9] A. Stroeer and A. Vecchio, “*The LISA verification binaries*,” *Class. Quantum Grav.* **23** S809-S817, (2006)
- [10] S. Nissanke *et al.*, “*Gravitational-wave emission from compact Galactic binaries*,” *Astrophys. J.* **758** (131) (2012)
- [11] C. Cutler and D.E. Holz, “*Ultra-high precision cosmology from gravitational waves*,” *Phys. Rev. D* **80**, 104009 (2009)
- [12] O. Jennrich, “*LISA technology and instrumentation*,” *Class. Quantum Grav.* **26** (15) 153001 (2009)
- [13] Gravitational Observatory Advisory Team, expected to submit a report to ESA in 2016
- [14] J. Sanjuan *et al.*, “*Note: Silicon carbide telescope dimensional stability for space-based gravitational wave detectors*,” *Rev. Sci. Instrum.* **83** (11), 116107 (2012)
- [15] J. Sanjuan *et al.*, “*Carbon fiber reinforced polymer dimensional stability investigations for use on the laser interferometer space antenna mission telescope*,” *Rev. Sci. Instrum.* **82** (12), 124501 (2011) (<http://link.aip.org/link/?RSI/82/124501>) DOI: 10.1063/1.3662470
- [16] A. Preston, “*Stability of materials for use in space-based interferometric missions*,” Ph.D. Dissertation, University of Florida (2010)

For additional information, contact Jeffrey Livas: Jeffrey.Livas@nasa.gov



Jeffrey Livas

Colloid Microthruster Propellant Feed System

Prepared by: John Ziemer (PI; JPL) and Morgan Parker (JPL)

Summary

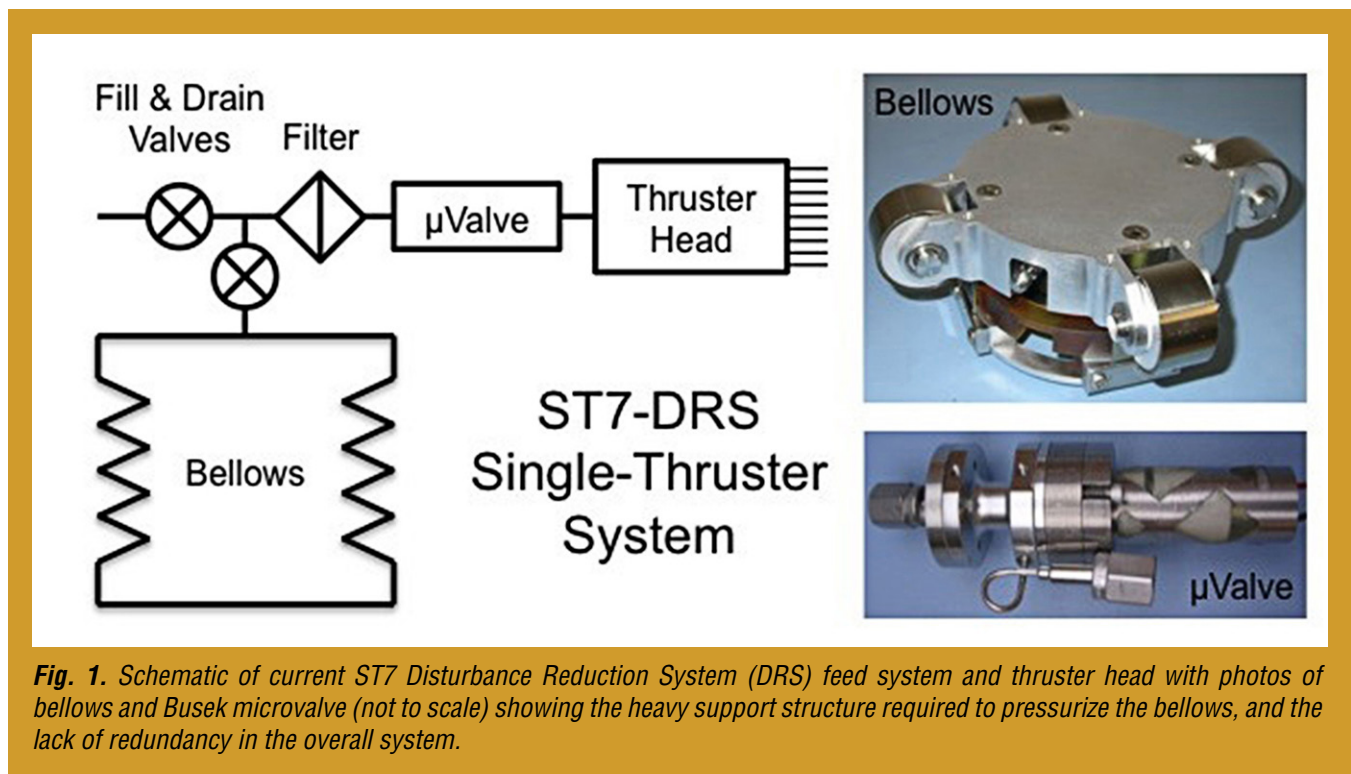
The Colloid Microthruster Propellant Feed System Project is a two-year technology development effort that began in early 2013, focusing on increasing the capacity and reliability of colloid microthruster feed systems. Delivered for a flight demonstration on the European Laser Interferometer Space Antenna (LISA) Pathfinder (LPF) mission in 2009, the Busek Colloid Micro-Newton Thruster (CMNT) represents the worldwide state-of-the-art in precision micro-propulsion along with lower-performance cold-gas thrusters. Precision micro-propulsion is required for drag-free operation of a space-based gravitational-wave observatory (GWO) and enables significant mass savings on exoplanet observatories by replacing reaction wheels and associated vibration-isolation stages for fine pointing. By using a new type of propellant storage tank, this technology development effort seeks to scale up propellant-handling capacity by a factor of 20 without significantly increasing cluster mass over the current CMNT architecture. This work also includes developing and integrating the next generation of precision propellant-flow control, the Busek microvalve, which includes reducing manufacturing complexity and increasing reliability by using a dual-string-redundant architecture. The ultimate objective at the end of this two-year project is to raise the system's Technology Readiness Level (TRL) to 5, in preparation for a long-duration test that would qualify the entire colloid microthruster system for a GWO mission.

This final report describes the successful completion of all environmental and performance tests for the new Colloid Microthruster Propellant Feed System. The following achievements have been accomplished:

- A new all-metal diaphragm tank has been developed with a 1.5 liter (2.25 kg) capacity for colloid thruster propellant and a GWO mission duration of at least five years.
 - All-304-stainless-steel construction provides long-term propellant storage compatibility and ease of cleaning and drying, and meets non-magnetic requirements.
 - Mass of less than 1 kg provides at least 10 kg mass savings over scaled Space Technology 7 (ST7) bellows tank and supporting structure.
 - New tank successfully passed TRL 5 tests – proof pressure tests, thermal and dynamic environments (by analysis), cycle tests (two complete cycles), and expulsion efficiency (>95%) tests.
- A new fully redundant string of next-generation Busek microvalves has been developed with associated accumulator and volume-compensator hardware and 3D-printed manifold.
- Next-generation Busek microvalve was developed under a Small Business Innovation Research (SBIR) program; Phase IIE provided matching funds for development of a new system including two valves in series.
 - New accumulator component prevents “water hammer” effect during operation; new volume compensator component provides “suck-back” that safely and rapidly shuts off propellant flow to thrusters; and new 3D-printed titanium manifold reduces mass and dead volume.
 - All new microvalve components passed thermal and dynamic testing to reach TRL 5.
 - A fully redundant-string feed system architecture (*i.e.*, tank, microvalve assembly, and supporting hardware) was assembled and tested in a simulated operational environment, demonstrating TRL 5 with expected beginning- and end-of-life performance and fully redundant flow control.
- Other associated hardware (latch valves, filters, *etc.*) were also tested at the system level for performance, and new processes for drying hardware and propellant as well as propellant loading have been developed and demonstrated.
- As-run test procedures and results, lessons learned, validated scaling relations, and suggested improvements for a TRL-6 flight-system design and test were captured for future applications.

Background

Almost all GWO concepts require precision microthrusters to meet mission science objectives by maintaining a drag-free environment for the inertial sensor instrument. Exoplanet observatories can also benefit from precision microthruster technology, replacing reaction wheels for spacecraft fine pointing without requiring elaborate and heavy vibration-isolation stages. The current state-of-the-art microthruster in the US is the Busek CMNT, originally developed under the New Millennium Program for ST7 and LPF technology demonstration mission. Two CMNT protoflight units, each with four thruster systems, passed environmental and spacecraft-level qualification testing [1]. In 2009, the units were delivered and integrated onto the LPF spacecraft, and are now awaiting launch in October 2015 for a 90-day demonstration mission. As shown in Fig. 1, the ST7 CMNT design includes a bellows propellant-storage tank, sized at 150 mL to provide up to 90 days of maximum thrust (30 μ N). A full CMNT system has been tested for 3478 hours (approximately 145 days) of near-continuous operation at an average thrust of about 18 μ N. However, as detailed in the 2011 Physics of the Cosmos (PCOS) Program Annual Technology Report (PATR) [2], two main issues remain for CMNT technology to reach TRL 6 for a future GWO mission. These are (1) developing and implementing a large enough propellant storage device, and (2) demonstrating system lifetime adequate for a full science mission of at least two years with adequate margin (150% of expected operational time and maximum expected propellant consumption).



Under the Strategic Astrophysics Technology (SAT) and Technology Development for Physics of the Cosmos (TPCOS) Program, we developed a new propellant storage tank and redundant feed system to TRL 5 that would eventually be included in a TRL-6 system-level lifetime demonstration. The tank is sized based on the longest expected mission duration of five years (Table 1), with margin, providing 2.25 kg or 1.5 liter of useable propellant. The tank uses a metal-diaphragm blow-down design for long-term propellant compatibility and to reduce mass by a factor of nearly 10 compared to the current state-of-the-art bellows design. Small metal-diaphragm propellant tanks have already been used in multiple US missile systems and for other space-based applications, but have not been demonstrated with colloid thrusters or ionic liquid propellants. The new feed system also includes the third generation of

Busek’s microvalve, recently developed under a NASA Phase II SBIR with a Phase IIE awarded based on this program. The microvalve is responsible for the picoliter-per-second propellant control from the tank to the thruster head, requiring parts with micron-level tolerances, critical alignments, and challenging acceptance-test protocols. While the ST7 Busek microvalve already provides the necessary performance, typical production times were 8-20 weeks per unit, including multiple iterations that did not meet leak rate, thermal performance, or cleanliness criteria (on average, only 16% of ST7 microvalves passed acceptance testing). Busek’s latest microvalve design focuses on manufacturability and reduced mass and cost, while maintaining performance. At the end of the program, a new tank and microvalve were tested in a relevant environment with an equivalent thruster head to reach TRL 5, demonstrating the required performance and lifetime capacity for a GWO.

	ST7-DRS Science / Attitude	LISA (7.5-year) Science / Attitude	GWO (2-year) Science / Attitude	GWO (5-year) Science / Attitude
Average Thrust (μN)	20 / N/A	10 / 30	10 / 30-100	10 / 30-100
Duration (hrs)	1400 / N/A	60000 / 6000	16000 / 1800	40000 / 4000
Total Impulse (Ns)	100	2800	800-1200	1900-2900
Propellant Mass (kg)	0.06*	1.5	0.4-0.6	1.0-1.5
* ST7 propellant tanks are sized for full thrust, 30 μN , for 90 days, and 0.15 kg of propellant.				

Table 1. The propellant mass requirements per thruster for all GWO concepts including both science and attitude operations (orbit maintenance/acquisition) demand larger tanks than what will be demonstrated on ST7 Disturbance Reduction System (DRS). The new tank holds 2.25 kg (1.5 L) of propellant, covering all GWO options. Total impulse and propellant mass numbers are based on sums of science and attitude modes.

The new feed system (shown schematically in Fig. 2) uses a more traditional diaphragm tank design, (Fig. 3). The thruster cluster mass can be nearly the same as ST7 despite the increase in propellant mass. This is achieved through a lightweight torispherical 304L stainless steel tank design with only 0.5 mm (20 mil) wall thickness made possible by the low feed pressures required [3]. The tank operates in blow-down mode from 4 Atm to 2.5 Atm. Although diaphragm tanks have been used extensively in space flight, our tank design is unique in that it uses an ionic liquid, EMI-Im (1-ethyl-3-methylimidazolium bis(trifluoromethylsulfonyl)imide) and compatible, non-magnetic stainless steel material for the shell and diaphragm. Standard elastomeric diaphragms used throughout the industry are not compatible with EMI-Im, and aluminum diaphragms used in some existing tank designs would suffer pitting corrosion. In addition, the torispherical tank design is easier to clean and dry than bellows, resulting in reduced risk of bubbles, contamination, and clogging in the feed system and thruster head. Compared to scaling up the original ST7 bellows system, the new feed system will realize mass savings of 19 kg per thruster cluster, corresponding to 57 kg mass savings per spacecraft and 171 kg mass savings per three-spacecraft mission.

The key challenges for the new feed system included:

Providing a chemically compatible, long-term propellant storage capability:

- EMI-Im colloid thruster propellant is not chemically compatible with many elastomers and metals over long periods of time or in high-temperature environments.

Providing for ease of cleaning and drying to prevent particulate and chemical contaminants:

- The smallest dimension within the feed system is on the order of 10 microns, which requires delicate cleaning and small-pore filters; and
- The EMI-Im propellant is hydrophilic and must to be kept at <150 ppm of water to prevent bubbles that clog feed system components and reduce thruster response time.

Providing full redundancy while meeting stringent flow-rate-control requirements:

- The ST7 colloid feed system is single-string, unacceptable for a future GWO flagship mission; and
- To provide precision thrust, the feed system must regulate to better than 12 nL/s (0.7 $\mu\text{L}/\text{min}$) flow rate with 40 pL/s resolution.

Following all standard flight practices for space-flight qualification of a liquid propellant feed system:

- Fully redundant liquid-fed propulsion feed system design practices are well understood; and
- Qualification standards for liquid propulsion feed systems are well documented.

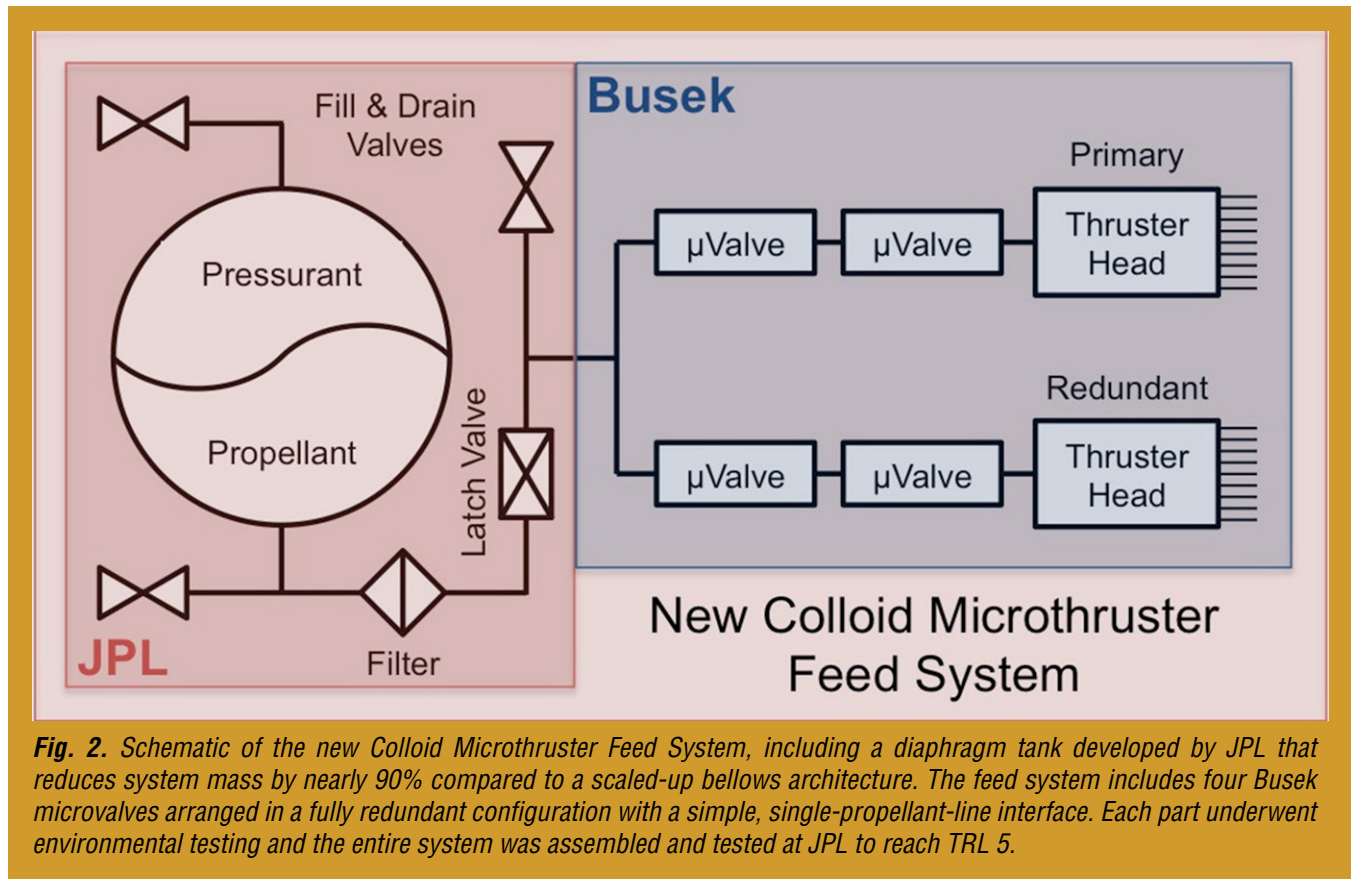


Fig. 2. Schematic of the new Colloid Microthruster Feed System, including a diaphragm tank developed by JPL that reduces system mass by nearly 90% compared to a scaled-up bellows architecture. The feed system includes four Busek microvalves arranged in a fully redundant configuration with a simple, single-propellant-line interface. Each part underwent environmental testing and the entire system was assembled and tested at JPL to reach TRL 5.

Objectives and Milestones

The objective of this project was to develop a lightweight (< 2 kg), five-year-capacity feed system for future GWO colloid-propulsion systems. This included a new, more reliable microvalve design and a metal diaphragm tank of 1.5-liter fuel capacity, both demonstrating TRL 5. In addition to component development, a complete feed system was assembled and tested consisting of the propellant tank, two serially mounted valves for redundancy, and other required commercial-off-the-shelf (COTS) feed system components to demonstrate system performance. In addition, we updated ST7 processes including cleaning; propellant loading and priming; as well as functional, acceptance, and qualification test procedures. The four main project objectives were:

1. **Design tank and feed system with a five-year GWO mission capacity and full redundancy.**
Use standard liquid propulsion feed system principles and practices to design a redundant colloid microthruster feed system, including interface and environmental requirements. Deliverables are feed system specifications and interface documents. **COMPLETE.**

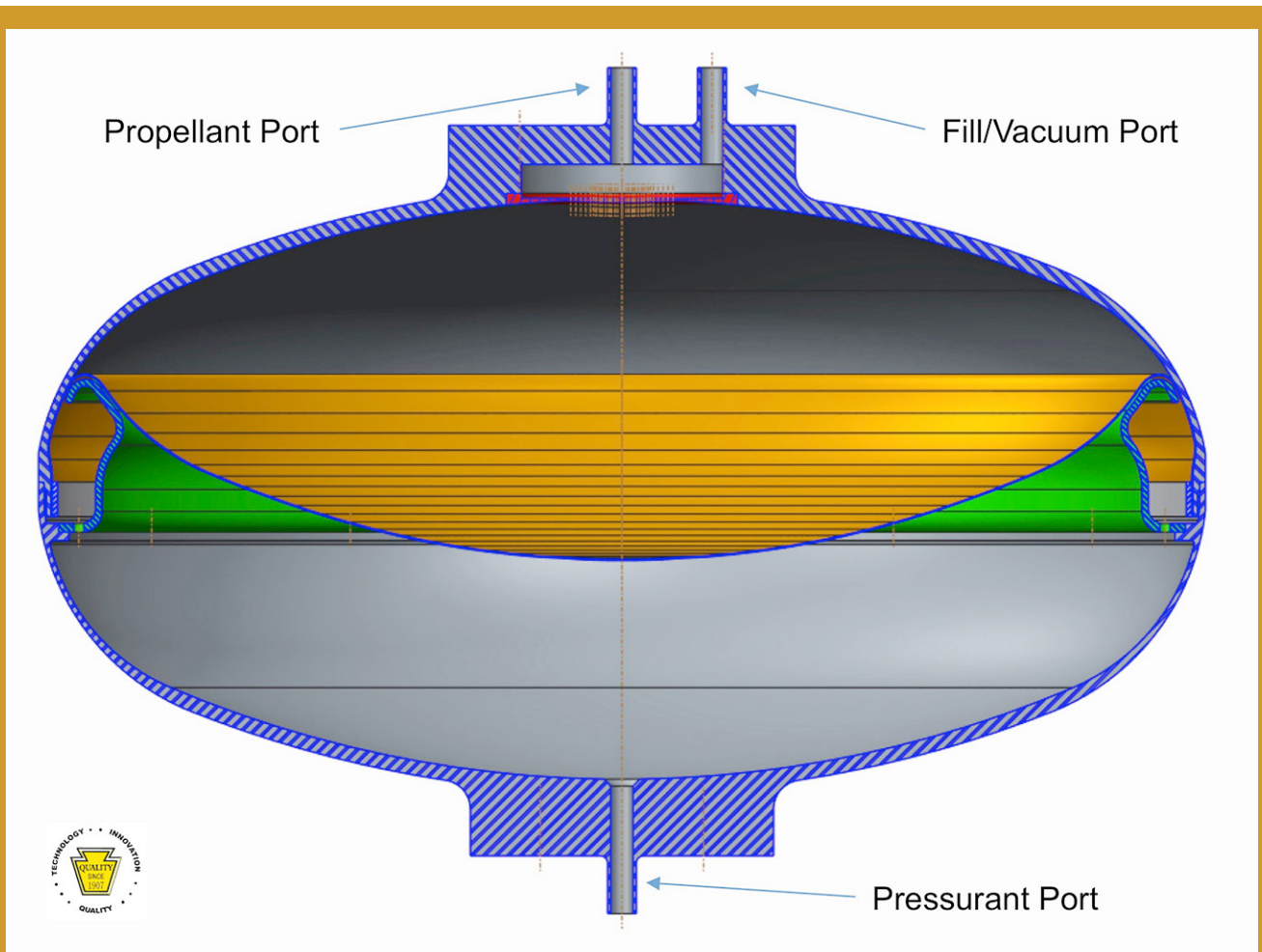


Fig. 3. Cut-away drawing of the new torispherical diaphragm tank designed by Keystone Engineering Company. The tank is constructed of non-magnetic stainless steel with enough volume (approximately 25 cm diameter and 14 cm height) to supply 1.5 liters of ionic liquid propellant, for greater than five years of operation, from 4 Atm at beginning of life to 2.5 Atm at end of life.

2. **Design, fabricate, and test the stainless steel diaphragm tank to reach TRL 5.**

Design and test tank to 1.25 times maximum design pressure (MDP), 5 Atm, (maximum expected operating pressure, MEOP, is 4 Atm) and 1.5 liter, or 2.25 kg, fuel capacity with >95% expulsion efficiency. JPL guided tank design, and Keystone Engineering Company manufactured the tank and performed cycle and proof testing. Deliverables were a tank design, stress report (including thermal and dynamic environment analysis), two tanks in place for destructive testing, and one prototype model (PM) tank delivered to JPL for integration tests (note that originally all tanks were to be delivered to JPL, but the vendor conducted the proof and cycle tests on two tanks to reduce cost to the project). **COMPLETE.**

3. **Design, fabricate, and test the microvalves to reach TRL 5.**

This work was performed by the microvalve supplier for ST7, Busek Co. Inc., leveraging experience gained with that program and the recently completed Phase II SBIR for microvalve development (note that our program benefited from an SBIR Phase IIE award for additional microvalve development). Deliverables included a valve and manifold design, and a microvalve assembly (containing two PM microvalves, manifold, and supporting hardware) for environmental testing conducted at Busek, and system integration with the new propellant tank at JPL. **COMPLETE.**

4. *Integrate and test feed system components.*

This objective included integration of the tank with a microvalve assembly, including other COTS feed system components modified for EMI-Im use. To keep testing costs down, no thrusters were installed. Instead, high-precision flow meters developed during the ST7 program were used as thruster simulators to verify system operation. The setup was used to develop and demonstrate feed system cleaning procedures, loading procedures, and full dynamic range control at the end of the task. **COMPLETE.**

The following are key task milestones (note that a delay in the tank procurement shifted some milestones that were originally in Year 1 to Year 2, but did not change the overall scope of the task).

Year 1 (January 2013 to December 2013):

- Busek placed on contract for microvalve and project support (completed Apr. 2013);
- Internal Design Review (completed May 2013);
- Prototype microvalve fabrication and test (completed Jul. 2013);
- Long-lead propellant tank procurement order submitted to vendor (completed Nov. 2013 – delay of seven months vs. original plan due to search for a new tank vendor; original vendor was acquired by another company that did not respond to request for proposal/quote); and
- Feed system component-level and system-level requirements (completed Dec. 2013).

Year 2 (January 2014 to December 2014, later extended to February 2015):

- Ground support equipment (GSE) design and part selection (completed Jan. 2014);
- Feed system COTS component down-select (completed Feb. 2014);
- Review of feed system and GSE design, test and integration processes (completed Mar. 2014);
- Development-model microvalve and volume compensator fabrication (completed Apr. 2014);
- Design Concept Review at Keystone Engineering facility (completed May 2014);
- Procurements placed for all GSE and COTS hardware (completed Jun. 2014);
- Development-model microvalve acceptance testing (completed Jul. 2014);
- Release final procedures based on Process Peer Review (completed Aug. 2014);
- Design of new microvalve support hardware and manifold (completed Aug. 2014);
- Fabrication and testing of new microvalve support hardware (completed Sep. 2014);
- Supporting feed system components delivery to JPL (completed Nov. 2014);
- Microvalve environmental testing (completed Nov. 2014);
- Tank cycle- and proof-testing (completed Nov. 2014);
- Tank delivery to JPL (completed Nov. 2014);
- Component-level environmental test results review (completed Dec. 2014);
- Microvalve development model delivery to JPL (completed Dec. 2014);
- GSE fabrication (completed Jan. 2015);
- Propellant drying (completed Jan. 2015);
- Full integration of feed system components (completed Jan. 2015); and
- Feed System functional tests and review (completed Feb. 2015).

Note that some delays in microvalve and tank fabrication pushed hardware delivery milestones back by one or two months. The main delays stemmed from having to find and switch to a new tank vendor, Keystone Engineering; and that after initial testing, Busek had to create two new components, an accumulator and a volume compensator, to meet the redundant feed system requirements.

Progress and Accomplishments

The Colloid Microthruster Propellant Feed System task started under contract at JPL in January 2013. The first six months focused on developing requirements, letting contracts for the tank, which incurred long delays due to a no-bid response from our original vendor, microvalve procurements,

and developing more detailed plans for testing to demonstrate TRL 5 [4]. In the second year through June 2014, we brought on a new vendor for the diaphragm tank, Keystone Engineering Company, successfully completed environmental testing of the Busek microvalve, developed designs for all GSE, and procured all components for the GSE and supporting commercial feed system components, latch valve and fill/drain valves [5]. After the initial Busek microvalve tests in July 2014, the project realized the need for two new components, an accumulator to protect against water-hammer effects between the valves, and a volume compensator to take up the extra propellant volume pushed forward when the microvalves close. Busek completed designs and functional tests for these new parts along with a 3D-printed titanium manifold in September 2014. By November 2014, both the tank and microvalve assemblies passed stress and environmental testing at their respective facilities. By January 2015, all components had arrived at JPL, the propellant had been dried, and all support equipment was integrated into a test fixture. Full functional tests were successfully completed in February 2015.

1. Design tank and feed system with a five-year-GWO-mission capacity and full redundancy.

Specifications and baseline requirements for the critical parts of the feed system, the tank and microvalve, were completed three months after the project started, in March 2013. Based on these specifications, the procurement of the microvalves from Busek Co., Inc. was initiated in April 2013, with an expected completion date one year later. Some delays for microvalve part manufacture, requirements flow-down from the actual tank design, and the need for two new components, the accumulator and volume compensator, required a two-month no-cost extension for Busek and the project. Fortunately, Busek was awarded an SBIR Phase IIE that gave matching funds to develop the additional hardware components necessary to integrate the microvalve into the new feed system. This work is described in more detail under Objective 3.

Initiation of diaphragm tank procurement met even greater schedule and budget difficulties, when the original vendor described in the proposal, AMPAC, was acquired by another company, Moog, Inc., which decided not to participate in this task. After months of searching, Keystone Engineering Company, which has developed many prototype and one-off tanks, indicated they would be interested in developing the new tank for our task. While the cost was slightly higher than the previous company's estimate, the schedule was shorter, which allowed the task to continue in the same two-year time frame. In addition, both Busek and Keystone agreed to perform environmental testing at their facilities which, together with a reduction in management and systems engineering at JPL, covered the additional tank contract cost. This work is described in further detail under Objective 2.

Objective 1 also includes the systems engineering for developing supporting hardware specifications, GSE design, and part procurement. All additional parts, including the commercial flight-like components in the feed system and a new propellant drying system, were delivered and tested. Vacco, Inc. supplied the feed-system latch valves as Engineering Model (EM) components with flight heritage traceability. The propellant drying system, the Rotavapor R-3, supplied by Buchi, was used for its large handling capacity (0.5 Liters) instead of custom GSE that was originally designed for this project. We chose to reduce cost by using commercial "flight-like" parts with traceable heritage and testing to qualified hardware instead of purchasing certified flight hardware.

2. Design, fabricate, and test the stainless steel diaphragm tank to reach TRL 5.

The diaphragm tank was designed, fabricated, and tested by Keystone Engineering Company. The tank is made of non-magnetic 304L stainless steel and has a total volume of 4 liters, nearly half of which was filled with 1.5 liters EMI-Im propellant at beginning of life. The tank has an MDP of 4 Atm for beginning-of-life operation and a blow-down ratio of 1.6 for an end-of-life pressure of 2.5 Atm. This capacity is actually 50% larger than originally planned (1 liter was the original goal for this project) due to the possibility of needing a higher operating pressure in the future. The expulsion efficiency was specified

to be greater than 99% with 25 expulsion cycles. However, the vendor quickly realized this would not be possible within the scope of the program, especially under the project's schedule constraints. We agreed to reduce the expulsion efficiency requirement to 95% (effectively adding 60 mL of residual propellant at end of life) to provide sufficient margin for cycle lifetime. Acceptance, qualification, expulsion, and burst test requirements were documented in a detailed specification. Keystone successfully passed a Design Concept Review in May 2014 (see cut-away drawing of the new torispherical diaphragm tank design in Fig. 3).

In November 2014, Keystone completed all required tests and delivered one prototype tank to JPL (Fig. 4). While the tank passed all pressurization proof and leak tests and requirements [6], the cycling tests of the two test tanks showed the diaphragm could only survive two complete cycles [7, 8]. On the third cycle of each test tank, the diaphragm ruptured. While this was not expected based on the design, it was clear that the diaphragm manufacturing method chosen (machined out of extruded stock) was not adequate. The colloid propellant tank is only expected to be filled and drained once (one complete cycle) but we believe we should have contingency for at least one additional fill and drain cycle. Although the Keystone tank successfully passed two complete cycles with $\geq 95\%$ expulsion efficiency, best flight practices require a 5 \times margin on cycle requirements. However, in our understanding, meeting mission margins is not required for TRL 5 demonstration. Moving toward TRL 6, Keystone developed a plan providing multiple options to increase cycle life.

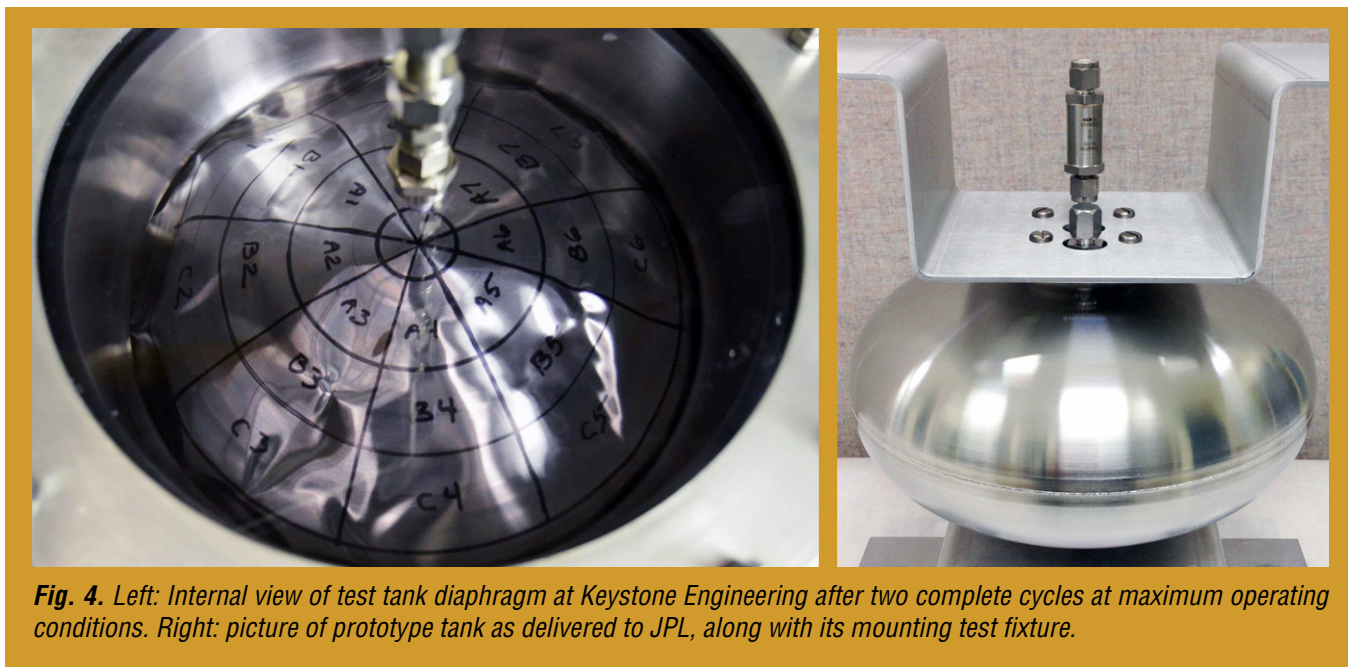


Fig. 4. Left: Internal view of test tank diaphragm at Keystone Engineering after two complete cycles at maximum operating conditions. Right: picture of prototype tank as delivered to JPL, along with its mounting test fixture.

The overall objective for tank development was to reach TRL 5 (including cycle and proof testing, as well as thermal environment analysis) with as light-weight a tank as possible, and we believe this has been achieved to the minimum set of requirements. We also prioritized ease of handling, cleaning, and drying which made the tank slightly heavier than a “flight-weight” tank, yet still remained under 1 kg. For future projects, significant time and effort will still be required to develop a qualifiable tank.

3. Design, fabricate, and test the microvalves to reach TRL 5.

One string of two Busek microvalves in series was developed and tested as part of this task. In the full feed system, a second identical string would also be present for redundancy, but was not included in this task to reduce cost. Furthermore, Busek found that additional hardware, a volume compensator

and accumulator, are necessary to meet performance requirements with two of the microvalves in series, which were not required for ST7. Development and environmental testing of these two new components was part of this task and the SBIR Phase IIE award.

The microvalve is designed to support flow rates up to an equivalent of 100 μN at 25°C (3.3 $\mu\text{L}/\text{min}$). Flow rates are controlled to 0.1- μN equivalent through two microvalves in series. Allowable input pressures are up to 4 Atm, matching the tank output specification, although expected operating conditions range from 2.5 to 4 Atm at end and beginning of life, respectively. Acceptance, qualification, leak-rate, and performance test requirements have been documented in a detailed specification.

Busek completed the development work on the third-generation microvalve in September 2013. The new microvalve (Fig. 5) is one quarter the size and made up of less than half the parts of the current state-of-the-art CMNT microvalve for ST7. Busek demonstrated 90% yield on microvalve fabrication through inspection and 90% yield through acceptance testing, resulting in 80% yield overall, compared to 16% overall yield during the ST7 flight hardware fabrication campaign. In addition, manufacturing and assembly time for a batch of four valves has been reduced to three weeks from a typical six-week cycle for two valves during ST7. The combination of yield and manufacturing improvements helped keep prototype and development model builds on schedule, and are expected to do the same for future flight mission implementations.

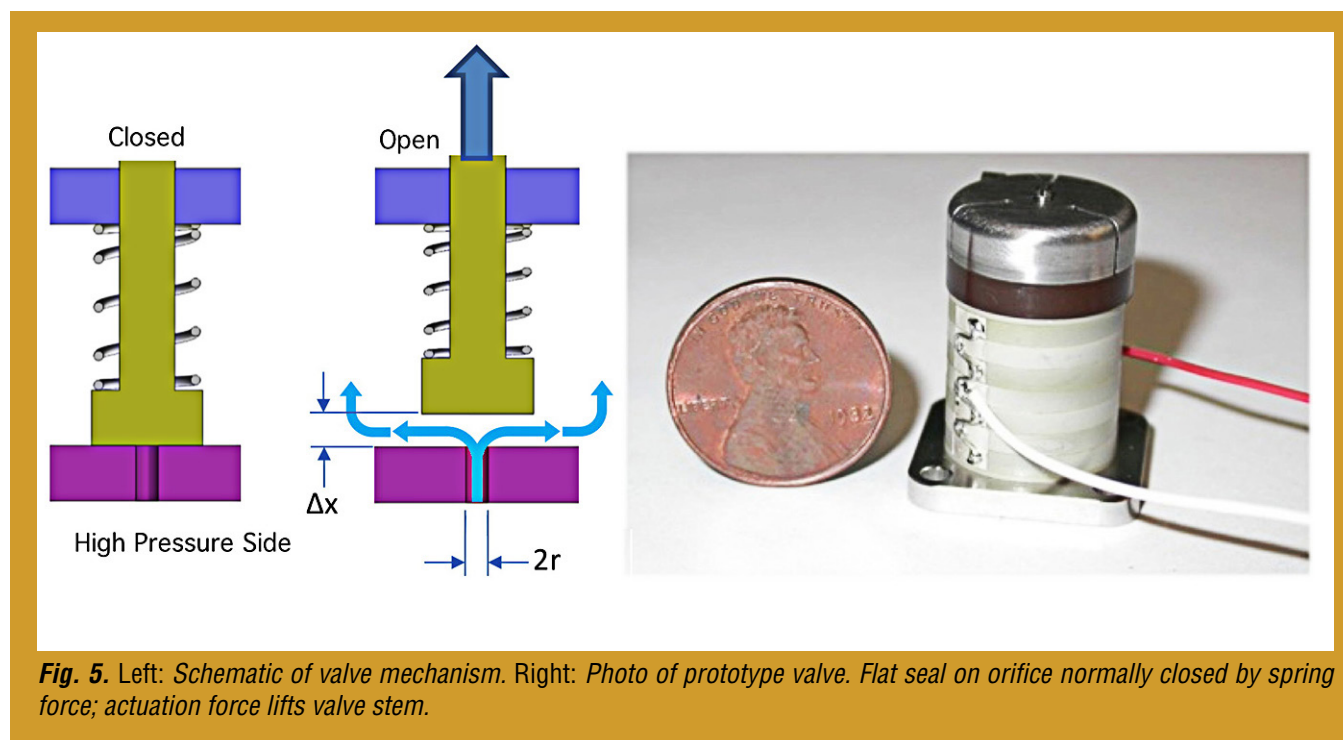
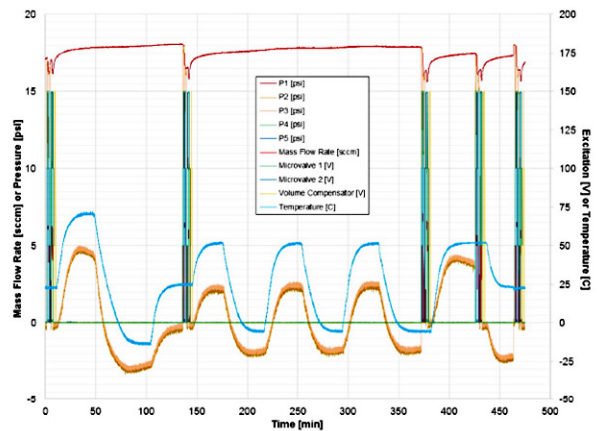
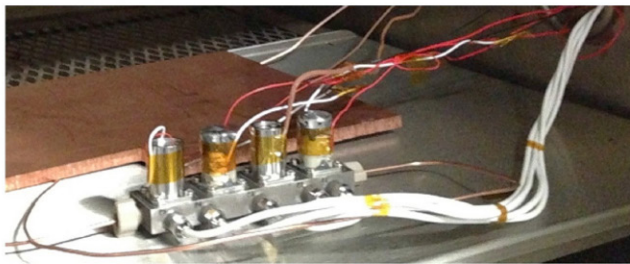
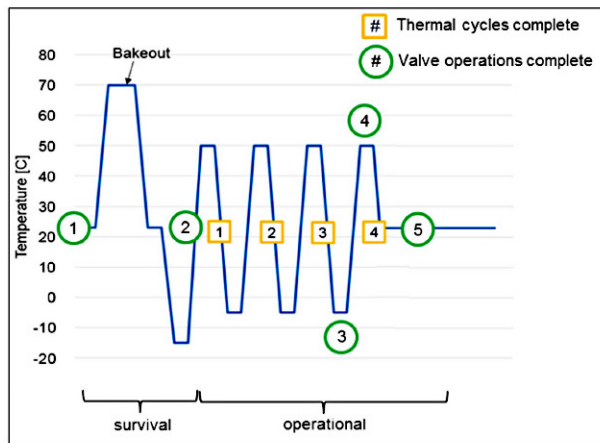


Fig. 5. Left: Schematic of valve mechanism. Right: Photo of prototype valve. Flat seal on orifice normally closed by spring force; actuation force lifts valve stem.

Busek completed thermal and vibration testing on the prototype units, showing acceptable flow characteristics before and after all tests. Dynamic environment test results have been documented in previous PATRs, with Fig. 6 showing a summary of prototype microvalve performance during various stages of the thermal test [9]. The pre- and post-test curves at ambient temperature show < 15 V shift in the response curve, meeting requirements and demonstrating TRL 5 for the assembly.

Busek delivered all components, including the new accumulator, volume compensator, and 3D-printed titanium manifold to JPL in December 2014, with integration and test support in February 2015.



- The thermal test was successful
- Feed system operated inside oven with N₂
- Operation included voltage sweep for all components and functional test of feed system
- Operations compared pre-test, at thermal extremes, post-test
- Feed system operated nominally throughout test

Fig. 6. Top left: graph of thermal conditions for the microvalve assembly. Bottom left: photo of microvalve assembly. Top right: thermal profile and pressure measurements. Bottom right: summary of thermal environment test results.

4. Integrate and test feed system components.

With all components delivered by the end of December 2014, JPL focused on component integration and propellant preparation in January 2015 and system-level testing in February 2015. All components were cleaned in JPL's propulsion component cleaning facility and brought to a Class 10,000 (ISO 7) clean room for assembly and integration. The EMI-Im propellant was delivered from Covalent and tested for water content. The result, at 350 ppm, was more than twice the 150 ppm allowable to prevent bubbles. The propellant was dried in three batches of 0.5 liter each using a Buchi Rotavapor R-3 evaporator/condenser unit, each to <100 ppm water, as demonstrated by Karl Fischer titration. Prior to filling, the tank was purged with 150°C dry nitrogen to remove water from the walls. The tank was then evacuated on both sides of the diaphragm and filled with propellant. Approximately 11 psi was required to move the diaphragm and fill the tank, as expected based on Keystone's tests of the test tanks. A high-capacity, 0.5-micron filter from Mott Corporation was selected based on an analysis from Mott on "dirt capacity" and pressure drop [10], which provided an acceptably low pressure drop (< 5 psi) for the required flow conditions. The entire feed system was then assembled; the tank was pressurized to beginning-of-life conditions (4 Atm), the most stressful for the system; and a sample of the propellant was extracted from the fill/drain port to prove water content was <150 ppm [11]. Propellant flow rate was measured by two methods, measuring the pressure drop across a precision capillary tube with known inner diameter and length and assuming Poiseuille flow, and measuring the output of the feed system on a mass balance over longer periods. Results from the two methods agreed to better than 4%.

Three conditions were successfully tested with complete flow-range demonstrations:

1. Beginning of life (4 Atm): primary microvalve in control (redundant microvalve wide open).
2. End of life (2.5 Atm): primary microvalve in control (redundant microvalve wide open).
3. End of life (2.5 Atm): redundant microvalve in control (primary microvalve wide open).

All three conditions showed acceptable and expected flow-rate range capability (0-100 μN) with the redundant microvalve also showing full control authority [12]. Figure 7 shows the test setup and propellant flow rate through the entire feed system under the first test condition. The expected hysteresis from the microvalve piezo-actuator is present as the flow rate is ramped up to maximum and down to shut-off conditions. The accumulator and volume compensator also functioned as expected.

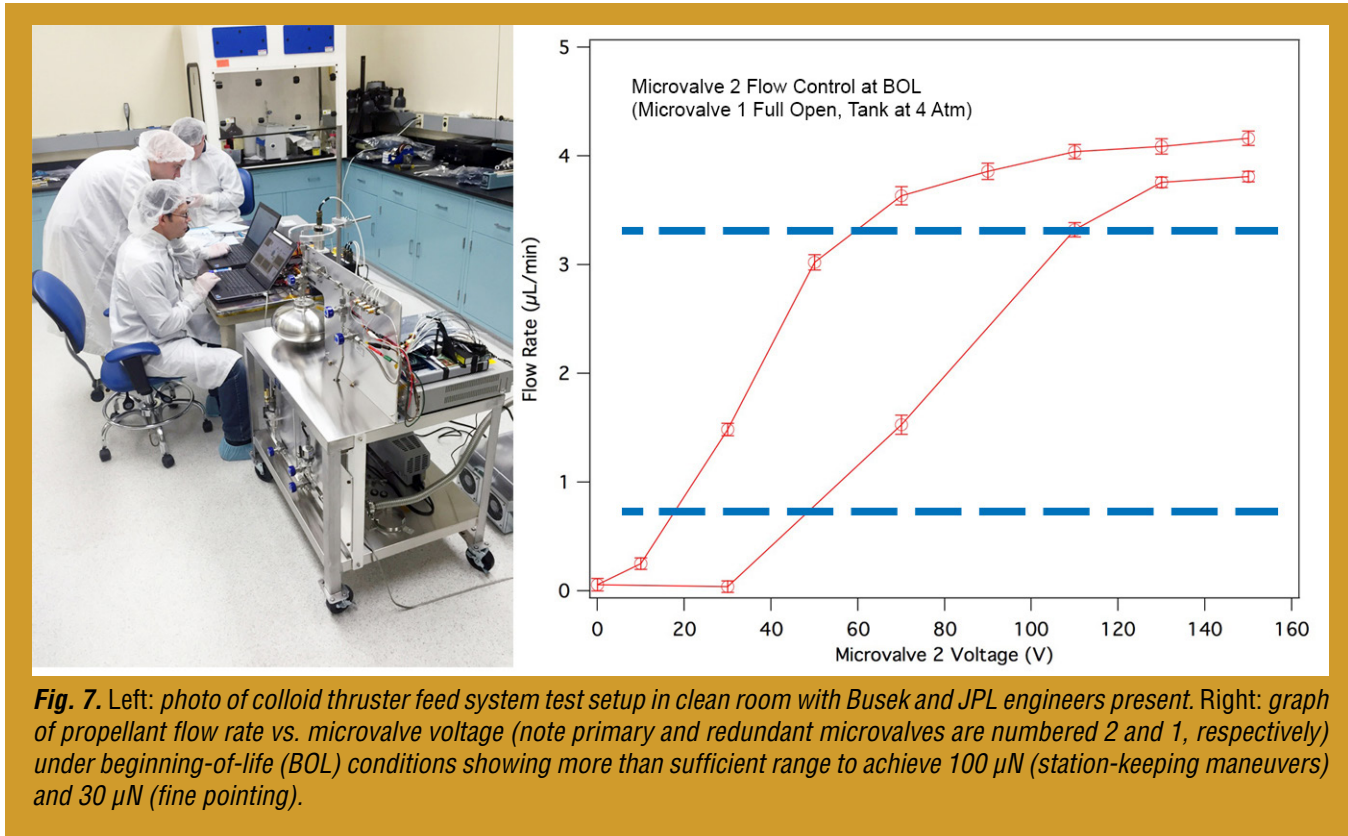


Fig. 7. Left: photo of colloid thruster feed system test setup in clean room with Busek and JPL engineers present. Right: graph of propellant flow rate vs. microvalve voltage (note primary and redundant microvalves are numbered 2 and 1, respectively) under beginning-of-life (BOL) conditions showing more than sufficient range to achieve 100 μN (station-keeping maneuvers) and 30 μN (fine pointing).

Path Forward

All objectives for this project have been completed, and we believe the new colloid microthruster feed system has achieved TRL 5. While improvements are needed, especially to the tank diaphragm construction, and further reductions in mass may be possible, the component-environmental and system-level performance tests using prototype hardware have shown the expected performance and the scaling relationships derived at the beginning of the project. Lessons learned have been captured for future use regarding feed system setup; propellant drying, filling, and testing; tank fabrication; microvalve assembly integration; and system-level testing.

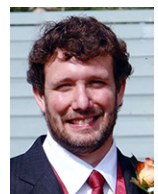
Until a particular GWO mission specifies mass, volume, interface, and environmental requirements that would allow design of a TRL-6-qualifiable unit, the next step in colloid thruster technology development should focus on thruster lifetime assessment and demonstration. This new TRL-5 feed system could be used for such a demonstration to advance technology readiness.

References

- [1] J.K. Ziemer *et al.*, "Colloid Micro-Newton Thrusters for the Space Technology 7 Mission," IEEE Aerospace Conference, Big Sky, Montana (2010)
- [2] NASA Physics of the Cosmos Program Office, "Program Annual Technology Report," (2011)

- [3] *“Space Systems-Metallic Pressure Vessels, Pressurized Structures, and Pressure Components,”* ANSI/AIAA S-080-1998 (September 13, 1999)
- [4] NASA Physics of the Cosmos Program Office, *“Program Annual Technology Report,”* (2013)
- [5] NASA Physics of the Cosmos Program Office, *“Program Annual Technology Report,”* (2014)
- [6] *“JPL Colloid Propellant Diaphragm Tank Stress Analysis Report,”* Keystone Engineering Report No. 1030051, Rev A (May 7, 2014)
- [7] *“JPL Colloid Propellant Diaphragm Tank Simulator 1 Test Report,”* Keystone Engineering Report No. 1030052 (September 30, 2014)
- [8] *“JPL Colloid Propellant Diaphragm Tank Simulator 2 Test Report,”* Keystone Engineering Report No. 1030053 (November 10, 2014)
- [9] *“As-Run Thermal Test Procedure,”* Busek Doc. #70011953 (November 2014)
- [10] *“Filter Dirt Loading Test Report,”* Mott Corporation, SO#2011584
- [11] *“As-Run Procedure for Transfer of EMI-Im into Propellant Tank and Loading of EMI-Im into Feed System,”* JPL internal procedure (February 17, 2015)
- [12] *“As-Run Feed System Operating Procedure,”* Busek Doc. #70011956 (February 26, 2015)

For additional information, contact John Ziemer: John.K.Ziemer@jpl.nasa.gov



John Ziemer

Directly Deposited Optical Blocking Filters for Imaging X-ray Detectors

Prepared by: Mark Bautz (PI; MIT Kavli Institute for Astrophysics & Space Research, MKI); S. Kassel (MKI); and K. Ryu and V. Suntharalingam (MIT Lincoln Laboratory); with special thanks to R. Masterson and the MIT Space Sciences Laboratory's REXIS team.

Summary

We aim to raise the Technology Readiness Level (TRL) of enhanced charge-coupled-device (CCD) detectors capable of meeting the requirements of X-ray grating spectrometers (XGS) and wide-field X-ray imaging instruments for small, medium, and large missions. Because they are made of silicon, all X-ray CCDs require blocking filters to prevent corruption of the X-ray signal by out-of-band, mainly optical and near-infrared (near-IR) radiation. We endeavor to replace the fragile, extremely thin, free-standing blocking filter that is current standard practice with a much more robust filter deposited directly on the detector surface.

High-performance, back-illuminated CCDs have flown with free-standing filters (*e.g.*, one of our detectors on Suzaku) and other, relatively low-performance CCDs with directly deposited filters have flown (*e.g.*, on the X-ray Multi-mirror Mission-Newton, XMM-Newton; Reflection Grating Spectrometer, RGS). However, a high-performance, back-illuminated CCD with a directly deposited filter has not yet been demonstrated. Our effort will be the first to show such a filter can be deposited on an X-ray CCD that meets the requirements of a variety of contemplated future instruments.

This Strategic Astrophysics Technology (SAT) program began on July 1, 2012. It is a collaboration between the MKI and MIT Lincoln Laboratory. The program is currently scheduled to end June 30, 2016.

Background

The past two decades have brought extraordinary progress in X-ray astronomy, in large measure as a result of unprecedented improvements in X-ray imaging and grating spectroscopy. Beginning with the launch of the Advanced Satellite for Cosmology and Astrophysics (ASCA) in 1993, and continuing to the present, concurrent operation of Chandra, XMM-Newton, Swift, and Suzaku, much of this success has been enabled by X-ray photon-counting CCD. CCDs will likely remain essential to many X-ray instruments for some time to come. In fact, three missions scheduled for launch in the next few years, the extended ROentgen Survey with an Imaging Telescope Array (e-ROSITA), Astrosat, and Astro-H, feature these detectors. Moreover, a number of future mission concepts include instruments relying on CCDs or other silicon-based X-ray imagers. Such instruments address a broad range of important scientific objectives. For example, as noted recently in the X-ray Mission Concepts Study Report (XCSR) commissioned by NASA's Program Office for the Physics of the Cosmos (PCOS) [1], several high-priority scientific questions identified by the 2010 Decadal Survey, *New Worlds, New Horizons in Astronomy and Astrophysics* (NWNH) [2] are best addressed by an XGS, which requires large-format X-ray imaging detectors. Specific science goals for an XGS and a Wide-Field Imager (WFI) are discussed in the report of the X-ray Community Science Team [1] and summarized in Table 1. The report notes an XGS could be deployed either alongside an X-ray micro-calorimeter on a Probe-scale mission, or as the sole instrument in a more modest, dedicated mission. XGS technology has therefore been identified as a priority 1 (highest-priority) need in the 2012 PCOS Program Annual Technology Report (PATR) [3]. Both

an XGS and a silicon-based, high-definition X-ray imager are key instruments for the X-ray Surveyor, a strategic mission concept identified as a priority by the NASA Astrophysics Roadmap “Enduring Quests, Daring Visions” [4], and now under study at NASA’s Marshall Space Flight Center (MSFC) [5].

Science Question	Measurement	Instrument
How does large-scale structure evolve?	Find and characterize the missing baryons via high-resolution absorption-line spectroscopy of the Warm-hot Intergalactic Medium (WHIM)	XGS
How does matter behave at high density?	Measure the equation of state of neutron stars through spectroscopy	XGS
How are black holes connected to large-scale structure?	Determine energetics and mass flows in Active Galactic Nuclei (AGN) outflows; probe hot galaxy halos via absorption spectroscopy	XGS
When did the first galaxies emerge and what were they like?	Identify high-redshift galaxies via gamma-ray bursts (GRB)	WFI
What new discoveries await in the time domain?	Monitor the entire sky with high sensitivity to find and study gravitational-wave sources and other transients	WFI

Table 1. High-priority science drivers for future instruments featuring large-format, imaging X-ray detectors (adapted from the PCOS X-ray Mission Concepts Study Report [1]). Directly deposited optical blocking filters (OBF) will improve performance and reliability, while reducing cost and risk of instruments addressing these questions.

Large-format, X-ray imaging detectors are also required for many missions envisaged for the Explorer program, which NWNH deemed “a crown jewel of NASA space science.” For example, an Explorer XGS has been proposed for a focused study of the cycles of baryons in and out of galaxies, and their role in galaxy evolution [6]. Other future Explorers will exploit the power of rapid-response X-ray imaging, so clearly demonstrated by Swift, but with much wider fields of view. As noted in [7], an X-ray WFI on an agile spacecraft can address with unprecedented sensitivity a variety of important science objectives ranging from the nature of the first galaxies to high-energy, time-domain astrophysics. An especially exciting prospect is identification of sources that may be detected by ground-based gravitational-wave observatories later in this decade [8, 9].

Our program aims to raise the TRL of advanced OBF technology required for these instruments. If successful, our effort will improve instrument sensitivity, robustness, and reliability. At the same time, it will reduce mass, complexity, risk, and cost. Our approach is to replace the fragile, free-standing, optical-blocking membrane of current practice with a filter deposited directly on the detector surface. A directly deposited filter can be thinner than a free-standing one, improving instrument sensitivity. Moreover, directly deposited filters do not require the heavy, complex, and expensive vacuum housings used in current instruments, and are of course much more robust than free-standing filters. The key challenge for our program is to demonstrate that blocking filters can be applied directly to the sensitive entrance surfaces of modern CCD detectors without compromising spectroscopic resolution.

To minimize cost, our program uses existing stocks of engineering-grade detectors produced for past programs at MIT Lincoln Laboratory. We apply so-called ‘back-illumination’ processing to these detectors, and then use coating facilities at Lincoln to apply blocking filters. X-ray and optical performance-testing is then conducted at MKI. We have also joined forces with REgolith X-Ray Imaging Spectrometer (REXIS), an MIT student instrument for NASA’s Origins Spectral Interpretation Resource Identification Security – Regolith Explorer (OSIRIS-REx) mission, to incorporate directly deposited blocking-filter technology into a flight program.

Objectives and Milestones

Silicon X-ray imaging detectors require blocking filters to prevent ambient visible and ultraviolet (UV) background light from adding noise and degrading X-ray spectral resolution. As noted above, most

such detectors flown to date have used fragile, free-standing filters comprised of thin plastic substrates coated with aluminum. Free-standing filters usually must be protected from ground-handling and launch acoustic loads using heavy vacuum enclosures equipped with complex door mechanisms. This project aims to show that adequate OBFs can be deposited directly on a detector, eliminating the need for fragile, freestanding filters. To the extent they eliminate plastic films, such filters could also improve soft-X-ray ($E < 1$ keV) detection efficiency.

A key challenge in this project is to demonstrate directly deposited OBFs provide the requisite optical blocking performance without compromising the spectral resolution of the detectors in the soft band. The latter depends critically on the electric fields present just inside the entrance surface of the detector, and these fields in turn require precisely controlled implant-density profiles. Our aim is to deposit blocking filters in such a way that the surface fields are unaffected by the deposition process or the filter itself. A secondary objective is to demonstrate such filters are sufficiently robust to survive the repeated thermal cycling any such detector is likely to experience.

Originally, we planned to complete the following four tasks:

Task 1: Select and thin existing CCID41 wafers and apply backside treatment

The target detectors for this project (Lincoln Laboratory model CCID41, now in use in Suzaku) were stored in wafer form as front-illuminated (FI) devices (typically four devices to a wafer). Using wafer-probe equipment, we identify functional devices. We then subject selected wafers to a custom, back-side treatment process, involving wafer thinning and molecular-beam-epitaxy passivation, which has already been shown to provide good X-ray results. Selected back-illuminated (BI) devices are packaged (removed from the wafer and installed in suitable test packages) for subsequent test at MKI.

Task 2: Establish baseline X-ray performance

We use established X-ray characterization facilities and procedures at MKI to verify suitable X-ray performance of the BI (but uncoated) devices.

Task 3: Apply filters and characterize filter-equipped devices

We use established thin-film deposition facilities at MIT Lincoln Laboratory to deposit aluminum blocking layers, and then package and test the filter-equipped devices. Filters are applied at the wafer level, with control areas masked to allow direct comparison of filtered and unfiltered areas of each device. We contemplate three cycles of filter deposition and test (one wafer per cycle), applying a relatively thick filter in the first cycle, and then continuing, after successful test, to progressively thinner filters. In so doing, we span the range of filter thicknesses required by future instruments. All filters will be capped with a 10 nm Al_2O_3 layer to improve robustness and provide UV blocking. Both optical rejection and X-ray spectral resolution will be measured in the characterization protocol.

Task 4: Test robustness and stability

To verify coating temporal stability and robustness to the repeated thermal cycling experienced by CCD detectors during instrument development and test, we will perform thermal cycling and long-term (6-8 month) stability measurements.

Soon after program start, we decided to alter the sequence of the program for two reasons. First, we discovered that a number of BI devices were already available at MIT Lincoln. To make best use of these, we needed to develop a filter deposition process that would accommodate individual chips as well as full wafers. Second, we learned that the MIT team developing REXIS wished to fly X-ray CCDs with directly deposited blocking filters. We decided to collaborate with REXIS because by doing so we gain the opportunity to demonstrate much higher TRL for our process than we could achieve in our

original program. REXIS is scheduled for delivery in 2015; OSIRIS-REx plans a 2016 launch. Although this collaboration has entailed some re-planning, we expect to achieve our objectives as scheduled.

Major milestones and our progress in achieving them are summarized in Table 2. We describe our progress in more detail in the following section.

Milestone at completion of:	Success Criteria	Status as of June 2015
1. BI processing	Wafer-probe testing of BI wafers shows: <ul style="list-style-type: none"> • ≥ 3 wafers with functional devices; and • ≥ 10 functional devices total. 	<ul style="list-style-type: none"> • Twelve FI wafers processed, yielding 33 devices with at least some functionality, of which eight are allocated to REXIS • Ten other functional BI devices identified as single chips
2. X-ray test of baseline BI device	X-ray performance demonstrated per protocol specified in proposal	• Complete; X-ray performance supports program objectives
3. 1 st device with thickest directly deposited filter	Packaged device delivered to MKI	• Complete (220 nm Al OBF)
4. X-ray and optical testing of device with thickest filter	X-ray and optical tests done per protocol specified in proposal	• Complete; three devices with 220 nm OBF characterized
5. X-ray and optical testing of device with thinnest filter	X-ray and optical tests done per protocol specified in proposal	• Complete; one device with 100 nm OBF and two with 70 nm OBF characterized
6. Long-term stability test	X-ray and optical tests done per protocol specified in proposal	• In progress: 8 months of planned 12 month test completed
7. Thermal cycle test	X-ray and optical tests done per protocol specified in proposal	• Planned for year 4 with REXIS flight instrument

Table 2. Project milestones and status.

Progress and Accomplishments

At the completion of the third year of our project, we have developed an OBF deposition process and thoroughly characterized X-ray and optical performance of BI CCDs with OBFs of a range of thicknesses (220, 100, and 70 nm Al) as specified in Milestones 1-6 in Table 2. Our principal results may be summarized as follows.

1. We demonstrated that it is feasible to deposit effective aluminum OBFs directly on high-performance BI CCDs with at most modest effect on X-ray spectral resolution.
2. The measured X-ray transmission of these OBFs is consistent with theoretical expectations.
3. The measured visible/near-IR transmission of these OBFs is consistent with the expected level of attenuation over most of the filter area, but, in a small fraction of pixels, higher than expected transmission is observed. The pixels exhibiting these so-called “pinholes” can have sensitivity to visible light that is 10 \times to 1000 \times theoretical expectations. We have evidence these pinholes are produced by irregularities on the detector surface. These irregularities, each extending over at most a few hundredths of a square micron of detector surface, seem to cause small breaks in the aluminum blocking layer. The irregularities in turn may be caused either by intrinsic roughness of the CCD surface or by sub-micron particulate contamination. The fraction of pixels exhibiting these pinholes can be reduced to 1% or less by (i) minimizing the density of sub-micron particles on the detector surface before aluminization and (ii) suitably orienting the detectors relative to the aluminum source during OBF deposition.
4. For very demanding optical blocking applications, in which visible/IR band attenuation factors greater than 10⁶ are required, we found that it may be necessary to take additional steps to prevent

light from entering the detector through its sidewalls and through the adhesive layer that affixes the detector to its package. We developed methods for doing this for the REXIS instrument.

- Interim results from our planned long-term stability tests show no change in visible/IR blocking performance of a directly deposited OBF after eight months of storage in a laboratory environment.

We discuss each of these results in turn.

1. Soft-X-ray spectral resolution with directly deposited blocking filters

Soft X rays (with energies below 1 keV) are photo-electrically absorbed within $\sim 1 \mu\text{m}$ of the entrance surface of a silicon detector, so good X-ray spectral resolution requires efficient collection of photoelectrons generated in this region. Precise doping of the entrance ('back') surface of the detector is necessary to produce the internal electric fields required to achieve this. We aimed to determine whether a metal OBF layer deposited directly on this surface would affect the spectral resolution of an X-ray CCD detector. In general, we find the OBF has little effect on spectral resolution except, possibly, at the lowest X-ray energies we studied ($E < 300 \text{ eV}$).

Figure 1 shows pulse-height spectra from representative devices. The back surfaces of these detectors were treated with MIT Lincoln Laboratory's molecular-beam epitaxy (MBE) process. One device has no OBF, and the other two have directly deposited aluminum OBFs with thicknesses of 70 nm and 220 nm, respectively. Identical exposure times to the same radioactive X-ray source were used to obtain the spectra. The source produces characteristic lines of C-K, V-L, O-K, and F-K, with energies ranging from 277 eV to 677 eV. As expected, X-ray absorption in the filters reduces the amplitudes of the lower-energy peaks. The figure also shows the OBFs produce relatively little change in the shapes and widths of the line-response functions.

Table 3 lists typical peak widths (full-width at half-maximum, FWHM) obtained from the different output nodes on each device. At 677 eV, all devices produce symmetrical peaks with essentially the same widths. At 525 eV, all peak widths are also quite comparable, given the expected systematic

measurement uncertainties (roughly 10% of peak width). The spectral resolution of all devices degrades to some extent at the lowest energies, and in each, the response at 277 eV shows a clear low-energy tail. We hypothesize the tail is a consequence of the relatively thick (20 nm) MBE layer applied in fabricating these devices. The FWHM at 277 eV is about 25% larger on the device with the thicker OBF than it is in the other two devices. The pre-OBF-deposition performance of this device is not known, so this difference can be regarded as an upper limit on the amount of low-energy broadening attributable to the OBF. Note that the unfiltered device and the device with the 70 nm-thick OBF show the same response widths at all three energies.

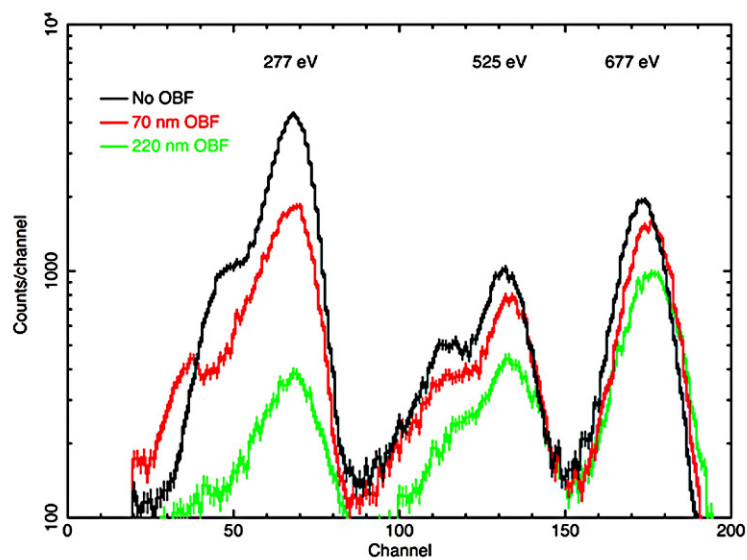


Fig. 1. Soft-X-ray response of a device with no OBF (black) and with directly deposited aluminum filters 70 nm (red) and 200 nm (green) thick. The filters have very little effect on spectral resolution.

Line Energy (eV)	Line width without OBF FWHM (eV)	Line width with 70 nm OBF FWHM (eV)	Line width with 220 nm OBF FWHM (eV)
277	59-74	62	75-92
525	70-92	68	76-96
677	61-78	59	61-75

Note: Data from device 53-1-4-3 (no OBF), 53-1-4-2 (70 nm-thick OBF) and device 53-1-7-1 (220 nm-thick OBF).

Table 3. Spectral resolution for devices without and with a directly deposited OBF.

2. X-ray transmission of OBFs

Measured X-ray transmission of a 70 nm-thick OBF is compared to expectations in Fig. 2, with generally good agreement. The data were obtained from a device (53-1-4-2) on which only part of the detector was covered by the OBF. Both covered and uncovered regions were exposed to a multi-line source like the one used to produce the spectra in Fig. 1, and transmission was determined from the line fluxes measured in the two regions. The red circles show measurements obtained by fitting Gaussian profiles to the data. Green crosses show fluxes obtained by summing over a spectral region within ± 3 standard deviations of line centers. The two methods agree reasonably well, except at the very lowest energy measured (183 eV) where the line profiles are distinctly non-Gaussian. Similarly, good agreement between measurements and expectations is obtained with 200 nm OBFs (see [10] for details).

3. Visible/near-IR transmission of directly deposited OBFs

Figure 3 shows the measured visible-band quantum efficiency (QE) of a device with a directly deposited blocking filter with a nominal thickness of 70 nm. The measurements agree reasonably well with a simple model of an aluminum layer over a thick silicon substrate. The aluminum thickness in the model has been adjusted to 63 nm to fit the data. The model assumes perfect internal CCD QE, which is certainly an overestimate redward of 600 nm, as the (thinned) detector’s sensitive volume (depletion region) is nominally 45 microns thick. A more sophisticated model, incorporating an accurate treatment of the internal detector efficiency, is clearly required to represent the data in the near-IR spectral band. The present results may indicate the OBF is somewhat more transparent in this spectral band than the simple model predicts.

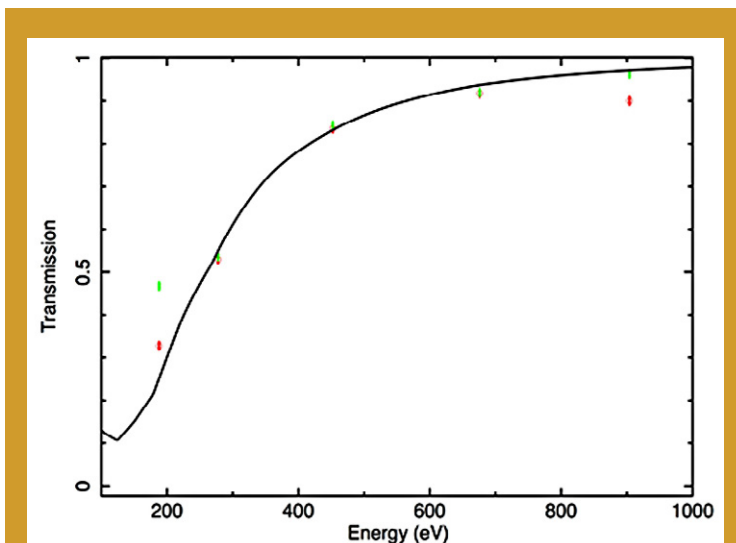


Fig. 2. Measured (points) and modeled (curve) X-ray transmission of 70 nm thick aluminum OBF. Red and green points obtained with different X-ray measurement methods discussed in the text.

Visible-band, flat-field exposures with both 220 nm-thick and 70 nm-thick OBFs show “pinhole-like” regions of relatively high transmission, as illustrated in Fig. 4. The image on the left of the figure shows pinholes in a 220 nm-thick OBF. The device was exposed to a fluence of 1.3×10^6 photons/pixel at 800 nm. A histogram of the 440,000 pixel amplitudes in the image is shown in the right panel. The theoretically expected transmission of this OBF is less than 10^{-9} , so if the OBF were perfect, all pixels would have zero amplitude, modulo the readout noise with root-mean-square (rms) width of a few electrons. The histogram shows that 99% of pixels are in fact consistent with zero amplitude, and about 1% of pixels are affected by pinholes with transmission ranging from about 10^{-6} to as high as 5×10^{-4} .

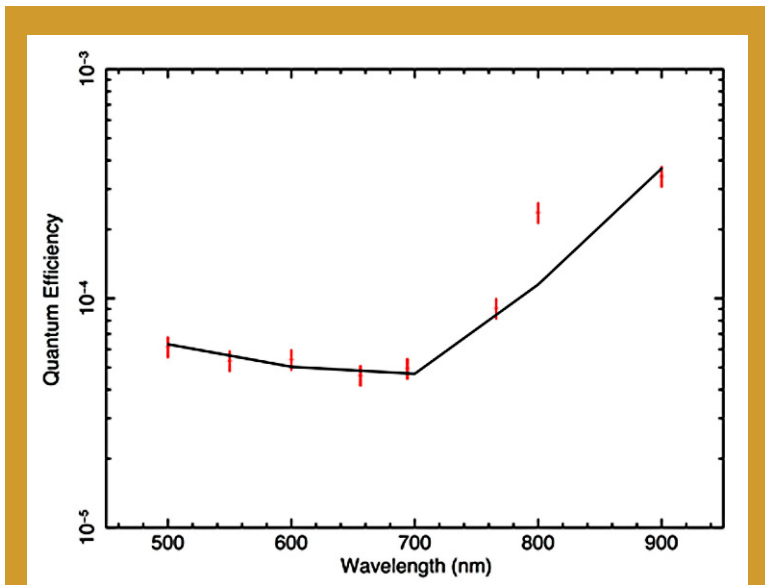


Fig. 3. Visible/near-IR QE of a CCD with a directly deposited blocking filter. Nominal filter thickness is 70 nm. The points are measured values; the line is a simple model of a 63 nm-thick OBF. Note: Data from device 53-1-4-2.

As discussed in detail in [10], we believe the pinholes are caused by surface irregularities present on the detector surface before the OBF is deposited. Several lines of evidence support this explanation. First, test coatings on quartz substrates do not show pinholes. Second, as shown in Fig. 5, scanning electron micrographs of deposited OBFs show texture with sizes (< 100 nm) and spatial density consistent with the observed number and transmission of pinholes. Third, the number of pinholes is dramatically reduced if an optically transparent, $1 \mu\text{m}$ -thick layer of photoresist is deposited on the detector surface before the aluminum OBF layer is deposited. Although such an interlayer is opaque to soft X rays and so could not be used on an X-ray sensor, this result does suggest there are no fundamental limitations to fabrication of a pinhole-free, directly deposited OBF.

Indeed, our success during the past year in reducing the pinhole fraction to less than 1%* for REXIS OBFs is further evidence in favor of this explanation for the origin of pinholes. Two measures in particular have proven effective. First, the interior surfaces of the coating chamber were aluminized after cleaning to minimize particulate contamination originating in the chamber walls. Second, the deposition geometry was changed so that the incident aluminum atoms approach the detector surface at about 45 degrees to the surface normal. The detector rotates about its surface normal during this process. This ‘angled-deposition’ allows the aluminum to cover the vertical sides as well as the tops of residual surface irregularities, and thus reduces the number of pinholes.

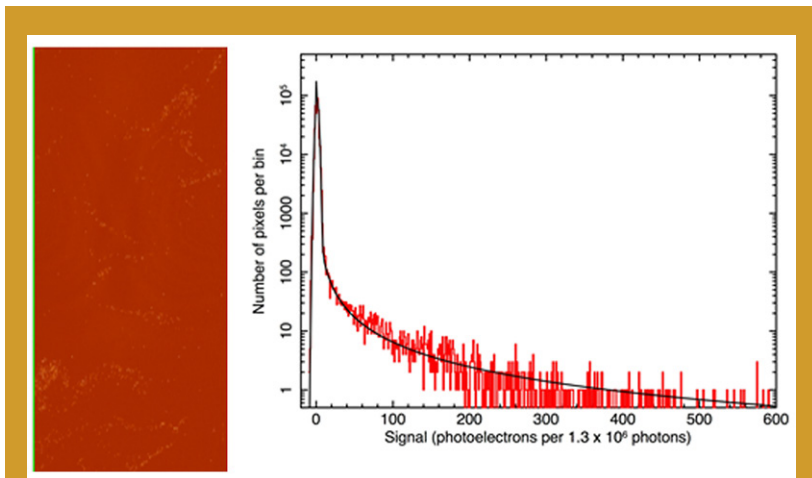


Fig. 4. Left: Image obtained using CCD with a 220 nm-thick OBF illuminated with 1.3×10^6 photons/pixel of 800 nm light. Pinholes (white spots) are evident. Right: Histogram of amplitudes of the 440,000 pixels in the image on the left. While 99% of pixels are in the peak, and are consistent with zero amplitude, about 1% of pixels show transmission greater than 10^{-6} .

4. Detector sidewall and bond-line leakage paths

The thickest OBF layers we tested, with 220 nm of aluminum, have a theoretical attenuation well in excess of a factor of 10^9 . The REXIS instrument, which will map fluorescent X-ray emission from the sunlit surface of asteroid RQ36, requires substantial optical

* Specifically, the mean fraction of pixels with optical density less than 7 (i.e. with pinholes) in 220 nm-thick OBFs in the 12 best REXIS flight devices is 0.76%; the root-mean-square pinhole fraction in this sample is 0.45%. An anomalous thirteenth device showed a pinhole fraction of 4.1%.

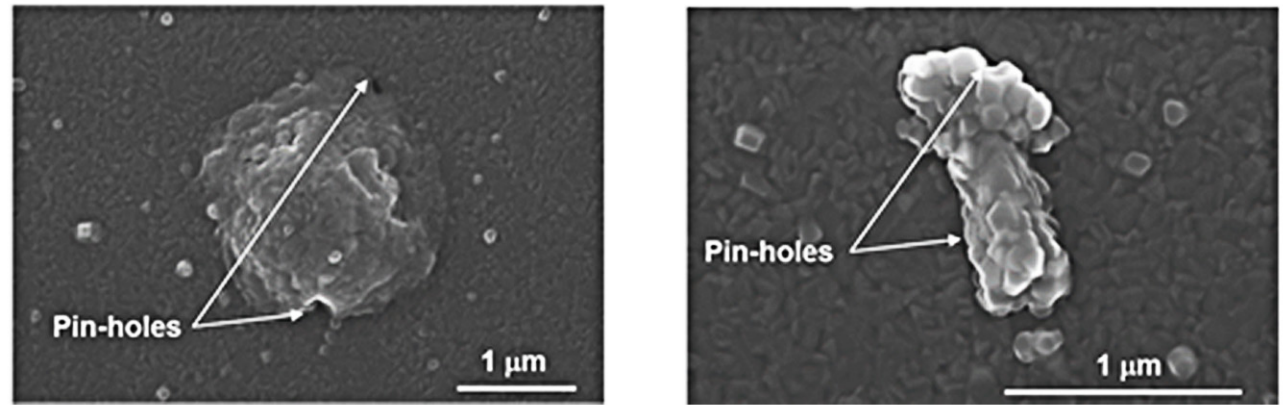


Fig. 5. Scanning electron micrograph images of an OBF directly deposited on the surface of a CCD.

blocking and is equipped with filters of this thickness. Our evaluation of directly deposited OBFs of this thickness revealed that to achieve very large attenuation (greater than a factor of 10^6 or so), one must block not only the light entering the entrance surface of the detector, but also light entering its thin side walls and even its mounting surface.

The effect and location of these leakage paths are illustrated in Fig. 6. The left panel shows a gray-scale image obtained by illuminating a CCD with a 220 nm-thick OBF. The white areas around the edges of the device have an attenuation factor of 10^7 or less. The right panel shows two leakage paths responsible for this effect. Light can enter the photosensitive regions of the device through its thin (45- μm -thick) sidewalls. Light can also penetrate the thin (~10- μm -thick) epoxy bond-line that attaches the CCD to the (photo-insensitive) silicon support wafer. A third leakage path, similar to the second but not shown in the figure, runs through a second, thicker epoxy bond-line that attaches the support wafer to the detector package, through the support wafer and into the detector from below. This third leakage path transmits mainly near-IR radiation to which the support wafer is relatively transparent.

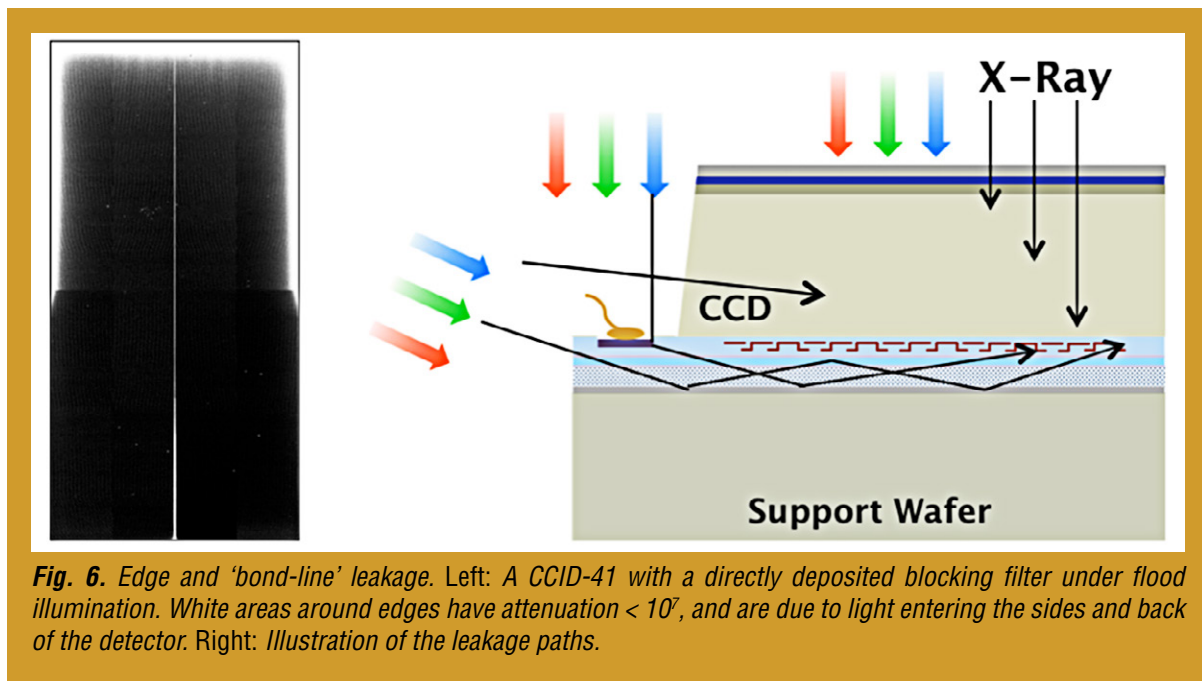


Fig. 6. Edge and 'bond-line' leakage. Left: A CCD-41 with a directly deposited blocking filter under flood illumination. White areas around edges have attenuation $< 10^7$, and are due to light entering the sides and back of the detector. Right: Illustration of the leakage paths.

Leakage through the two paths shown in Fig. 6 was reduced to levels acceptable to REXIS by depositing an additional 100 nm of aluminum using the angled-deposition geometry described in the previous section. This coating covers the detector sidewalls and the bond-line between the detector and the support wafer. In addition, the REXIS team qualified two effective countermeasures against bond-line leakage at the bottom of the support wafer. One method was to coat the bottom of the support wafer with black paint, using a suitable adhesion promoter. The other method was to deposit a 300 nm-thick aluminum layer on the bottom surface of the support wafer. REXIS has adopted the latter approach because it permits a flatter surface coating that can be applied more quickly.

5. Long-term stability of directly deposited OBFs

The final task in our original program is to evaluate the long-term stability of directly deposited OBFs. We began this process in September 2014 with a baseline evaluation of device 53-1-17-2, which is equipped with a 100 nm-thick OBF. We have monitored this device periodically since then, and as of this writing (June 2015) we have not detected any significant change in OBF performance. In particular, Fig. 7 compares pinhole maps obtained for this device before and after eight months of laboratory storage. The images have been scaled to correct for light-source-intensity differences so that the mean of the amplitudes of a set of randomly selected pinhole pixels is the same in both images. To date, we find no evidence for change over time in the optical blocking properties of this OBF. We plan to extend this stability test to at least a year's duration.

Path Forward

In the final year of our program, we plan to continue the long-term stability and thermal cycle tests begun this year, through a total duration of at least one year (milestone 6 in Table 2). We will also support evaluation of the REXIS flight focal plane and its directly deposited OBFs (Fig. 8) through environmental (vibration and thermal) testing. Success in these tests, expected by autumn 2015, will achieve milestone 7 and establish the TRL of directly deposited OBFs at 6.

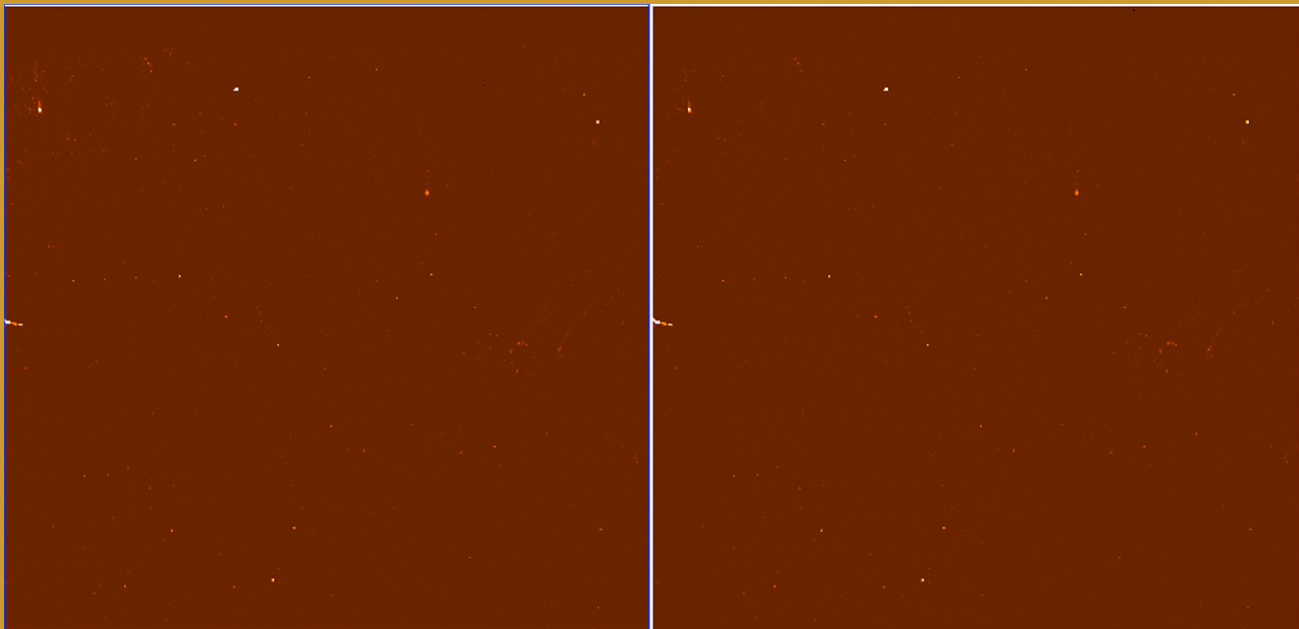


Fig. 7. Pinhole maps of a randomly chosen, 400×400 pixel section of CCD 53-1-17-2, equipped with a 100-nm-thick directly deposited aluminum OBF, obtained in September 2014 (left) and June 2015 (right). These images demonstrate the stability of the OBF over an eight-month period of laboratory storage.

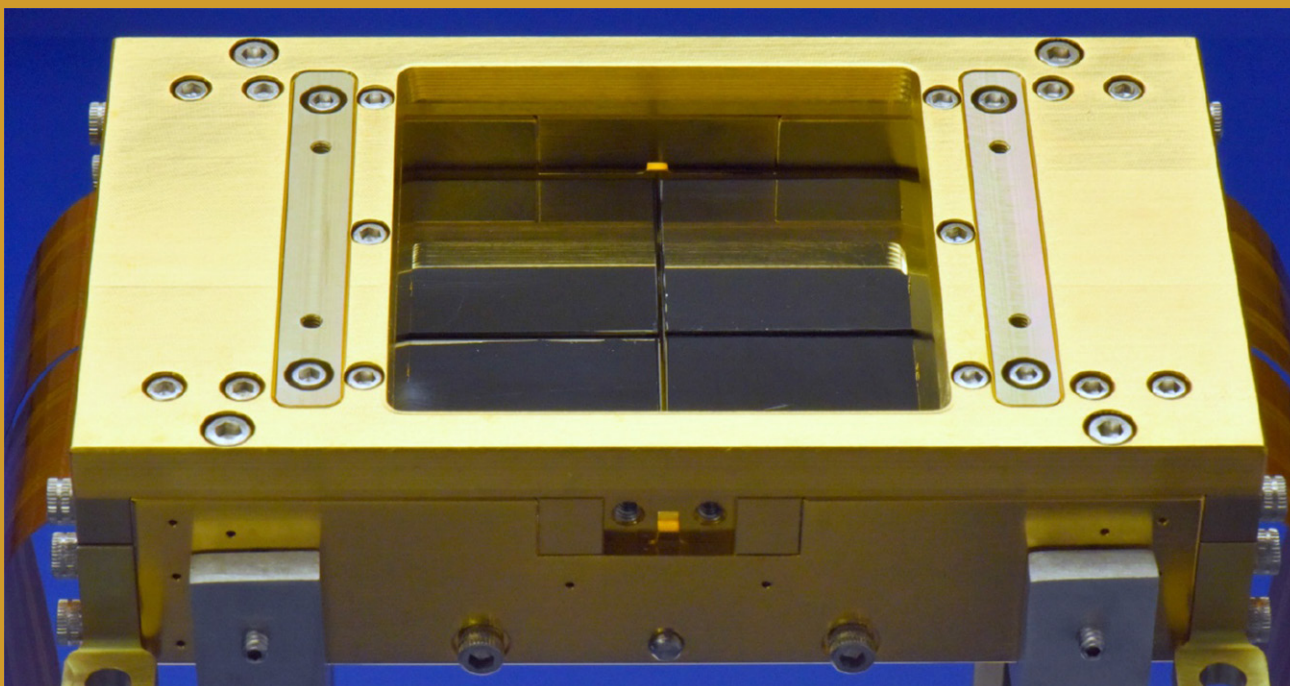


Fig. 8. The REXIS Detector Assembly Module features four MIT/Lincoln CCDs, each with a directly deposited optical-blocking filter. With successful completion of REXIS environmental testing, expected later this year, directly deposited OBF technology will achieve TRL 6. Image courtesy of MIT Lincoln Laboratory and MIT Space Sciences Laboratory.

References

- [1] X-ray Community Science Team, X-ray Science Support Team, and X-ray Engineering Support Team, “*X-ray Mission Concepts Study Report*” (2012)
- [2] National Academy of Science, Board on Physics and Astronomy, “*New Worlds, New Horizons in Astronomy and Astrophysics*” (2010)
- [3] NASA Physics of the Cosmos Program Office, “*NASA Physics of the Cosmos Program Annual Technology Report*” (2012)
- [4] NASA Astrophysics Roadmap Team, C. Kouvelioutou, Chair, “*Enduring Quests, Daring Visions: NASA Astrophysics in the Next Three Decades*” (2013)
- [5] M. Weisskopf *et al.*, “*Beyond Chandra – The X-ray Surveyor*,” Proc. SPIE 1505.00814 (2015)
- [6] R. Smith *et al.*, “*Arcus: an ISS-attached high-resolution X-ray grating spectrometer*,” Proc. SPIE **9144**, id. 9144Y, (2014)
- [7] N. Gehrels, S. Barthelmy, and J. Cannizzo, “*Time-Domain Astronomy with Swift, Fermi and Lobster*,” Proc. IAU, **Vol. 285**, pp. 41-46, (2012)
- [8] Laser Interferometer Gravitational-wave Observatory (LIGO) Scientific Collaboration, “*Predictions for the rates of compact binary coalescences observable by ground-based gravitational-wave detectors*,” Classical and Quantum Gravity, **Vol. 27**, p. 173001, (2010)
- [9] B.D. Metzger and E. Berger, “*What is the Most Promising Electromagnetic Counterpart of a Neutron Star Binary Merger?*” Astrophysical Journal, **Vol. 746**, p. 48, 2012.
- [10] K. Ryu *et al.*, “*Development of CCDs for REXIS on OSIRIS-REx*,” Proc. SPIE **9144**, 91444O-1 (2014)

For additional information, contact Mark Bautz: mwb@space.mit.edu



Mark Bautz

Fast Event Recognition for the ATHENA Wide-Field Imager

Prepared by: David N. Burrows (PSU)

Summary

High-throughput X-ray missions of the future, including proposed Explorer missions like Joint Astrophysics Nascent Universe Satellite (JANUS) and X-ray Time Domain Explorer (XTiDE), the proposed International Space Station (ISS) mission Arcus, the European Space Agency (ESA) Advanced Telescope for High ENergy Astrophysics (ATHENA) mission, and the notional X-ray Surveyor mission, will use active pixel sensors (APS) with very high readout speeds that are too fast for software event recognition. Under this Strategic Astrophysics Technology (SAT) program, we are developing a high-speed event recognition module called a Frame Builder, running on a field-programmable gate array (FPGA), based on a prototype design developed for our JANUS Small EXplorer (SMEX) proposal. The purpose of this project is to advance the Frame Builder from Technology Readiness Level (TRL) 3 to at least 4.

Background

For the past two decades, the state-of-the-art detector for X-ray astronomy missions has been the CCD detector. X-ray CCD instruments use a technique of “event recognition” to read images, scan them for X-ray events, and telemeter only X-ray events; compressing the data rate from these instruments by more than a factor of 500. These algorithms are well-proven in flight and have been shown to produce data quality indistinguishable from laboratory analysis of full CCD images [1, 2].

Objectives and Milestones

Technical Approach and Methodology

The primary objectives of this proposal are to design and build a prototype breadboard version of a high-speed Frame Builder, and to advance the design to TRL 4. This board must extract X-ray events from the high-speed data stream from an APS; in other words, it performs event recognition and data compression. The existence of high-speed, radiation-tolerant Field Programmable Gate Arrays (FPGAs) makes this feasible. During Phase A of our JANUS proposal, we developed a preliminary design concept for this circuitry that is at TRL 3. We will now implement our event recognition algorithms on a low-fidelity breadboard Event Recognition Processor (ERP) and demonstrate basic functionality and high-speed operation in our laboratory to achieve TRL 4.

Event Recognition

Most pixel data obtained with a CCD or APS are “empty,” containing only read noise (Fig. 1). Reducing the data to fit satellite telemetry bandwidth requires extracting candidate X-ray signals from this data stream, a process we refer to as “event recognition,” and passing them to the flight software for characterization and transmission to the ground. The spatial distribution of charge generated by X-ray interactions has characteristic features: charge is usually deposited in 1–4 pixels, depending on exactly where the photon lands within the pixel [3]. For example, if a photon hits near a pixel boundary, the charge cloud produced in the detector will be split between the adjacent pixels (Fig. 1). By contrast, background events due to charged-particle interactions in the detector tend to deposit large amounts of charge across many adjacent pixels (Fig. 2). Thus, classifying the “morphology” of an event allows it to be interpreted as either an X-ray or background event with high confidence [4]. Amplitude windows provide a second powerful discriminator, since charged particles deposit charge packets in the deep depletion region of an active pixel detector that are much larger than

those produced by X-rays in the instrument bandpass. These techniques have been used for several decades, achieving charged-particle rejection efficiencies of order 99.9% in X-ray CCD data [4 – 8]. Because they depend primarily on photoelectric absorption in pixelated silicon detectors, the same techniques apply to active pixel detectors.

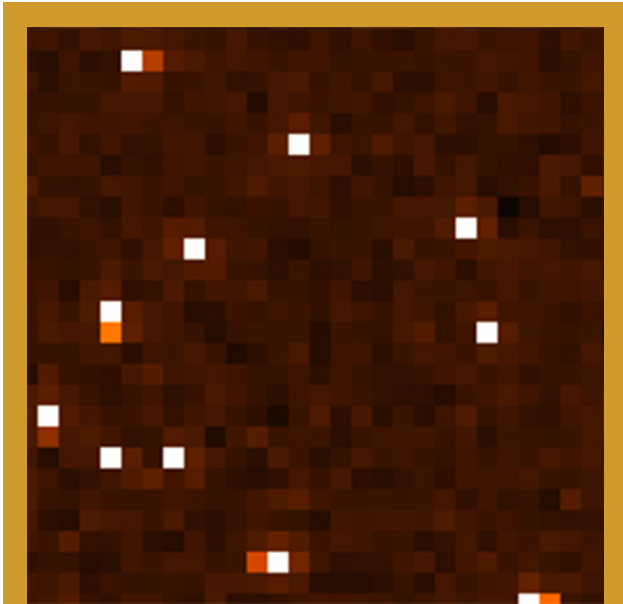


Fig. 1. Small portion of a single frame of ground test data from hybrid CMOS detectors developed by PSU, where color indicates the signal in each pixel. Most pixels show read noise (dark red/black). A few isolated bright pixels (white) represent X-ray events depositing their energy into single pixels. Several events are also seen in which the charge is spread into adjacent pixels, indicating the photon was absorbed near a pixel boundary [3].

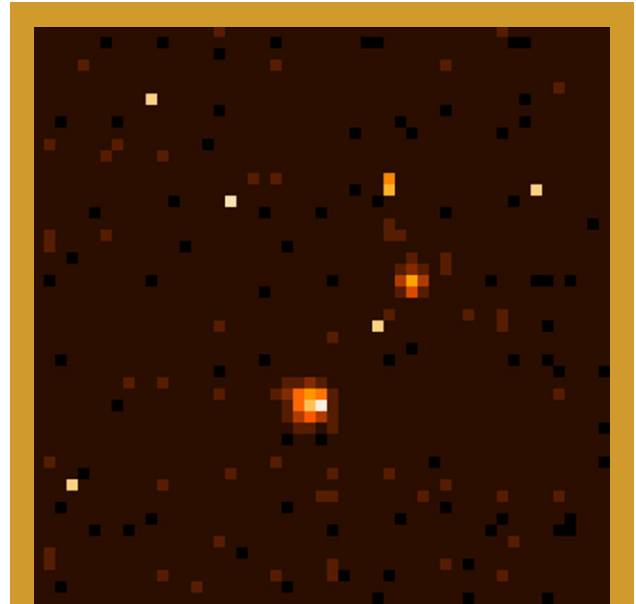


Fig. 2. Small portion of a single frame of flight data from the Swift X-Ray Telescope (XRT) CCD. Most pixels show read noise. A few isolated bright pixels (white/yellow) represent X-ray events depositing their energy into one or two pixels. Two broad, “blobby” events are from cosmic-ray interactions in the detector, which produce wide charge clouds, easily distinguished from X rays.

Frame-Builder Concept

The Frame Builder is an FPGA-based board that performs high-speed processing of active-pixel frames and identifies candidate X-ray events. A block diagram of the main functions of the Frame Builder is shown in Fig. 3. The Frame Builder consists of a high-speed data capture and demultiplexing block, masking of bad pixels, event detection and grading (event recognition), and an output buffer (not shown). A full-scale Frame Builder must be able to combine data from multiple readout channels. The required logic is very similar to that which we designed for JANUS and updated for the International X-ray Observatory (IXO) Wide Field Imager. Under this grant we will implement a single-channel version of the Frame Builder to test our ability to process data accurately at speeds approaching those required by future instruments, including the ATHENA WFI.

Implementation of a Single-Channel Event Recognition Processor

The heart of the Frame Builder is the ERP, as shown in Fig. 3. The ERP accomplishes the event recognition task through signal processing and pattern matching. The input data have already had any necessary bias and gain corrections applied and have been demultiplexed to determine the (X, Y)

location and signal value of each pixel. The data are temporarily stored in high-speed FPGA memory. A sliding 3×3 window is then virtually scanned across the three-row pixel buffer and each 3×3 “neighborhood” is searched for a local maximum (that exceeds an adjustable threshold) in the central pixel. When one is found, this pixel is identified as a possible X-ray event, and the event is graded, using an uploadable lookup table to assign event grades. The event is then formatted and passed to the output telemetry stream as a 3×3 “neighborhood” or as an X-ray with position, energy (E), and grade (depending on the instrument telemetry mode).

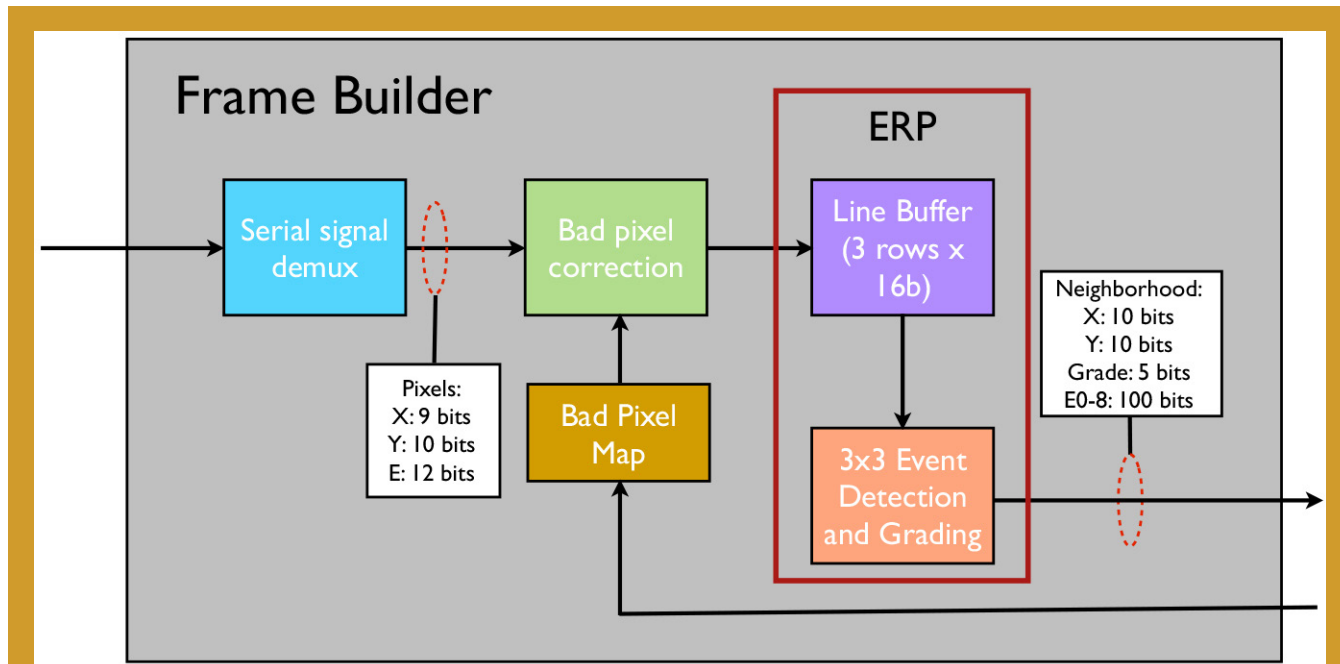


Fig. 3. A simplified block diagram of the Frame Builder. High-speed serial digital data are demultiplexed and bad pixels are zeroed as needed. The data are then inserted into a three-line buffer in the ERP and scanned for valid X-ray events using a sliding 3×3 pixel window. Event grades are encoded based on a simple comparator with a settable threshold. Output data are 3×3 “neighborhoods” centered on candidate X-ray events. Bit assignments shown are nominal.

The basic processing implied in the previous sentence has been implemented in software by all three of our groups (PSU in our laboratory CCD and CMOS cameras and on Satellite de Aplicaciones Cientificas-B (SAC-B) and Swift; MIT on Advanced Satellite for Cosmology and Astrophysics (ASCA), Chandra, and Suzaku; and SAO in their laboratory CMOS cameras). We will begin by implementing the version used on Swift. Similarly, various grading schemes have been used in previous missions, ranging from the ASCA grades (0-7) to the Chandra Advanced CCD Imaging Spectrometer (ACIS) system, in which a bit is assigned to each of the eight surrounding pixels in a 3×3 neighborhood, resulting in grades from 0 to 255. We will use the ACIS system for our testing.

For this project, we will implement the single-channel ERP shown in Fig. 4. This will provide a proof-of-concept for a hardware implementation of the critical function of this board, identification, and grading of X-ray events in a data stream. TRL 4 testing will be done at simulated data rates ranging from 1200 kilobits per second (kbps), the speed of the Swift software implementation, to 1 gigabyte per second (GBps).

The ERP will be implemented on a Xilinx Virtex-5 FPGA. The Virtex-5 OpenSPARC Evaluation Platform (Fig. 5) is a PCI Express board (equivalent to the Xilinx ML509 board) that facilitates development and testing of the FPGA in a host PC. This board allows us to test the most critical portions of the design at a variety of operating speeds in a simple, convenient test environment, with minimal development costs.

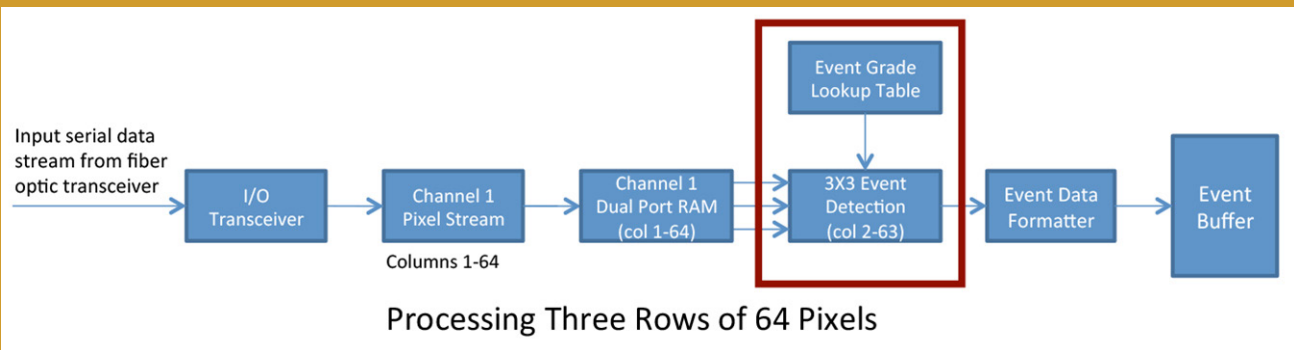


Fig. 4. A single-channel implementation of the ERP, capable of handling a string of events from a 64-row-wide strip of an APS or CCD (figure shows processing schematic for three rows of 64 pixels). We will test this using fixed data patterns. The architecture allows row widths up to 1024 columns. Events from rows 1 and 64 cannot be fully processed in this breadboard implementation because they do not have a full 3×3 pixel “neighborhood” available to classify the event grade.

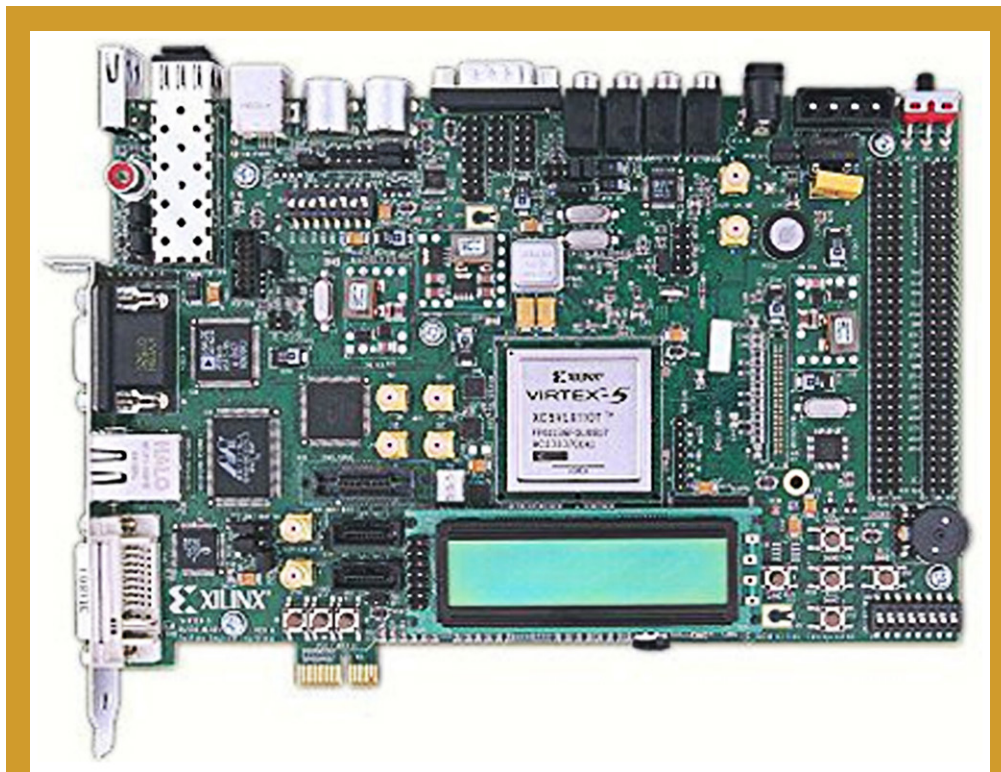


Fig. 5. The Virtex-5 OpenSPARC Evaluation Platform is specifically designed to be a flexible development board for testing high-speed Virtex-5 class FPGAs.

We will begin with a very simple three-row implementation to verify ERP functionality over a range of operating speeds. We will pay particular attention to jitter sensitivity and timing difference between commercial and flight-qualified versions of the Virtex-5 chip, but will concentrate on proving the concept on the commercial version, since that satisfies TRL 4 requirements.

Once the basic building blocks have been tested, we will implement and test the complete single-channel ERP block (Fig. 4) capable of handling data from a 64×64 detector (or a 64-column segment of a larger detector). This gives us a reasonable image size on which to test the algorithms against input test patterns, and will also allow us to perform tests on a real APS in our laboratory once the tests using simulated data are complete. However, the architecture will allow expansion up to 1024-column-wide devices.

The total data rate from the WFI will be about 1.5 GBps, but this will be divided into at least six data streams that can be processed in parallel by the Frame Builder. Thus, the effective data rate for any single data stream in the Frame Builder is 0.25 GBps. To achieve sufficient margin, we will test up to a readout speed of 1 GBps. We will verify the algorithm is functioning as expected at slow clock speeds (150 kilopixels per second, the speed we currently use in our laboratory cameras) before incrementally increasing the effective clock speed to the GBps goal. FPGA timing and performance will be verified at each clock speed, and the design will be modified as necessary to solve any problems found at high readout speeds.

Progress and Accomplishments

Task List

This effort extends over two years (Fig. 6). In the first year, the work will focus on implementing the ERP design in the FPGA and testing the basic event detection logic on a simple single-channel segment. This work will be done jointly by the PSU Department of Astronomy and Astrophysics (Astro) and the PSU Applied Research Laboratory (ARL), and will be completed by the end of Year 1 (Calendar Year, CY, 2015). Further testing will continue into Year 2, with TRL 4 demonstrated by the end of the effort. MIT and SAO will participate throughout the project via annual meetings at PSU, monthly telecons, and annual joint trips to WFI consortium meetings.

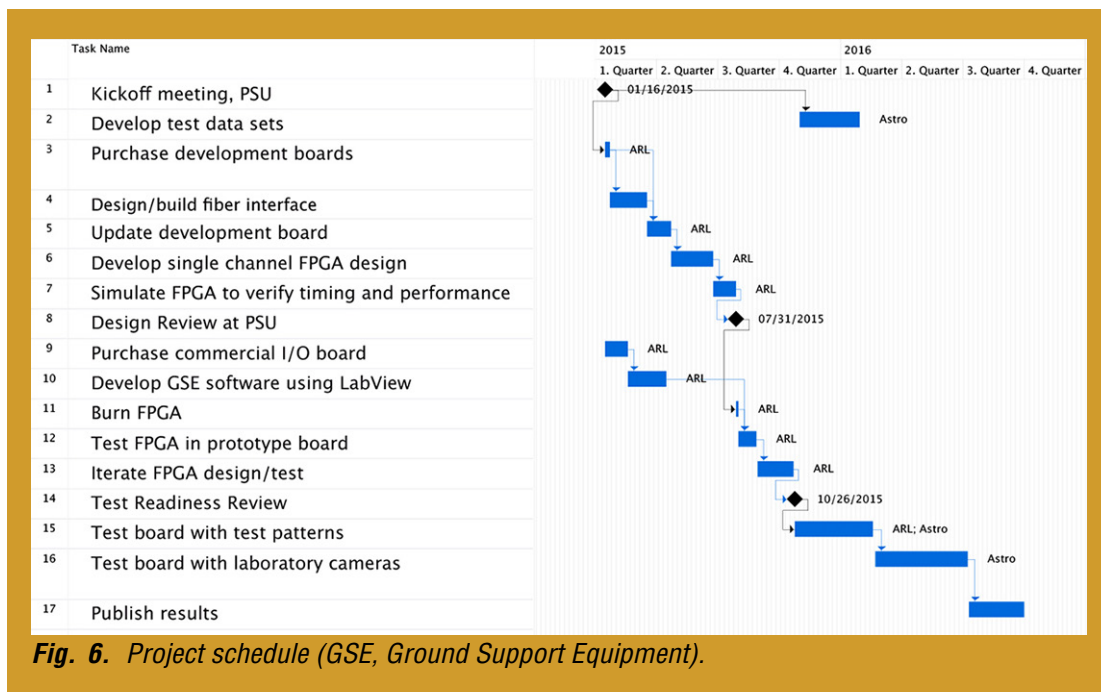


Fig. 6. Project schedule (GSE, Ground Support Equipment).

Progress to Date

Here is the state of progress to date by task number:

1. Complete.
2. Started. The first set of test data sets is complete, and software for generating arbitrary test data sets for use in later stages of testing is complete.
3. Complete.
4. We have modified our plans for the data interface. The data interface architecture has been defined, and a preliminary RS-232 data interface is complete. We are in the process of upgrading this to a high-speed data interface. The fiber-optics interface has been postponed until Year 2.
5. Postponed to Year 2.
6. The overall architecture design is complete. Design work is beginning on a three-row, 64-column implementation of the basic ERP. This work is slightly behind our original schedule due to personnel availability.

Path Forward

The remaining tasks have not yet started. Major tasks and milestones are shown in Table 1.

CY 2015	CY 2016
Kickoff meeting (1/16/15)	Test pattern performance verification (2/19/16)
Design review (7/31/15)	Realistic data testing (7/09/16)
Test breadboard version (8/28/15)	Test report completion (8/20/16)
Test Readiness Review (10/26/15)	Publication of results (12/20/16)

Table 1. Key program tasks and milestones with completion dates.

References

- [1] L. J. Cawley *et al.*, “*CCD x-ray detectors: on-board data processing*,” in O. H. W. Siegmund and John V. Vallerga (eds.), *EUV, X-Ray, and Gamma-Ray Instrumentation for Astronomy VI*, **Vol. 2518** of Society of Photo-Optical Instrumentation Engineers (SPIE) Conference Series, 179–187 (1995)
- [2] J. E. Hill *et al.*, “*Readout modes and automated operation of the Swift X-ray Telescope*,” in K. A. Flanagan and O. H. W. Siegmund (eds.), *X-Ray and Gamma-Ray Instrumentation for Astronomy XIII*, **Vol. 5165** of Society of Photo-Optical Instrumentation Engineers (SPIE) Conference Series, 217–231 (2004)
- [3] J. Hiraga *et al.*, “*Subpixel Spatial Resolution of the X-Ray Charge-Coupled Device Based on the Charge Cloud Shape*,” *Japanese Journal of Applied Physics*, **40**, 1493 (2001)
- [4] D. H. Lumb and A.D. Holland, “*Event recognition techniques in CCD X-ray detectors for astronomy*,” *Nuclear Instruments and Methods in Physics Research A*, **273**, 696 (1988)
- [5] D. H. Lumb and A.D. Holland, “*Background rejection techniques in CCD X-ray detectors for astronomy*,” *IEEE Transactions on Nuclear Science*, **35**, 534 (1988)
- [6] D. H. Lumb, “*Particle background in CCD detectors*,” in O. H. W. Siegmund (ed.), *EUV, X-Ray, and Gamma-Ray Instrumentation for Astronomy IV*, **Vol. 2006** of Society of Photo-Optical Instrumentation Engineers (SPIE) Conference Series, 300–306 (1993)
- [7] A. Owens and K.J. McCarthy, “*Energy deposition in X-ray CCDs and charged particle discrimination*,” *Nuclear Instruments and Methods in Physics Research A*, **366**, 148 (1995)
- [8] J. A. Mendenhall and D. N. Burrows, “*CCD Sounding Rocket Observation of the High-Latitude Soft X-Ray Background*,” *Astrophys. J.*, **563**, 716 (2001)

For additional information, contact David Burrows: burrows@astro.psu.edu



David Burrows

Demonstrating Enabling Technologies for the High-Resolution Imaging Spectrometer of the Next NASA X-ray Astronomy Mission

Prepared by: Caroline Kilbourne (PI; NASA/GSFC); Joseph Adams, Simon Bandler, and Stephen Smith (NASA/GSFC); Joel Ullom, W. Bertrand Doriese, and Johnathon Gard (NIST/Boulder); and Kent Irwin (Stanford University)

Summary

In order to enable the next generation of high-resolution X-ray imaging spectrometers for astrophysics, we are developing large-format arrays of X-ray microcalorimeters and their readout. Specifically, we have been developing Transition Edge Sensor (TES) arrays and a Time-Division-Multiplexed (TDM) Superconducting QUantum Interference Device (SQUID) readout. These spectrometers have very high spectral resolution and quantum efficiency, combined with the ability to observe extended sources without spectral degradation. The current program has been supported by the Strategic Astrophysics Technology (SAT) program since 2013, and is the work of a collaboration between our research groups at NASA/GSFC (PI C. Kilbourne); National Institute of Standards and Technology (NIST), Boulder (lead J. Ullom); and Stanford University (lead K. Irwin). These groups have been collaborating on microcalorimeter spectrometer technology development since 1998. This collaboration previously brought a TES detector and readout system to Technology Readiness Level (TRL) 4 (per both NASA and the European Space Agency, ESA, as part of the formulation of the International X-ray Observatory, IXO). The goal of the ongoing program is to advance key components of an X-ray microcalorimeter imaging spectrometer from TRL 4 to 5, and to advance a number of important supporting technologies to at least TRL 4.

The prospects for future missions that will benefit from the successes of this research program changed in June 2014 with the choice of the Advanced Telescope for High-ENergy Astrophysics (ATHENA) [1] for the European L2 (large mission) opportunity. One of the two instruments for this mission, the X-ray Integral Field Unit (X-IFU), is a high-resolution imaging X-ray spectrometer. The use of TES microcalorimeters, originally pioneered by our collaboration and under development in our SAT program, is currently assumed for this instrument [2]. Very recently, both NASA and the PI of X-IFU, Dr. Didier Barret, have communicated interest in designating the X-IFU microcalorimeter array as one of NASA's principal contributions to ATHENA, with ESA's concurrence. As a consequence, this collaboration submitted a new SAT proposal entitled "Providing Enabling and Enhancing Technologies for a Demonstration Model of the ATHENA X-IFU" to cover our contribution to X-IFU technology development in fiscal years 2016 and 2017. In fact, our pivot towards ATHENA has already begun, resulting in a change of emphasis in our current program as explained in the Background section.

The primary goal of the current project has been to advance the core detector-system technologies to a strong demonstration of TRL 5. The criteria for TRL 5 depend on specific mission requirements, as, in fact, does the meaning of "core technology." In the absence of a single mission to drive the requirements, we planned a demonstration based on a basic element common to various mission concepts at the time of the proposal: a kilo-pixel array with a 0.25 mm pitch, capable of achieving 3 eV resolution at count rates up to 50/s/pixel. This "core" constituted the entire focal plane array in one mission concept (the first version of the ATHENA spectrometer, in fact), and part of the instrument capabilities in several others, thus the anticipated TRL-5 demonstration of the common element will be an important milestone towards any future X-ray imaging spectrometer.

Additional objectives of this program have been to develop and demonstrate two important related technologies to at least TRL 4 that would allow an expanded focal plane and higher per-pixel count rates without greatly increasing mission resource requirements. The project also includes development of a design concept and critical technologies needed for the thermal, electrical, and mechanical integration of the detector and readout components into the focal-plane assembly. The switch from preparing technologies to enable a variety of X-ray spectroscopy missions to instead developing technologies for one specific mission has had the greatest impact on the plans for these related technologies.

Background

The ability to perform broadband imaging X-ray spectroscopy with high spectral and spatial resolution was an essential capability of the IXO mission concept. Despite the fourth-place ranking of IXO in the 2010 National Research Council (NRC) decadal review of astrophysics, “New Worlds, New Horizons” (NWNH), the IXO science focus was strongly endorsed in the review, as was investing in its key technologies. Quoting the NWNH, “*Because of IXO’s high scientific importance, a technology development program is recommended this decade with sufficient resources.*” The technology development program we are pursuing is a response to this endorsement, to enable a mission with a science focus similar to IXO. The science case is the study of the universe of extremes, from black holes to large-scale structure. The main goals are structured around three main topics – “black holes and accretion physics,” “cosmic feedback,” and “large-scale structure of the universe.” Underpinning these topics is the study of hot astrophysical plasmas that broadens the scope of this science to virtually all corners of astronomy.

The reference detector technology we have been developing consists of Mo/Au TES thermometers (operated at < 0.1 K) with close-packed Bi/Au thermalizing X-ray absorbers on a 0.25-0.3 mm pitch. In our baseline TDM concept [3], outputs from the dedicated input SQUIDs of individual TES pixels are coupled to a single amplifier, and multiplexing is achieved by sequential switching of these input SQUIDs.

The integrated detector system reached TRL 4 in March 2008 with the successful demonstration [4] of multiplexed (2 columns \times 8 rows) readout of 16 different pixels (in an 8 \times 8 array) similar to those in the current reference design. Reaching this milestone showed the baseline technology approach is fundamentally sound. The detector pixels were sufficiently uniform to permit good performance under common bias, and the modest degradation of detector performance while multiplexed was consistent with models. Resolution across 16 multiplexed pixels ranged from 2.6 to 3.1 eV, and the pulse time constant was 0.28 ms. This “2 \times 8 demo” achieved the most fundamental goal of a demonstration of TRL 4 (as articulated in NASA Procedural Requirements NPR 7123.1B and expanded in [5]) – basic technological components were integrated to establish that they will work together. The performance approached the requirements of potential system applications in terms of resolution, speed, pixel scale, and quantum efficiency.

We are very close to completing the demonstration we defined as necessary for TRL 5:

“Demonstrate multiplexed (3 columns \times 16 rows) readout of 48 different flight-like pixels. The pixels shall be placed on a 0.25 mm pitch in a 32 \times 32 (or greater) array, and more than 95% of pixels must achieve better than 3 eV resolution at 6 keV, using an analysis method consistent with the requirement of 80% live-time at an X-ray rate of 50/s/pixel.”

We expect to complete this milestone by the end of 2015.

To reach TRL 5, the demonstration must be done in a relevant environment. Vibration testing of an array is required to validate the pixels’ mechanical design. Radiation testing of the detectors and readout is necessary to validate robustness in the space environment. Preliminary vibration testing is planned this year, but radiation testing has been deferred, in part because the readout planned for X-IFU is different

from the baseline of our development program to this point in time. The baseline readout for X-IFU is Frequency-Division Multiplexing (FDM) [6], in which the TESs are biased with AC signals of different frequencies, which act as carriers for the slower thermal signals.

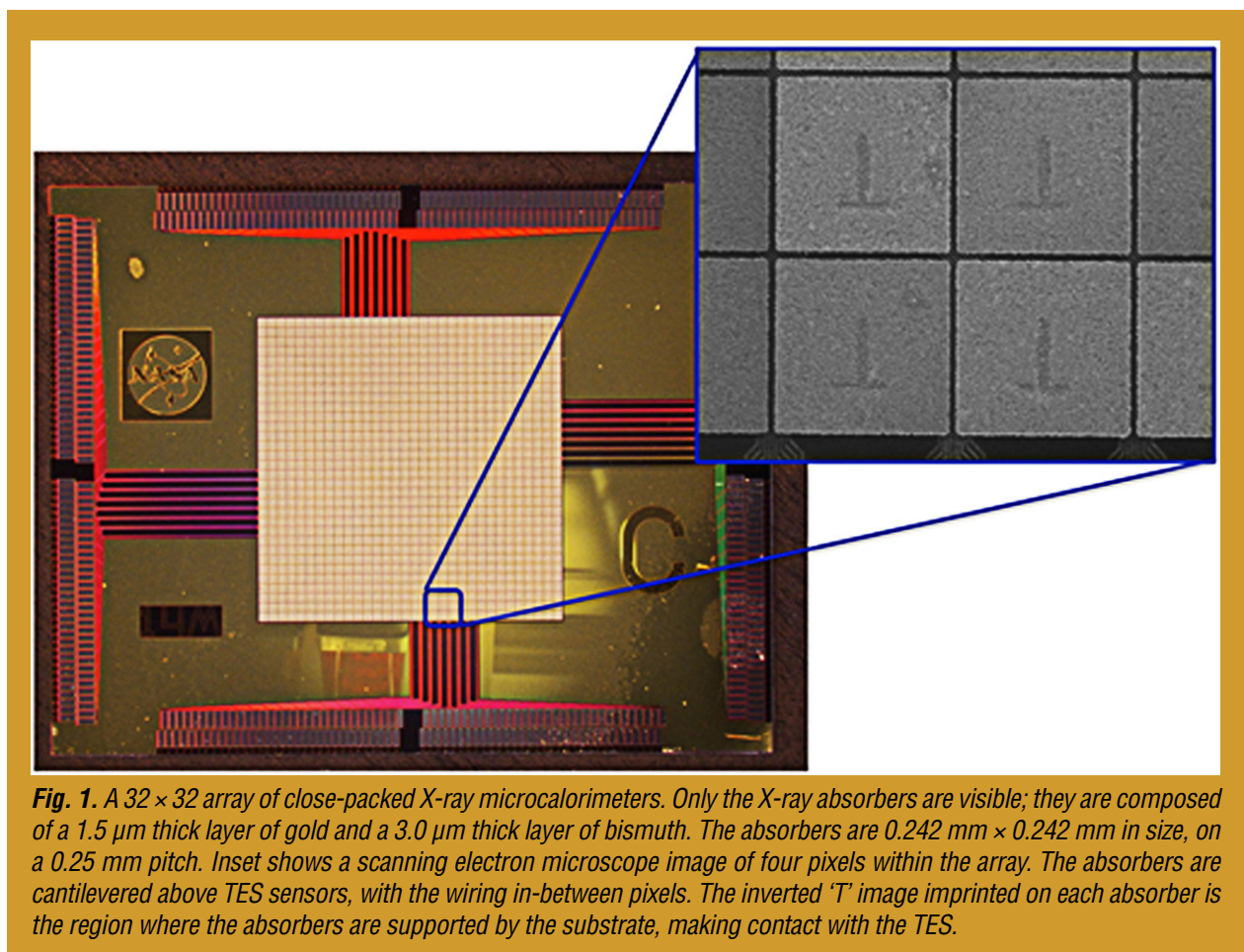
One of the related technologies we proposed to develop to at least TRL 4 is position-sensitive TES devices. Position-sensitive devices enable a large expansion of the field-of-view coverage at the cost of degraded (though still very high) energy resolution. Such a compromise in resolution is not currently under consideration for X-IFU, thus this line of development has fallen in priority.

The other related technology we are developing towards TRL 4 is Code-Division Multiplexing (CDM). CDM is a switched-multiplexing system like TDM. In TDM, only one TES channel is on at a time, whereas in CDM all channels are always on, but are switched in polarity according to a matrix of combinations, thus avoiding the aliased noise of TDM. We consider the continued development of TDM important despite the X-IFU baseline of FDM because it is a core capability that could be vital to future NASA missions, or even ATHENA, if FDM development, which presently lags TDM, runs into unexpected difficulties. CDM is compatible with the TDM infrastructure, but provides increased design margin.

Progress and Accomplishments

Multiplexed Readout of Large-Format Arrays

Production of 32×32 TES arrays, such as shown in Fig. 1, is routine. The pixels are on a 0.25 mm pitch. All pixels are wired out to the edge of the array, but, on these test devices, only 256 of the pixels (25%) have wiring going to bond pads around the circumference of the silicon carrier wafer.



Significant improvements have now been made throughout the multiplexer system. These include:

- New room-temperature amplifier for > 20 MHz bandwidth (increased from ~ 2 MHz);
- Hardware and firmware upgrades to enable 32 bits of data to be streamed in 16 master-clock cycles;
- New multiplexer (mux) chips with reduced intrinsic multiplexer cross talk;
- New mux chips with intrinsic flux noise reduced to $< 0.4 \mu\Phi_0/\sqrt{\text{Hz}}$; and
- Increased frequencies of two important poles in the system.

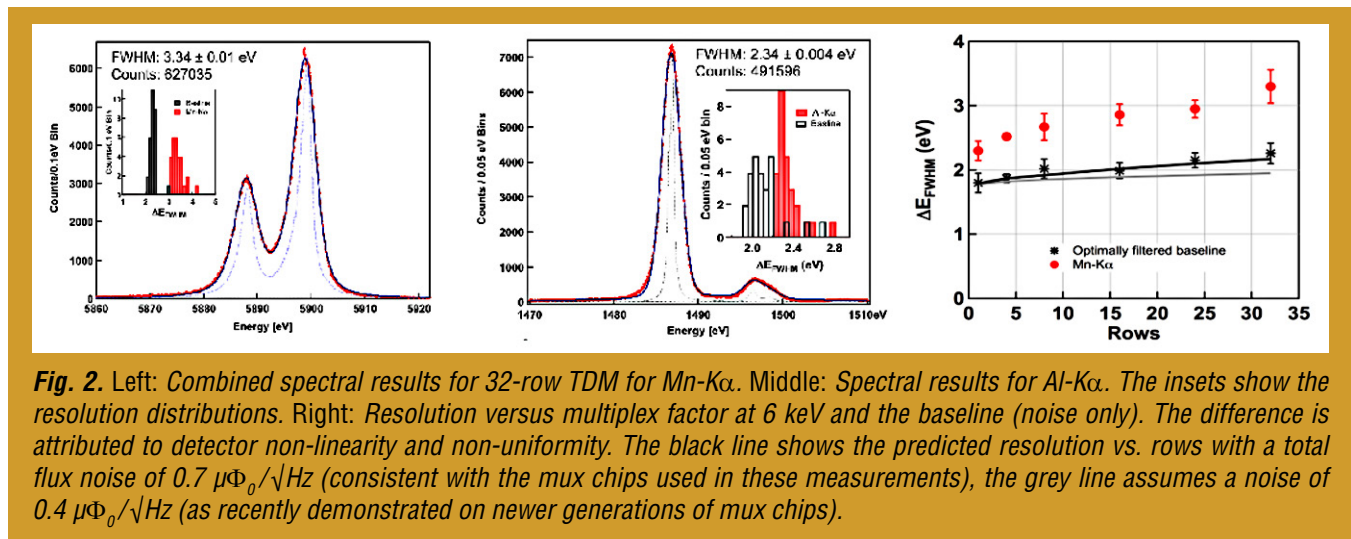
These improvements meet the combined requirements on row-switching time and noise, but they are not yet implemented together in a single readout chain. The present test platform at GSFC utilizes an eight-column focal-plane assembly that is presently configured with multiplexer chips and second-stage SQUID amplifiers of different designs. This mixed configuration enables direct comparison of important performance metrics such as noise, cross-talk, and bandwidth for the different SQUID multiplexing architectures under consideration. Because of the differences, however, rows cannot be addressed across the columns, limiting our initial results to a single column. Furthermore, the particular 32×32 TES array used for these measurements exhibited some non-ideal characteristics, including lower-than-targeted T_c (~ 82 mK) and a larger-than-standard T_c gradient across the array. These effects resulted in non-uniformity across the array and decreased detector linearity with respect to energy.

Despite these less-than-ideal characteristics, excellent performance has been achieved (Fig. 2). We have multiplexed 16 rows in a single column with an average resolution of 2.86 ± 0.17 eV at 6 keV. For 32 rows at 6 keV, the average was slightly worse, not due to TDM limitations but rather the non-uniformity in pixel response resulting from non-ideal magnetic field conditions. At 1.5 keV, we have achieved 2.34 ± 0.1 eV. Performance is improved at lower energy, consistent with the non-linearity of the detector. Thus, for a single column, we are very close to reaching the original milestone. However, because the T_c is lower than the design value, the critically damped time constant is $\sim 40\%$ longer than that needed to meet the original count-rate requirement.

Given the original requirements, the main array technology is approaching TRL 5.

New Multiplexer Chip and Series Array Designs

In each readout channel (or “column”), there are two integrated-circuit chips that are operated inside the cryostat. One is a series array (SA) of SQUIDs that provides amplification, and the other is the multiplexer chip that switches the different signals into that amplifier. Over the last year, we developed several new chip designs that have not yet been integrated into full TES readout demonstration systems. The development



goals have been to decrease the system noise, increase the row-switching speed, and increase the interoperability of components at the system level. We describe several of these new components below.

Low-resistance series arrays: Our newest SAs (dubbed “medium-power SAs” because they dissipate less power in the ~300–700 mK stage where they operate) are made of six “banks” of 64 elements each. The six banks can be wired (in fabrication) to attain various series-parallel combinations. The most-tested combination has two banks in series and three in parallel, and has dynamic resistance of several hundred Ohms. This resistance combined with the capacitance of the readout lines creates a pole in the readout bandwidth in the 5 MHz range. These series arrays are typically then shunted with a chip resistor of about 150 Ω to move this pole closer to 10 MHz.

Recent testing of a new series-parallel combination, in which all six banks are wired in parallel, yields a dynamic resistance of 50–60 Ω with no external resistive shunting required. The resulting bandwidth pole is increased to near 20 MHz, which allows series-array-only settling times of ~50 ns. When coupled to a workhorse two-stage SQUID multiplexer chip, this new SA allows fully switched system settling times as fast as 190 ns; our previous state-of-the-art had been 240 ns. With the new room-temperature digital electronics described in the next section, we have recently recorded TES-pulse data with row times of 240 ns, a significant improvement over our previous state-of-the-art of 320 ns. These series arrays are thus now approaching the combined performance (noise and bandwidth) needed for the full X-IFU (TDM/CDM-style) readout chain.

Flux-actuated TDM multiplexer chips: Our new TDM SQUID-multiplexer chips use “Zappe-style” [7, 8] flux-actuated switches. Each first-stage SQUID (SQ1) is a four-element series-array. All SQ1s in a readout column are DC biased in series. The row-address currents in this architecture do not directly bias the SQ1s, but rather actuate a SQUID switch. Thus the SQ1 DC voltage bias bypasses all SQ1s except the one per column that is addressed.

There are three main advantages to this new architecture:

- The optimal row-address current is now based on geometry, rather than on SQ1 critical current. Previously, SQ1 critical currents had to be well-matched across columns (chips) to allow optimal SQUID performance. Now, SQ1 critical currents need only be matched within a column (within a chip), which will lead to a higher yield of usable components.
- The first-stage SQUID can have dynamic resistance of 20 Ω or higher (was previously several Ohms). This allows higher bandwidth in the pole determined by the mux chip’s connection to the series-array SQUID.
- The switches add the multiplexed signals together without a second-stage SQUID, which was previously used for signal summation, removing potential bandwidth poles and improving total SQUID noise.

These new chips have achieved SQ1-referred system noise as low as $0.33 \mu\Phi_0/\sqrt{\text{Hz}}$ in the configuration in which they will be used. The SQ1-only contribution is $0.27 \mu\Phi_0/\sqrt{\text{Hz}}$, which will meet presumed X-IFU TDM/CDM requirements.

Flux-actuated, 32-channel CDM multiplexer chips: Our new CDM SQUID-multiplexer chips use the same Zappe-style flux-actuated switches as described above. Here, each SQ1 is a six-element series array. As expected, more elements improve the noise: here the full system noise is as low as $0.17 \mu\Phi_0/\sqrt{\text{Hz}}$. We have recently yielded a pair of 32-channel CDM chips of this flux-switched architecture and will use them to read out TESs by the end of Fiscal Year (FY) 2015.

Digital Electronics and Signal Processing

Significant progress has also been made to further increase multiplexer digital-feedback speed, increasing the clock speed from 50 MHz to 125 MHz. We have produced a functional implementation

of a commercial PCIe development board with a NIST 16-channel fiber-optic receiver daughter card and validated data rates up to 200 MB/s. It was necessary to update the firmware with a data-encoding scheme and signal-alignment controls to ensure data fidelity. We have successfully demonstrated operation at 125 MHz with parallel data streaming that allows switching between consecutive rows within 160 ns. Further firmware modifications were made to the row-addressing card to enable matrix-selection schemes required for CDM chips. Additional progress has been made with power handling and delivery within the readout electronics.

The data acquisition software has been updated to support the new PCIe development board and has been successfully integrated with the real-time pulse analysis suite developed for Astro-H ground testing.

Kinematic Mounts of Focal-Plane Components

We have designed kinematic mounts for two detector arrays and an anti-coincidence detector on three separate levels. A first mechanical model (used for fit-checks and verifying the assembly process) has been fabricated. A second iteration using the design materials will be produced. A mechanical model of a full-scale array chip (with perimeter long enough to accommodate pads for all channels) has also been produced and will be iterated to accommodate the mount design. Thermal-cycle and vibration tests can then be performed. Figure 3 shows the first mechanical model array and Fig. 4 shows a series of kinematic mount frames holding dummy detectors.

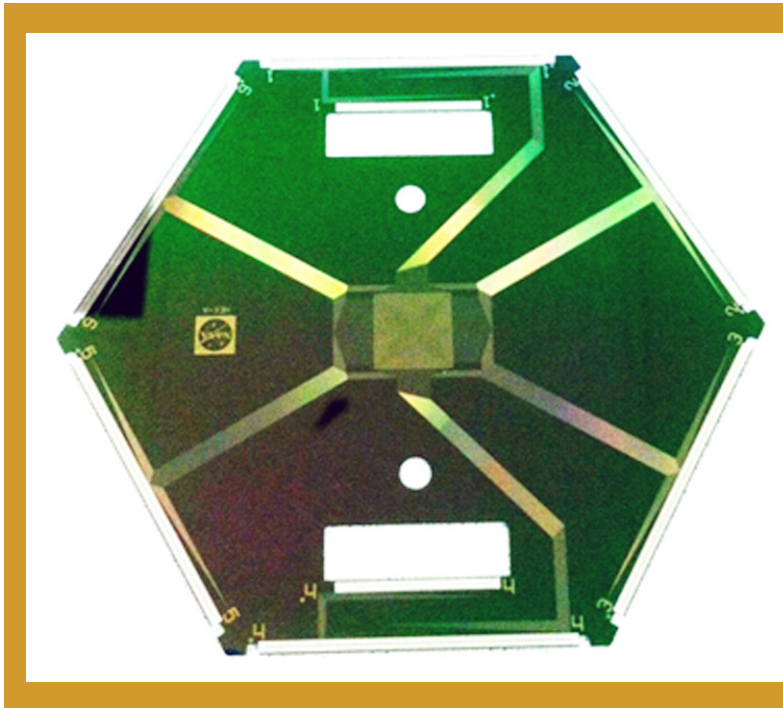


Fig. 3. Prototype fully wired kilo-pixel array chip with 1024 bond-pad pairs to all main array TESs and 128 bond pads routed to rectangular holes for incorporation of a second array. The size is 72 mm corner-to-corner (opposite vertices). The circular holes are for use with an earlier design for the kinematic mounting.

Path Forward

The path to completing the performance demonstration associated with TRL 5 for the core technologies is short. Given a detector of suitable T_c and heat-sinking, our recent improvements in TDM architecture are sufficient to complete a 16-row demonstration as specified in the TRL-5 demonstration milestone. Meeting requirements with at least three columns is essential for TRL 5. We will convert the present multi-configuration test platform to a uniform configuration (with optimal mux chips, second stage SQUID amplifiers, and room-temperature electronics) and complete this demonstration in platforms at both GSFC and NIST before the end of FY 2015. Similarly, a 3×32 row demonstration with a slower detector and reduced maximum count-rate capability will also be achievable.

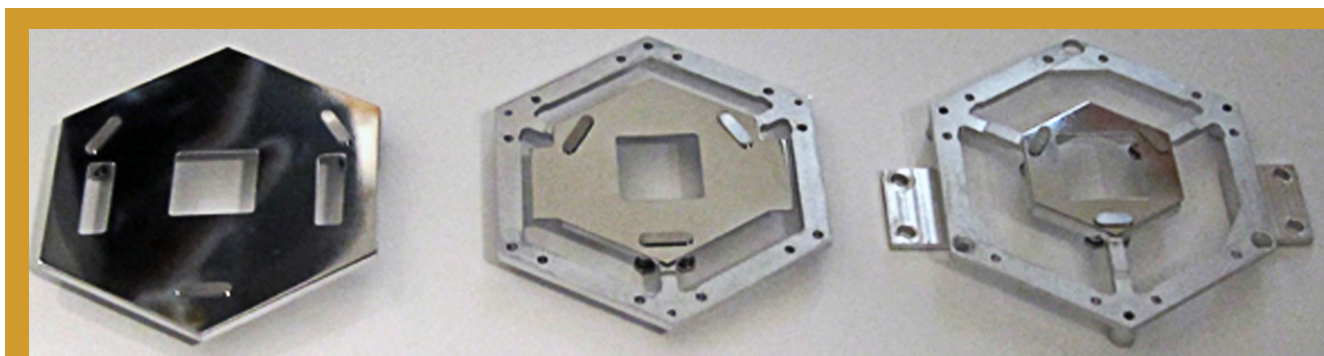


Fig. 4. Three kinematic mount frames with dummy main array, sub-array, and anti-coincidence detector. The three detectors are integrated onto their frames separately and then the frames are integrated.

The X-IFU requirements are in the process of being refined. Serious consideration is being given to the possibility of making the array with two different types of pixels; so the focal-plane coverage, counting-rate, and energy-resolution requirements do not have to be met by a single compromise pixel design. If a central region of smaller pixels is designed to handle bright point sources, the speed of the pixels in the main part of the array can be reduced. Interest in this possibility has been motivated by our collaboration's progress with fine-pitch TES arrays [9] (not SAT-funded). Such pixels can be optimized for either high count-rate capability and high dynamic range, or higher energy resolution at reduced dynamic range. We have been supporting the X-IFU trade studies of array configurations. The outcome of this study will determine the readout requirements of the FDM readout, or an equivalent TDM or CDM readout.

Because the baseline X-IFU FDM readout applies an AC bias to the TES thermometers, we need to characterize and optimize performance under AC bias. Such research is the main component of the related program in which our collaboration is engaged (PI: J. Ullom, "Technology Development for an AC-Multiplexed Calorimeter for ATHENA"). That effort will merge with our overall effort to support early technology demonstrations for the X-IFU.

References

- [1] K. Nandra *et al.*, "ATHENA, the Advanced Telescope for High ENergy Astrophysics," a mission proposal submitted to ESA's L2 large mission opportunity, recently accepted (2014)
- [2] D. Barret *et al.*, "The Hot and Energetic Universe: The X-ray Integral Field Unit (X-IFU) for ATHENA+," astro-ph arXiv:1308.6784 (2013)
- [3] J.A. Chervenak *et al.*, "Superconducting multiplexer for arrays of transition edge sensors," Appl. Phys. Lett., **74**, 4043-4045 (1999)
- [4] C.A. Kilbourne *et al.*, "Multiplexed readout of uniform arrays of TES x-ray microcalorimeters suitable for Constellation-X," Proc. SPIE **7011**, 701104 (2008)
- [5] J.C. Mankin, "Technology Readiness Levels," NASA White Paper (1995)
- [6] R. den Hartog *et al.*, "Baseband Feedback for Frequency-Domain-Multiplexed Readout of TES X-ray Detectors," AIP Conf. Proc. **1185**, 261-264 (2009)
- [7] H.H. Zappe, "Josephson quantum interference computer devices," IEEE Trans. on Magnetics, **13**, 41-47 (1977)
- [8] J. Beyer and D. Drung, "A SQUID multiplexer with superconducting-to-normal conducting switches," Superconductor Sci. and Technol., **21**, 105022 (2008)
- [9] S.R. Bandler *et al.*, "Advances in Small Pixel TES-Based X-Ray Microcalorimeter Arrays for Solar Physics and Astrophysics," IEEE Trans on Appl. Sup., **23**, (3), 2100705 (2013)



For additional information, contact Caroline Kilbourne: caroline.a.kilbourne@nasa.gov

Reflection Grating Modules: Alignment and Testing

Prepared by: Randall L. McEntaffer (University of Iowa)

Summary

Future X-ray missions from Explorers to Probes to large mission concepts designed for soft X-ray spectroscopy will require instrumentation capable of delivering the effective area and spectral resolving power needed to meet their science requirements. Key science goals addressing the cycles of galactic matter and energy feedback, as well as distribution of hot matter in the universe, can be realized through diffraction-grating-based spectrographs. The soft X-ray energy regime below 2 keV contains the majority of spectral features expected from astrophysical plasmas at the relevant temperatures. Diagnostics of key absorption and emission features are achieved with adequate sensitivity and resolution. Spectrometers utilizing X-ray diffraction gratings can provide the performance required to achieve the science goals. However, current technologies require development in the areas of grating alignment, array population, and performance testing to qualify grating spectrometers for these future opportunities.

This document details the plans for a new Strategic Astrophysics Technology (SAT) program with a period of performance spanning calendar years 2015 and 2016. Here, we describe the development efforts for an Off-Plane X-ray Grating Spectrometer (OP-XGS) [1] with an emphasis on the alignment and testing of gratings within their module housings. These developments leverage heavily from associated NASA programs including: 1) a past SAT program (“Off-plane Grating Arrays for Future Missions”) that concentrated on the very initial trade studies necessary to identify grating fabrication, alignment, and testing techniques, 2) a Roman Technology Fellowship (RTF) dedicated to developing our grating fabrication methodology, and 3) an Astrophysics Research and Analysis (APRA) grant for suborbital flight of an OP-XGS. Although previous developments made in these programs were crucial for this SAT [1-7], they are not described in exhaustive detail here in order to concentrate on future efforts specific to alignment and testing of grating modules. To further these efforts, the University of Iowa has partnered with NASA’s Marshall Space Flight Center (MSFC) and Goddard Space Flight Center (GSFC). Collaborators at GSFC are providing X-ray telescopes to be used during performance testing while MSFC is providing testing facilities and support at their Stray Light Facility (SLF) X-ray beamline. The ultimate goal of this project is to populate and qualify a flight-like grating module with several large-format, high-fidelity gratings to create an OP-XGS subsystem that is ready for incorporation into the next spectroscopic X-ray observatory.

Background

The purpose of this study is to advance high-throughput, high-spectral-resolving-power, X-ray spectroscopy and its application in future NASA missions. Specifically, the project will concentrate on improving the Technology Readiness Level (TRL) of off-plane reflection-grating spectroscopy for soft X-rays (0.2 – 2.0 keV). This technology has applications in a variety of NASA missions from suborbital rockets, to Explorer-class missions, to large observatories. An OP-XGS was included in the instrument suite for the International X-ray Observatory (IXO) during the last Decadal Survey, which spurred many follow-on studies including mission concepts such as the Advanced X-ray Spectroscopic Imaging Observatory (AXSIO), the Notional X-ray Grating Spectrometer (N-XGS), and the Square Meter Arcsecond Resolution Telescope for X-rays (SMART-X). Currently, an OP-XGS forms the backbone of an Explorer mission concept, Arcus, submitted in response to the 2014 Explorer Announcement of Opportunity (AO) [8], and is included as a spectrometer concept for the X-ray Surveyor large mission concept. Progress made during the development of the OP-XGS has been detailed in the three previous Program Annual Technology Reports (PATRs) of the Physics of the Cosmos (PCOS) Program. The PCOS program identified X-ray reflection gratings as a critical technology for development in this decade to

address X-ray science goals. In this role, we also contributed a development roadmap detailing the efforts and milestones necessary to advance the OP-XGS to flight readiness, incorporated into the most recent PCOS Technology Development Roadmap (TDR).

Soft X-ray grating spectrometers with high throughput and high spectral-resolving power can address many top science questions such as:

- What controls the mass-energy-chemical cycles within galaxies?
- How do baryons cycle in and out of galaxies, and what do they do while they are there?
- What are the flows of matter and energy in the circumgalactic medium?
- How do black holes work and influence their surroundings?
- How do massive stars end their lives?
- What controls the masses, spins, and radii of compact stellar remnants?

These science questions can be addressed with high-quality X-ray spectra as specifically stated in the 2010 Decadal Survey, *New Worlds, New Horizons in Astronomy and Astrophysics* (NWNH). At the lowest energies, the most efficient method of obtaining high spectral-resolving power is grating spectrometers.

To achieve these science goals, the OP-XGS must be capable of producing spectral-resolving powers ($\lambda/\delta\lambda$) better than 1500, with high throughput over the soft X-ray energy band. The major limiting factor is meeting the spectral-resolving-power requirement. In the context of off-plane reflection gratings, this requires customization of the groove profile to obtain blazed facets with high groove density that varies along the groove direction. In a parallel RTF effort, we are developing a new fabrication method using common lithographic techniques borrowed from the semiconductor industry. Electron-beam (e-beam) lithography enables tight control over the groove profile during recording, while various etching steps can be used to shape the facets to the desired blaze. An optimal groove profile will cancel any grating-induced aberrations to the telescope focus while maximizing throughput and resolving power over our wavelength band of interest. We will use gratings fabricated during the RTF in the current SAT study to populate our grating modules. The design of the grating module has gone through several iterations during the previous SAT program. This design has been refined through testing and analysis leveraged from the APRA program and concept mission studies. In the course of our current SAT, we will implement this design to house our gratings. During module population, alignment tolerances must be met so that every spectrum from every grating overlaps at the focal plane without alignment-induced distortion. We have previously analyzed our alignment tolerances, assessed required metrology, and developed a concept alignment methodology. Therefore, given these previous developments, our development plan for the current SAT can be described at the highest level as two main paths:

- Implementation of our alignment methodology; and
- Performance-testing of aligned modules.

Objectives and Milestones

High diffraction efficiency and high spectral-resolving power have been demonstrated for off-plane reflection gratings. Prototype gratings have been shown to place > 40% of incident light into diffracted orders while also achieving spectral resolving powers > 3000 in the soft X-ray band. These demonstrations place off-plane gratings at TRL 4. While single, prototype gratings have proven the capability of the off-plane design, aligned arrays of large-format, blazed gratings need to be fabricated and tested to prove the technology for flight missions. A program of grating fabrication, alignment, and performance/environmental testing is necessary to bridge the current technology gap and achieve flight readiness.

The milestones needed to achieve our goals for this SAT (implementation of alignment methodology and performance-testing of aligned modules) are listed below with projected completion dates.

1. Quantify alignment tolerances – completed 1st quarter of 2015.
2. Formulate alignment methodology – completed 2nd quarter of 2015.
3. Design medium-fidelity grating mount – completed 2nd quarter of 2015.
4. Fabricate medium-fidelity grating mount – 3rd quarter of 2015.
5. Install alignment fixtures and metrology in the lab – partially completed, continued in 3rd quarter of 2015.
6. Align multiple gratings into mount – 3rd quarter of 2015.
7. Performance and environmental testing of a medium-fidelity module of aligned gratings – 4th quarter of 2015.
8. Improve grating alignment methodology informed by test results – 4th quarter 2015/1st quarter of 2016.
9. Publish results of our findings – 1st quarter of 2016.
10. Design and fabricate high-fidelity grating mount – 1st quarter of 2016.
11. Implement alignment improvements – 1st/2nd quarter of 2016.
12. Align multiple large-format gratings into mount – 2nd/3rd quarter of 2016.
13. Performance and environmental testing of a high-fidelity module of aligned, large-format gratings – 3rd/4th quarter of 2016.
14. Publish results of our findings – 4th quarter 2016/1st quarter of 2017.

In the previous PATR, we provided an extensive list of milestones relevant to the broad development of an OP-XGS. Many of those milestones have been accomplished in the previous SAT or through efforts in our parallel programs or concept mission studies. Several milestones are in process in these parallel programs, and only those dealing with module alignment and testing are detailed here.

Progress and Accomplishments

The current SAT program has just begun, so progress and accomplishments specific to this program are quite limited. However, the work of the past SAT program, as well as our parallel efforts of the RTF, APRA, and concept mission studies have allowed us to make much headway in anticipation of these efforts. We have detailed some of these past accomplishments in several publications [1-7], and discuss here our most recent endeavors applicable to the ongoing SAT.

Much of the effort during this SAT involves X-ray performance-testing. Over the past several years, we have developed a successful record of performance testing gratings for diffraction efficiency and spectral-resolving power; the latter being the largest hurdle for qualifying grating spectrometers for future missions. During previous resolving-power tests at the MSFC SLF (in late 2012), we were limited by source diffusivity; the optics were capable of resolving the electron impact spot on the X-ray source anode. Therefore, while we were able to measure the theoretical resolution of 900 ($\lambda/\Delta\lambda$) for 1st order Mg K α (1.25 keV), higher-order resolutions did not scale accordingly and were limited to 1300. We then moved testing to the GSFC facility (in late 2013/early 2014) where the much longer 600-m beam line allowed for a discrete source. This resulted in a new record for spectral resolving power for a telescope-fed reflection grating with a measured value of ~2100 at 3rd order Mg K α . However, we found that this number was limited by the stability of the CCD which is cantilevered from the main optics chamber and simply supported. Since this measurement, the MSFC SLF has been upgraded to address the previous source issue while the large instrument chamber allows for maximal stability of system components with new support stages for the GSFC optics, Iowa gratings, and MSFC CCD. Preliminary analysis of data obtained late in 2014 shows excellent results. Using the Al K α line, we were able to

detect all orders from -6^{th} to $+6^{\text{th}}$. At 6^{th} order, the spectral line spread function was dominated by the natural width of the Al $K\alpha_1$ and $K\alpha_2$ lines which are only separated by 0.43 eV. This demonstrated another record for X-ray spectral-resolving power, at 3250 (Fig. 1).

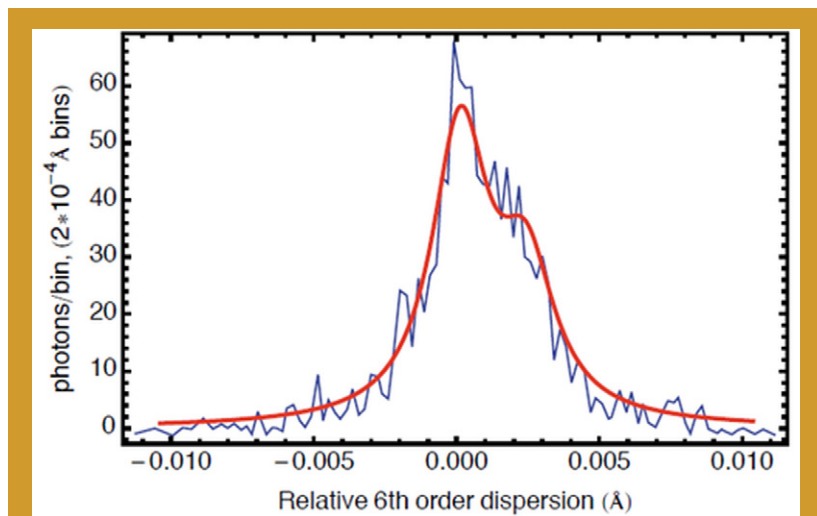
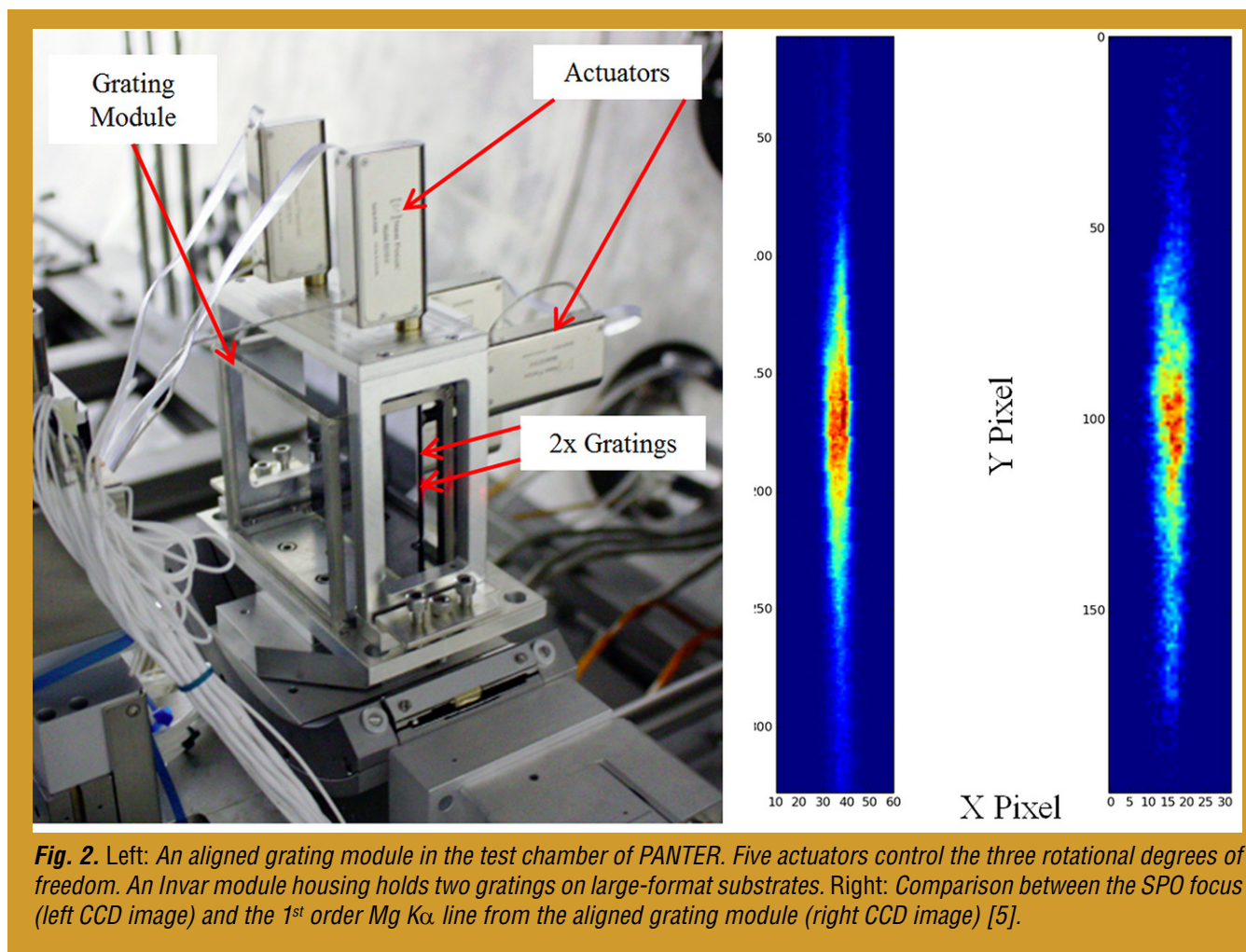


Fig. 1. Spectral resolving power test data (blue histogram) for 6^{th} order Al $K\alpha_1$ and Al $K\alpha_2$ at 8.340 and 8.342 Å, respectively. The red line is the expected Lorentzian response as determined from a fit to the zero order line spread function. The resulting spectral resolving power is 3250.

tolerance (tens of microns vs. a few). Therefore, we had to find a new substrate material, which also involved revisiting and tweaking our fabrication method. The trade study resulted in changing to fused silica as the substrate of choice, which provided many benefits. For example, fused silica wafers could be bought off-the-shelf at the required thickness (0.5 mm) and figure. In addition, the new final step of our process involves nano-imprint replication of the silicon wafer groove profile into UV-cured resist. This enables mass production of gratings via replication into a mechanically robust resist, while concurrently exploiting the transparent nature of the fused silica substrates.

In addition to completing the grating substrate trade study, our rocket and Arcus analyses resulted in several iterations of grating module design and alignment methodologies. One of the later iterations was fabricated, implemented, and tested. The performance test was performed at the Max Planck Institute for extraterrestrial Physics PANTER X-ray test facility and utilized a Silicon Pore Optics (SPO) module as the telescope. The SPOs form the basis of the telescope for the European Space Agency (ESA) Advanced Telescope for High-ENERgy Astrophysics (ATHENA) X-ray observatory and are also proposed for use onboard Arcus. The test concentrated on our ability to align two gratings within a module using an “active” alignment methodology. This involves mounting a reference grating within the module while the position of a second grating is actively manipulated during X-ray testing to overlap spectra at the focal plane. A detailed description of the alignment tolerances and module design can be found in Allured *et al.* [6]. Figure 2 shows the aligned grating module within the PANTER test chamber. The module itself is made of Invar, heat treated to match the Coefficient of Thermal Expansion (CTE) of silicon. A larger alignment mount houses five pico-actuators that control the three rotational degrees of freedom while the translational degrees of freedom are controlled mechanically. The first-order diffracted spectral line of Mg $K\alpha$ is also shown in comparison to the SPO focus. Once aligned, we showed that the gratings contributed no additional aberration to the line-spread function which was dominated by the quality of the telescope focus [5].

A small Explorer concept mission named Arcus was studied over the last 1.5 years, culminating in a proposal submitted near the end of 2014. During this time, we studied alignment tolerances and methodologies in detail. We also performed similar tolerance analysis for an upcoming suborbital rocket payload flying the same gratings. This enabled a detailed understanding of our tolerances, how they depend on spacecraft configuration, and what strategies can be used to achieve them. The tolerance analysis led to a reevaluation of our grating substrate material. Previously, we were etching grooves directly into silicon wafers. However, typical wafers have a bow in their flatness that is beyond the acceptable range for our grating figure



The PANTER testing signified a major step for OP-XGS studies, as not only was it the first time that we aligned gratings to this level, it also shed light on several flaws in the module design and limitations of our alignment methodology. These findings led to another iteration which has recently completed the design phase and is currently entering implementation. The alignment setup is shown in Fig. 3. Briefly, it consists of a laser source that is expanded to sample nearly the entire grating surface, which is then analyzed by a Wave-Front Sensor (WFS) to determine the grating figure and normal. Using this information, each grating in the module is positioned relative to the previous grating in the stack using a hexapod to control the grating position and a separate stage stack to control module position. Measuring the grating figure and attitude by the WFS during module population ensures that each grating is placed in the proper orientation. Additional measurements of the grating surfaces relative to a fiducial flat on the module mount are made using a theodolite. These ensure proper referencing of each grating and provide an alignment reference for X-ray testing. We have begun implementation of this methodology in our lab (milestones 4 and 5 above) with population of modules soon to follow (milestone 6).

As mentioned above, we have recently improved our blazed-grating fabrication recipe to include replication onto flat fused-silica substrates. While not a direct effort of this SAT, gratings fabricated in this manner will be used, so their developmental status is important. In efforts leading up to the aforementioned PANTER testing, we successfully fabricated off-plane, radial-profile, blazed gratings using our entire fabrication process. We first etched into a 10° off-axis cut <111> silicon wafer to form our radial, blazed-profile master, which was subsequently imprinted into UV resist on a fused-silica

wafer. This was tested in the Littrow configuration with the SPO optics to determine that the grating induced no aberration into the telescope-dominated line-spread function, while also exhibiting a strong blaze effect by preferentially diffracting onto one side of zero order [7]. Figure 4 show a comparison between the 0th, +1st and -1st order Mg K α lines. The calculated half-energy widths (HEWs) demonstrate that the zero-order profile is maintained, thus leading to the conclusion that there is no dispersion-based aberration contributing to the line-spread function. This 10° blazed grating placed twice as much flux into -1st order in comparison to +1st order. In addition, we successfully fabricated 29.5° and 54.7° blazed gratings in silicon wafers to verify production of the high blaze angles typically needed for future X-ray spectrometers (Fig. 4). We tested the 29.5° blazed grating at PANTER as well, and showed line-spread function agreement along with a very strong blaze function – the relative efficiency of +1st order was 43 times that of -1st order with +2nd order almost twice as strong as +1st order [7].

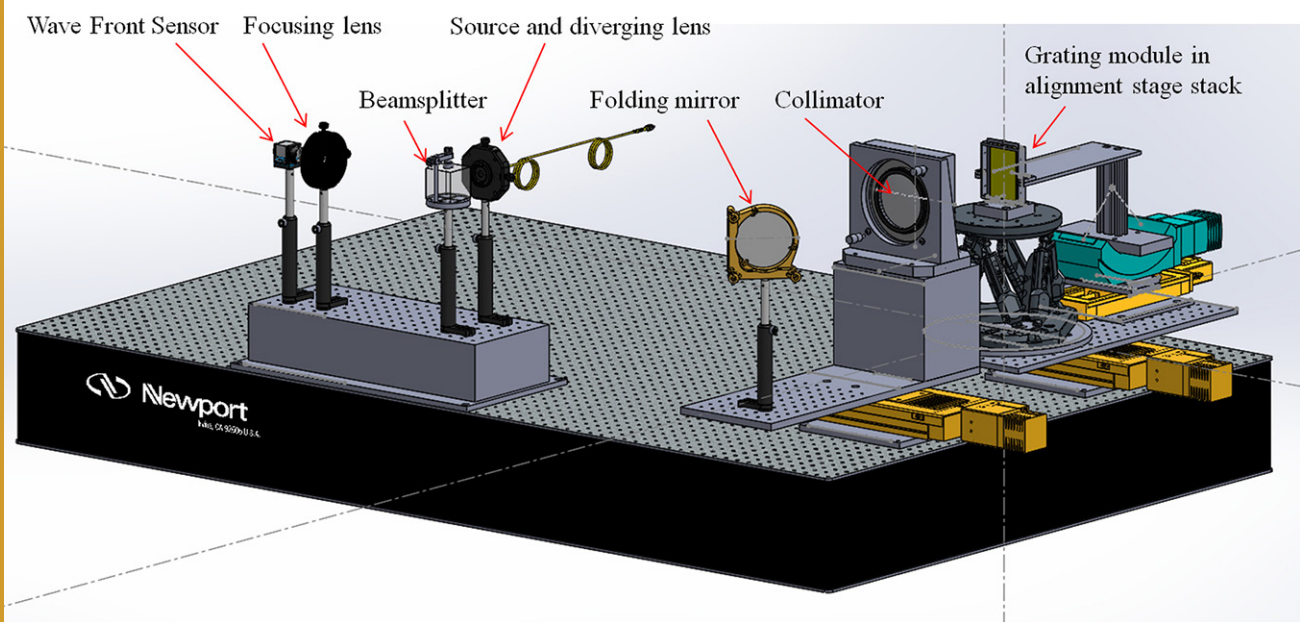


Fig. 3. An engineering model of the alignment setup. A wave front sensor measures the figure and attitude of each grating as it is placed within the module. Not shown is the externally located theodolite used to measure the grating surfaces relative to a fiducial flat on the grating module.

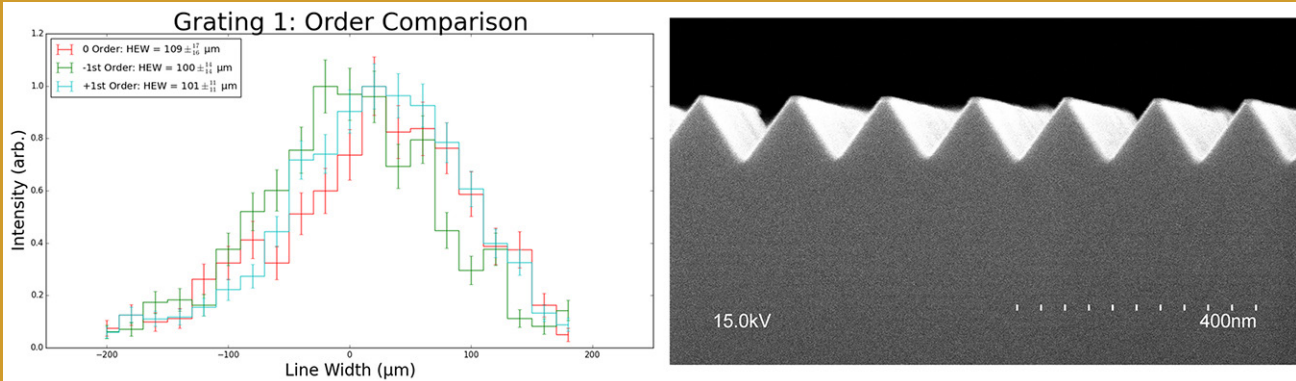


Fig. 4. Left: Comparison between the 0th (red data points), +1st (blue), and -1st (green) order lines of Mg K α . The HEWs remain constant with dispersion. Right: Scanning Electron Micrograph (SEM) image of a cleaved <100> wafer following our etch recipe. The triangular groove features with smooth sidewalls are created by KOH etching to the <111> planes resulting in a 54.7° blazed profile.

Path Forward

In the coming years, our efforts will concentrate on achieving the list of milestones presented above. The initial steps of quantifying our alignment tolerances, formulating our methodology, and designing the grating mount have all been accomplished prior to submission of this report. As described in the previous section, much of this took place prior to the start of 2015 and was supported by parallel efforts. The next steps are to implement this methodology and align gratings into a mount. For the first year's efforts we plan to use our existing prototype gratings. These are small-format, 25 mm × 32 mm, but will be replicated onto large fused-silica substrates, 75 mm × 96 mm, to simulate the relevant size and substrate material of future flight gratings. The grooved area will be used during X-ray performance testing to ensure that our optical alignment methodology results in aligned diffraction arcs. The initial goal is to test our methodology on just one grating member. This will identify any poor assumptions and/or bad designs, enabling us to make quick changes before attempting multiple-grating alignment. We are testing with a slumped glass telescope consisting of three mirror shells provided by GSFC and known as the Technology Development Module (TDM). These shells span ~8 mm of radial space, allowing us to test X-ray alignment of at least four gratings. The performance tests will be performed at the MSFC SLF. We will measure spectral-resolving power pre- and post-environmental testing to verify the mounting structure. The results of these tests may verify our methods, or identify problems. If the former, then we will repeat the Year 1 tasks in Year 2, using a grating that is grooved over the entire 75 mm × 96 mm substrate (again, these large-format, blazed gratings will be provided through our RTF program). If the latter, then we have allotted time in the schedule to alter our setup based on issues found during testing, and then implement our improved strategy. This will still be performed using a large format, 75 mm × 96 mm grating and a module mount of appropriate material and scale to be considered high-fidelity and flight-like. Following each test campaign we plan to publish our results in a peer-reviewed journal.

References

- [1] R.L. McEntaffer, C. DeRoo, T. Schultz, B. Gantner, J. Tutt, A. Holland, S. O'Dell, J. Gaskin, J. Kolodziejczak, W.W. Zhang, K.-W. Chan, M. Biskach, R. McClelland, D. Iazikov, X. Wang, and L. Koecher, "First results from a next-generation off-plane X-ray diffraction grating," *Experimental Astronomy*, **36**, 389, 17 pages (2013)
- [2] R. Allured and R.L. McEntaffer, "Analytical Alignment Tolerances for Off-Plane Reflection Grating Spectroscopy," *Experimental Astronomy*, **36**, 661, 17 pages (2013)
- [3] R. Allured, B.D. Donovan, and R.L. McEntaffer, "Alignment Tolerances for Off-Plane Reflection Grating Spectrometry: Theoretical Calculations and Laboratory Techniques," *Proc. SPIE*, **8861**, 88611C (2013)
- [4] C. DeRoo, R.L. McEntaffer, T. Schultz, W.W. Zhang, N.J. Murray, S.L. O'Dell, and W. Cash, "Pushing the boundaries of x-ray grating spectroscopy in a suborbital rocket," *Proc. SPIE*, **8861**, 88611B (2013)
- [5] H. Marlowe *et al.*, "Performance Testing of a Novel Off-plane Reflection Grating and Silicon Pore Optic Spectrograph at PANTER," arXiv:1503.05809 (2015)
- [6] R. Allured, B. Donovan, V. Burwitz, C. DeRoo, H. Marlowe, B. Menz, D. Miles, J. Tutt, and R.L. McEntaffer, "Co-Alignment of Off-Plane Reflection Gratings at PANTER," in preparation (2015)
- [7] C. DeRoo *et al.*, "Line Spread Functions of Blazed Off-Plane Gratings Operated in the Littrow Mounting," in preparation (2015)
- [8] R.K. Smith *et al.*, "Arcus: an ISS-attached high-resolution x-ray grating spectrometer," *Proc. SPIE*, **9144**, 91444Y (2014)

For additional information, contact Randall McEntaffer: randall-mcentaffer@uiowa.edu



Development of 0.5-Arcsecond Adjustable Grazing-Incidence X-ray Mirrors for the SMART-X Mission Concept

Prepared by: Paul B. Reid (PI; SAO) and Stuart McMuldloch (SAO)

Summary

“Development of 0.5-Arcsecond Adjustable Grazing-Incidence X-ray Mirrors for the SMART-X Mission Concept” is a Strategic Astrophysics Technology (SAT) program that began in April 2015 and is scheduled to run through the end of calendar year (CY) 2016. This program follows an earlier Astrophysics Research and Analysis (APRA) project, co-funded by Space Technology Mission Directorate (STMD), working on the development of adjustable high-resolution X-ray optics. This report captures progress made in both projects since the summer of 2014. The program seeks to develop a modular, highly nested, grazing-incidence X-ray mirror assembly composed of bimorph adjustable X-ray mirror segments to achieve 0.5-arcsec imaging while also achieving extremely low mirror assembly mass-per-unit-effective-area (e.g., $< 500 \text{ kg/m}^2$ effective area, compared to $\sim 16,000 \text{ kg/m}^2$ for Chandra). Our technology will enable large-area, high-resolution imaging X-ray telescope mission concepts such as the Square Meter Arc-second Resolution Telescope for X-rays (SMART-X) [1], or equivalently, the 2013 NASA Astrophysics Roadmap committee-recommended X-ray Surveyor [2] mission concept. X-ray Surveyor (XRS) will study the early universe (growth of structure, merger history of black holes), as well as feedback and evolution of matter and energy.

Our adjustable-optics technology eliminates the figure errors and unwanted distortions usually inherent in thin lightweight mirrors. We use a thin (nominally $1.5 \mu\text{m}$) film of the piezoelectric material, lead zirconate titanate (PZT), sputtered as a continuous film on the back of thin (0.4 mm) thermally formed glass Wolter-I mirror segments (a continuous ground electrode is first applied to the back surface). A pattern of independently addressable platinum (Pt) electrodes is deposited on top of the PZT layer, forming individual piezo cells. Applying a low ($< 10\text{V}$) DC voltage between a cell's top electrode and the ground electrode creates an electric field that produces a local strain in the piezo material parallel to the mirror surface. This strain causes localized bending in the mirror, called an influence function. By supplying an optimally chosen voltage to each of the individual cells, one can change the amplitude of each influence function to minimize figure errors in the mirror, thereby improving imaging performance. This allows us to correct mirror figure errors from fabrication, distortions introduced during mounting, and any gravity-release errors. Figure correction is implemented once on the ground during a calibration step post-mirror alignment and mounting. Having the ability to adjust and correct the figure of thin mirror segments, increases their performance from the 10-arcsec resolution level to 0.5 arcsec. We have shown through simulations improvements from ~ 7 -arcsec half-power diameter (HPD) to less than 0.5-arcsec HPD using exemplar mirror-figure data and modeled influence functions [3].

Beside the adjustable-optics and XRS teams at the Smithsonian Astrophysical Observatory (SAO), significant contributors to the adjustable-optics team are our colleagues at Penn State University (PSU) Materials Research Institute, where Dr. Susan Trolier-McKinstry, supported by Margeaux Wallace, develops the PZT processes.

This program began at SAO in April this year. Our early progress to date is in performing Structural Thermal and Optical Performance (STOP) analyses to examine the performance sensitivity of mirror-assembly temperature control, and the sensitivity of that control to the mirror-mounting scheme –

namely whether the mirrors are supported at their forward and aft ends, or supported at their sides. Also important as part of this initial design study is the relative correctability of any mount-induced and/or temperature-related distortions.

Background

XRS will be able to address a plethora of important science goals: growth of supermassive black holes (SMBH) and strong gravity effects; evolution of large-scale structure and detection of the warm-hot interstellar medium (WHIM); and active galactic nuclei (AGN) feedback and cycles of matter and energy. It will be able to carry out surveys to the Chandra deep-fields depth over 10 deg^2 ; study galaxy assembly processes to $z = 2.5$; track the evolution of group-sized objects, including those hosting the first quasars, to $z = 6$; and open new opportunities in the time domain and high-resolution spectroscopy.

Over the past few years, we have developed the concept of the adjustable-optic X-ray telescope. The challenge is to develop a mirror assembly, equivalent to the Chandra High-Resolution Mirror Assembly (HRMA), to a high level of technical readiness over the next several years to provide Chandra-like 0.5-arcsec HPD angular resolution with large effective area. The goal is 2.3 m^2 at 1 keV, or ~ 30 times that of Chandra, which would be a tremendous increase (a factor-of-four increase in area from Palomar to Keck was considered a breakthrough at the time).

Our baseline plan for SMART-X optics uses slumped-glass mirror segments with deposited piezoelectric actuators energized to correct mirror figure errors from 10 arcsec HPD (achieved for the International X-ray Observatory, IXO; and Advanced X-ray Spectroscopic Imaging Observatory, AXSIO) [4] to better than 0.5-arcsec HPD. The slumped-glass mirror segments developed for IXO/AXSIO represent the current state-of-the-art in lightweight optics. Another approach to develop adjustable X-ray optics simultaneous to our work relied on gluing individual, thick (0.2 mm) ceramic piezoelectric actuators to thin mirrors. This resulted in large ‘print-thru’ errors in the mirror figure [5]. Our approach builds on the mirror development for IXO/AXSIO, in terms of the thermally formed substrates, as well as mirror alignment and mounting. The addition of the piezoelectric layer is essentially just a single process step in the mirror-fabrication process. Our approach resolves the two main problems with lightweight slumped-glass mirrors: (1) it corrects for the low-frequency figure errors that result from a combination of mandrel and thermal-forming errors, and (2) it corrects after the fact for deformations introduced in coating and mounting thin, flexible mirrors. In addition, the ability to make an on-orbit correction of mirror figure is critical for telescopes with apertures larger than can be tested with full aperture on the ground (*i.e.*, larger than Chandra).

Our development plan contains two major activities:

1. Flight-like mounting of aligned mirrors in a modular housing that maintains sub-arcsec alignment through the application of launch loads, and after (spacecraft) thermal survival temperature cycling.
2. Connection of control signals and power to the adjustable optics in their flight-like housing, without introducing loads into the mirrors and without losing connection after launch.

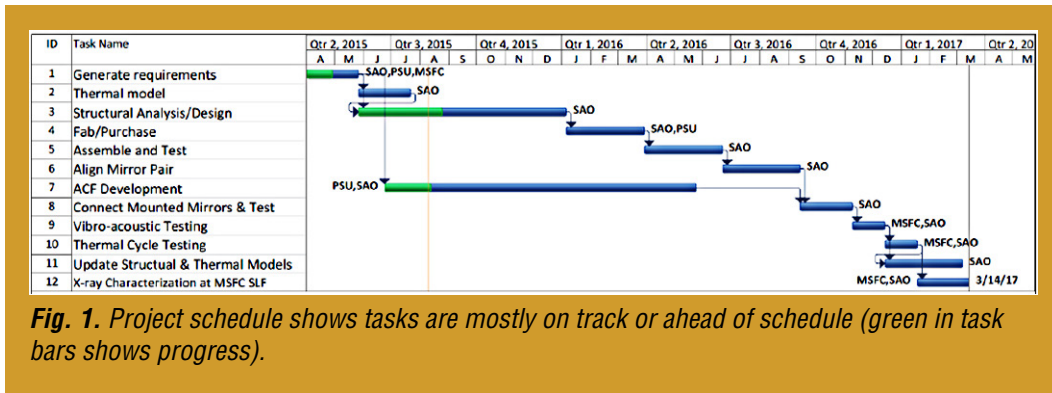
We will generate requirements for an adjustable-optic mirror assembly capable of achieving 0.5-arcsec HPD. This includes iterative error-budgeting and thermal and structural modeling, balancing the difficulty of achieving multiple mirror-assembly requirements.

We will develop, design, and model a flight-like mounting able to support multiple, closely spaced shells of adjustable-mirror segments. This will entail structural and thermal modeling to ensure compatibility with system requirements. Subsequently, we will develop hardware to implement and test the designs.

We will explore the use of Anisotropic Conductive Films (ACFs) for connecting control and power lines to the mirror segment. ACFs are film adhesives with uniformly dispersed conductive particles several micrometers in diameter in a low-temperature thermo-setting resin [6-9]. They are used routinely in connecting to LCD and OLED displays and connecting bare chips directly onto glass, because they are extremely thin and allow a high connection density without difficult alignment. They are standard products manufactured by companies such as Hitachi and 3M, among others. We will investigate the deformations introduced into the mirrors by ACFs by measuring mounted mirror figures before and after bonding ACF connections onto the mirror. We will also investigate thermal effects on ACF-induced stresses under temperature changes resulting from the differing coefficients of thermal expansion (CTEs) of the ACF and the mirror segment, and we will also explore the best location structurally to make the connections without degrading mirror effective area, while mitigating attachment-related stresses. Lastly, the ACF connections will be in place before vibro-acoustic and thermal cycling tests, and we will test for functionality after these environmental tests. This effort comprises about 10% of our budgeted work and will be performed at PSU, environmental tests at the NASA Marshall Space Flight Center (MSFC), and non-environmental testing at SAO.

Objectives and Milestones

SAO began the project in April 2015 and has made good progress against the baseline plan. Figure 1 shows the annotated baseline schedule from our proposal.



Progress and Accomplishments

Major work has been progressing in the areas of system requirements and finite element modeling. In this earliest phase, we focus on the performance impact of different mounting schemes. A structural model was developed for a mounted pair of mirror segments, and thermal gradients and ambient temperature changes were applied to the mounted mirror segments (Tasks 1, 2, and 3 in Fig. 1). We will compute the sensitivities of imaging performance to on-orbit thermal conditions via ray-tracing of the modeled deformations. Two different mounting configurations are modeled: (1) mirror attachment points on the forward and aft ends, and (2) mirror attachment points on the side edges of the mirror segments. Initially, this study is for a conic mirror shell with a 1-m radius-of-curvature and 400 mm circumferential dimension at its leading edge, with an axial dimension of 200 mm and primary mirror cone angle of 0.025 radians (1.43°). The mirrors are modeled as a (multilayer) stack of materials to reflect the actual current state of design:

- 0.05 μm Ir X-ray reflective surface layer, sputtered material;
- 0.05 μm Cr coating binder and stress compensation layer, sputtered material;
- 400 μm Corning Eagle glass substrate;
- 0.05 μm Ti sputtered protective layer;
- 0.10 μm Pt sputtered ground electrode;
- 1.5 μm PZT sputtered piezoelectric material; and
- 0.10 μm Pt sputtered top electrode.

The housing is designed to provide a CTE-matched structure in which to mount the mirror. Housing-wall thicknesses are modeled as 6 mm. Properties for the housing used in analysis are based on a near-zero CTE quasi-isotropic M55J/954-3 carbon fiber/cyanate core with 23.6 ppM/°C CTE aluminum facesheets. For 6 mm total thickness, a 4.92-mm composite core with 0.54-mm thick aluminum facesheets provides an effective CTE of 3.17 ppM/°C, which matches the Corning Eagle glass substrate and is within 50 ppB/°C of the mirrors. For this analysis, the housing is modeled with isotropic properties rather than as a composite laminate structure.

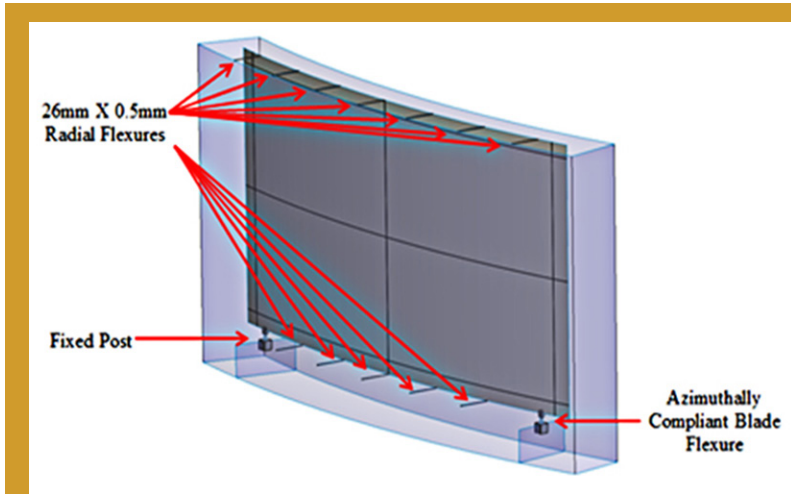


Fig. 2. Modeled primary-mirror mounting structure. Two fixed supports are used as in SAO's APRA development: 6 degree-of-freedom (dof) fixed support and a tangential flexure (azimuthally compliant blade flexure). Twelve additional radial wire flexures are used (seven at the forward end and five at the aft end) to provide radial positioning of the mirror edges.

Different mirror-mounting solutions were designed and analyzed for mirror deformations under a +1°C change in nominal temperature (soak) and 1°C axial, azimuthal, and diametric gradients over the mirror (temperature changes are relative to the conditions at mirror bonding during assembly). The design intent is to support the mirror against rigid-body translations and rotations while also providing additional radial constraints to restrain the mirrors against deformations caused by temperature soaks. An example of the mounting and model for a primary mirror is shown in Fig. 2.

Figure 3 shows the radial figure error due to a 1°C change in ambient temperature for the same mirror. Uniform displacement of the mirror (effectively a change in mirror radius) is included in the figure. Displacement amplitudes range from ~2.77 μm to ~3.29 μm. In addition to the ~3 μm change in average radius error, the temperature change introduces ~0.06 μm root-mean-square (rms) error.

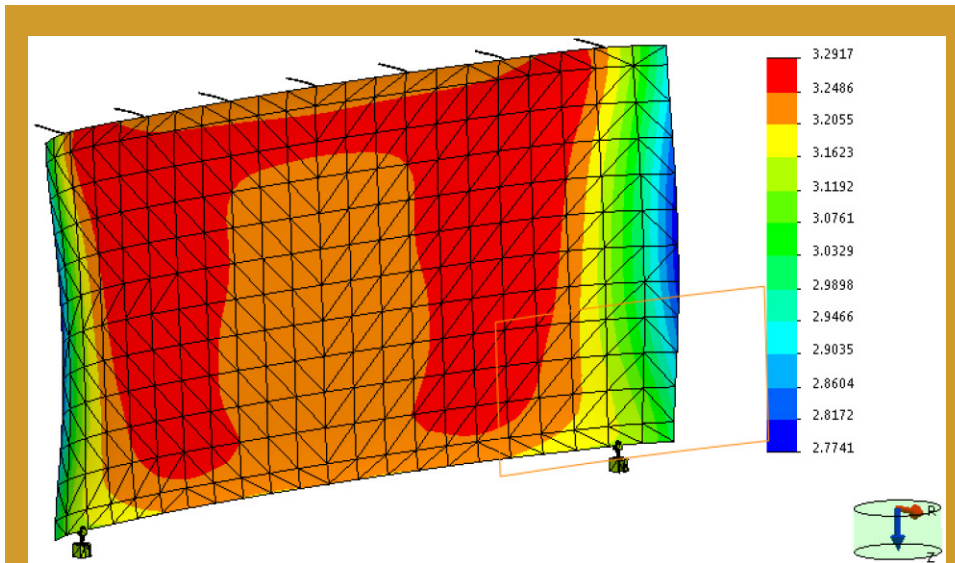


Fig. 3. Radial deformations produced in the primary mirror due to a temperature change of 1°C. Deformations include ~3 μm average radius change, as well as axially and azimuthally varying errors.

Finite element modeling will be repeated for the same thermal conditions for the secondary mirror. The combination of the two mirrors will be ray-traced to understand the performance impacts of the various conditions.

At this point, we have not yet analyzed the output distortions from the finite element modeling so we have no new information regarding thermal sensitivities.

Path Forward

In the near term, we will continue our activities investigating the structural and thermal aspects of our system. We are focusing on extending the planned test design for Technology Readiness Level (TRL) 4 to larger, full-size mirrors, with many shell segments per module. We will explore the allowable thermal control system requirements consistent with the mount concept and the error budget. We will examine how installing subsequent mirror segments into a module impacts the alignment of already-installed segments – what we refer to as the impact of “packing” the module. All these activities will also include ray-tracing to understand performance implications. We will also model the effects of launch loads and conceptual first mode to ensure that no permanent adverse changes occur due to launch and/or gravity release. Upon completion of the modeling and design efforts, we will start parts procurement and fabrication in order to implement the multi-shell design concept for testing.

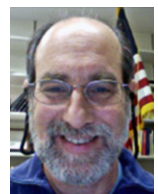
Miscellaneous

SAO continues to show strong institutional support for the adjustable X-ray optics program, providing funds for internal research and development activities in addition to creating a three-year postdoctoral fellowship – the Leon Van Speybroeck Fellowship in X-ray Optics. This institutional support has helped us advance ahead of schedule and reduce the overall project risk.

References

- [1] A. Vikhlinin *et al.*, “*SMART-X: Square Meter Arcsecond Resolution x-ray Telescope*,” SPIE Proc. **8443**, 844316 (2012)
- [2] “*Enduring Quests, Daring Visions*,” NASA Astrophysics Roadmap, Dec. (2013)
- [3] T. Aldcroft *et al.*, “*Simulating correction of adjustable optics for an X-ray telescope*,” SPIE Proc. **8503**, 85030F (2012)
- [4] W.W. Zhang *et al.*, “*Lightweight and high angular resolution x-ray optics for astronomical missions*,” SPIE Proc. **8147**, 81470K (2011)
- [5] C. Feldman *et al.*, “*The performance of thin shell adaptive optics for high angular resolution x-ray telescopes*,” SPIE Proc. **7803**, 78030N (2010)
- [6] J. Liu, “*Conductive Adhesives for Electronics Packaging*,” Electrochemical, Port Erin, 12 (1999)
- [7] S. Ganesan and M. Pecht, “*Lead-free Electronics*,” (Wiley, New Jersey), 437 (2006)
- [8] W.S. Kwon and K.W. Paik, “*Experimental Analysis of Mechanical and Electrical Characteristics of Metal-Coated Conductive Spheres for Anisotropic Conductive Adhesives (ACAs) Interconnection*,” IEEE Trans. Compon. Packag. Technol. **29**, 528 (2006)
- [9] K.W. Jang *et al.*, “*Material properties of anisotropic conductive films (ACFs) and their flip chip assembly reliability in NAND flash memory applications*,” Microelectron. Reliab. **48**, 1052 (2008)

For additional information, contact Paul Reid: preid@cfa.harvard.edu



Advanced Packaging for Critical-Angle X-Ray Transmission Gratings

Prepared by: Mark L. Schattenburg (PI; MIT), Ralf K. Heilmann (MIT), and Alex R. Bruccoleri (Izentis)

Summary

Critical-Angle Transmission (CAT) gratings combine the advantages of traditional phase-shifting transmission gratings – *e.g.*, relaxed alignment and figure tolerances, low mass, transparency at high energies; with the advantages of blazed reflection gratings – *e.g.*, high diffraction efficiency and high resolving power due to utilization of higher diffraction orders. In combination with grazing-incidence X-ray mirrors and CCD detectors, they promise a five- to 10-fold increase in efficiency and a three- to five-fold improvement in resolving power over existing X-ray grating spectrographs [1]. Development of CAT grating fabrication technology has been supported by NASA under the Strategic Astrophysics Technology (SAT) program since January 2012.

During the past year, NASA support has enabled the acquisition and development of a set of key etching and processing tools. Improved processes developed with these tools has enabled the fabrication of gratings with significantly improved quality. This new process utilizes a combination of Deep Reactive Ion Etch (DRIE) and potassium hydroxide (KOH) polishing steps. The combined dry- and wet-etch techniques lead to the predicted blazing and record diffraction efficiencies about 1.5× better than our previous best results, as confirmed by X-ray synchrotron tests.

Background

Absorption- and emission-line spectroscopy, with the performance made possible by a well-designed CAT X-ray grating spectrometer (CATXGS), will target science objectives concerning the large-scale structure of the universe, cosmic feedback, interstellar and intergalactic media, and stellar accretion. A CATXGS-carrying mission can address the kinematics of galactic outflows, hot gas in galactic halos, black hole growth, the missing baryons in galaxies and the Warm-Hot Intergalactic Medium, and the effect of X-ray radiation on protoplanetary disks. All of these are high-priority International X-ray Observatory (IXO) science questions described in the 2010 Decadal Survey, *New Worlds, New Horizons in Astronomy and Astrophysics* (NWNH) [2], and are addressed further in the NASA X-ray Mission Concepts Study Report [3]. A number of mission concepts submitted in response to NASA Request for Information (RFI) NNH11ZDA018L could be enabled by a CATXGS; these include Advanced X-ray Spectroscopic Imaging Observatory (AXSIO), Astrophysics Experiment for Grating and Imaging Spectroscopy (AEGIS), and Square Meter Arcsecond Resolution X-ray Telescope (SMART-X), as well as the Notional X-ray Grating Spectrometer (N-XGS) studied by the X-ray Community Science Team (CST) [4-6] or future Explorers. Also, an X-ray Surveyor – a mission described in the 2013 “Enduring Quests, Daring Visions” Astrophysics Roadmap [7] – is on a short list of possible mission concepts considered for further study in preparation for the 2020 Decadal Survey [8]. A core instrument for an X-ray surveyor would be a grating spectrometer, for example one similar to the CATXGS design for SMART-X.

The soft X-ray band contains many important diagnostic lines (C, N, O, Ne, and Fe ions). Imaging spectroscopy with spectral resolution better than 2 eV has been demonstrated with small transition edge-sensor-based microcalorimeter arrays, providing resolving power over 3000 above 6 keV. However, toward longer wavelengths, energy-dispersive detectors cannot provide the spectral resolution required to address several of the NWNH high-priority science objectives. The only known technology providing high spectral-resolving power in this band is wavelength-dispersive, diffraction-grating-based spectroscopy.

The technology currently used for grating-based soft X-ray spectroscopy was developed in the 1980s. The Chandra High-Energy Transmission-Grating Spectrometer (HETGS) carries polyimide-supported

gold gratings with no more than 10% diffraction efficiency in the 1-5 nm band, but the whole moveable grating array only weighs about 10 kg. The X-ray Multi-mirror Mission – Newton (XMM-Newton) Reflection Grating Spectrometer (RGS) has more efficient grazing-incidence reflection gratings, but its mass is high (>100 kg) and it has low spectral-resolving power (~300). CAT gratings combine the advantages of the HETGS and RGS gratings, and promise higher diffraction efficiency over a broad band, with a resolving power greater than 3000 for a 10 arcsec Point Spread Function (PSF) telescope. These gratings also offer near-ideal synergy with a calorimeter-based imager, since CAT gratings become increasingly transparent at higher energies. Thus, high-resolution spectroscopy could be performed with a CATXGS in tandem with a calorimeter over the range of ~0.2 to tens of keV on a larger mission such as an X-ray Surveyor. Figures-of-merit for many types of observations, such as the accuracy of line-centroid measurement in absorption-line spectroscopy, could be improved by more than an order of magnitude over Chandra and XMM. The new patented CAT grating design relies on the reflection (blazing) of X rays from the sidewalls of free-standing, ultra-high aspect-ratio, sub-micron-period grating bars at grazing angles below the critical angle for total external reflection. Fabrication combines advanced novel methods and tools from the semiconductor and Micro-Electro-Mechanical Systems (MEMS) industries with patterning and fabrication methods developed at MIT over several decades.

We plan to bring CAT grating technology to Technology Readiness Level (TRL) 6 by the end of 2018 to reduce technology risk and cost for future CATXGS-bearing missions before they enter Phase A. We therefore want to demonstrate efficient, large-area (over 30 mm × 30 mm) CAT grating facets with minimal blockage from support structures. Facets will be mounted to thin and stiff frames, which can then be assembled into grating arrays with sizes on the order of 1 m².

Objectives and Milestones

The objective of this project is to demonstrate an aligned array of large-area, high-efficiency CAT gratings with minimal blockage by support structures, providing resolution over 3000 in the soft X-ray band, and maintaining its performance after appropriate vibration, shock, and thermal testing. The array will consist of so-called grating facets mounted to a Grating Array Structure (GAS). Facets are comprised of a grating membrane, etched from a silicon-on-insulator (SOI) wafer, and a facet frame that holds the membrane.

Key project milestones:

1. Develop silicon lattice-independent anisotropic etch capable of achieving the required aspect ratios for 200 nm-period gratings (DRIE at University of Michigan tool, completed in 2011).
2. Develop process for free-standing, large-area gratings with hierarchy of low-blockage supports (completed in 2012).
3. Combine (completed in 2013) and optimize (ongoing) dry- and wet-etch processes to obtain smooth grating-bar sidewalls and narrow Level 1 (L1) supports; produce free-standing, large-area gratings with hierarchy of low-blockage supports (demonstrated, improving yield); and test X-ray efficiency (ongoing).
4. Select, acquire, install, and test advanced DRIE tool at MIT (completed in 2014).
5. Demonstrate CAT grating resolving power in an X-ray imaging system. Repeat with more than one grating or small array (Calendar Year, CY, 2015/16, in preparation).
6. Develop grating facet/frame design, process for integration of CAT grating membrane and frame, and alignment of facets on a breadboard GAS (Fiscal Year, FY, 2015/16).
7. Environmental and X-ray tests of grating facets (FY 2016).

Progress and Accomplishments

The key challenges in the fabrication of CAT gratings lie in their structure – small grating period (200 nm), small grating duty cycle (~40 nm-wide grating bars with 160 nm spaces between), and large depth

(4-6 μm) result in ultra-high aspect ratios (100-150), and they require nm-smooth sidewalls. In addition, the gratings should not be supported by a membrane, but rather be freestanding. Structures with such an extreme combination of geometrical parameters – or anything similar – have never been made before.

Prior to SAT support, we fabricated small KOH-wet-etched CAT grating prototypes that met all these requirements, and measured their efficiency at a synchrotron source, demonstrating good agreement with theoretical predictions [9, 10]. Due to their extreme dimensions and the requirement to be freestanding, CAT gratings must be supported by slightly “bulkier” structures. We use a so-called L1 cross-support mesh (period \sim 5-20 μm), integrated into the SOI device layer, and etched at the same time as the CAT gratings. Unfortunately, the wet-etch that provides the nm-smooth CAT grating sidewalls leads to widening L1 supports with trapezoidal cross sections and unacceptable X-ray blockage.

DRIE is an alternative process that can provide the required etch anisotropy for CAT grating bars and L1 supports simultaneously. To make large-area, freestanding gratings, we also use this process to fabricate a high-throughput hexagonal Level 2 (L2) mesh, etched out of the much thicker (\sim 0.5 mm) SOI handle layer (Fig. 1). We developed a process that allows us to DRIE the CAT grating bars and the L1 supports out of the thin SOI device layer (front side), stopping on the buried oxide (BOX) layer, and to subsequently etch the L2 mesh with a high-power DRIE into the back side, again stopping on the BOX layer. The BOX layer is removed with a hydrofluoric acid (HF) etch, and the whole structure is critical-point-dried in liquid CO_2 . We fabricated several 31 mm \times 31 mm samples with decent yield [11].

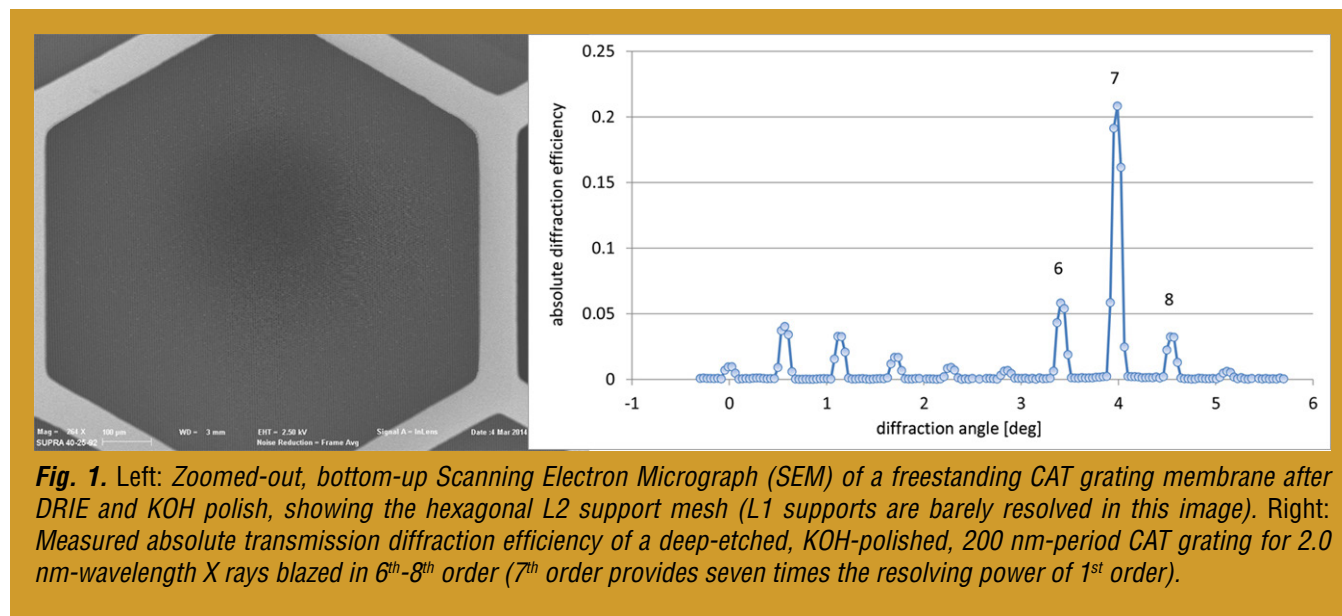
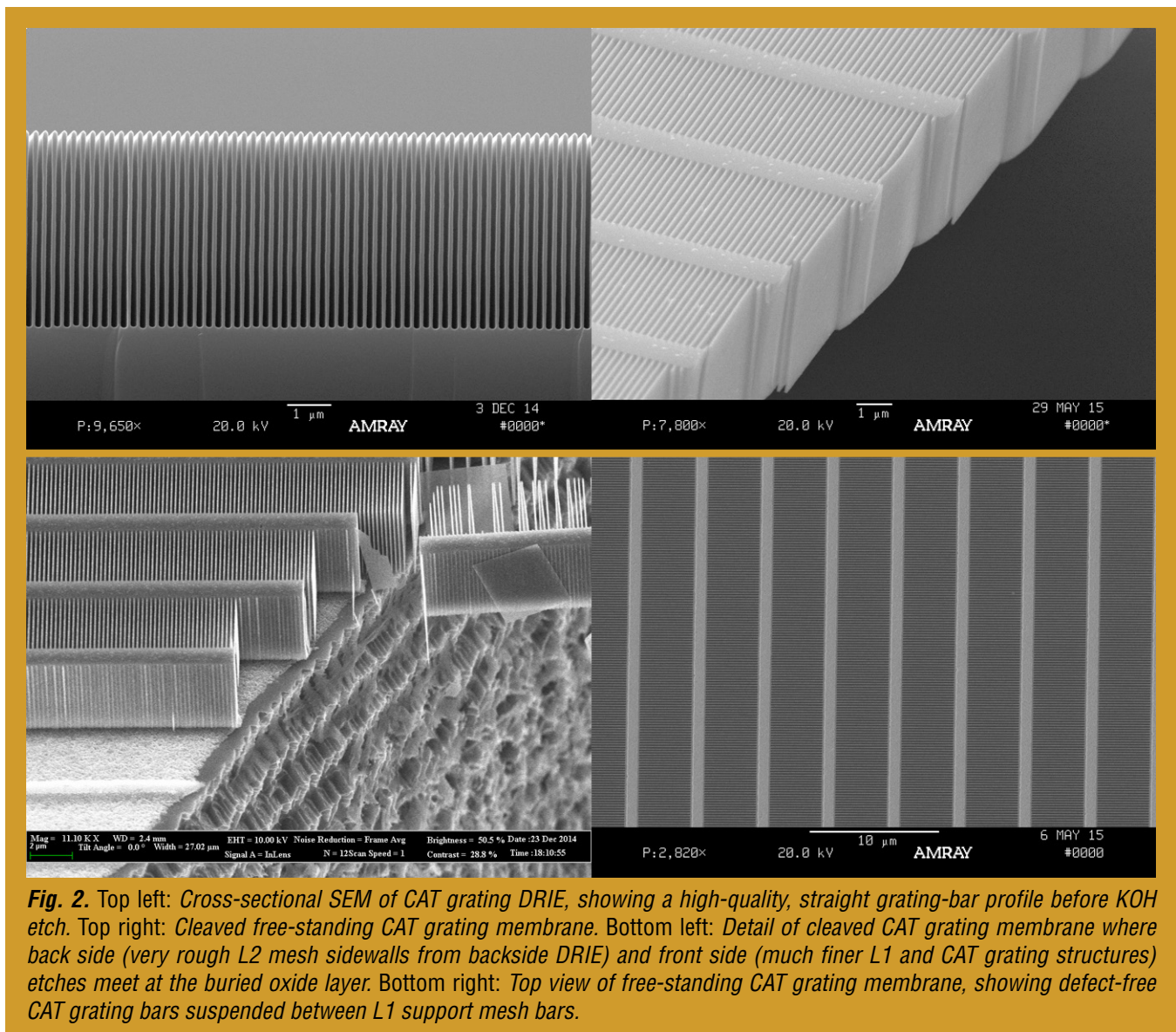


Fig. 1. Left: Zoomed-out, bottom-up Scanning Electron Micrograph (SEM) of a freestanding CAT grating membrane after DRIE and KOH polish, showing the hexagonal L2 support mesh (L1 supports are barely resolved in this image). Right: Measured absolute transmission diffraction efficiency of a deep-etched, KOH-polished, 200 nm-period CAT grating for 2.0 nm-wavelength X rays blazed in 6th-8th order (7th order provides seven times the resolving power of 1st order).

Unfortunately, DRIE leaves the sidewalls of etched structures with several nm of roughness, detrimental to CAT grating efficiency. In 2012 – 2013, we developed a combined DRIE/KOH approach on bulk silicon that follows DRIE with a relatively short KOH “polishing” step that reduces sidewall roughness, and straightens and thins the grating bar profile [12]. In 2014, we transferred and modified our new process to be compatible with the more delicate double-sided processing on SOI wafers for large-area, freestanding gratings (Figs. 1 and 2).

Up to a year ago, all of the above DRIE steps were done remotely at a University of Michigan open user facility [13, 14]. Since then, we have been able to use a newly acquired DRIE tool in our lab at MIT. During this last year we greatly improved DRIE grating bar profile control and surpassed the etch performance of the Michigan tool. We now routinely achieve constant-thickness or slightly retrograde bar profiles (Fig. 2). These improved grating bars survive vastly longer wet etch (sidewall polishing) times in concentrated KOH, up to 40 minutes, presumably leading to smoother sidewalls and thus higher reflectivity and diffraction



efficiency. We just X-ray-tested a number of CAT gratings with varying KOH etch times and are currently analyzing the data. Preliminary results show record X-ray diffraction efficiency on blaze, about 1.5× better than our previous best results (> 31% absolute efficiency, sum of blazed orders; Fig. 1). We are continuing to add yield-enhancing steps to the fabrication sequence, such as addition of an integrated L2 mesh (aligned with the backside L2 mesh) to the front side to strengthen the grating membrane (batch in progress).

Path Forward

We are working on fabrication-yield improvements to produce a number of high-quality samples for X-ray resolution tests. If satisfactory performance is achieved, we will focus on the following milestones, subject to funding:

1. Design of brass-board GAS, alignment verification, and environmental test of grating array (FY 2015/16).
2. Scale up grating fabrication, frame design, and membrane/frame integration to full size (mission-dependent, FY 2016/17).
3. Design and build GAS prototype (FY 2017).
4. Environmental and X-ray tests of GAS populated with full-size gratings (FY 2017/18).

References

- [1] R. K. Heilmann, J. E. Davis, D. Dewey, M. W. Bautz, R. Foster, A. Bruccoleri, P. Mukherjee, D. Robinson, D. P. Huenemoerder, H. L. Marshall, M. L. Schattenburg, N. S. Schulz, L. J. Guo, A. F. Kaplan, and R. B. Schweickart, “*Critical-Angle Transmission Grating Spectrometer for High-Resolution Soft X-Ray Spectroscopy on the International X-Ray Observatory*,” Space Telescopes and Instrumentation 2010: Ultraviolet to Gamma Ray, M. Arnaud, S. S. Murray, T. Takahashi (eds.), Proc. SPIE **7732**, 77321J (2010).
- [2] Blandford *et al.*, “*New Worlds, New Horizons in Astronomy and Astrophysics*,” National Academy of Sciences, (2010).
- [3] “*X-ray Mission Concepts Study Report*” (2012).
- [4] Jay A. Bookbinder, Randall K. Smith, Simon Bandler, Michael Garcia, Ann Hornschemeier, Robert Petre, and Andrew Ptak, “*The Advanced X-ray Spectroscopic Imaging Observatory (AXSIO)*,” Proc. SPIE **8443**, Space Telescopes and Instrumentation 2012: Ultraviolet to Gamma Ray, 844317 (2012).
- [5] M. W. Bautz, W. C. Cash, J. E. Davis, R. K. Heilmann, D. P. Huenemoerder, M. L. Schattenburg, R. McEntaffer, R. Smith, S. J. Wolk, W. W. Zhang, S. P. Jordan, and C. F. Lillie, “*Concepts for High-Performance Soft X-Ray Grating Spectroscopy in a Moderate-Scale Mission*,” Space Telescopes and Instrumentation 2012: Ultraviolet to Gamma Ray, T. Takahashi, S. S. Murray, and J.-W. A. den Herder (eds.), Proc. SPIE **8443**, 844315 (2012).
- [6] A. Vikhlinin, P. Reid, H. Tananbaum, D. A. Schwartz, W. R. Forman, C. Jones, J. Bookbinder, V. Cotroneo, S. Trolrier-McKinstry, D. Burrows, M. W. Bautz, R.K. Heilmann, J. Davis, S. R. Bandler, M. C. Weisskopf, and S. S. Murray, “*SMART-X: Square Meter Arcsecond Resolution X-Ray Telescope*,” Space Telescopes and Instrumentation 2012: Ultraviolet to Gamma Ray, T. Takahashi, S. S. Murray, and J.-W. A. den Herder (eds.), Proc. SPIE **8443**, 844316 (2012).
- [7] “*Enduring Quests, Daring Visions*,” Astrophysics Roadmap (2013)
- [8] P. Hertz, “*Planning for the 2020 Decadal Survey: An Astrophysics Division White Paper*” (2015).
- [9] R. K. Heilmann, M. Ahn, E. M. Gullikson, and M. L. Schattenburg, “*Blazed High-Efficiency X-Ray Diffraction via Transmission through Arrays of Nanometer-Scale Mirrors*,” Opt. Express **16**, 8658 (2008).
- [10] R. K. Heilmann, M. Ahn, A. Bruccoleri, C.-H. Chang, E. M. Gullikson, P. Mukherjee, and M. L. Schattenburg, “*Diffraction Efficiency of 200 nm Period Critical-Angle Transmission Gratings in the Soft X-Ray and Extreme Ultraviolet Wavelength Bands*,” Appl. Opt. **50**, 1364-1373 (2011).
- [11] A. Bruccoleri, P. Mukherjee, R. K. Heilmann, J. Yam, M. L. Schattenburg, and F. DiPiazza, “*Fabrication of Nanoscale, High Throughput, High Aspect Ratio Freestanding Gratings*,” J. Vac. Sci. Technol. B **30**, 06FF03 (2012).
- [12] A. R. Bruccoleri, D. Guan, P. Mukherjee, R. K. Heilmann, and M. L. Schattenburg, “*Potassium Hydroxide Polishing of Nanoscale Deep Reactive-Ion Etched Ultrahigh Aspect Ratio Gratings*,” J. Vac. Sci. Technol. B **31**, 06FF02 (2013).
- [13] D. Guan, A. R. Bruccoleri, R. K. Heilmann, and M. L. Schattenburg, “*Stress Control of Plasma Enhanced Chemical Vapor Deposited Silicon Oxide Film from Tetraethoxysilane*,” J. Micromech. Microeng. **24**, 027001 (2014).
- [14] R.K. Heilmann, A.R. Bruccoleri, D. Guan, M.L. Schattenburg, “*Fabrication of large-area and low mass critical-angle x-ray transmission gratings*,” R.K. Heilmann, A.R. Bruccoleri, D. Guan, M.L. Schattenburg, Proc. SPIE **9144**, Space Telescopes and Instrumentation 2014: Ultraviolet to Gamma Ray, 91441A (2014).

For additional information, contact Mark Schattenburg: marks@space.mit.edu



Mark Schattenburg

Technology Development for an AC-Multiplexed Calorimeter for ATHENA

Prepared by: Joel Ullom (PI; NIST/Boulder); Caroline Kilbourne and Simon Bandler (NASA/GSFC); and Kent Irwin (Stanford University)

Summary

We are developing large-format arrays of X-ray microcalorimeters and the associated readout that will enable the next generation of high-resolution X-ray imaging spectrometers for astrophysics. These spectrometers have very high spectral resolution and quantum efficiency, combined with the ability to observe extended sources without spectral degradation. The goal of this program is to advance a readout architecture for an X-ray microcalorimeter imaging spectrometer from Technology Readiness Level (TRL) 3 to 4. The key components are (1) the use of an Alternating Current (AC) bias for microcalorimeter sensors and (2) frequency-division-multiplexed readout. This work is a collaboration between the National Institute of Standards and Technology (NIST), Boulder (Principal Investigator, PI, J. Ullom); GSFC (lead C. Kilbourne); and Stanford University (lead K. Irwin). The work is supported by the Strategic Astrophysics Technology (SAT) program. It began in Fiscal Year (FY) 2015, and is supported through FY 2016. The scientists in our groups have been collaborating on technology development for an imaging X-ray microcalorimeter spectrometer since 1998. This heritage has focused on Transition Edge Sensor (TES) microcalorimeter arrays with a different readout architecture: Direct-Current (DC) bias and time-division multiplexing.

The prospects for future missions using X-ray microcalorimeters changed in June 2014 with the choice of the Advanced Telescope for High ENergy Astrophysics (ATHENA) [1] for the European Space Agency (ESA) L2 (large mission) opportunity. One of the two instruments for this mission, the X-ray Integral Field Unit (X-IFU), is a high-resolution imaging X-ray spectrometer. The use of TESs for the X-ray microcalorimeters, originally pioneered by our collaboration, is currently assumed for this instrument [2]. The baseline readout for X-IFU is frequency-division multiplexing (FDM) [3], in which the TESs are biased with AC signals of different frequencies, which act as carriers for the slower thermal signals. In anticipation of the selection of ATHENA and the baseline instrumentation for the X-IFU, we initiated this study of AC multiplexing of our TES microcalorimeters.

Very recently, both NASA and the PI of X-IFU, Dr. Didier Barret, have communicated interest in designating the X-IFU microcalorimeter array as one of NASA's principal contributions to ATHENA, with ESA's concurrence. As a consequence, this collaboration submitted a new SAT proposal entitled "Providing Enabling and Enhancing Technologies for a Demonstration Model of the ATHENA X-IFU" to cover our contribution to X-IFU technology development in FY 2016 and 2017. One component of that program is to ensure that the pairing of the US sensors with the baseline X-IFU readout can meet mission requirements. The current project allows us to get a valuable early start on that study and optimization.

Background

The ability to perform broadband imaging X-ray spectroscopy with high spectral and spatial resolution has been a core requirement of recent X-ray satellite mission concepts. Multiplexed microcalorimeter arrays provide this capability. The technology development program we are pursuing is a response to this need and is now directed towards ATHENA. The science case is the study of the universe of extremes, from black holes to large-scale structure. The main goals are structured around three main topics – "black holes and accretion physics," "cosmic feedback," and "large-scale structure of the universe."

Underpinning these topics is the study of hot astrophysical plasmas that broadens the scope of this science to virtually all corners of astronomy. The ATHENA science case is very similar to that endorsed in the 2010 NRC decadal review of astrophysics for the International X-ray Observatory concept.

The baseline readout architecture for the X-IFU on ATHENA is FDM. The AC signals from different TESs are measured by a shared Superconducting Quantum Interference Device (SQUID) current amplifier. To date, the resolutions achieved using DC-biased TESs have not been reproduced in AC-biased TESs. The best results with AC-bias are from the Space Research Organization Netherlands (SRON) group, which reported a full-width at half maximum (FWHM) resolution of 3.6 eV at 5.9 keV using transformer coupling to low-resistance Mo/Au GSFC devices [4, 5]. Under DC-bias, these same devices yielded 2.3 eV FWHM at 5.9 keV. Since the essential principle of AC-bias has been demonstrated, its current TRL is 3. If we succeed in improving the AC-biased performance to levels that meet the X-IFU specifications, then we will have increased the TRL of AC bias to 4. Thus, we will initially attempt to advance the TRL for reading out single pixels in large arrays of TESs with AC bias. We will attempt to demonstrate a FWHM energy resolution performance of less than 2.5 eV at 6 keV at an input X-ray count-rate of 50 counts per second, with 80% throughput for high-resolution events. While the final ATHENA mission requirements are still under development, this level of sensor performance is likely to be satisfactory.

Objectives and Milestones

The primary goal of the current project is to advance the technical readiness of the AC-biased readout of X-ray microcalorimeters from TRL 3 to 4. This advance requires work on both single TES devices and on small numbers of devices operating together. For single devices, we will compare sensor resolution under AC and DC bias, and compare properties that affect the energy resolution such as transition shape and noise. Studies of small numbers of devices operating together will allow interaction pathways within the AC-readout architecture to be identified and characterized. Interactions between sensors are a potential source of energy resolution degradation.

The behavior of a TES is more complicated than that of a temperature-dependent resistor because of the role of superconductivity. Noise and responsivity depend on both the current and the temperature in the device. Under AC bias, the current is constantly changing even though the temperature is very close to fixed. This current variation is one possible reason why results under AC bias are not as mature as those under DC bias. We will study how the properties of TES devices under AC bias compare to those under DC bias. We will focus on Mo/Au TES thermometers developed at GSFC that are currently the baseline sensor technology for the X-IFU, but will also study other TES designs insofar as these can provide insight into the details of AC bias. This work encompasses both the fundamental physics of TES devices and the role of the readout SQUID and feedback system in determining performance levels.

Our key upcoming milestones are as follows:

- Study AC-biased TES performance using readout components from the European ATHENA team;
- Use a novel, open-loop readout architecture based on microwave SQUID amplifiers to separate the effects of the readout system from the TES; and
- Study interactions among small numbers of AC-biased TES devices.

Progress and Accomplishments

Single-Calorimeter Testing

Since our recent work on TES microcalorimeters used DC bias, this project requires the development of an AC-biased measurement capability. This capability is being developed at both GSFC and NIST Boulder but with different approaches, explained below, to maximize the prospects for project success.

Work toward single-calorimeter testing at GSFC is organized to maximize the use of readout components from European institutes collaborating on the ATHENA mission. At a meeting at GSFC between SRON, NIST, and GSFC scientists, several options for setups to characterize microcalorimeters under AC bias were considered in detail. Following the meeting, it was decided that the most time- and resource-efficient option was to reproduce a version of the test setup used at SRON rather than design a new system. This setup will include low-temperature components supplied by SRON including the LC filters, transformer chips, sum-point chips, and the PC board for routing wires. This setup will also use the same two-stage SQUIDs used by SRON that will be provided by VTT in Finland. The room-temperature electronics necessary to read out the devices under AC bias will also be the same as currently used by SRON, including an analog amplifier and electronics capable of carrying out base-band feedback, necessary for reading out multiple pixels at one time using FDM. The housing for the electronics and the interface connectors will be developed and machined at GSFC.

Most of the low-temperature components have been located and tested at SRON and will be sent to GSFC in the coming weeks. The electronics will take longer to develop. While we await this new set of electronics, GSFC and SRON scientists will begin testing some new GSFC X-ray microcalorimeters using an existing test setup at SRON. Three new sample detector chips have been identified as suitable for the next tests under AC bias, and are being prepared for shipment in the coming weeks. These have been characterized at GSFC under DC bias, and will now be tested under AC bias at SRON. These experiments will be the next critical tests needed to study the different physics between the AC- and DC-biased cases. The first of these will consist of current-voltage (I-V) measurements of TESs of different sizes, in particular studying the I-Vs for very small TESs, from 140 microns down to 8 microns, without X-ray absorbers attached. The second detector chip will allow investigation of the properties of TESs in the size range of 100 to 140 microns, with the TESs having Bi/Au absorbers and microstrip wiring attached. The third detector chip will have TESs designed for better performance under AC bias, based on previous studies of the performance of TESs with different normal-metal features.

The AC-bias testing effort at NIST is organized to maximally separate the contribution of the readout system from that of the TES microcalorimeter in assessments of detector performance. The non-linear response of SQUID amplifiers is typically mitigated by magnetic flux or current feedback. Feedback is particularly important in FDM because of the large amplitude of fast-carrier signals and the requirement that one SQUID simultaneously measure the signal from many sensors. As a result, FDM system performance can depend strongly on the particular feedback implementation and feedback systems with additional capability are likely to be needed [3].

To assess the fundamental limits of sensor performance under AC bias free of any effects related to a particular feedback system, test capability is under development at NIST based on microwave SQUID techniques, in which the readout SQUID is operated open-loop with flux-ramp modulation [6]. The SQUID is embedded in a passive microwave resonator and probed using microwave tones. This approach provides very large readout bandwidths without use of feedback.

The design of the readout box is under development at NIST (Fig. 1). It allows flexibility in both the choice of TES microcalorimeters and the configuration of the AC-bias circuit. The box will accommodate different versions of the SRON LC-filter chips and the SRON transformer chips. To connect the existing filter and transformer chips to all the various TES designs to be tested in this project, we will fabricate coplanar waveguide bus-bar chips that allow MHz frequencies to be routed flexibly to the different detector chips and the microwave MUX readout.

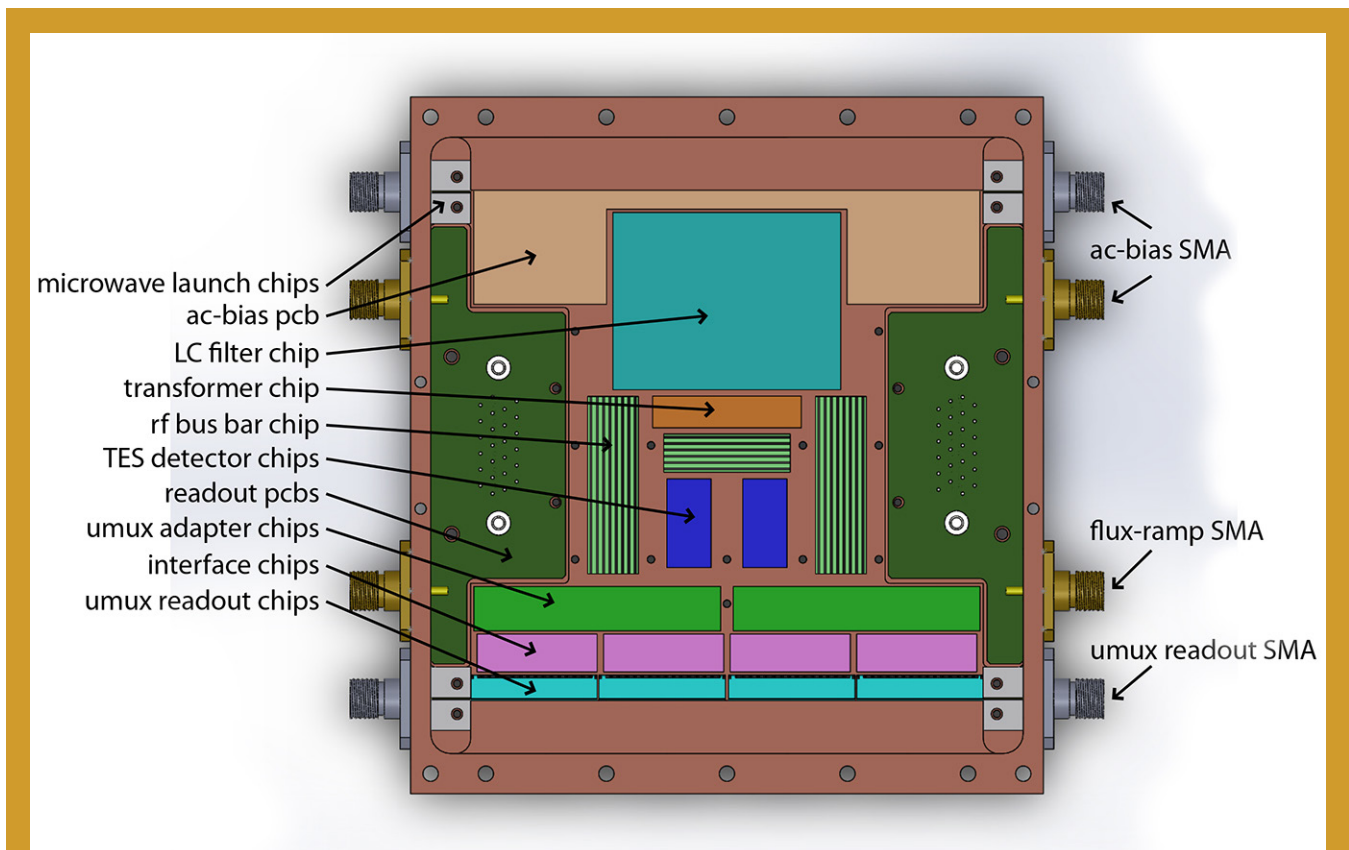


Fig. 1. Sample box design for testing of TES microcalorimeters under AC bias using high-bandwidth microwave SQUID readout. All AC signals can be supplied using wideband SMA connectors. A key to the circuit components that populate the sample box is shown at left (RF, radio frequency; PCB, printed circuit board; umux, microwave SQUID multiplexer; SMA, subminiature version A). This box will be sent out for manufacture before Sep. 1, 2015.

We are developing a microwave multiplexing circuit with sufficient readout and flux-ramp modulation-lines bandwidth to sample the AC TES response at frequencies of multiple MHz. To achieve these modulation frequencies, the flux ramp is routed to the microwave MUX chips on high-bandwidth coaxial cables. The sample box also contains four high-bandwidth SMA (Sub-Miniature version A) connections for the AC bias of the TESs. These coaxial cables are not strictly necessary to achieve the bias frequencies proposed for ATHENA (1-4 MHz), and would increase the power load for a large array. However, for this project, the extra bandwidth lets us focus on the physics of the AC bias, instead of worrying about cabling contributions to the response. Separate circuit boards will have the components necessary to achieve the voltage bias for the TES. There will be board designs for both the resistive shunt typical for DC-biased TESs and the reactive biasing presently favored for ATHENA.

Having microwave SQUID amplifiers optimized for measurements at high sample rates is crucial for the planned work. As shown in Fig. 2, we have designed a microwave SQUID amplifier for AC-biased TES applications that should have 10 MHz of bandwidth with an input-referred current noise below $40 \text{ pA}/\sqrt{\text{Hz}}$. We will be fabricating and testing this design in the remainder of FY 2015.

Multi-Pixel Testing

Interactions among pixels are possible with any readout scheme. In the second year of this effort, we will begin to study these interactions for AC-biased pixels measured using FDM. This work will exploit the test capabilities presently under development.

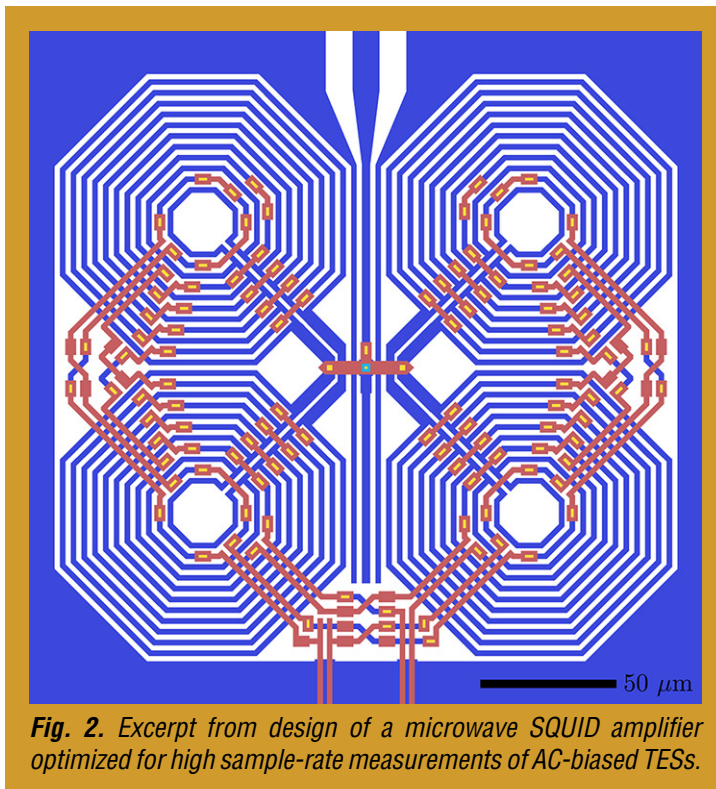


Fig. 2. Excerpt from design of a microwave SQUID amplifier optimized for high sample-rate measurements of AC-biased TESs.

Path Forward

Close study of the behavior of TES microcalorimeters under AC bias is needed to see if performance levels comparable to those under DC bias can be achieved consistently. Achieving consistent agreement between AC- and DC-biased performance will advance the TRL of AC-biased TES microcalorimeters from 3 to 4. We are pursuing a two-pronged approach to address this question. In one effort, we maximize the use of cold and warm readout electronics under development in Europe for ATHENA. In the other, we use an emerging, high-bandwidth readout architecture that will allow us to separate noise contributions of the readout system from those of the sensors. Our studies focus on the GSFC microcalorimeters presently baselined for the X-IFU. Using these devices and, as needed, other test structures, we will assess whether particular sensor designs are more compatible than others with AC bias. In particular, we will assess whether the underlying resistance mechanism in the

sensor affects compatibility. Electrical resistance is governed by weak-link effects in small sensors and by phase-slip lines in larger sensors. The normal-metal features commonly used to engineer the transition shape and suppress high-frequency noise may also play a role in the behavior under AC bias; different designs for these features will also be assessed.

References

- [1] K. Nandra *et al.*, “ATHENA, the Advanced Telescope for High ENergy Astrophysics,” a mission proposal submitted to ESA’s L2 large mission opportunity, recently accepted (2014)
- [2] D. Barret *et al.*, “The Hot and Energetic Universe: The X-ray Integral Field Unit (X-IFU) for ATHENA+,” astro-ph arXiv:1308.6784 (2013)
- [3] R. den Hartog *et al.*, “Baseband Feedback for Frequency-Domain-Multiplexed Readout of TES X-ray Detectors,” AIP Conf. Proc. **1185**, 261-264 (2009)
- [4] H. Akamatsu *et al.*, “Single Pixel Characterization of X-Ray TES Microcalorimeter Under AC Bias at MHz Frequencies,” IEEE Trans. Appl. Supercon. **23** 2100503 (2013)
- [5] H. Akamatsu *et al.*, “Performance of TES X-ray Microcalorimeters with AC Bias Read-Out at MHz Frequencies,” J. Low Temp. Phys. **176** 591 (2014)
- [6] J. Mates *et al.*, “Demonstration of a multiplexer of dissipationless superconducting quantum interference devices,” Appl. Phys. Lett. **92** 023514 (2008).

For additional information, contact Joel Ullom: joel.ullom@nist.gov



Next-Generation X-ray Optics: High Angular Resolution, High Throughput, and Low Cost

Prepared by: William W. Zhang (PI; NASA/GSFC) and Stephen L. O'Dell (NASA/MSFC)

Summary

This work continues technology development of X-ray optics for astronomy. Since Fiscal Year (FY) 2012, the Strategic Astrophysics Technology (SAT) program has funded this effort, which the Constellation-X project initiated and the International X-ray Observatory (IXO) project continued. This is an effort by the NASA Goddard Space Flight Center (GSFC) with collaboration from the NASA Marshall Space Flight Center (MSFC). We believe this technology development has achieved Technology Readiness Level (TRL) 5 for building 10-arcsec X-ray mirror assemblies as of May 2015, and is on track to achieve TRL 5 for building 5-arcsec X-ray mirror assemblies by December 2016.

The objective is to advance astronomical X-ray optics by at least an order of magnitude in one or more of three key metrics from the state-of-the-art represented by the four major X-ray missions currently in operation: Chandra, X-ray Multi-mirror Mission – Newton (XMM-Newton), Suzaku, and Nuclear Spectroscopic Telescope Array (NuSTAR). These metrics are (1) angular resolution, (2) mass per unit area, and (3) production cost per unit area. The modular nature of this technology renders it appropriate for missions of all sizes, from Explorers that can be implemented by the end of this decade, to Probes and flagship missions that can be implemented during the next decade.

Key areas of technology development include (1) fabrication of substrates, (2) thin-film coating of these substrates to make X-ray mirror segments, (3) alignment and (4) bonding of mirror segments into mirror modules, and (5) systems engineering to ensure all spaceflight requirements are met. In previous years, our emphasis was on steadily improving angular resolution, achieving X-ray images with a half-power diameter (HPD) of 8 arcsec. During the past year, consolidating our prior progress on improving angular resolution, we placed the emphasis of our work on improving the environmental robustness of mirror modules, stability over time and against thermal vacuum, and production process reliability. We expect to improve image quality further, to better than 5 arcsec over the next two years, and to better than 1 arcsec by the end of this decade.

Background

The last five centuries of astronomy are a history of technological advancements in optical fabrication and optical-systems integration. Furthering our understanding of the cosmos requires telescopes with ever-larger collecting area and ever-finer angular resolution. In the visible and other wavelength bands, where radiation can be reflected at normal incidence, a large mirror area alone directly translates into a large photon-collecting area. However, due to its grazing-incidence nature, an X-ray telescope requires a combination of both large area and thin mirrors to increase photon-collecting area.

Three metrics capture the essence of an X-ray optics technology: (1) angular resolution, (2) mass per unit collecting area, and (3) production cost per unit collecting or mirror area. Table 1 compares these metrics with Chandra, XMM-Newton, Suzaku, and NuSTAR. The X-ray optics of each observatory represents a scientifically useful compromise between the three metrics that was implementable in its specific technological, budgetary, schedule, and spaceflight opportunity context.

Mission	Launch Year	Mirror Technology	Angular Resolution HPD (arcsec)	Mass per Unit Collecting Area @ 1 keV (kg/m ²)	Production Cost per Unit Collecting Area @ 1 keV (2013 \$/m ²)
Chandra	1999	Ground and polished Zerodur™ shells	0.5	18,000	~9,800
XMM-Newton	1999	Electroformed nickel shells	15	3,200	~360
Suzaku	2005	Epoxy-replicated aluminum segments	120	400	~88
NuSTAR	2012	Slumped-glass segments	58	400	~80
NGXO Current Status	N/A	Slumped-glass segments	8	~400	~80
Near-Term (2-yr) Objective	N/A	Polished and light-weighted single-crystal-silicon segments	5	~400	~80
Long-Term (5-10 yrs) Objective	N/A	Polished and light-weighted single-crystal-silicon segments	<1	~400	~80

Table 1. Comparison of the objectives of this technology effort, Next Generation X-ray Optics (NGXO), and its future goals, with the state of the art as represented by the four major X-ray missions currently in operation. Given the difficulty in ascertaining cost of a specific mission component, the costs stated here are estimates.

Compared with Chandra, this technology would lower mass and cost per unit collecting area by nearly two orders of magnitude. Compared with XMM-Newton, it would reduce mass per unit collecting area by a factor of eight and cost by a factor of three, while significantly improving angular resolution. Compared with Suzaku and NuSTAR, it would improve angular resolution by an order of magnitude, while preserving their advantages in mass and cost per unit collecting area.

A salient feature of this technology is that it utilizes a hierarchical segmented design, as did Suzaku and NuSTAR. Such a design incorporates modularity and scalability, enabling use of mass production to minimize production cost, and enabling missions of any size, from small Explorer missions to large flagship missions. Small and large mirror assemblies differ only in the number of identical mirror modules that need to be constructed, aligned, and integrated. Each of these modules would typically measure 200 mm × 200 mm × 400 mm (optical axis direction), with a mass of about 10 kg, rendering them easy to handle. Construction of many identical modules lends itself to mass production, offering substantial cost and schedule savings, as well as risk-management advantages.

Objectives and Milestones

In the near term (two years or less), we expect to demonstrate an entire process for making mirror modules that produce X-ray images better than 5 arcsec HPD in a consistent and repeatable manner, and that can pass all environmental tests required for spaceflight. In the long term (next five to 10 years), we expect to continue to improve every aspect of the process toward better angular resolution from 5 arcsec to less than 1 arcsec, with the ultimate goal of achieving diffraction-limited X-ray optics in the 2020s.

The same set of milestones can be used to measure progress toward realizing both near-term and long-term objectives. They differ only in the X-ray image quality, measured in arcsec. Each step or milestone has two metrics: image quality and consistency. The steps are as follows:

1. Fabrication of mirror substrates.
2. Maximizing X-ray reflectivity by coating substrates with thin-film iridium or other material.
3. Alignment of individual mirror segments and pairs of mirror segments.

4. Bonding of mirror segments to a housing.
5. Construction of mirror modules, requiring co-alignment and bonding of multiple mirror segments.
6. Environmental tests of mirror modules, with mirror module X-ray performance tests before and after environmental tests.

Environmental tests include vibration, acoustic, and thermal-vacuum. X-ray performance tests include measurement of point spread function and effective area at representative X-ray energies – *e.g.*, 1.5 keV (aluminum $K\alpha$), 4.5 keV (titanium $K\alpha$), and 8.0 keV (copper $K\alpha$).

Progress and Accomplishments

In the past year, we made progress in every area of the technology: substrate fabrication; coating; mirror alignment; mirror bonding; and module design, analysis, construction, and testing.

Substrate Fabrication

Although not an emphasis of our FY 2015 work, we continued refining and simplifying the glass-slumping process, routinely fabricating 6-arcsec mirror substrates to support the development of subsequent technology steps. We have also provided glass substrates to other groups to facilitate their X-ray optics development. These include Dr. Brian Ramsey at MSFC for his effort of using differential deposition to improve their figure, Dr. Melville Ulmer at Northwestern University for his effort of using magnetic smart material to improve their figure, and Dr. Giovanni Pareschi at the Istituto Nazionale di Astrofisica (INAF) Osservatorio Astronomico di Brera for his effort of developing a mirror integration process.

Meanwhile, in a concurrent effort funded by the Astrophysics Research and Analysis (APRA) program under the Research Opportunities in Space and Earth Sciences (ROSES), we advanced the technology of making lightweight, single-crystal-silicon mirror substrates. We developed a polishing and light-weighting process that can make cylindrical mirror substrates of better than 3-arcsec image quality. In the remainder of FY 2015 and in FY 2016, we expect to make Wolter-I mirror substrates that are of similar image quality, completing the transition from glass substrates to silicon substrates.

Coating

Mirror substrates require an optical coating (*e.g.*, 20-nm iridium) to enhance X-ray reflectivity. The stress of an iridium film, typically several Giga-Pascal, severely distorts the figure of a thin substrate, greatly degrading its imaging quality. In FY 2014, we optimized thermal annealing parameters, reducing coating stress sufficiently to enable coated mirror segments to meet requirements for a 5-arcsec mirror assembly. Our experimental effort of further optimization of the coating process was thwarted by our lack of access to a coating chamber, which was taken over by the Neutron-star Interior Composition Explorer (NICER) project. Our coating investigation work will resume at the end of FY 2015 when NICER will have finished its work with the coating chamber.

Mirror Segment Alignment

The alignment of each mirror segment entails closed-loop operation of a hexapod, a beam of laser light, and an optical CCD imager. The alignment step must meet two requirements. First, it must maneuver the mirror segment into its prescribed location and orientation to achieve the best possible image in conjunction with other mirror segments. Second, it must hold the mirror segment steady in the optimal configuration for a sufficient time for it to be permanently affixed to the module housing.

During the past year, we reached an understanding of the alignment hexapod drift. In consultation with the hexapod manufacturer, we identified the underlying cause of the drift: thermal change of actuators. Unfortunately, there is no ready once-and-done fix. As a result, we have implemented a 30-minute wait after final mirror alignment before bonding. This “cool-off” period has proven to be effective in ameliorating mirror alignment drift during bonding.

Mirror Segment Bonding

Building on work done in previous years, we tested and implemented a totally new apparatus for bonding mirrors, dubbed the “bond-gap-control apparatus.” Although conceptually identical to the procedure we have used for several years, this new apparatus quantifies several aspects of the bonding process, including precise setting and verification of epoxy bond gap, and precise measurement of force exerted on the mirror segment. To date, we have completed a preliminary trial of this apparatus and expect that it will enable us to achieve more precise bonding going forward, achieving both better image quality and higher mechanical strength.

In addition, we conducted numerous cycles of curing epoxy-bonded mirrors to investigate their stability over time and in vacuum. We demonstrated that it is possible to cure a mirror module at an elevated temperature without degrading its image quality, resulting in a more optically stable and mechanically stronger module. We shall conduct more trials of this experiment in FY 2016 to confirm and optimize both the bonding and thermal cure processes.

Mirror Module Design, Analysis, Construction, and Testing

Our systems engineering effort in the past year has focused on thermal analysis. We constructed a finite-element-analysis model to investigate generic on-orbit thermal conditions under which a mirror assembly must operate to achieve a specified image quality. We compared a mirror assembly built with glass mirror substrates and one with silicon mirror substrates, and concluded that the silicon one is far superior. This is primarily because of silicon’s lower coefficient of thermal expansion and higher thermal conductivity compared to glass. In FY 2016, we will consolidate this work and arrive at an approximate thermal design for a generic mirror assembly.

In addition, we conducted structural finite element analyses of the stress that a typical mirror segment would experience during launch. We concluded that for a mirror segment with an axial length of 200 mm, 10 epoxy bonds (five on each azimuthal end) are optimal. Our current six epoxy bonds per mirror is sub-optimal in that, if one bond fails for whatever reason, its neighboring bonds would bear too high a load, causing them to fail as well, resulting in a cascade of bond failures. This result is being empirically verified and will be addressed in future module designs.

Path Forward

We intend to maintain the tremendous momentum of technology development, in order to build and test Technology Development Modules (TDMs) with progressively better angular resolution. The momentum of this effort is evidenced by the spectacular progress over the past few years: 17 arcsec in FY 2012, 11 arcsec in FY 2013, and 8 arcsec in FY 2014 (Fig. 1). We expect to build TDMs with at least five pairs of mirror segments that can produce better than 5 arcsec HPD images by December 2016, readying this technology for a Medium-class Explorer (MIDEX) mission opportunity that NASA HQ is expected to release in late 2016 or 2017, as well as for the European Space Agency (ESA) Advanced Telescope for High-ENergy Astrophysics (ATHENA) mission.

The 8-arcsec HPD of current TDMs has two major contributions – mirror substrates and gravity distortion during X-ray testing in a horizontal beam. As such, our path to 5 arcsec HPD images is as follows:

- Consolidate the current alignment and bonding process to achieve consistency; build more TDMs to be tested for both performance and environmental robustness; transition from 2nd generation Kovar housing to 3rd generation E60 housing, which can accommodate more than three pairs of mirror segments;

- Transition from slumped glass to polished and light-weighted single-crystal-silicon substrates, achieving better than 3-arcsec HPD substrates, needed to achieve 5-arcsec HPD TDMs; and
- Complete modification of an existing 600-m X-ray beam line to enable a TDM to be tested with its optical axis in the vertical direction, reducing gravity-induced distortion by more than an order of magnitude.

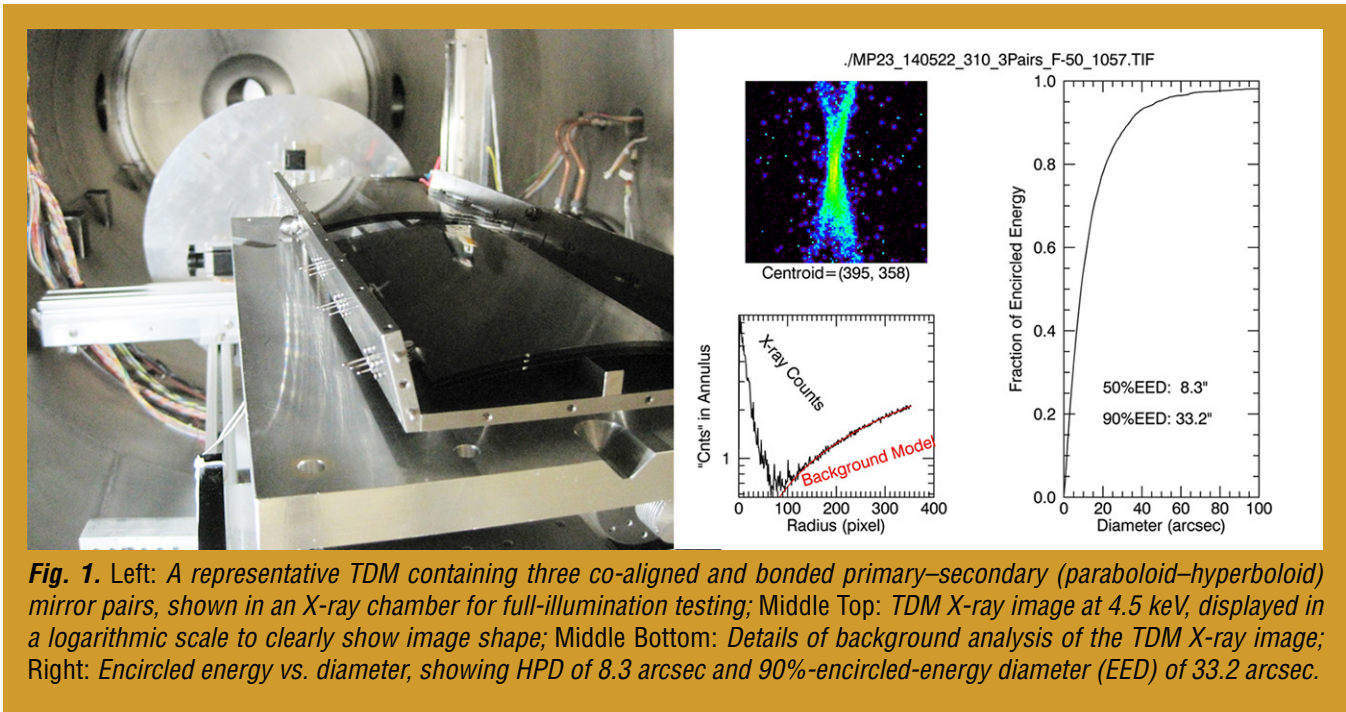


Fig. 1. Left: A representative TDM containing three co-aligned and bonded primary–secondary (paraboloid–hyperboloid) mirror pairs, shown in an X-ray chamber for full-illumination testing; Middle Top: TDM X-ray image at 4.5 keV, displayed in a logarithmic scale to clearly show image shape; Middle Bottom: Details of background analysis of the TDM X-ray image; Right: Encircled energy vs. diameter, showing HPD of 8.3 arcsec and 90%-encircled-energy diameter (EED) of 33.2 arcsec.

We anticipate that successful completion of the above three tasks will lead to TDMs with better (possibly significantly better) than 5 arcsec HPD. At that point, we shall conduct a detailed error analysis to determine the remaining dominant contributors to image blur. These contributors, which likely include coating stress and distortion due to epoxy bonding, will become natural targets for our future work.

For additional information, contact William Zhang: william.w.zhang@nasa.gov



William Zhang

Planar Antenna-Coupled Superconducting Detectors for CMB Polarimetry

Prepared by: James J. Bock (Jet Propulsion Laboratory, California Institute of Technology)

Summary

We are developing advanced antenna-coupled superconducting detector-array technology for the NASA Inflation Probe, a future satellite dedicated to comprehensive measurements of Cosmic Microwave Background (CMB) polarization in NASA's Physics of the Cosmos (PCOS) office. This Strategic Astrophysics Technology (SAT) program will extend the demonstrated frequency range of antennas down to 40 GHz and up to 270 GHz, and develop dual-band antennas that offer a higher density of detectors, a valuable resource in a 100 mK space-borne focal plane. We are carrying out a systematic study of polarized beam-matching of new tapered antennas in representative optical systems. We are testing cosmic-ray susceptibility in antenna-array wafers and developing methods to mitigate thermal response due to hits in the silicon frames. Finally, we will characterize noise stability and magnetic susceptibility in a microwave-resonator Superconducting QUantum Interference Device (SQUID) multiplexing system that offers significant resource savings compared with current time-domain or frequency-domain multiplexing. The technology is advanced by rapidly integrating arrays in ground-based and sub-orbital experiments, and guided by our experience developing an earlier generation of bolometers for space readiness for the European Space Agency (ESA) Planck satellite.

Antenna-coupled detectors have the requisite attributes – sensitivity, frequency coverage, and control of systematic errors – called for in community studies of space-borne CMB polarization experiments. The arrays provide integral beam-formation, spectral-band definition, and polarization analysis; and scale to operate over the wide-frequency range of 30 – 300 GHz required to remove galactic foregrounds at near-background-limited sensitivity. The devices have rapid response speed and $1/f$ noise stability for slow-scanning observations without requiring an additional level of signal modulation.

This two-year program began in October 2013, and includes Jeff Filippini, Chao-Lin Kuo, Roger O'Brient, Anthony Turner, and Alexis Weber. Most notably this year, antenna-coupled bolometer-array technology made leading measurements of B-mode polarization on degree angular scales at 150 GHz, with the Keck Array data surpassing the sensitivity of Background Imaging of Cosmic Extragalactic Polarization 2 (BICEP2) and demonstrating consistent polarization measurements. The effort has now progressed to implementing new 95- and 220-GHz bands to better separate CMB and galactic foreground signals. In January 2015, the Spider balloon experiment flew with six full focal planes operating at 95 and 150 GHz. The detectors performed well in the closest scientific environment to space, with low photon backgrounds, slow-scanned observations, and a difficult cosmic-ray environment.

Background

The importance of CMB polarization research has been recognized in national reports including the 1999 National Academy Report, the 2001 Decadal Survey, and the 2003 National Research Council (NRC) report "Connecting Quarks with the Cosmos." In 2005, the Task Force on CMB Research stated that its first technology recommendation was "*technology development leading to receivers that contain a thousand or more polarization sensitive detectors*", and that "*highest priority needs to be given to the development of bolometer-based polarization sensitive receivers.*" The Astro2010 decadal report endorsed a CMB technology program of \$60M-\$200M, its second-ranked medium initiative for space. In addition, the decadal report states the amount could be increased to \$200M following a mid-decade

review of the state of CMB polarization measurements. The CMB Technology Roadmap ranked detector arrays as its highest priority of CMB technologies, recommending a program that takes maximum advantage of operating the arrays in sub-orbital and ground-based CMB polarization experiments.

The Inflation Probe (IP) will measure CMB polarization over the entire sky to cosmological and astrophysical limits. The CMB is thought to carry a B-mode polarization signal imparted by a gravitational-wave background produced by the Inflationary expansion $\sim 10^{-32}$ seconds after the Big Bang. The Inflationary polarization signal is sensitive to the energy scale and shape of the Inflationary potential, and can be clearly distinguished from polarization produced by matter-density variations due to its distinctive B-mode spatial signature. A detection of the Inflationary polarization signal would do more than just confirm Inflation — the amplitude of gravitational waves depends on the model and energy scale of Inflation, so detection would distinguish between models and constrain the physical process underlying Inflation. Such a measurement has profound implications for cosmology and bears on the current frontiers of fundamental physics: the union of general relativity and quantum mechanics, string theory, and the highest accessible energies.

The IP will also map the CMB polarization pattern produced by gravitational lensing. Intervening matter between us and the surface-of-last-scattering slightly distorts the background CMB polarization, imparting a B-mode signal that peaks at arc-minute angular scales and probes the evolution of large-scale structure, which is sensitive to neutrino mass and dark energy. The CMB lensing signal is related to the projected gravitational potential of this matter, and provides a powerful combination with dark-energy surveys such as baryon acoustic oscillations and weak lensing.

The most recent definition study of the IP in 2008-9 developed the basis for space-borne CMB polarization measurements, incorporating wide participation across the CMB community, and leading to a series of consensus papers on the scientific and technical case. High-sensitivity detector arrays were identified as the key technology, operating over a wide range of frequencies to accurately measure and remove polarized galactic foregrounds. The detector system must demonstrate extreme $1/f$ noise stability, forward-beam definition with stray-light immunity, Radio Frequency (RF) and magnetic shielding, excellent spectral-band and time-constant matching, and cosmic-ray insusceptibility. Alternate implementations have been proposed, including an ESA medium-class mission and the Japanese Aerospace eXploration Agency (JAXA) LiteBIRD concept. Furthermore, a NASA Explorer mission may be possible if the technologies are sufficiently mature.

Antenna-coupled Transition-Edge-Sensor (TES) bolometer arrays (Fig. 1) are a scalable, planar-focal-plane architecture that coherently sums an array of individual slot antennas with a microstrip feed network, controlling the phase and electric-field amplitude distributed to each slot. The planar antenna enables customized shaping of the detector beam-pattern for controlling the detector illumination on critical optical surfaces. The antenna operates in two polarizations: an array of horizontal slots couples to one detector, and an interleaved array of vertical slots couples to another. The spectral band is defined by a three-pole RF microstrip filter. Power from the antenna is deposited in a meandered Au resistor on a thermally isolated bolometer, detected by a Ti/Al TES detector and read out by a multiplexed SQUID current amplifier. As shown in Fig. 1, this technology has now been demonstrated in scientific observations in spectral bands centered at 95, 150, and 220 GHz.

Planar antennas are entirely lithographed and avoid coupling optics such as feedhorns or hyper-hemispherical lenses, ideal for a low-mass 100 mK focal plane. The devices can cover the wide range of frequencies by scaling the antenna with wavelength and keeping the detector element essentially unchanged. The antennas demonstrate excellent polarization properties and the lithographed filters provide reproducible control of the spectral band. The Ti TES detectors give predictable noise properties and low-frequency noise stability appropriate for slow-scanned observations from space.

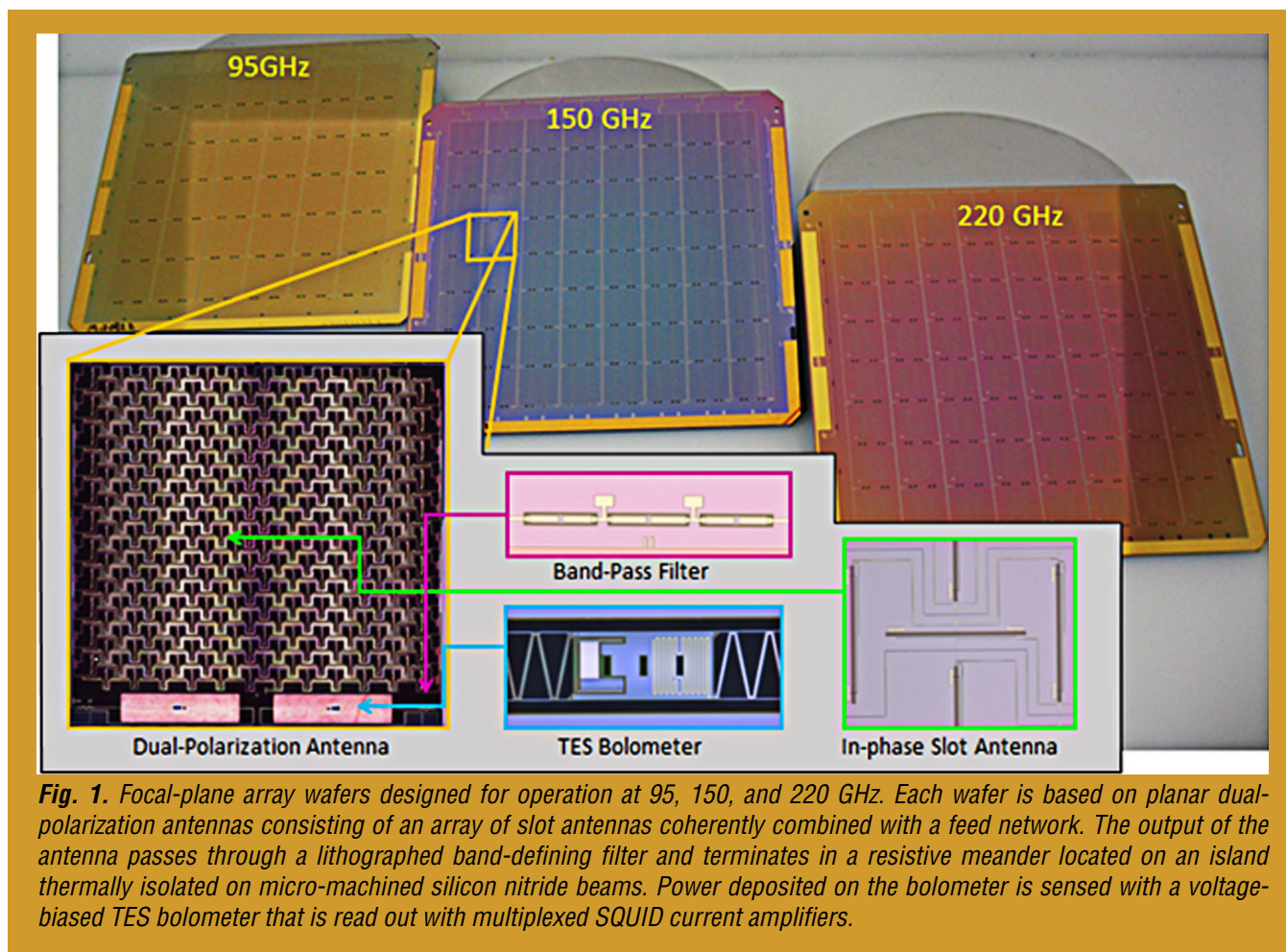


Fig. 1. Focal-plane array wafers designed for operation at 95, 150, and 220 GHz. Each wafer is based on planar dual-polarization antennas consisting of an array of slot antennas coherently combined with a feed network. The output of the antenna passes through a lithographed band-defining filter and terminates in a resistive meander located on an island thermally isolated on micro-machined silicon nitride beams. Power deposited on the bolometer is sensed with a voltage-biased TES bolometer that is read out with multiplexed SQUID current amplifiers.

Current State of CMB Polarization Measurements

In March 2014, the BICEP2 instrument, using antenna-coupled detector technology, announced the detection of degree-scale B-mode polarization at 150 GHz. New data from the Keck Array at 150 GHz were recently added to BICEP2. With comparable sensitivity, the Keck Array data are consistent with the BICEP2 signal, passing this mutual consistency check as well as a comprehensive battery of internal consistency tests. These measurements are near the depth that the IP will reach, although restricted to a small patch instead of covering the entire sky. The consistency at this level of high sensitivity demonstrates the necessary control of systematic errors, a critical milestone for space readiness.

The BICEP2/Keck and Planck teams carried out a combined analysis in order to assess the level of galactic foregrounds to the total signal amplitude. The joint data set combines the extreme sensitivity of BICEP2/Keck at 150 GHz with the wide frequency range of Planck in seven polarized spectral bands. The result leads to a detection of polarized emission from galactic dust, and the inflationary CMB polarization is not detected ($r < 0.12$ at 95% confidence). However, one must note that the statistical errors increase significantly due to the additional noise involved in subtracting the galactic dust component. While the best fit to the data gives a positive value of r , the current statistical significance is weak given the current statistical errors. In the coming year, multi-frequency data using new arrays developed for 95 and 220 GHz will significantly improve the statistical errors in foreground separation. As well as demonstrating the array technology, these results bear directly on the scientific goals of the IP, and the sensitivity and frequency coverage needed for discriminating foregrounds in a future space-borne measurement.

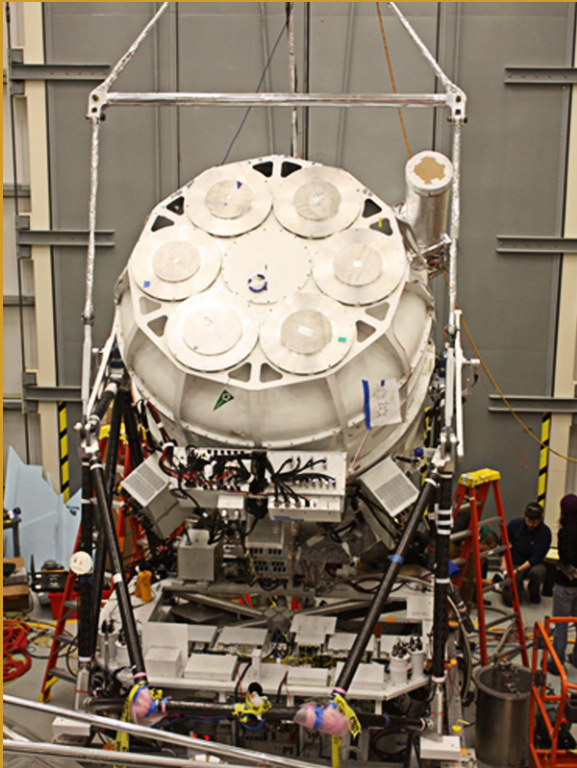


Fig. 2. The Spider balloon experiment in the final stages of assembly for its successful 2015 Antarctic long-duration balloon flight. The detectors performed well under low photon background and high cosmic-ray rate carrying out slow-scanning observations under conditions representative of a space environment.

Antenna-Coupled TES Bolometers Fly on Spider

In January 2015, the Spider long-duration balloon experiment (Fig. 2) flew from Antarctica with six focal plane arrays with 24 wafers of antenna-coupled TES bolometers operating at 95 and 150 GHz. A long-duration balloon flight is the closest suborbital scientific representation of a space mission, and the Planck mission was preceded by the Balloon Observations Of Millimetric Extragalactic Radiation and Geophysics (BOOMERanG) and Archeops balloon flight demonstrations. The Spider detectors were slowly scanned across the sky, with a low photon background and a hostile cosmic-ray environment. Early detector sensitivity and noise stability results are shown in Fig. 3. The noise performance is stable enough that an additional level of signal modulation is not needed, avoiding the complexity and single-string risk of a cryogenic, broadband, spinning wave-plate.

Objectives and Milestones

Instruments such as BICEP2 and the Keck Array demonstrate antenna-coupled bolometers are scientifically capable in ground-based observations. This SAT program advances the detector attributes needed for space-borne observations, specifically developments related to frequency coverage, focal-plane packaging, cosmic-ray susceptibility, multiplexing, and noise stability. The tasks for our

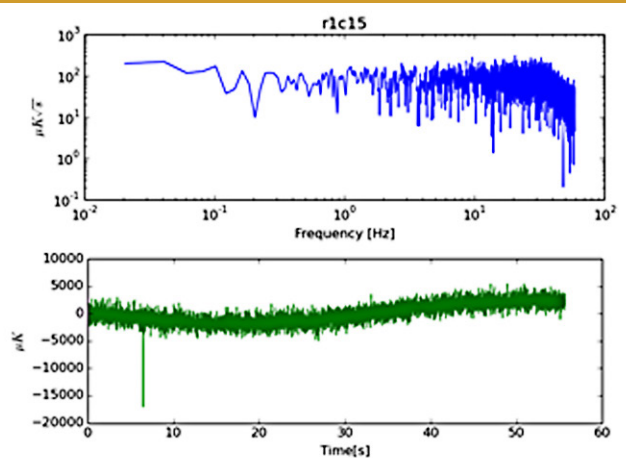
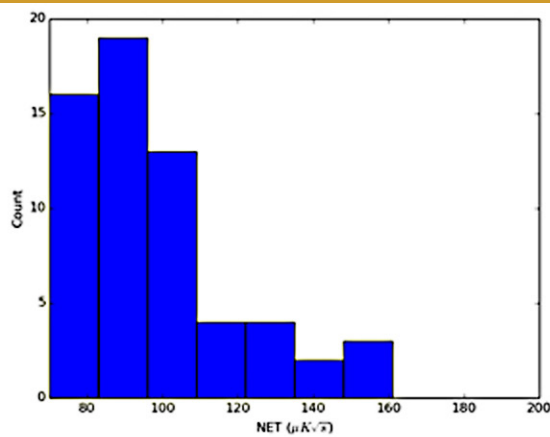


Fig. 3. Left: Distribution of preliminary on-sky noise equivalent temperature (NET) from one of Spider's 150-GHz focal plane arrays. The NET is calculated from the mean noise between 0.5 and 2 Hz with a preliminary calibration obtained from mapping RCW38. Right top: On-sky noise power spectrum for one bolometer channel over a 60s period when the telescope was pointed. Right bottom: Time stream of the same channel during scanning observations, where the CMB dipole is visually evident in the data.

SAT program builds on current antenna-coupled detector technology to address specific challenges for a space mission as follows:

- Extend the frequency range to bands at 40 GHz and 270 GHz;
- Develop dual-band devices operating at 220 and 270 GHz;
- Fully demonstrate the optical performance of tapered antennas in a modular housing;
- Measure and reduce the cosmic-ray particle susceptibility; and
- Characterize the noise stability and magnetic susceptibility of RF-multiplexed readouts.

Progress and Accomplishments

Last year, we successfully completed loss testing in deposited dielectric materials, including Plasma-Enhanced Chemical Vapor Deposition (PECVD) silicon oxide, silicon nitride, and amorphous silicon. Amorphous silicon showed the best loss characteristics; however, we found that it produced a number of high-impedance shorts in the antennas. We then fabricated full antennas from sputtered silicon oxide and PECVD silicon nitride, finding that the uniformity (evidenced by beam matching) was noticeably better for silicon oxide. For the time being, silicon oxide remains our default dielectric material in spite of presenting a ~10% propagation loss in our current antenna designs.

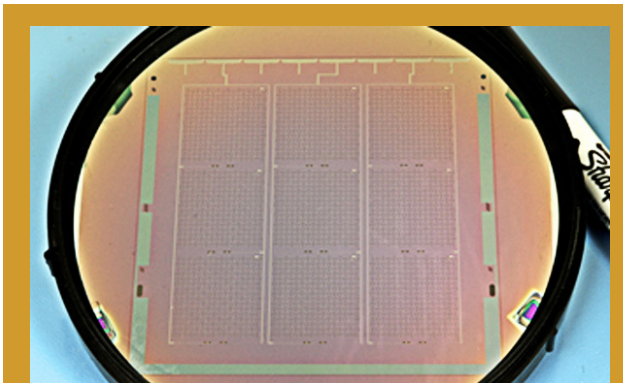


Fig. 4. Wafer with nine 40-GHz antennas fabricated at the JPL micro devices lab. The devices are completed and ready for cryogenic testing and optical characterization.

We then developed antennas for extending the range of demonstrated frequencies. As shown in Fig. 4, we have completed an array wafer at 40 GHz. The array will be characterized as soon as 40-GHz optical components are completed. Several science-grade wafers were produced for 220 GHz. As shown in Fig. 5, the spectral band is ~10 GHz higher than the target center frequency but well-matched to the atmospheric window, and the arrays show excellent system optical efficiencies. The 220-GHz design has been operating on the Keck Array since February 2015, and we are carefully monitoring its performance, in particular the level of atmospheric noise. It is possible that observations in the 200- to 300-GHz window will prove more effective from a ground-based site than from a balloon-borne observatory.

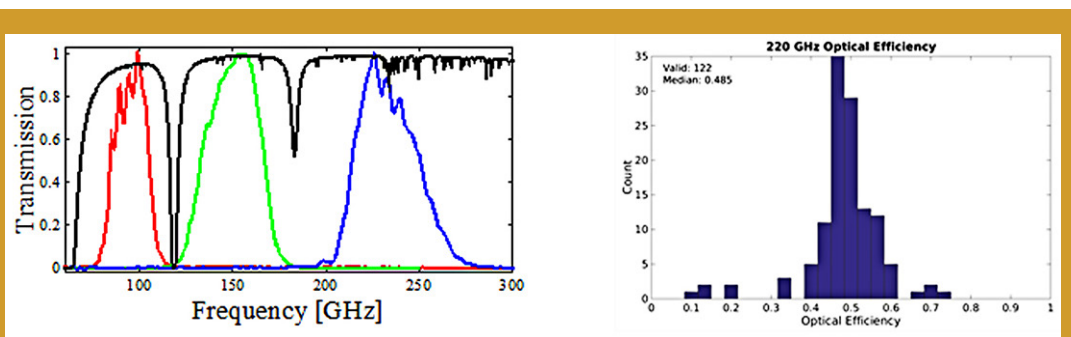
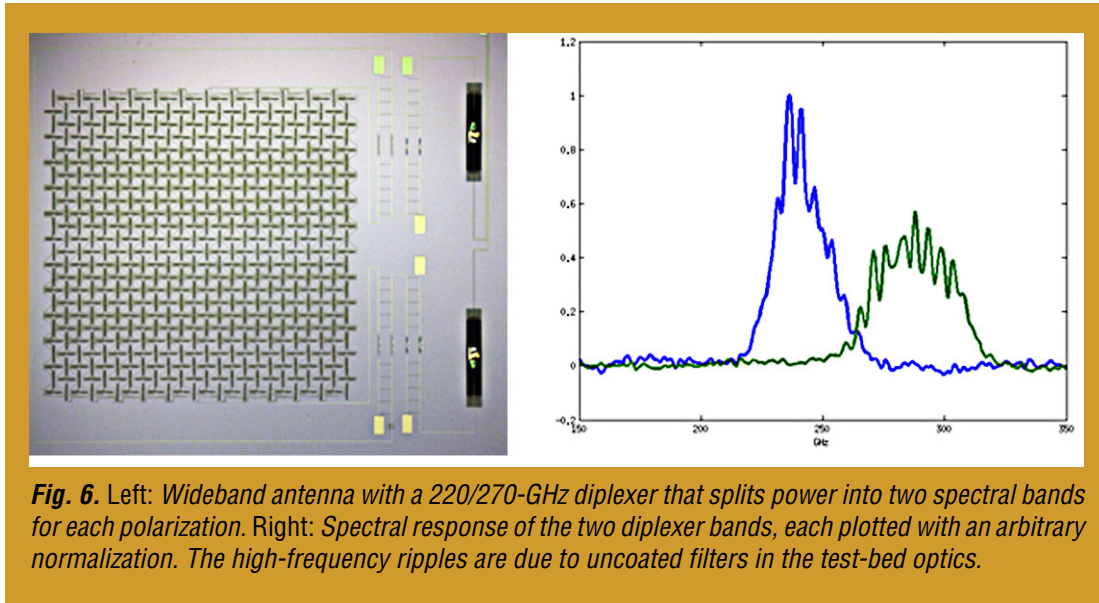


Fig. 5. Left: Measured spectra from 95-, 150-, and 220-GHz focal-plane tiles. The designs are chosen to operate within atmospheric windows. Right: Histogram of measured optical efficiencies of a recent 220-GHz focal-plane array, giving an array median optical efficiency of 48%. These measurements include all losses in the detectors, as well as losses in a system of low-pass filters and the cryostat window, but do not include efficiency through the telescope that would be part of a full instrument.

We also produced a first-generation array for 270 GHz that performed well. Based on the results, we are now planning a second-generation 270-GHz design to more closely match the response of the antenna and filter.

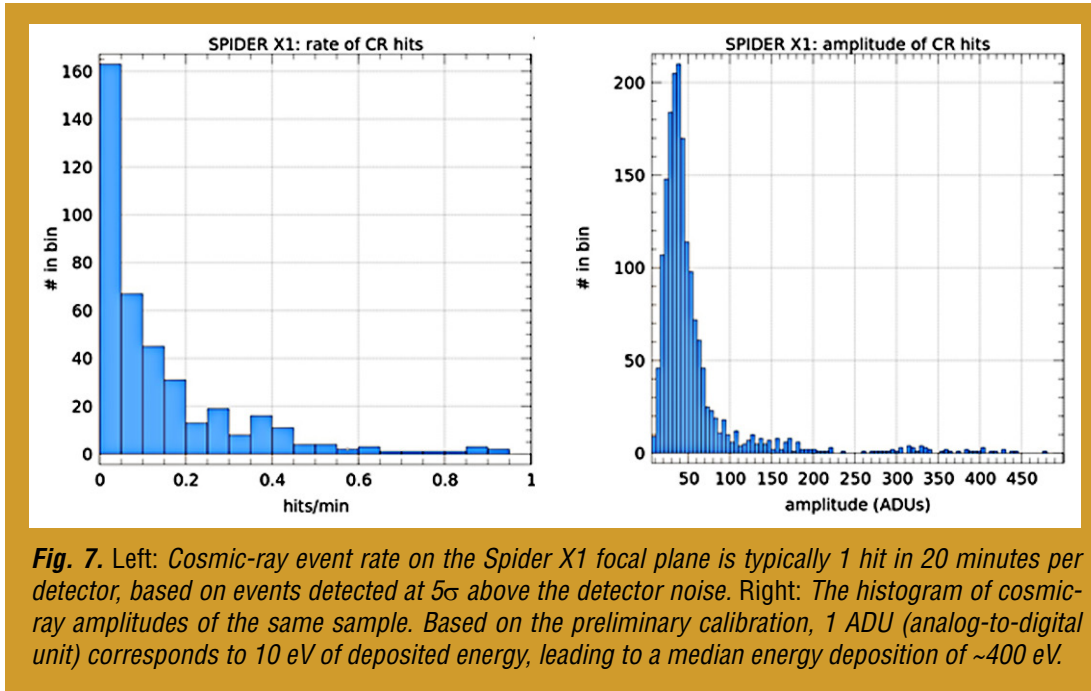
We have also been developing a dual-frequency antenna. A first version of this device, shown in Fig. 6, uses a diplexer and band-pass filters to split the response into two spectral bands. In parallel, we are developing an antenna with wider bandwidth using a resonant stub to better match the real and imaginary components of the complex antenna impedance. The first-generation device clearly functions as intended, although the optical efficiency in the upper band is lower than expected, and the antenna bandwidth was not as wide as we expected from RF simulations. We are now developing a second-generation device with improved components.



We have completed several wafers with a moderate degree of beam tapering, obtained by designing the power splitters in the antenna feed network to produce a Gaussian illumination rather than a top-hat function. These wafers have been assembled into focal-plane modules, and were optically tested end-to-end in a representative optical system in the BICEP3 experiment. Beam properties were measured at the telescope aperture and in the far field of the telescope. We are now in the process of analyzing the data to determine the degree of matching with these tapered antennas, and to characterize the effect of electromagnetic interactions between the antenna and the module frame. Some effects from the frame are visible, indicating there is room for improvement in the frame corrugations. These measurements are a first step toward characterizing antennas with more tapering that are appropriate for coupling to an ambient-temperature reflecting telescope.

To characterize the susceptibility of the antenna-coupled TES detectors to cosmic rays, we are first completing a test of a modified Planck bolometer. Planck detectors suffered from a high rate of cosmic-ray events in space at L2, and our analysis of the flight data indicates the dominant population arises from hits in the Si frame, which then lead to thermal events sensed by the bolometer. New devices with a high-heat-capacity material (PdAu) deposited on the frame have been fabricated and await testing at 100 mK in a particle-beam facility in France, to be directly compared with an unmodified Planck flight-spare detector. The Spider balloon flight served as a first test of the cosmic-ray performance of antenna-coupled bolometers. The in-flight data reveal that the fraction of observing time lost to particle events is negligible, indicating that the cosmic-ray cross-section is smaller than the spider-web bolometers flown on Balloon-borne Large-Aperture Sub-millimeter Telescope (BLAST) and BOOMERanG. Based on

30 minutes of Spider data at float (Fig. 7), the median rate is 0.05 hits/minute, significantly lower than the rate in BLAST (1.5–6 hits/minute) and BOOMERanG (0.5 hits/minute) in the same environment. Event amplitudes based on a first-order calibration are 0.1 – 2 keV, with a median of 0.4 keV. Events that cause a DC-level discontinuity or drive a detector or SQUID readout unstable are extremely rare. We are continuing to analyze the flight data to search for and characterize common-mode events, due to hits in either the frame or the multiplexed readout. Pending the conclusion of these two investigations, we will assess whether the antenna-coupled arrays would benefit from a high-heat-capacity material, which can be patterned behind the Nb ground plane.



Finally, our collaborators at the National Institute of Standards and Technology (NIST) have made progress on the microwave SQUID multiplexer, which has been operated with a 67-element TES instrument. Recent noise testing of the readout system gives a white noise level of 17 pA/ $\sqrt{\text{Hz}}$, competitive with that of time-domain-multiplexed SQUIDs. Crosstalk has been demonstrated to be below 0.1% on neighboring channels for large signals ($> 1 \phi_0$). Noise testing of TES detectors operated under dark conditions, and read out with a ROACH-based (Reconfigurable Open Architecture Computing Hardware) system, shows white-noise levels consistent with expectations from detector-thermal-fluctuation noise. These measurements indicate that the readout system does not degrade the detector sensitivity at frequencies above 1 Hz.

Table 1 shows project milestones by topic, with each milestone’s schedule and status.

Path Forward

Developing antennas for extended frequencies will continue, with upcoming tests of the 40-GHz devices. We are also planning to develop second-generation 270-GHz and dual-band devices based on the performance we have achieved with the first-generation devices. Improved wide-band and 270-GHz designs will quickly improve the current situation with monitoring galactic dust emission and will find immediate application in ground-based experiments and the second flight of Spider. The particle susceptibility of the arrays on Spider looks very encouraging, and we will be able to assess the need for frame mitigation on the arrays once the Planck device testing and Spider data analysis completes. The SQUID uMUX development will need to address noise stability below 1 Hz, after which we will characterize susceptibility to magnetic fields.

Topic	Milestone	Schedule and Status
Antennas for Extended Frequencies	Dielectric Loss and Uniformity Characterize loss and uniformity of SiO ₂ and Si ₃ N ₄	September 2012 - May 2014 Completed
	40-GHz Arrays Demonstrate antennas for the 40-GHz frequency band	October 2014 – August 2015 Fabrication completed, devices awaiting test
	220-GHz Arrays Develop arrays for 220 GHz	January 2014 - February 2014 Completed; arrays fielded in Keck Array
	270-GHz Arrays Develop arrays for 270 GHz	August 2014 – December 2015 1 st generation arrays tested; 2 nd generation in design
Multi-Color Antennas	Wide-Band Antenna Develop wide-band antenna for 220/270-GHz diplexer	August 2014 – December 2015 1 st generation device tested; 2 nd generation in design
	Diplexer and Filters Develop and test diplexer + filter components	August 2014 – December 2015 1 st generation device tested; 2 nd generation in design
	220/270-GHz Diplexed Antenna Develop integrated device: antenna, diplexer, and filters	August 2014 – December 2015 1 st generation device tested; 2 nd generation in design
Tapered Antennas	Module Verification Develop and test designs for B-shielding and frame electromagnetic interaction	January 2014 – September 2014 Full modular array fabricated and tested
	Far-Field Beam Maps with Telescope Test tapered antenna in representative optical system	January 2014 – June 2015 Far-field beam tests in BICEP3 completed
Particle Susceptibility	Frame Response of Single-Element Device Test Planck devices with modified frame to minimize events	January 2014 – August 2015 Frame-mitigation devices awaiting test
	Cosmic-Ray Events in Spider Arrays Determine cosmic-ray properties of arrays in balloon environment	January 2015 – October 2015 Flight data under analysis
	Design to Minimize Array Frame Hits Implement frame mitigation on arrays if necessary	November 2015 - Dec 2015 Design pending results of above tests
SQUID μ MUX	Demonstrate Noise Properties at NIST Determine noise properties of μ MUX	January 2014 – July 2015 Measured as 17 pA/ $\sqrt{\text{Hz}}$ to 1 Hz, some pickup
	Magnetic Susceptibility Tests Determine system B-field susceptibility	July 2015 – December 2015 Test with reference magnetometer

Table 1. Project milestones, schedule, and status by topic.

Publications

- [1] P. Ade *et al.*, “Antenna-Coupled TES Bolometers Used in BICEP2, Keck Array, and SPIDER,” ApJ in press (arXiv 1502.00619) (2015)
- [2] BICEP2/Keck and Planck Collaborations, “Joint Analysis of BICEP2/Keck Array and Planck Data,” PRL, **114**, 1301 (2015)
- [3] BICEP2/Keck Array Collaboration, “BICEP2/Keck Array V: Measurements of B-Mode Polarization at Degree Angular Scales and 150 GHz by the Keck Array,” ApJ in press (arXiv 1502.00643) (2015)
- [4] BICEP2 Collaboration “BICEP2 III: Instrumental Systematics,” ApJ in press (arXiv 1502.00608) (2015)
- [5] BICEP2/Keck Array Collaboration, “BICEP2/Keck Array IV: Optical Characterization and Performance of the BICEP2 and Keck Array Experiments,” ApJ in press (arXiv 1502.00596) (2015)
- [6] K.S. Karkare *et al.*, “Keck Array and BICEP3: Spectral Characterization of 5000+ Detectors,” SPIE **9153E**, 3BK (2014)
- [7] I. Buder *et al.*, “BICEP2 and Keck Array: Upgrades and Improved Beam Characterization,” SPIE **9153E**, 12B (2014)

For additional information, contact James Bock: james.j.bock@jpl.nasa.gov



James Bock

Superconducting Antenna-Coupled Detectors and Readouts for Space-Borne CMB Polarimetry

By James Bock (JPL)

Abstract:

We propose to develop advanced, high-sensitivity millimeter-wave detector arrays for measuring the polarization of the cosmic microwave background (CMB). The arrays are based on planar antennas that provide beam collimation, polarization analysis, and spectral band definition in a compact lithographed format that eliminates discrete fore-optics such as lenses and feedhorns. The antennas are coupled to transition-edge superconducting bolometers, read out with multiplexed SQUID current amplifiers.

This development is directed to advance the technology readiness of the Inflation Probe mission in NASA's Physics of the Cosmos program. The Inflation Probe is a fourth-generation CMB satellite that will measure the polarization of the CMB to astrophysical limits, characterizing the inflationary polarization signal, mapping large-scale structure based on polarization induced by gravitational lensing, and mapping Galactic magnetic fields through measurements of polarized dust emission. The inflationary polarization signal is produced by a background of gravitational waves from the epoch of inflation, an exponential expansion of space-time in the early universe, with an amplitude that depends on the physical mechanism producing inflation. The inflationary polarization signal may be distinguished by its unique 'B-mode' vector properties from polarization from the density variations that predominantly source CMB temperature anisotropy.

Our development is based on previous Strategic Astrophysics Technology (SAT) funding that developed detector array technology that has been successfully demonstrated in demanding ground-based and balloon-borne CMB experiments. We have fully tested complete arrays operating at 220 GHz, and developed new antennas for 40 and 270 GHz. We have also completed a wide-band antenna and diplexer suitable for multi-band operations. We have developed a focal plane sub-array assembly that enables modular testing and replacement for making large focal planes. Detector arrays recently flew on the Spider long-duration balloon experiment for characterizing the effects of cosmic rays on the detectors.

We propose to develop new capabilities appropriate for space operation, leveraging demonstration on sub-orbital platforms where possible. We will develop arrays of wide-band 250-GHz detectors optimized for sensitive measurements of polarized Galactic dust emission from ground-based and sub-orbital platforms. We will extend the operation of antennas to higher frequencies with the development of an antenna for 350 GHz. We will develop a high-density detector module assembly that enables a densely sampled focal plane at 250 GHz, which also provides higher detector count in upcoming experiments. We will measure the Radio-Frequency susceptibility of a focal plane array, and study potential improvements using a high-pass edge filter. We will measure the low-level integrated spillover of highly tapered antennas appropriate for a passively cooled reflecting space telescope, and complete full beam-line particle testing of wafers designed to mitigate cosmic ray events in the detector frame. Finally, we will determine the uniformity of deposition equipment at JPL for scaling up to 150-mm wafer production.

For additional information, contact James Bock: james.j.bock@jpl.nasa.gov

Telescope Dimensional Stability Study for a Space-Based Gravitational-Wave Mission

By Jeffrey Livas (GSFC)

Abstract:

Gravitational waves are on the brink of discovery all across the frequency spectrum. The Advanced Laser Interferometer Gravitational-Wave Observatory (LIGO) network will be starting science operations to cover frequencies above 10 Hz. Pulsar timing consortia such as NANOGrav expect to see gravitational waves at frequencies of order 30 nHz (corresponding to a period of one year), and the detection of B-mode polarization in the cosmic microwave background is the subject of multiple current research efforts, including BICEP2 and the Planck Mission. The study of the gravitational universe is the science theme of the L3 launch opportunity of European Space Agency's Cosmic Visions program. However, multiple expected discoveries across the spectrum before the end of the decade will increase the urgency and importance of observing the rich variety of fascinating astrophysical sources in the 0.0001-to-1 Hz band that can be observed only from space.

All viable space-based gravitational wave mission concepts use telescope designs with similarly challenging requirements that are slightly different from the usual imaging telescope specifications. Two particularly difficult ones are the dimensional stability and stray light requirements. The telescope is directly in the laser interferometric metrology path and therefore must be dimensionally stable. Picometer level stability over timescales compatible with the measurement band (~10,000 seconds) is needed for gravitational wave observations. A sensitive detector and simultaneous transmit/receive operation impose a strong requirement for low levels of stray light.

Our previous research has identified an off-axis design as most suitable for achieving low stray light performance, and we are currently working to experimentally validate models that identify particulate contamination of the tertiary and quaternary mirrors as the primary sources of stray light once the surface roughness is sufficiently good. We have also demonstrated dimensional stability of an on-axis silicon carbide metering structure. The next step is to put these key pieces together.

We propose to fabricate a telescope with a realistic off-axis design, a metering structure made of flight-like lightweight materials with high stability mirror mounts, and excellent scattered light performance, and to verify that it can meet the requirements for precision interferometric metrology.

For additional information, contact Jeffrey Livas: Jeffrey.Livas@nasa.gov

High-Efficiency Feedhorn-Coupled TES-Based Detectors for CMB Polarization Measurements

By Edward Wollack (GSFC)

Abstract:

The development of large format focal planes of sensitive detectors that have excellent systematic control is essential for future space-borne measurements of the cosmic microwave background that will search for evidence of inflation. We have developed and demonstrated detectors that utilize a unique combination of a highly symmetric electromagnetic design and a single-crystal silicon material system that results in high transmission efficiency, the required sensitivity, and low cross-polarization response. We propose a two-year technology maturation effort that will focus on implementing these detectors in large focal planes that are compatible with the space environment.

For additional information, contact Edward Wollack: edward.j.wollack@nasa.gov

Appendix C – Developing the Future Astrophysics Workforce

Strategic Astrophysics Technology (SAT) projects mature technologies that enable the strategic astrophysics missions of the next decade or two. Student involvement may offer a minor strength in assessing individual proposals. However, without a trained astrophysics workforce, we will be unable to deploy new technologies into groundbreaking missions. Some of the students and postdocs participating in current SAT projects may become Principal Investigators (PIs) in their own right in 10-30 years, developing technologies for missions 50 years into the future. This demonstrates the SAT program's far-reaching impact, in that directly or indirectly, it enables the astrophysics missions of the next half century. Below we introduce some of the many students and postdocs whose work supported our current portfolio of Physics of the Cosmos (PCOS) SAT projects. We would be surprised if we don't meet them again at conferences, and as PIs, technologists, and researchers supporting flight missions enabled by the technologies they worked on early in their careers.



Dr. Ryan Allured

Leon van Speybroeck Fellow in X-ray Optics, Ph.D., University of Iowa

PI: Paul Reid

"Working on the adjustable X-ray optics program has been a truly rewarding experience. I have been able to collaborate with some of the best scientists in my field across a variety of world renowned institutions. This has helped me develop my expertise such that I now consider myself one of their peers. I feel well-prepared to lead efforts in optical design, modeling and simulation, and experiment design and implementation. I have also had the opportunity to mentor an undergraduate student in this field, and I hope to continue mentoring students as I continue my career."



Lindsey Barner

Undergraduate student, mechanical engineering, Messiah College

PI: William Zhang

"At NASA Goddard, I had the opportunity to work for Next Generation X-ray Optics (NGXO) as a mechanical engineering intern in 2015. Working alongside NGXO served as a fantastic learning experience both academically and professionally. My work focused on developing the process that mounts ultra-thin X-ray mirrors inside their telescopic modules. This involved establishing and testing hypotheses, compiling procedures and results, Computer-Aided Design (CAD), finite element analysis, and critical load analysis. In culmination, this advanced NGXO's techniques for bonding mirrors, an optimization process that is essential to the project's development.

"Not only was I able to work alongside NGXO in its pursuit of unprecedented X-ray technology, but I was able to build on my evolving skills as an aspiring engineer. Immersed in an environment of frequent discussion, compelling ideas, and passionate problem-solving, I had the opportunity to constantly inquire and learn. This thoroughly catalyzed my curiosity and gave me a genuine desire to invest in the project's success. Whether suggesting a new idea, asking for clarification, or advocating a method, I learned to take initiative and communicate with confidence. In context of a team, these skills are essential to cooperative success. In addition to building professional skills, this position strengthened my technical skills. My problem-solving and critical thinking abilities were constantly challenged; I continually learned new methods and principles. This internship had a major impact on my skillset and interest in engineering.

"My excellent experience in this position is chiefly due to an outstanding mentor. He balanced giving constructive, encouraging guidance with giving freedom and independence. I was comfortable seeking help when necessary, yet empowered to seize my own ideas and test their potential. Undoubtedly, this energized my work and enhanced my learning. My only request of NASA's internship program is to encourage this empowering mentor-mentee relationship as much as possible. Its product is nothing short of an intern's best work."



Alexander Bruccoleri

Ph.D. from MIT, based on SAT project work; started a company (Izentis, LLC) and currently consults for the project.

PI: Mark Schattenburg

“Working in the Space Nanotechnology Lab has given me a unique experience of both design and hands-on skills developing hardware for X-ray telescopes. This helped me start a business to continue developments of a broad range of technologies that interest me. This includes innovative rocket technology aimed at improving propellant efficiency via power-beaming energy from the ground. This technology could significantly reduce launch costs to space, radically changing how society and business utilize space. My company also developed a variety of nanofabrication technologies to make high-efficiency diffraction gratings for X-ray

spectrometers on space telescopes. These gratings will give future astronomers better tools to study high energy sources such as neutron stars and black holes.”



Robby Buttles

Undergraduate student, University of Maryland College Park

PI: Jeffrey Livas

“I worked with Dr. Livas and Dr. Ira Thorpe on the Laser Interferometer Space Antenna (LISA) program and on various tasks around the lab. I had to extensively use Matlab to analyze and optimize the use of lasers in the lab in order to find lab lasers that worked well in pairs (i.e., reached the same wavelength/frequency) far from mode hops. As well, I performed data analysis on the crosstalk data from the Photo Receivers developed for LISA. While working on this task, I developed a filing system for the data collection of the Photo Receivers’ crosstalk with Matlab. In addition to these duties, I performed troubleshooting and optimized LabView code to make the Photo Receiver crosstalk measurements. Lastly, I simulated and designed the

Photo Receiver circuit on Cadence and LTSpice. I discovered that a simple model did not accurately represent the circuitry in the Photo Receiver and the fluctuation in the phase difference that changing temperatures caused.

“As part of my internship, I gave a talk at the branch lunch on the details of my work, and participated in the Goddard Summer Intern Poster Session. During the internship I learned how to use oscilloscopes, network analyzers, and lock-in amplifiers. I also learned how to use Matlab, LabView, Cadence, and LTSpice.”



Chih-Hao Chang

Ph.D. from MIT with contribution from SAT project work; now a professor at North Carolina State University.

PI: Mark Schattenburg

“I was involved with the SAT project for six years, and it was extremely fruitful. Working at the intersection of optics, nanofabrication, and precision engineering, I was exposed to technology beyond my imagination. It was extremely inspirational to be a part of large team that shared a common goal. This research experience forms the key foundation for my professional training, and has encouraged me to pursue a career in academia. To this day, my group continues working and collaborating with NASA on nanostructured materials for space applications.”



Casey DeRoo

Graduate student, University of Iowa Presidential fellow

PI: Randall McEntaffer

"I've been fortunate to have the opportunity to work on the development of off-plane X-ray diffraction gratings from the ground-up. By endeavoring to establish a well-characterized fabrication process for these gratings, I've gained valuable microfabrication knowledge and skills that I know will serve me well in future efforts to ready new technology for broader use. I've also gained valuable experience designing mission concepts and optical systems through my work on the Off-plane Grating Rocket Experiment (OGRE). I feel that the well-rounded experience I've had in my research group equip me to develop, characterize, and test nascent technologies in optics, as well as apply my knowledge of technology development and mission

design to see a project through to flight."



Ben Donovan

Undergraduate student and rising Senior, Univ. of Iowa, "summer student"

PI: Paul Reid

"I am so fortunate to have had the opportunity to work with Paul Reid and the adjustable X-ray optics program at the Smithsonian Astrophysical Observatory for the past two summers. The project and the people involved have taught me a tremendous amount about X-ray astronomy and have developed my skills as a researcher a great deal. The experiences I gained while working on the project solidified my passion for astronomical research and my decision to pursue astronomy as a career. I am sad to be leaving such a great project, but am excited to see what the future holds."



Daniel Hirsh

NASA/GSFC Intern, Spring 2015; The City College of New York

PI: William Zhang

"The NGXO group is developing mirrors that will form the lens of the next generation x-ray telescope. While laser interferometers are used to profile the surface of the final, polished mirrors, they have an extremely limited measurement range that prohibits their use for other purposes. In order to profile the mirror surfaces at earlier stages of polishing, or the tools themselves, a different type of scanner is necessary. The purpose of my project is to design a scanner using a laser displacement sensor, which works on geometric rather than superposition principles, and a linear stage. A scanner was designed to meet the requirements of the NGXO group and software was written to interface with the scanner. The software

consisted of hardware-level drivers as well as a full Graphical User Interface (GUI) application designed to handle all scanning tasks, diagnostic scanning tasks, and to view and analyze resulting data sets. Tests were conducted to determine the optimum hardware settings and scan methodologies, and final results exceeded the group's requirements."



Hudson Loughlin

Student, James Madison High School; Vienna, VA; Will attend Princeton starting fall 2015

PI: Jeffrey Livas

"I worked in the lab last year, took the Electrostatic Discharge (ESD) instructor lead course and the SATERN laser safety course last summer, and am familiar with laser and ESD safety. Working in the lab, I have experience with spectrum analyzers, soldering, coding with Matlab, using LT spice, and analyzing the input current noise of quadrant photoreceivers. In addition, I have experience working with op-amp circuits and the direct and indirect methods used to calculate the equivalent input current noise of these circuits. I also gained an understanding of the evolved Laser Interferometer Space Antenna (eLISA) mission and the photo-receiver's role in this mission. Outside the Gravitational Astrophysics lab, I have experience working with circuitry

and electronics from my participation in Science Olympiad."



Jaime McCarrell

Undergraduate student, mechanical engineering, Trine University

PI: William Zhang

"This summer I was an intern with the NGXO program. Exposure to different building and manufacturing processes was common throughout the 10-week duration. Some of the subjects briefly addressed included water filtration, design, machining, tolerances, glass cutting, and computer programming. The aspect of machine creation and assembly was the major focus during my time with NGXO. Two functioning lapping machines, one rotary table and one cylindrical, were created and successfully implemented into the mirror fabrication process. This introduced the difficulty of correct assembly, and the challenge of maintaining different precision levels needed in each step.

"Working with the NGXO team has exposed me to a true professional work environment. Attending status meetings and being included in discussion of possible problems was very informative. I have been shown great examples of respectful discussions, where every opinion is taken seriously. I have also been taught many different things about X-ray astronomy, mirror creation, and all of the exciting things happening at GSFC. I never felt uncomfortable asking for clarification or help; everyone was always willing to take time to explain or help in any way possible. I thoroughly enjoyed this internship and feel it would be a great and well-rounded educational opportunity for any student. It was filled with hands-on projects and the excitement of ongoing progress."



Jake McCoy

Graduate student, University of Iowa, NASA Space Technology Research Fellowships (NSTRF) fellow

PI: Randall McEntaffer

"My career thus far as a graduate research assistant at the University of Iowa has given me valuable experience in several aspects of instrumentation for X-ray spectroscopy. Having hands-on practice with operating detectors and designing digital electronics for the Off-plane Grating Rocket for Extended Source Spectroscopy (OGRESS) payload helped solidify my understanding of the back-end workings of a space observatory system. Currently, I am supported by NSTRF to develop efficient, high-resolution X-ray reflection gratings using techniques in electron-beam lithography. Through testing these gratings at synchrotron and beamline facilities, I will

gain experience integrating together X-ray optics and detectors as a complete system. By graduation, I will be prepared well to serve as a principal investigator for future missions and a contributor to the fields of space technology and astrophysics."



Thomas Rogers

Graduate student, University of Colorado, former NESSF recipient; OGRESS rocket lead.

PI: Randall McEntaffer

“For the past three years, I acted as the lead project scientist for the development and launch of a soft x-ray spectrograph sounding rocket payload. This work has given me exposure to the full cycle of a typical science mission, including proposing for funding, designing the instrument, fabricating and assembling the components, laboratory calibrations, launch operations, and flight data analysis. Throughout the process, I have collaborated extensively with personnel at Wallops Flight Facility and White Sands Missile Range. I also had the opportunity to manage and mentor both an undergraduate and junior graduate student. This project has given me extensive hands-on experience in project management, systems engineering, and X-ray astronomy.”



Ryan Stein

MSc in Physics from Towson University, now graduate student at University of Maryland, College Park

PI: Jeffrey Livas

“During this past summer, I was awarded an internship at NASA GSFC under the mentorship of Dr. Jeffrey Livas and Dr. Shannon Sankar. The bulk of my work at GSFC was electronics-related; in particular, the goal of the project was to develop a low-noise photo-detector circuit with a dynamic range of 10^{10} W and sensitivity on the order of a few pW (10^{-12} W). This photo-detector circuit was primarily intended for scattered-light measurements in relation to the proposed space gravitational-wave detector, called Laser Interferometry Space Antenna or LISA. In one of the proposed designs of LISA, the light scattered off the secondary mirror of the telescope would be a significant source of noise in phase measurements. This photo-detector circuit was basically comprised of an integrating photodiode circuit and an anti-aliasing filter. Part of this process included a thorough analysis of the electronic noise characteristics of both circuits. The noise analysis of these circuits allowed me to develop a fair amount of experience with a 2-channel signal analyzer and circuit simulations with LTspice. I also gained experience with optics through testing the photo-detector with 1064-nm YAG lasers in various setups.”

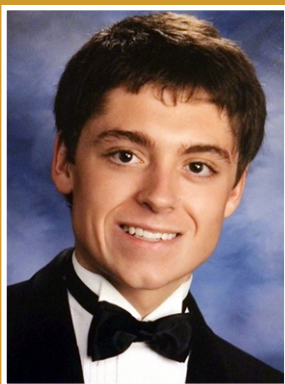


Dr. James H. Tutt

*Postdoctoral Research Scholar, Dept. of Physics & Astronomy, U. of Iowa
Moved to Iowa from a collaborating international institution, the Open University in the UK*

PI: Randall McEntaffer

“As a postdoc with experience in using solid-state detectors for X-ray detection, the SAT project enabled me to gain understanding of the systems-level engineering challenges further up the optical path. During my PhD, I was only concerned with the detection of photons as they reached the focal plane. Now, through developing the setup that will allow us to co-align X-ray gratings, I am gaining valuable experience in understanding a soft X-ray spectrometer as a complete and complex system.”



Connor Zipfel

NASA GSFC Intern, Spring 2015; University of Maryland, College Park

PI: William Zhang

“Working as an intern on the NGXO team at NASA GSFC has given me substantial insight into the research and development and engineering design processes. Through my contributions to NGXO, I’ve obtained a better understanding of the essence of performing months of trial and error experimentation. I’ve also sharpened key mechanical engineering skills and learned how to bridge the gap between physical theories taught in school and real-life scenarios.

“While performing experimentation, I’ve noticed the importance of patience and attention to detail. Although it may not be the easiest means of obtaining information, sequential testing with single variable isolation (changing one variable at a time) has always provided the most groundbreaking results. Attention to small details has proven to minimize failure propagation and result in higher-quality experiments.

“The engineering design work I performed with NGXO has been well-rounded. I’ve utilized CAD and C programming language to model and program an apparatus that will have improved features from a previous version. I performed mechanics and analysis calculations to fine-tune the parameters of the apparatus. I’ve also attended weekly meetings, to which I routinely provided work status updates. Finally, I developed an understanding of how product vendors operate.”

Beyond those featured above in their own words, many more students and postdocs participate in current SAT projects, or participated in the past, each making his or her unique contribution while gaining valuable research and development knowledge and experience.



Minseung Ahn

Graduated with Ph. D. based on SAT project work, now staff engineer at Intel

PI: Mark Schattenburg

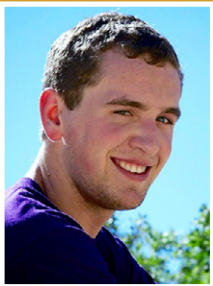


Dr. Sagi Ben Ami

Einstein Fellow, Weizmann Institute, Israel

PI: Paul Reid

Supported development of adjustable-mirror lifetime testing, measuring piezoelectric cell current, and in-situ measurement of piezoelectric cell temperature and strain using on-cell semiconductor strain gauges.



Ben Donovan

Undergraduate student, University of Iowa, awarded a prestigious University of Iowa fellowship based on his work

PI: Randall McEntaffer

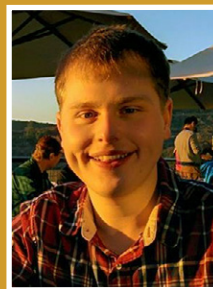
Ben also works summers with Paul Reid on adaptive X-ray optics, as described earlier.



Jay Fucetola

Graduate student, mechanical engineering, MIT Working on grating support mesh patterning for Critical-Angle Transmission (CAT) gratings.

PI: Mark Schattenburg



Jonathon Hunacek

Caltech graduate student, NSF fellowship

PI: James Bock

Studied the spectroscopic performance of 220-GHz antennas and filters, which can be used to determine the loss properties of the superconducting transmission lines used in these detectors. Improvements in mm-wave transmission may enable a new generation of lithographed spectrometers based on applications of similar methods and components used in antenna-coupled detectors.



Dong Gaun

Graduate student, mechanical engineering, MIT

PI: Mark Schattenburg

Developed stress-controlled Silicon-on-Insulator (SOI) wafers for CAT gratings. Graduated 2014, now works for Oracle.



Sinan Kefeli

Caltech graduate student

PI: James Bock

Tested antenna-coupled focal plane arrays for operating at high frequencies, in the 200-300-GHz atmospheric window. These devices enable high-sensitivity measurements of polarized Galactic dust emission, a leading foreground in the search for inflationary B-mode polarization from the Cosmic Microwave Background, from ground-based and sub-orbital observatories. Sinan is currently analyzing the on-sky performance of two 230-GHz focal plane arrays being used in the Keck Array experiment from the South Pole.



Kenneth Heitritter

Undergraduate student; physics, astronomy, and mathematics, University of Iowa

PI: Randall McEntaffer

Carried out data analysis.



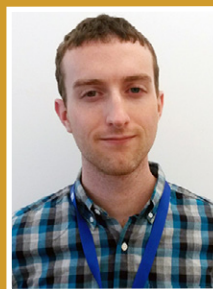
Howard Hui

Caltech graduate student

PI: James Bock

Assisted in developing modular focal plane elements that incorporate readout and amplification behind the focal plane array. These elements enable

the construction of arbitrarily large millimeter-wave focal planes. Howard is applying this technology towards his thesis experiment, the Background Imaging of Cosmic Extragalactic Polarization 3 (BICEP3) polarization experiment that operates from the South Pole.



Shawn Kilpatrick

Undergraduate student, University of Iowa

PI: Randall McEntaffer

Worked on preliminary grating testing.



Hannah Marlowe
Graduate student, University of Iowa, NASA Earth and Space Science Fellowship (NESSF) fellow

PI: Randall McEntaffer



Roger O'Brient
JPL NASA Postdoctoral Program fellowship

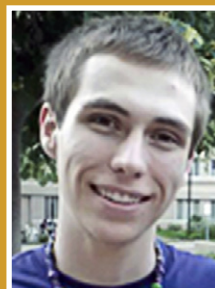
PI: James Bock

Designs novel antennas and filters for the antenna-coupled detectors program, and analyzes their performance using finite-element methods. Roger recently developed a new antenna with broad frequency response to enable sensitive high-frequency polarization measurements for studying the early universe.



Drew Miles
Undergraduate student, University of Iowa, awarded a prestigious University of Iowa fellowship based on his SAT work

PI: Randall McEntaffer



Tom Peterson
Undergraduate student, University of Iowa, awarded a prestigious University of Iowa fellowship based on his work

PI: Randall McEntaffer



Pran Mukherjee

PI: Mark Schattenburg

Worked as postdoctoral fellow for one year on SAT project, now works for a Boston software company



Julie Rose
Graduate student, aero/astro engineering, University of Maryland, College Park

PI: Jeffrey Livas



Matthew Neuman
Undergraduate student, mechanical engineering, University of Maryland, College Park

PI: Jeffrey Livas

Worked in the Gravitational-Astrophysics Laboratory during the summer of 2015 on a variety of projects related to developing a prototype telescope for a space-based gravitational-wave detector. Designed and rapid-prototyped a holder to place an aperture at the intermediate image plane in the telescope. It fit perfectly, as you can see by his smile in the picture, where he has just installed it in the telescope. In addition, developed a thermal model of the telescope using SolidWorks and sorted out the differences between the design and "as-built" versions of the telescope mechanical model. Also helped repair several models and demonstrations used for public outreach.

Worked in the Gravitational-Astrophysics Laboratory during the summer of 2015 with Shannon Sankar to align and test a prototype telescope for a space-based gravitational-wave mission. The telescope was delivered by the vendor in early June but was disassembled to avoid damage during shipping. Helped reassemble the telescope and align it. Had laser safety, ESD, and cleanroom training. Also developed some software for a MATLAB model of the telescope.



Shannon Sankar

*University of Colorado
postdoctoral fellow*

PI: Jeffrey Livas

In his third year in this position, working on the design and testing of a telescope for a space-based gravitational-wave detector. Participated in all facets of the work, including developing sensitive instrumentation for measuring scattered light, writing MATLAB models for analyzing data and the telescope design, and working on petaled masks for scattered light suppression. Also assisted with writing a follow-on SAT proposal that was just selected for funding. Certified for laser safety, ESD, cleanroom operation, and has taken scattered-light training using a non-sequential ray-tracing program. His current research is to validate a scattered-light model using a telescope delivered at the beginning of June 2015.

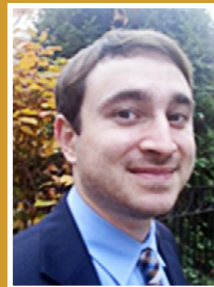


Si Tan

*Student, Stanford University
Mechanical Engineering*

PI: John Lipa

Developed pre-stabilizer cavity system and optics.



Garrett West

Graduate student, University of Rochester, transitioned to civil servant optical designer at NASA/GSFC Code 551, currently working on the James Webb Space Telescope (JWST).

PI: Jeffrey Livas

Contributed optical design and tolerancing work for a prototype telescope for a space-based gravitational-wave mission. In July 2015, Garrett received the Applied Engineering & Technology Directorate (AETD, Code 500) Excellence Award for Rookie of the Year.



Alberto Stochino

Stanford University postdoctoral fellow

PI: John Lipa

Developed and tested laser stabilization system.



Andrew John Heaton Sutton

JPL NASA Postdoctoral Program fellow

PI: William Klipstein

The project involved developing signal processing systems and an optical test bed for demonstrating the Differential Wavefront Sensing (DWS) technique for LISA. DWS provides sensing and control of the relative tilt between lasers exchanged between satellites. DWS is also required by the Gravity Recovery and Climate Experiment (GRACE) Follow-On Laser Ranging Interferometer (LRI), which utilized the LISA DWS algorithms and test bed to successfully demonstrate its wavefront sensing and control. Andrew did the primary work on this DWS.

Appendix D – Acronyms

A

AAS	American Astronomical Society
AC	Alternating Current
ACFs	Anisotropic Conductive Films
ACIS	Advanced CCD Imaging Spectrometer
ADC	Analog-to-Digital Converter
ADR	Adiabatic Demagnetization Refrigeration
ADU	Analog-to-Digital Unit
AEgis	Astrophysics Experiment for Grating and Imaging Spectroscopy
AETD	Applied Engineering & Technology Directorate
AGN	Active Galactic Nuclei
AIP	American Institute of Physics
AIP	Astrophysics Implementation Plan
AO	Announcement of Opportunity
AOM	Acousto-Optic Modulator
APRA	Astrophysics Research and Analysis
APS	Active Pixel Sensor
ARL	Applied Research Laboratory
ASCA	Advanced Satellite for Cosmology and Astrophysics
ASE	Amplitude-Stimulated Emission
ASM	All-Sky Monitor
ATHENA	Advanced Telescope for High-Energy Astrophysics
ATLAST	Advanced Technology Large-Aperture Space Telescope
AXSIO	Advanced X-ray Spectroscopic Imaging Observatory

B

BAT	Burst-Alert Telescope
BI	Back-Illuminated
BICEP	Background Imaging of Cosmic Extragalactic Polarization
BLAST	Balloon-borne Large Aperture Submillimeter Telescope
BOL	Beginning of Life
BOOMERanG	Balloon Observations Of Millimetric Extragalactic Radiation and Geophysics
BOX	Buried Oxide
BPF	Band-Pass Filter

C

CAD	Computer-Aided Design
CAT	Critical-Angle Transmission
CATXGS	Critical-Angle Transmission X-ray Grating Spectrometer
CCD	Charge-Coupled Device
CDM	Code-Division Multiplexing
CDR	Critical Design Review
CMB	Cosmic Microwave Background
CMNT	Colloid Micro-Newton Thruster
CMOS	Complementary Metal Oxide Semiconductor
CNR	Carrier-to-Noise (density) Ratio
COPAG	Cosmic Origins Program Analysis Group
Co-PI	Co-Principal Investigator
COR	Cosmic Origins
COTS	Commercial off the Shelf

CRESST Center for Research and Exploration in Space Science & Technology
CST Community Science Team
CTA Cherenkov Telescope Array
CTE Coefficient of Thermal Expansion
CY Calendar Year

D

DC Direct Current
DRIE Deep Reactive Ion Etching
DRS Disturbance Reduction System
DWS Differential Wavefront Sensing

E

EC Executive Committee
ECL External Cavity Laser
eLISA evolved Laser Interferometer Space Antenna
EM Electro-Magnetic
EM Engineering Model
EOM Electro-Optic Modulator
eROSITA extended ROentgen Survey with an Imaging Telescope Array
ERP Event Recognition Processor
ESA European Space Agency
ESD Electro-Static Discharge
EUSO Extreme Universe Space Observatory
eV electron-Volt
ExEP Exoplanet Exploration Program
ExoPAG Exoplanet Exploration Program Analysis Group

F

FDM Frequency-Division-Multiplexing
FI Front-Illuminated
FM Flight Model
FPC Fabry-Perot Cavity
FPGA Field Programmable Gate Array
FWHM Full-Width at Half-Maximum
FY Fiscal Year

G

GAS Grating Array Structure
GBps Gigabyte per second
GEMS Gravity and Extreme Magnetism SMEX
GFE Government-Furnished Equipment
GOAT Gravitational Observatory Advisory Team
GPS Global Positioning System
GRACE Gravity Recovery and Climate Experiment
GRB Gamma-Ray Bursts
GRS Gravitational Reference Sensor
GSE Ground Support Equipment
GSFC Goddard Space Flight Center
GUI Graphical User Interface
GW Gravitational Wave
GWO Gravitational-Wave Observatory

H

HETGS High-Energy Transmission Grating Spectrometer
HEW Half-Energy Width

HPD	Half-Power Diameter
HQ	Headquarters
HRMA	High-Resolution Mirror Assembly
I	
IF	Intermediate Frequency
ILRC	International Laser Radar Conference
INAF	<i>Istituto Nazionale di Astrofisica</i> (Italian National Institute for Astrophysics)
INFN	<i>Istituto Nazionale di Fizica Nucleare</i> (Italian National Institute for Nuclear Physics)
IR	Infrared
IRAD	Internal Research and Development
ISS	International Space Station
I-V	Current-Voltage
IXO	International X-ray Observatory
IXPE	Imaging X-ray Polarimeter Explorer
J	
JANUS	Joint Astrophysics Nascent Universe Satellite
JAXA	Japanese Aerospace eXploration Agency
JEM	Japanese Experiment Module
JPL	Jet Propulsion Laboratory
JWST	James Webb Space Telescope
K	
kbps	kilo-bit per second
L	
LADEE	Lunar Atmosphere and Dust Environment Explorer
LATOR	Laser Astrometric Test of Relativity
LCD	Liquid Crystal Display
LCRD	Laser Communication Relay Demonstration
LD	Laser Diode
LIDAR	Light Detection and Ranging
LIGO	Laser Interferometer Gravitational-Wave Observatory
LISA	Laser Interferometer Space Antenna
LiteBIRD	Lite (Light) satellite for the studies of B-mode polarization and Inflation from cosmic background Radiation Detection
LPF	LISA Pathfinder
LPF	Low-Pass Filter
LRI	Laser-Ranging Interferometer
LRP	Laser-Ranging Processor
LTP	LISA Technology Package
LUVOIR	Large UV/Optical/IR
L1	Level 1
L2	Level 2
L2	Second large space mission of ESA's Cosmic Visions program
L3	Third large space mission of ESA's Cosmic Visions program
M	
MAXI	Monitor of All-sky X-ray Image
MBE	Molecular-Beam Epitaxy
MDP	Maximum Design Pressure
MEMS	Micro-Electro-Mechanical System
MEOP	Maximum Expected Operating Pressure

MIDEX Medium-class Explorer
 MIT. Massachusetts Institute of Technology
 MKI MIT Kavli Institute
 MPPC Multi-Pixel Photon Counter
 MSFC Marshall Space Flight Center
 MSM. Magnetic Smart Material
 mux multiplexer

N

NANOGrav North American Nanohertz Observatory for Gravitational Waves
 NASA National Aeronautics and Space Administration
 Near-IR Near-Infrared
 NESSF. NASA Earth and Space Science Fellowship
 NET Noise-Equivalent Temperature
 NGO. New Gravitational-wave Observatory
 NGXO. Next-Generation X-ray Observatory
 NICE-OHMS Noise-Immune Cavity-Enhanced Optical-Heterodyne Molecular Spectroscopy
 NICER. Neutron-star Interior Composition Explorer
 NISP Near-Infrared Spectrometer and Photometer
 NIST. National Institute of Standards and Technology
 NITPC. Negative-Ion Time Projection Chamber
 NPR NASA Procedural Requirements
 NPRO Non-planar Ring Oscillator
 NRC National Research Council
 NSF. National Science Foundation
 NSSC. NASA Shared Services Center
 NSTRF NASA Space Technology Research Fellowship
 NuSTAR Nuclear Spectroscopic Telescope ARray
 NWNH New Worlds, New Horizons in Astronomy and Astrophysics (2010 Decadal Survey)
 N-XGS. Notional X-ray Grating Spectrometer

O

OBA Optical Bench Assembly
 OBE Optical Bench Electronics
 OBF Optical Blocking Filter
 OGRE Off-plane Grating Rocket Experiment
 OGRESS Off-plane Grating Rocket for Extended-Source Spectroscopy
 OLED Organic Light-Emitting Diode
 OPA Optical Power Amplifier
 OP-XGS Off-Plane X-ray Grating Spectrometer
 OSIRIS-REx. Origins, Spectral Interpretation, Resource Identification, and Security-Regolith Explorer
 OWL. Orbiting Wide-angle Light collectors

P

PAG Program Analysis Group
 PAN-STARRS Panoramic Survey Telescope and Rapid-Response Systems
 PATR. Program Annual Technology Report
 PCB Printed Circuit Board
 PCIe Peripheral Component Interconnect express
 PCOS Physics of the Cosmos
 PDR Preliminary Design Review
 PECASE. Presidential Early Career Award for Scientists and Engineers

PECVD Plasma-Enhanced Chemical Vapor Deposition
 PER Polarization Extinction Ratio
 PER Pre-Environmental Review
 PHARAO *Projet d'Horloge Atomique par Refroidissement d'Atomes en Orbit* (On-Orbit Cooled-Atom Atomic Clock Project)
 PhysPAG Physics of the Cosmos Program Analysis Group
 PI Principal Investigator
 PID Proportional Integral Differential
 PLC Planar Linear Cavity
 PM Prototype Model
 PMS Phase-Measurement Subsystem
 POET Polarimetry of Energetic Transients
 PRAXyS Polarimeter for Relativistic Astrophysical X-ray Sources
 PRN Pseudo-Random Noise
 PSF Point Spread Function
 PSU Penn State University
 PTA Pulsar Timing Array
 PTB *Physikalisch-Technische Bundesanstalt* (German Institute for Science and Technology)
 PZT PieZo-electric Transducer

Q

QE Quantum Efficiency

R

R&D Research and Development
 REXIS REgolith X-ray Imaging Spectrometer
 RF Radio Frequency
 RFI Request for Information
 RFQ Request for Quotes
 RGS Reflection-Grating Spectrometer
 RIO Redfern Integrated Optics
 rms root mean square
 ROACH Reconfigurable Open Architecture Computing Hardware
 ROSES Research Opportunities in Space and Earth Science
 RTF Roman Technology Fellowship
 RXTE Rossi X-ray Timing Explorer

S

SA Series Array
 SAC-B Satelite de Aplicaciones Cientificas
 SAG Science Analysis Group
 SAO Smithsonian Astrophysical Observatory
 SAT Strategic Astrophysics Technology
 SBIR Small Business Innovation Research
 SBS Stimulated Brillouin Scattering
 SEM Scanning Electron Micrograph
 SGO Space-based Gravitational-wave Observatory
 SGR Soft-Gamma Repeater
 SIG Science Interest Group
 SiPM Silicon Photomultiplier
 SLF Stray-Light Facility
 SMA Sub-Miniature version A

SMART-X Square Meter, Arcsecond Resolution Telescope for X-rays
SMBH Supermassive Black Hole
SMD Science Mission Directorate
SMEX Small Explorer
SOI Silicon-on-Insulator
SOTA State of the Art
SPO Silicon-Pore Optics
SQUID Superconducting QUantum Interference Device
SRON Space Research Organization Netherlands
SR&T Supporting Research and Technology
SST Science Study Team
STAR Space-Time Asymmetry Research
STMD Space Technology Mission Directorate
STOP Structural-Thermal-Optical Performance
ST7 Space Technology 7

T

TDM Technology Development Module
TDM Time-Division Multiplexing
TDR Technology Development Roadmap
TES Transition-Edge Sensor
TES Transition-Edge Superconducting
TFB Tapered Fiber Bundle
TMB Technology Management Board
TPC Time Projection Chamber
TPCOS Technology development for Physics of the Cosmos
TRL Technology Readiness Level

U

UHECR Ultra-High-Energy Cosmic Ray
ULE Ultra-Low Expansion
umux Microwave SQUID multiplexer
US United States
USO Ultra-Stable Oscillator
USRA Universities Space Research Association
UV Ultraviolet

W

WDM Wavelength-Division Multiplexer
WFI Wide-Field Imager
WFIRST Wide-Field Infrared Survey Telescope
WFS Wavefront Sensor
WHIM Warm-Hot Intergalactic Medium

X

XCSR X-ray mission Concepts Study Report
XGS X-ray Grating Spectrometer
X-IFU X-ray Integral Field Unit
XMM-Newton . . . X-ray Multi-mirror Mission-Newton
XRS X-Ray Surveyor
XRT X-Ray Telescope
XTiDE X-ray Time Domain Explorer

